



## Durham E-Theses

---

### *Investigating antimicrobial resistance mechanisms in Neisseria gonorrhoeae using peptide probes*

BURTON, MATTHEW,FRANCIS

#### How to cite:

---

BURTON, MATTHEW,FRANCIS (2009) *Investigating antimicrobial resistance mechanisms in Neisseria gonorrhoeae using peptide probes* , Durham theses, Durham University. Available at Durham E-Theses Online: <http://etheses.dur.ac.uk/185/>

#### Use policy

---

The full-text may be used and/or reproduced, and given to third parties in any format or medium, without prior permission or charge, for personal research or study, educational, or not-for-profit purposes provided that:

- a full bibliographic reference is made to the original source
- a [link](#) is made to the metadata record in Durham E-Theses
- the full-text is not changed in any way

The full-text must not be sold in any format or medium without the formal permission of the copyright holders.

Please consult the [full Durham E-Theses policy](#) for further details.

---

Academic Support Office, Durham University, University Office, Old Elvet, Durham DH1 3HP  
e-mail: [e-theses.admin@dur.ac.uk](mailto:e-theses.admin@dur.ac.uk) Tel: +44 0191 334 6107  
<http://etheses.dur.ac.uk>



**Investigating antimicrobial resistance  
mechanisms in  
*Neisseria gonorrhoeae* using  
peptide probes**

**Matthew F. Burton**

**PhD Thesis**

**Supervisor: Dr P. G. Steel**

**Department of Chemistry**

**2009**

## Abstract

### **Investigating antibiotic resistance mechanisms in *Neisseria gonorrhoeae* using peptide probes**

The continuing evolution of antibiotic resistance strains of *Neisseria gonorrhoeae* coupled with the paucity of new antimicrobial agents makes the treatment of gonococcal infections challenging. A major cause of resistance is the expression of a multidrug efflux pump termed MtrCDE, which exports a wide range of antimicrobial agents. Efflux pumps are membrane-bound systems and consequently challenging to study and target with drugs. The transcriptional regulator (MtrR) of the efflux pump, however, is a soluble protein and therefore more amenable to study and drug target validation investigations. This thesis serves to investigate the hypothesis that substrates for the MtrCDE efflux pump are also ligands for the regulator MtrR.

Isothermal titration calorimetry (ITC) was used to show that MtrR binds commercial antibiotics and antimicrobial peptides.  $\beta$ -lactam antibiotics not only bind MtrR but are hydrolysed by the multidrug protein. Evidence for this novel enzymatic activity is provided by ITC, mass spectrometric and microbiological techniques.

A series of peptides derived from LL-37 were synthesised and screened for binding to MtrR. A key region of LL-37 with a higher affinity to MtrR than the natural product was then identified. The peptide binding site in MtrR was elucidated via a photoactivated peptide binding study. Electrophoresis mobility shift assays indicated that the peptides do not induce derepression of the genes controlled by MtrR, although the peptide derivatives of LL-37 were shown to be substrates for the MtrCDE efflux pump.

## **Copyright**

The copyright of this thesis rests with the author. No quotations from it should be published without prior consent and information derived from it should be acknowledged.

## **Declaration**

The work was conducted in the Department of Chemistry at Durham University between October 2005 and September 2009. In January 2007, a one month placement was undertaken at Cambridge Research Biochemicals. This work has not been submitted to any other university. It is my own work, unless otherwise stated.

## Acknowledgements

I would like to thank my supervisor Patrick Steel for support and guidance throughout the project.

I am grateful to Alison White for facilitating my placement at Cambridge Research Biochemicals and to Dr John McDermot and Johann Eksteen for training me in many aspects of peptide chemistry.

To the biologists of CG209, particularly Dr David Dixon, Dr Mark Skipsy, Dr Ian Cummins and Dr Melissa Brazier-Hicks, thanks for your help and support over recent years.

Thanks also to my friends in CG1 and around the department for making the past four years a pleasurable experience. A big thanks goes to Ehmke for the many helpful discussions and to Aileen and Jon for proof reading this thesis.

I would also like to thank Prof. Judith Howard and Dr Susan Frenk for the encouraging discussions over the past four years.

Finally, a special thanks to my partner Tessa, for everything you have done to help and support me over the past four years. Without your care and support, none of this would have been possible.

## Abbreviations

[ $\alpha$ ]	Specific rotation
ABC	ATP binding cassette
ABPP	Activity based protein profiling
ACT	Activotec
ACVS	Alanine cysteinyl valine synthetase
AMP	Antimicrobial peptide
ATP	Adenosine triphosphate
<i>bla</i>	$\beta$ -Lactamase (gene)
BOP	Benzotriazole-1-yl-oxy-tris-(dimethylamino)-phosphonium hexafluorophosphate)
<i>t</i> -Bu	<i>tert</i> -butyl
$^{\circ}\text{C}$	Degrees Celsius
CAS	Clavulanic acid synthase
$\text{CCl}_4$	Carbon tetrachloride
$\text{CDCl}_3$	Deuterated chloroform
CID	Collision induced dissociation
$\delta$	Chemical shift in parts per million
DBD	DNA binding domain
DCB	Dichlorobenzoylchloride
DCM	Dichloromethane
DIC	Diisopropylcarbodiimide
DIPEA	Diisopropylethylamine
DMAP	4-( <i>N,N</i> -dimethylamino)pyridine
DMF	Dimethylformamide
DMSO	Dimethyl sulfoxide
DNA	Deoxyribonucleic acid
DOACS	Deacetylcephalosporin synthase
DOPC	Dioleoylphosphatidylcholine
DPPC	Dipalmitoylphosphatidylcholine
DPPG	Dipalmitoylphosphatidylglycerol
DTT	Dithiothreitol
EB	Ethidium bromide
ECD	Electron capture dissociation
EDTA	Ethylenediametetracetic acid
EGFR	Epidermal growth factor receptor
EMSA	Electrophoresis mobility shift assay
ESI	Electrospray ionisation
FDA	Fluorescein diacetate
Fmoc	9-fluorenylmethoxycarbonyl
FT-ICR	Fourier transform ion cyclotron resonance
HATU	2-(1H-7-Azabenzotriazol-1-yl)--1,1,3,3-tetramethyluronium hexafluorophosphate
HBTU	O-Benzotriazole- <i>N,N,N',N'</i> -tetramethyl-uronium-hexafluoro-phosphate
hCAP18	Human cathelicidin antimicrobial protein-18
HGT	Horizontal gene transfer

HIV	Human immune deficiency virus
HPLC	High-performance liquid chromatography
HRMS	High-resolution mass spectrometry
HTH	Helix-turn-helix
IM	Inner membrane
IPNS	Isopenicillin synthase
IPTG	Isopropyl $\beta$ -D-1-thiogalactopyranoside
ITC	Isothermal titration calorimetry
<i>J</i>	Coupling constant (in NMR spectrometry)
LB	Luria broth
LCA	Lithocholic acid
LPS	Lipopolysaccharide
LTA	Lipoteichoic acid
MALDI	Matrix-assisted laser desorption ionisation
MATE	Multidrug and toxic compound extrusion
MeOH	Methanol
MFS	Major facilitator superfamily
MHB	Müller hinton broth
MIC	Minimum inhibitory concentration
MSNT	1-(mesitylene-2-sulfonyl)-3-nitro-1H-1,2,4-triazole
<i>mtr</i>	Multiple transferable resistance
NMR	Nuclear magnetic resonance
OD	Optical density
OM	Outer membrane
PBP	Penicillin binding protein
PC	Phosphatidylcholine
PI	Propidium iodide
PICC	Proximity induced covalent capture
PS	Phosphatidylserine
PyBOP	Benzotriazol-1-yl-oxytrypyrrolidinophosphonium hexafluorophosphate
QRDR	Quinolone resistance determinant region
RND	Resistance nodulation and division
rRNA	Ribosomal ribonucleic acid
SDS-PAGE	Sodium dodecylsulphate polyacrylamide gel electrophoresis
SM	Sphingomyelin phospholipid
SMR	Small multidrug resistance
SOC	Super optimal broth with catabolite repression
SPPS	Solid phase peptide synthesis
TEMED	N,N,N',N'-tetramethyl-1,2-ethylenediamine
TFA	Trifluoroacetic acid
TFE	Trifluoroethanol
TLR	Toll-like receptor
TO	Thiazole orange
TOF / TOF	Time of flight / time of flight
tRNA	Transfer Ribonucleic Acid
WT	Wild type
<i>v / v</i>	Volume per unit volume



<b>1 Introduction</b> .....	13
<b>1.1 Antimicrobial resistance</b> .....	13
1.1.1 Overview of antibiotics and bacterial resistance .....	13
1.1.2 Antimicrobial resistance mechanisms.....	16
1.1.2.1 Genetic features of bacteria that contribute to resistance.....	16
1.1.2.2 Decreased cell permeability .....	18
1.1.2.3 Inactivation of the drug compound .....	20
1.1.2.4 Mutation of active site residues .....	21
1.1.2.5 Up-regulation of chromosomal resistance genes .....	23
<b>1.2 Efflux pumps</b> .....	23
1.2.1 Introduction .....	23
1.2.2 Overview of efflux pumps in <i>N. gonorrhoeae</i> .....	25
1.2.3 The MtrCDE efflux pump from <i>N. gonorrhoeae</i> .....	26
<b>1.3 Transcriptional regulation of efflux pumps</b> .....	27
1.3.1 Introduction .....	27
1.3.2 The TetR family of transcriptional regulators.....	31
1.3.2.1 Structural studies on TetR family proteins .....	31
1.3.2.2. Functional studies of TetR proteins: Electrophoretic mobility shift assays.....	33
1.3.2.3. Functional studies of TetR proteins: Isothermal Titration Calorimetry .....	34
1.4 MtrR from <i>N. gonorrhoeae</i> .....	36
1.4.1 Genetic origin and structure of the mature protein .....	36
1.4.2 Effect of oligonucleotide mutations on MtrR function.....	37
1.4.3 MtrR regulatory network.....	38

1.5	<i>Project hypothesis and aims</i> .....	39
<b>2</b>	<b>MtrR interaction with peptide antibiotics</b> .....	<b>41</b>
2.1.1	Introduction .....	41
2.1.2	$\beta$ -lactam antibiotics .....	41
2.1.3	Cellular target and bacterial resistance to $\beta$ -lactams .....	46
2.1.4	Mechanism determination by mass spectrometry .....	49
2.1.5	Non-classical $\beta$ -lactamases .....	51
<b>2.2</b>	<b><i>Results and discussion</i></b> .....	<b>52</b>
2.2.1	Introduction .....	52
2.2.2	Origin, overexpression and purification of MtrR.....	52
2.2.2	MtrR and antibiotics ITC binding study.....	55
2.2.3	Specificity of ligand binding.....	58
2.2.4	Mass spectrometric inhibitor study .....	61
2.2.6	Visualisation of results using a homology model of MtrR .....	67
2.2.7	Site directed mutagenesis studies.....	69
<b>2.3</b>	<b><i>Summary</i></b> .....	<b>76</b>
<b>2.4</b>	<b><i>Conclusions</i></b> .....	<b>76</b>
<b>3</b>	<b>Peptide probes for MtrR</b> .....	<b>78</b>
<b>3.1</b>	<b><i>Introduction</i></b> .....	<b>78</b>
<b>3.2</b>	<b><i>Antimicrobial peptides as substrates for microbial efflux pumps</i></b> .....	<b>78</b>
<b>3.3</b>	<b><i>Antimicrobial peptides</i></b> .....	<b>80</b>
3.3.1	Introduction .....	80
3.3.2	Cathelicidins .....	80

3.3.3 Human antimicrobial peptide LL-37.....	81
3.3.4 Bioactivity.....	82
3.3.5 Structure.....	84
3.3.6 Molecular mode of action.....	90
3.3.7 Interactions with mammalian cellular proteins.....	93
3.3.8 Interactions with DNA.....	95
3.3.9 Conclusions.....	96
<b>3.4 Interaction studies.....</b>	<b>97</b>
3.4.1 Activity based protein profiling.....	98
3.4.1.1 Photoactivated activity based protein profiling.....	99
3.4.1.2 Benzophenone containing photoactivated ABPP.....	100
3.4.1.3 Techniques for analysing ABPP experiments.....	102
<b>3.5 Results and discussion.....</b>	<b>103</b>
3.5.1 Introduction.....	103
3.5.2 Peptide synthesis plan.....	105
3.5.3 Results of peptide synthesis.....	109
3.5.3.1 Automated synthesis.....	109
3.5.3.2 Manual synthesis.....	111
3.5.3.3 Microwave synthesis.....	113
3.5.3.4 Summary.....	114
3.5.4 ITC binding studies.....	115
3.5.4.1 Screening of synthetic peptides by ITC.....	115
3.5.4.2 Conclusion.....	118

3.5.5 Photoactivated peptide substrates.....	119
3.5.5.1 <i>Introduction</i> .....	119
3.5.5.2 <i>X-ray crystallographic trials</i> .....	119
3.5.5.3 <i>Photoaffinity peptides</i> .....	121
3.5.5.4 <i>Summary</i> .....	133
3.5.5.5 <i>Conclusion</i> .....	134
3.5.6 Electrophoretic gel mobility shift assays .....	134
3.5.6.1 <i>Introduction</i> .....	134
3.5.6.2 <i>MtrR:DNA complex</i> .....	135
3.5.6.3 <i>Development of EMSA conditions</i> .....	136
3.5.6.4 <i>Conclusions</i> .....	139
3.5.7 Are the peptide fragments substrates for the mtrCDE efflux pump? .....	140
3.5.7.1 <i>Introduction</i> .....	140
3.4.2 Peptide bioactivity .....	141
3.4.4 Summary .....	151
3.4.5 Conclusions.....	151
<b>4. Conclusions and further work</b> .....	<b>152</b>
<b>4.1 Conclusions</b> .....	<b>152</b>
4.2.1 Introduction.....	153
4.2.2 Development of cathelicidin peptide screening .....	153
4.2.3 Conclusion .....	156
4.3.1 Solution phase synthesis .....	157
<b>5. EXPERIMENTAL</b> .....	<b>160</b>

<b>5.1 Chemistry</b> .....	160
5.1.2 General procedures.....	160
5.1.3 Peptide synthesis.....	162
5.1.3.1 General procedures.....	162
5.1.3.2 Synthesis of LL-37 and derivatives .....	164
5.1.4. Synthesis of benzophenone labelled peptides .....	170
5.1.4.1 Benzophenone-FLRNLVPRTES (243) .....	170
5.1.5 Photoactivated binding studies.....	170
5.1.6 Synthesis of PC-8.....	171
5.1.7 Synthesis of PG-1 .....	172
5.1.8 Pseudo proline synthesis .....	172
<b>5.2 Biology</b> .....	176
5.2.1 General Procedures.....	176
5.2.2 Overexpression and purification of MtrR .....	177
5.2.3 MtrR mutant proteins.....	178
5.2.4 Construction of BL21AI and KAM3 <i>E. coli</i> containing pET28a-MtrR plasmid .....	178
5.2.4.1 Plasmid prep from BL21-AI (pET21a-mtrR).....	178
5.2.4.2 Transformation of XL-10 with pET21a-mtrR .....	179
5.2.4.3 Excision of mtrR gene from pET21a and purification of the mtrR gene .....	179
5.2.4.4 Ligation of mtrR gene into pET 28a .....	180
5.2.4.5 Transformation of Kam3 (DE3) cells with pET28-mtrR.....	180
5.4.5 Analysis of covalent modification of MtrR by small molecule probes using trypsin digests and mass spectrometry .....	180

5.2.6 $\beta$ -lactamase activity of MtrR as determined by growth curve analysis using Kam3 <i>E. coli</i> expressing MtrR.....	181
5.2.7 Analysis of bacterial cultures by Flow Cytometry .....	182
5.2.8 Isothermal Titration Calorimetry.....	182
5.2.9 Subcellular localisation of MtrR by Western blot.....	182
5.2.10.1 Concentration of oligonucleotides .....	183
5.2.10.2 Biotin 3' end labelling of DNA .....	184
5.2.10.3 Annealing of labelled oligonucleotides .....	184
5.2.10.4 Preparation of 4 % bis-acrylamide gels.....	184
5.2.10.5 DNA / Protein / ligand binding reactions .....	185
5.2.10.6 Gel electrophoresis.....	185
5.2.10.7 Electrophoretic transfer of binding reaction to membrane.....	185
5.2.10.8 Detection of Biotin-labelled mtrR DNA by chemiluminescence.....	186
5.2.11 Antibacterial activity of synthetic peptides as determined by growth curve analysis using Kam3 <i>E. coli</i> expressing full, or elements of, MtrCDE .....	186
5.2.11.1 FLASHSCAN method.....	186
<b>6 References</b> .....	<b>188</b>
<b>7 Appendix</b> .....	<b>211</b>

# 1 Introduction

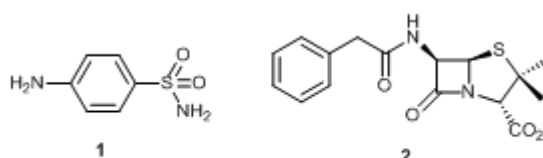
This thesis describes research carried out using a combination of peptide chemistry, biophysical and microbiological techniques, to investigate antimicrobial resistance mechanisms in *Neisseria gonorrhoeae*. More specifically, this research focuses on the transcription regulator protein MtrR, its ability to bind a range of synthetic peptides and commercial antibiotics and ultimately how these binding events regulate the expression of a multidrug efflux pump.

The following chapter provides an overview of antibiotic resistance mechanisms in bacteria, highlights the importance of multidrug, membrane bound transport systems (efflux pumps), and discusses the role of the transcriptional regulator in the expression of efflux pumps. Chapter 2 describes the characterisation of a previously unknown secondary function of MtrR, namely a  $\beta$ -lactamase function. Chapter 3 details the design, synthesis and evaluation of natural product-derived peptides to probe how MtrR responds to binding ligands. The use of a photoactivated peptide as a ligand for MtrR enables the first characterisation of the ligand binding domain of MtrR to be reported. Chapter 4 concludes the thesis and consider future work arising from this thesis. Chapter 5 provides experimental procedures.

## 1.1 Antimicrobial resistance

### 1.1.1 Overview of antibiotics and bacterial resistance

The introduction of antimicrobial agents such as sulphanilamide (1) and benzyl penicillin (2) in the early 20<sup>th</sup> Century greatly improved patient survival rates (Figure 1).



**Figure 1** Structures of the first synthetic, commercial antibiotics sulphanilamide (1) and benzyl penicillin (2)

The success of these antibiotics was curtailed by the rapid evolution of resistant bacteria, which is exemplified by the development of penicillin resistance in *Staphylococcus aureus*.<sup>1</sup> In 1940 more than 85 % of *S. aureus* strains were susceptible to less

than 0.1  $\mu\text{g} / \text{mL}$  benzyl penicillin, whilst by 1947 susceptibility had decreased to 30 %. This considerable increase in resistant strains is a powerful example of how quickly antibiotic resistance can (and does) develop.

The concept of 'resistance' is a subjective notion with several definitions listed in the literature. The World Health Organisation defines resistance as when 5% of infections are not cured by treatment with the recommended antibiotic.<sup>2</sup> Clinicians and infection control specialists define resistance on the basis of 'breakpoint' concentrations, whereby a breakpoint is defined as "*a discriminating concentration used in the interpretation of results of susceptibility testing to define isolates as susceptible, intermediate or resistant.*"<sup>3</sup> Concentrations are determined by monitoring bacteria growth at different concentration, with a resistant organism showing no reduction in population size, even at high antibiotic concentrations. The concentration of an antibiotic required to prevent bacterial growth is termed the 'minimum inhibitory concentration' (MIC) and levels of resistance in pathogenic bacteria are frequently quoted as n-fold increases compared to the susceptible strain. For example the MIC for ciprofloxacin against *N. gonorrhoeae* is 0.03 mg / mL in susceptible strains and 0.06 mg / mL in resistant strains.<sup>3</sup> This thesis adopts the conventional biochemical definition of resistance, namely as the observation of decreased susceptibility towards an antimicrobial agent due to the presence of a selective advantage.<sup>4</sup>

In order to combat bacterial resistance, intensive research during the mid-twentieth century led to the development of several classes of antibiotic (Table 1). Despite the structural diversity of antimicrobial compounds bacteria have continued to respond through the evolution of resistant strains. For example the relatively new antibiotic linzolid (**3**) is no longer effective at inhibiting protein synthesis in all strains of *S. aureus* due to the emergence of strains with mutations in the antibiotic target site, the 23S subunit in RNA.<sup>5</sup>

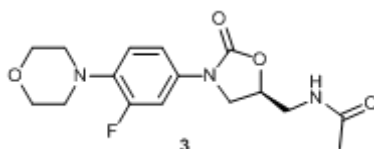


Figure 2 Linzolid (3)



Antibiotic		Cellular target	Bacterial resistance mechanism	Representative organisms with resistance phenotype	Ref
Class	Examples				
β-lactam	Benzylpenicillin	Cell wall biosynthesis (transpeptidase)	β-lactamase Mutations in PBP's Active efflux	<i>Staphylococcus aureus</i> <i>Neisseria gonorrhoeae</i>	6
	Cephalosporin				
Cyclic peptide	Vancomycin	Cell wall biosynthesis (transglycosylation)	Alterations in LPS / LTA Target site mutation	<i>Clostridium difficile</i> . <i>Staphylococcus aureus</i>	7
	Polymixin	Outer membrane integrity	Modification of LPS	<i>Pseudomonas aeruginosa</i>	
	Daptomycin		Unknown	MRSA	
Macrolide	Erythromycin	Protein synthesis (50S RNA subunit)	Methylation of target RNA Esterase Active efflux	<i>Staphylococcus aureus</i> <i>Escherichia coli</i>	41
Tetracycline	Tetracycline Tigecycline	tRNA 30S subunit	Oxidation of tetracycline Efflux	<i>Enterobacteriaceae</i>	8
Aminoglycoside	Gentamycin Kanamycin	Protein synthesis (50S and 30S subunits)	N-acetylation, O-phosphorylation N-nucleotidylation of drug	<i>Staphylococcus aureus</i> Staphylococci, <i>Staphylococcus aureus</i>	33
Quinolones	Nalidixic Ciprofloxacin	DNA gyrase topoisomerase IV	Mutations in target proteins Efflux	<i>Staphylococci</i> , <i>streptococci</i> and <i>enterococci</i>	9
Oxazolidinone	Linezolid	Protein synthesis (23S subunit of 50S)	Mutation in 23S subunit of RNA	<i>Staphylococcus aureus</i>	5

Table 1 Summary of common clinically used antibiotics, bacterial targets, resistance mechanisms and species.

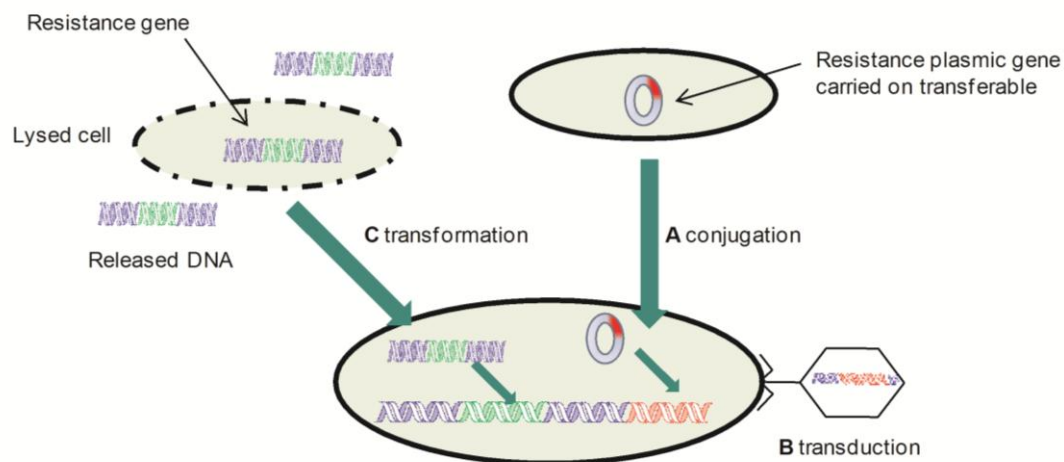
The predominance of resistant bacterial strains coupled to the paucity of new antimicrobial agents now severely compromises the treatment options for a wide range of infections including meningitis (*Neisseria meningitidis*)<sup>10</sup>, hospital-acquired infections (*Clostridium difficile*, *Methicillin resistant Staphylococcus aureus*),<sup>11</sup> and sexually transmitted infections (STI). Recent figures for STI's highlight these problems, with resistance in *N. gonorrhoeae* to fluoroquinolones currently between 10 and 27 % of isolates across Europe but more than 50 % in Australia and up to 98 % in China.<sup>12</sup> The World Health Organisation (WHO) recommends that antimicrobial agents are no longer used to treat infections where resistance is seen in 5% of the community; consequently since 2009 fluoroquinolones are no longer recommended for the treatment of *N. gonorrhoeae*. Third generation cephalosporins are now recommended but, worryingly, resistant isolates have already been reported in Japan.<sup>13</sup> This rapid increase in antibiotic resistance, coupled with the increasing number of cases and its frequent co-infection with HIV has driven research to understand antimicrobial resistance mechanisms in *N. gonorrhoeae* in the hope of developing new antimicrobial agents.

### **1.1.2 Antimicrobial resistance mechanisms**

#### ***1.1.2.1 Genetic features of bacteria that contribute to resistance***

Important influences on the continued evolution of bacterial resistance are increased usage of antibiotics (in both a clinical setting and in the food chain) and greater mobility of people across the world.<sup>14</sup> The presence of antibiotics in the environment increases the selective pressure on bacteria and the increased movement of people across the globe enhances the rate of transmission of resistance genes. Bacteria can accept resistance genes from other bacteria of the same strain, or a different strain via fundamental processes referred to as horizontal gene transfer (HGT, also known as horizontal evolution, Figure 3).<sup>15,16</sup>

Bacteria lacking a particular resistance feature (*e.g.* a  $\beta$ -lactamase) can accept a plasmid from a species of bacteria that contains the desired resistance element (*e.g.* *bla* gene) in a process referred to as conjugation (A, Figure 2).<sup>11</sup> The acquired plasmid is integrated into the bacterial genome causing the recipient bacteria to display the resistance phenotype (*e.g.*  $\beta$ -lactamase). Furthermore, gene sharing by conjugation in bacteria



**Figure 3 Genetic mechanisms used by bacteria to enhance antibiotic resistance**

enables genes encoding a beneficial mutation to be transferred to other bacteria, accelerating bacterial evolution and species survival.<sup>17</sup> In transduction, genes are transferred between bacteria through the use of bacteriophages (B, figure 3). The final method of transformation describes the ability of bacteria to incorporate DNA segments that have been released by other bacteria after cell lysis (C, figure 3). These genetic bacterial features underpin the mechanisms used by bacteria to decrease susceptibility to antimicrobial agents.

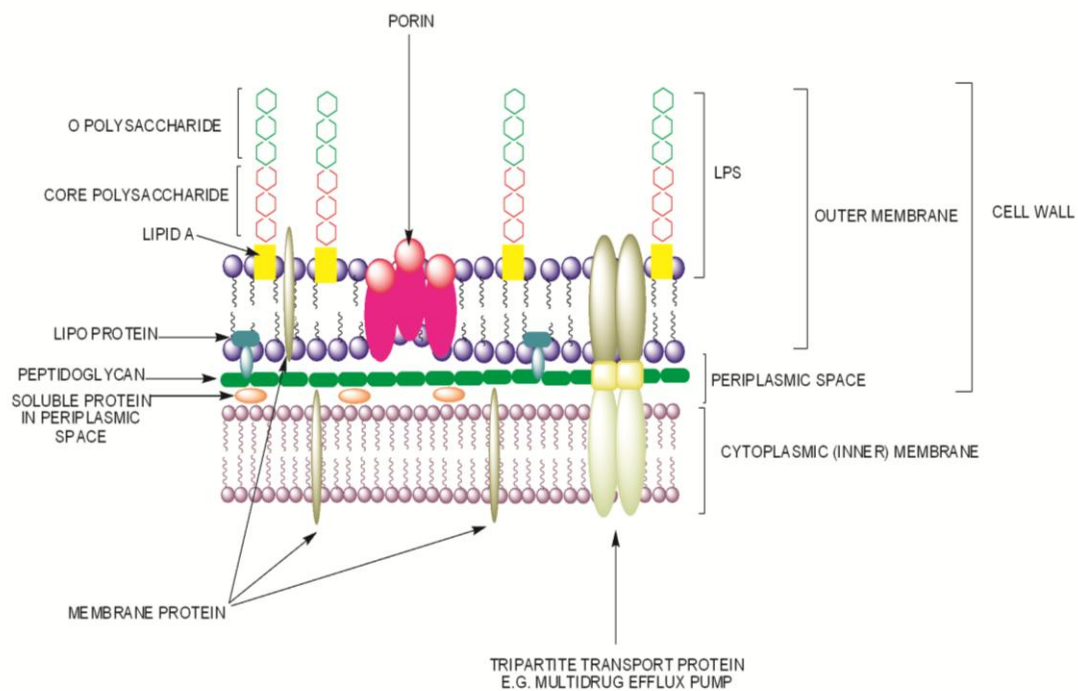
In addition to horizontal evolution, there is a process called vertical evolution.<sup>18</sup> This genetic feature refers to spontaneous mutations that occur in and confer increased resistance to antibiotics. Mutations are generally uncommon events, occurring at a frequency of 1 event per  $10^7$ – $10^{10}$  bacteria, but may result in the development of resistance during antimicrobial therapy in organisms that are initially susceptible, for example a mutation in the coding region of a protein. An example of this would be mutation in RNA at the binding site of fluoroquinolone antibiotics that abrogates drug binding, which will be discussed in more detail later.<sup>19</sup>

As a result of these genetic features, five principle resistant phenotypes exist, *viz.* decreased cell permeability, inactivation of the drug compound, modification of the target site, up-regulation of resistance gene transcription and decreased cellular

concentration. Each mechanism will be discussed using examples from the literature, with specific reference to *N. gonorrhoeae*, the pathogen of interest in this thesis.

### 1.1.2.2 Decreased cell permeability

An innate resistance feature of bacteria is the cell membrane and associated structures (e.g. peptidoglycan), which provides a natural barrier to antimicrobial agents. *N. gonorrhoeae* possesses a double cell membrane and is classified as a Gram negative bacterium as it does not retain the crystal violet dye (Figure 4). Other Gram negative pathogenic organisms include *E. coli*, *P. aeruginosa* and *V. Cholera*. Between the inner membrane (IM) and the outer lipid bilayer (OM) is the periplasmic space and peptidoglycan, linked to the OM by lipoproteins. Lipopolysaccharides (LPS) are anchored to the surface of the outer membrane and play a key role in pathogenicity and resistance.<sup>20</sup>

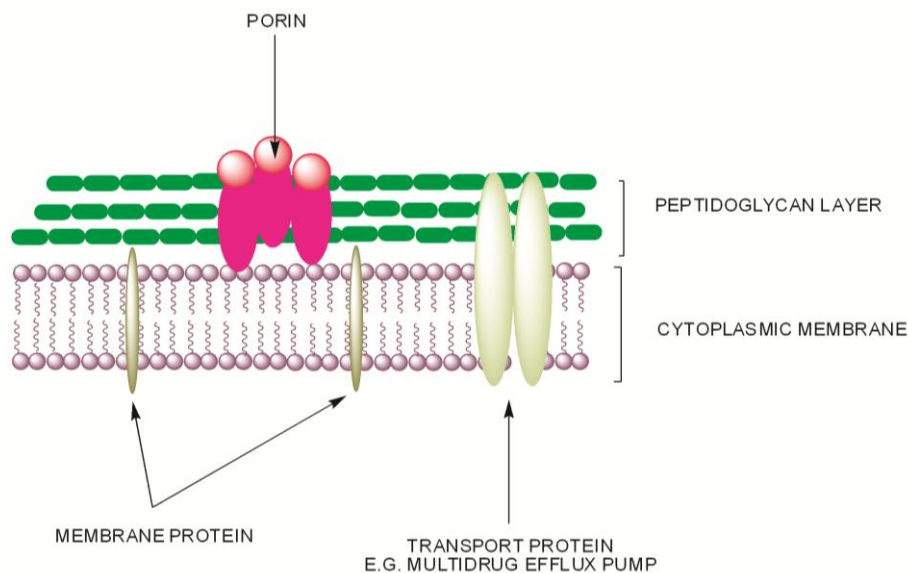


**Figure 4 Structure of the Gram negative cell membrane (Image drawn in ChemDraw, adapted from Stryer, *Biochemistry* and Albert *et al*, *The Molecular Biology of the Cell*)**

Large cationic antibacterial agents such as antimicrobial peptides, aminoglycosides and macrolides bind to the negatively charged lipopolysaccharide on the outer surface of Gram negative bacteria and then enter the cell via diffusion through the lipid bilayer.<sup>21</sup> Decreasing the overall negative charge of the OM is a key strategy utilised by *N. gonorrhoeae* to resist cationic antimicrobial agents. The acylation (with

phosphoethanolamine) of the phospho head group of lipid A in the gonococcal OM decreases the anionic character and hydrophobicity of the membrane increasing cell survival in the presence of cationic host defence peptides and human serum.<sup>22,23</sup> Further modification to the cell envelope in *N. gonorrhoeae* is achieved by *O*-acylation of peptidoglycan conferring resistance to host defence secreted lysozyme.<sup>24</sup>

In contrast to Gram negative bacteria, Gram positive bacteria have a very thick layer of peptidoglycan, which does retain the crystal violet dye (Figure 5). A second major component of the Gram positive cell wall is lipoteichoic acids that are an important virulence factor in infections.<sup>25</sup>



**Figure 5 Structure of the gram positive cell membrane**

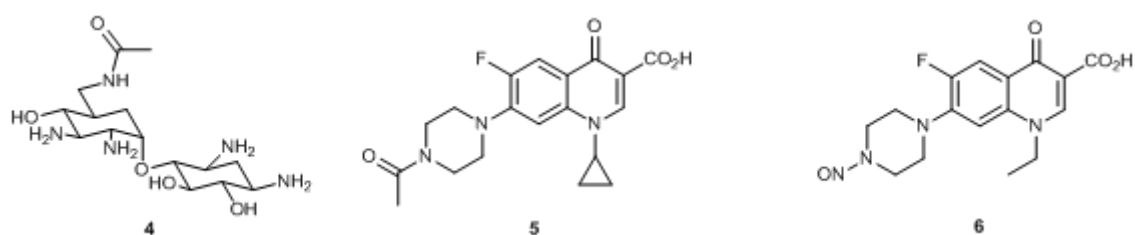
The cell membrane also contains a number of protein channels called porins. Porins are non-selective mono or trimeric protein channels present in Gram negative and Gram positive bacteria, that enable nutrient molecules (often hydrophilic) to enter the cell.<sup>21</sup> Small antibiotics such as  $\beta$ -lactams, tetracycline, fluoroquinolones and chloramphenicol also enter bacteria through these protein channels. In order to lower cell permeability to antibiotics, bacteria can decrease production of porin proteins, but this compromises bacterial viability. A more selective evolutionary advantage comes from mutations in the primary structure of the porin, particularly in flexible loops at the entry to the protein channel. A typical example of this is the *penB* mutation of the porin IB in *N. gonorrhoeae* that encodes amino acid replacements G $\rightarrow$ K alone or G $\rightarrow$ D and A $\rightarrow$ D in the entry loops

of the porin.<sup>26</sup> The increased negative charge resulting from these point mutations decreases the translocation of benzyl penicillin into the cell, however, the increase in MIC as a result of *penB* are only seen in conjunction with a mutation in another resistance element, *mtr*. This will be discussed in more detail in section 1.1.4.<sup>27,28</sup>

### 1.1.2.3 Inactivation of the drug compound

If the antimicrobial agent passes through the membrane one mode of resistance used by bacteria is to detoxify the compound by chemical modification, in a process analogous to the phase I and phase II metabolism in humans.<sup>7</sup>  $\beta$ -Lactam containing antibiotics are susceptible to enzymatic degradation (phase I process) by extended spectrum  $\beta$ -lactamases<sup>29</sup>, metallo- $\beta$ -lactamases<sup>30</sup> and AmpC enzymes.<sup>31</sup> A detailed review of  $\beta$ -lactamases can be found in Chapter 2. Other examples of phase I type metabolism are hydrolases present in pathogenic organisms include erythromycin esterases in *E. coli* and *S. aureus*. Aminoglycosides are subject to enzymatic modification to give *O*-phosphorylated, *N*-adenylated or *N*-acetylated compounds, for example *N*-acetylated kanamycin (**4**, Figure 6). The modification of the antibiotic disrupts a crucial hydrogen bonding interaction necessary for the drug to locate in the binding site on the ribosome, thus conferring resistance to the antibiotic.<sup>32</sup> Chloramphenicol and streptogramin are also prone to *O*- or *N*-acetylation.<sup>33</sup>

The survival advantage that *N*-acetylation confers is exemplified by the acetylation of aminoglycosides in *E. coli*.<sup>34</sup> *N*-acetyl-ciprofloxacin (**5**) has a four fold higher MIC than its unmodified parent drug.



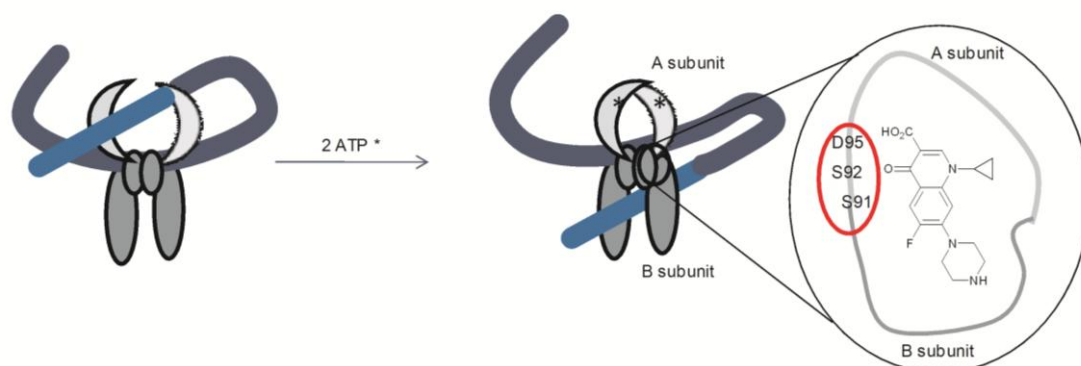
**Figure 6** Deactivated antibiotics by bacterial enzymes: 6'-*N*-acetyl kanamycin (**4**); *N*-acetyl ciprofloxacin (**5**) and *N*-nitroso norfloxacin (**6**).

Furthermore fluoroquinolone detoxification enzymes have been observed in soil bacteria, and these are capable of *N*-nitrosation (**6**).<sup>35</sup> Such transformations are not currently seen

in clinical strains but due to genetic transfer mechanisms between bacteria it is possible for such detoxification mechanisms to become more common.

#### 1.1.2.4 Mutation of active site residues

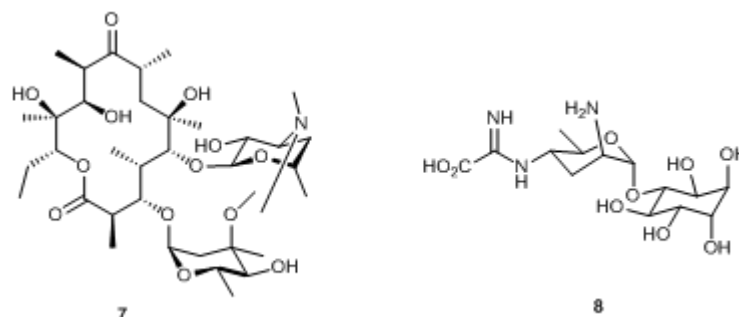
A further means that bacteria have developed for preventing antibiotics binding to their target site, are point mutations in the amino acid sequence of the binding site, as highlighted earlier in Table 1. Fluroquinolones target DNA gyrase and specific mutations in the amino acid sequence in topoisomerase IV and in DNA gyrase (subunits GyrA and GyrB) decrease fluoroquinolone binding to the protein-DNA complex.<sup>36,37</sup> The point mutations are species specific but are primarily localised to a region of the protein called the quinone resistance determinant region (QRDR) although there are more recent reports of mutations occurring outside this region.<sup>38</sup> In *N. gonorrhoeae*, a charged amino acid (Asp 95) is replaced with a neutral asparagine, alanine or glycine in the QRNR, with the probable result being disruption of hydrogen bonding networks in the protein : DNA complex.<sup>39</sup>



**Figure 7** Cartoon representation of DNA gyrase. Fluoroquinolones bind at the interface of the A and B subunits inhibiting DNA repair. The amino acids highlighted in the red circle correspond to the quinolone resistant determinant region (QRDR) on the A subunit in *N. gonorrhoeae*, the region in which most amino acid mutations are found that abrogate drug binding.

Macrolides target bacterial ribosomes and inhibit protein synthesis by blocking the elongation of peptide chains.<sup>40</sup> Oral pathogenic species of *N. gonorrhoeae* were isolated which contain an rRNA methylase that transfers a methyl group to adenine at position 2142 on the 23S rRNA, consequently disrupting the binding of erythromycin (7, Figure 8) to the ribosome subunit and thus conferring resistance to 7 and other macrolides.<sup>41,42</sup>

A further RNA modification that disrupts macrolide binding is a C → T mutation at position 2605 in 23S rRNA.<sup>43</sup>



**Figure 8** Macrolide antibiotic erythromycin (7) and aminoglycoside antibiotic kasugamycin

The precise structural effects of the base alteration in the gonococcal ribosome is not known but based on related literature studies it can be hypothesised that the cytosine to thymidine substitution alters the conformation of peptidyltransferase loop 5, lowering the binding affinity of macrolide antibiotics to RNA.<sup>44</sup> The 16S subunit has also been shown to contain nucleotide mutations that confer resistance to aminoglycoside kasugamycin (8, Figure 8) although the molecular basis for this decreased susceptibility is yet to be established.<sup>45,46</sup>

Mutations are also seen in penicillin binding proteins (PBP), the cellular target of penicillin type antibiotics and by altering the amino acids at the antibiotic binding site, PBP's become resistant to penicillin. The X-ray crystal structure of PBP2 from *N. gonorrhoeae* has recently revealed that the insertion of an aspartic acid at position 345 near the active site of the enzyme is not the sole mutation responsible for lowering the affinity of PBP2 for penicillin as previously thought.<sup>47</sup> Four mutations at the C-terminal region of the enzyme decrease the acylation rate 4.9 fold compared to 5.2 fold for the 345a insertion. The C-terminal mutations include P → S and P → A / G which alter the orientation of the helix they occupy modulating the position of amino acids in the hydrogen bonding network of the bound penicillin : enzyme complex. Such detailed analysis at the atomic level is crucial in order to understand the molecular changes that cause drug resistance and is a theme developed in the Result and Discussion chapters of this thesis.



### **1.1.2.5 Up-regulation of chromosomal resistance genes**

The mechanisms discussed so far principally involve the modification of drugs through enzymatic means or the mutation of resistance related proteins. In addition to these mechanisms, chromosomally encoded proteins may be up-regulated in order to negate the effects of the drug. Examples of this are the increase in penicillin binding proteins (PBP) and the increase in membrane bound transport proteins for the active efflux of the toxic agents. The multi-protein systems capable of recognising and removing diverse antimicrobial agents from inside the cell are termed multidrug efflux pumps and these are a major resistance feature in pathogenic bacteria. The structure, function and regulation of these efflux systems is discussed in more detail in the following section.

## **1.2 Efflux pumps**

### **1.2.1 Introduction**

Efflux of antibiotics via a membrane bound, multi-protein transport system was first demonstrated for the export of tetracycline in *E. coli*.<sup>48</sup> Efflux pump genes are predominantly found on the bacterial chromosome indicating that antibiotic efflux is an evolutionary capability arising from an enhanced intrinsic ability to extrude diverse structures, rather than an acquired function resulting from horizontal gene transfer of plasmid DNA encoding antibiotic specific transporters.<sup>49</sup> A further indication of the origin of efflux pump genes is revealed by the high number of efflux pump genes present in non-pathogenic bacterial species where there is a lack of clinical antibiotics, and also the unusually broad specificity of multidrug transporter proteins that are encoded across not only bacterial species but also animals kingdoms.<sup>50, 51</sup>

Analyses of the evolutionary origin, amino acid sequence and structure of efflux pump proteins has resulted in efflux pumps being grouped into one of 5 categories (Figure 9): ATP-binding cassette (ABC), major facilitator superfamily (MFS), resistance / nodulation / cell division (RND), small multidrug resistance (SMR) or multidrug and toxic compound extrusion (MATE).<sup>52</sup>

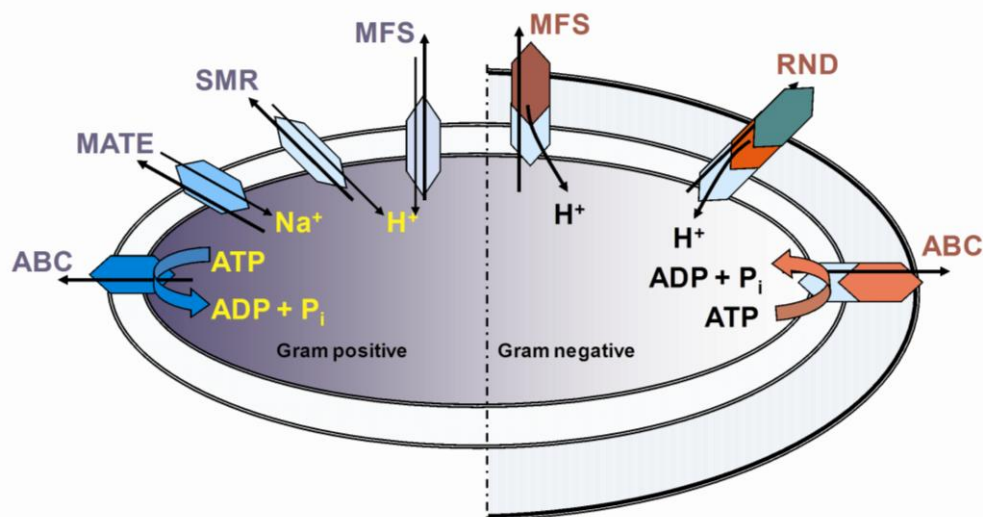
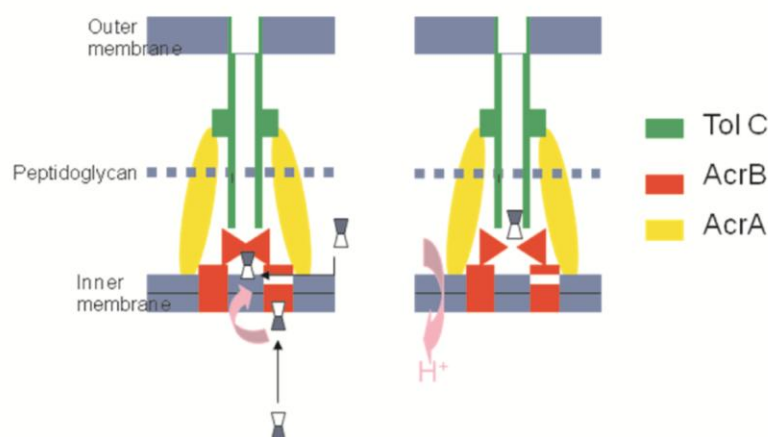


Figure 9 Bacterial efflux pumps and energy sources

Further classification of the multidrug transporters arises from the energy source for drug translocation. The RND, MFS and SMR families are proton driven pumps.<sup>53</sup> The ABC system links ATP hydrolysis to drug translocation and the MATE class is a Na<sup>+</sup> / H<sup>+</sup> antiporter system.<sup>54</sup> A detailed study of each class of efflux pump is outside the scope of this thesis, but will focus on the RND class to which the gonococcal system belongs. The RND designation applies to the transport protein of the efflux pump and proteins of this class have 12 transmembrane spanning (TMS) regions, with two large loops between TMS 1 and 2 and 7 and 8. Examples of this class include AcrB from *E. coli*,<sup>55</sup> MexB and MexD from *P. aeruginosa*<sup>56</sup> and MtrD from *N. gonorrhoeae*.<sup>57</sup> To achieve efflux of the antibiotic across the cell envelope, the transport protein associates with an outer membrane protein and the complex is held together by a membrane fusion protein.<sup>58</sup>

The best studied example of an RND transport system is AcrAB–TolC from *E. coli*, where AcrA is the membrane fusion protein, AcrB is the transporter protein and TolC is the outer membrane protein.<sup>55</sup> It is proposed that AcrB is in constant contact with the membrane fusion protein AcrA, but the outer membrane protein TolC is only recruited when a ligand is bound to the inner membrane protein. The presence of ‘vestibule’ areas



**Figure 10 Schematic representation of active efflux through the AcrAB–TolC system**

in the periplasmic region of enable hydrophilic drugs such as carbenicillin to be collected in the periplasm and exported (Figure 10). The precise mechanism of translocation is still a matter for debate, however, Asp407, Asp408, Lys940, and Arg971 are proposed to form ion pairs and are deprotonated in the unliganded resting state. On binding of a ligand and remote proton binding, the ion pairs become charged causing a conformational change in the protein complex opening the pore to the outer membrane protein thus allowing export of the ligand. The structure and function of the AcrAB–TolC system serves as a model system for the less well studied gonococcal efflux systems.

### 1.2.2 Overview of efflux pumps in *N. gonorrhoeae*

Three efflux pump systems have so far been identified in *N. gonorrhoeae* conferring high levels of antimicrobial resistance to a range of antimicrobial agents. Antibacterial fatty acids are exported through the FarAB efflux pump and macrolides are transported through the MacAB system.<sup>59,60</sup> Both FarAB and MacAB are composed of an inner membrane (transport) protein (FarA and MacA respectively) and a membrane fusion protein (FarB and MacB respectively) and require an outer membrane protein for export of the drug out of the cell. The outer membrane protein used is MtrE, from the MtrCDE efflux pump that recognises numerous toxic compounds of different structures.<sup>61,62</sup> The MtrCDE and FarAB efflux pumps are both regulated by the regulator protein MtrR. The products of the multiple transferable resistance (*mtr*) locus, in particular MtrR, are the main focus of this thesis and are introduced in more detail below.

### 1.2.3 The MtrCDE efflux pump from *N. gonorrhoeae*

MtrCDE is a tripartite protein pump composed of the RND family protein MtrD, an inner membrane protein (IMP) with 43 % identity to AcrB from *E. coli*.<sup>57</sup> MtrC, a membrane fusion protein (MFP) has 45 % identity to AcrA. The outer membrane protein (OMP) MtrE is 22% homologous to TolC.<sup>63,64</sup> MtrC is located in the periplasm and acts as the connection between MtrD and MtrE, as in the related AcrAB–TolC system. A further IMP, MtrF, has been linked to efflux of antimicrobials in *N. gonorrhoeae* and may function in conjunction with MtrCDE in conferring high level resistance.<sup>65</sup>

As yet, there are no crystal structures of the constituent proteins in the MtrCDE efflux pump. Insights into the structure of the gonococcal multidrug transporter have recently been revealed by solution state characterisation of the multidrug complex.<sup>66</sup> The 44 kDa lipoprotein MtrC was shown by mass spectrometry to exist as a stable hexamer, whereas the OMP MtrE formed trimers indicating that MtrC interacts with MtrE in a 6 : 3 ratio. This finding is supported by analysis of Isothermal Titration Calorimetry (ITC) data that indicates MtrC interacts with MtrE, *viz.* two MtrC units interact per MtrE unit. No interaction was seen between MtrD and MtrE, and only a weak interaction was detected by pull down assays between the IMP and OMP, compared to a strong interaction between the MFP and IMP and MFP and OMP.

A wide range of antimicrobial agents are substrates for the gonococcal efflux pump. Large cyclic compounds such as azithromycin (**9**) and spectinomycin (**10**), planar aromatics such as tetracycline (**11**) and detergents (**10**) are all substrates.<sup>66</sup> The human

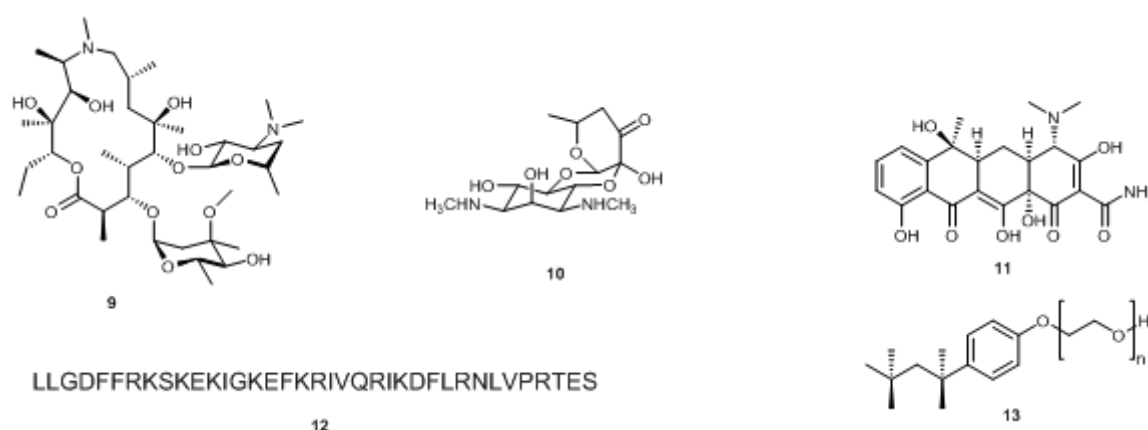


Figure 11 MtrCDE efflux pump substrates; azithromycin (**9**), spectinomycin (**10**), Tetracycline (**11**), human cathelicidin antimicrobial peptide (**12**) Triton X-100 (**13**)

antimicrobial peptide LL-37 (**12**) is also a substrate, which makes the specificity of the MtrCDE pump unusually broad. The ability the MtrCDE efflux pump to recognise peptide substrates is discussed further in Chapter 3.<sup>67</sup> Studying membrane proteins, and multi-protein membrane systems is very demanding due to protein insolubility in aqueous solutions (without detergents). Consequently protein efflux pumps themselves represent challenging drug targets and not easily amenable to (bio-) chemical investigation. Efflux pump genes are tightly regulated by transcriptional regulators, that are also proposed to be multidrug recognition proteins. Transcriptional regulators are soluble proteins and thus present themselves as tractable drug targets. Understanding the molecular basis of efflux pump regulation would enable the development of new classes of antimicrobial agents. To this end, the concept of transcriptional regulators is introduced in the next section, with particular attention devoted to the MtrR protein that controls the expression of the MtrCDE efflux pump.

### **1.3 Transcriptional regulation of efflux pumps**

#### **1.3.1 Introduction**

Transcriptional control of efflux pump genes can be maintained by either a two-component or single component system. In the former system a cell-surface bound kinase undergoes autophosphorylation (at a specific histidine residue) in response to a specific stimulus.<sup>68</sup> The phosphoryl group is then transferred to an aspartate residue of the cognate response regulator that will be activated, for example in *E. coli* the MdtABC RND pump is regulated by BaeSR, a two component system (Figure 12).<sup>69</sup> This system is an example of positive regulation, that is the regulator when bound to DNA recruits other activating proteins ultimately enabling the RNA-polymerase to bind.

In a single component system, the efflux pump genes are under the control of a regulator that responds to stimulus by an intracellular ligand, as exemplified by the TetR system (Figure 13). With regard to the regulation of bacterial export systems, two protein families (AraC and MerR, Figure 14 A and B) function as activators of gene transcription and a further two classes (MarR and TetR, Figure 14 C and D) function as repressors.<sup>49</sup>

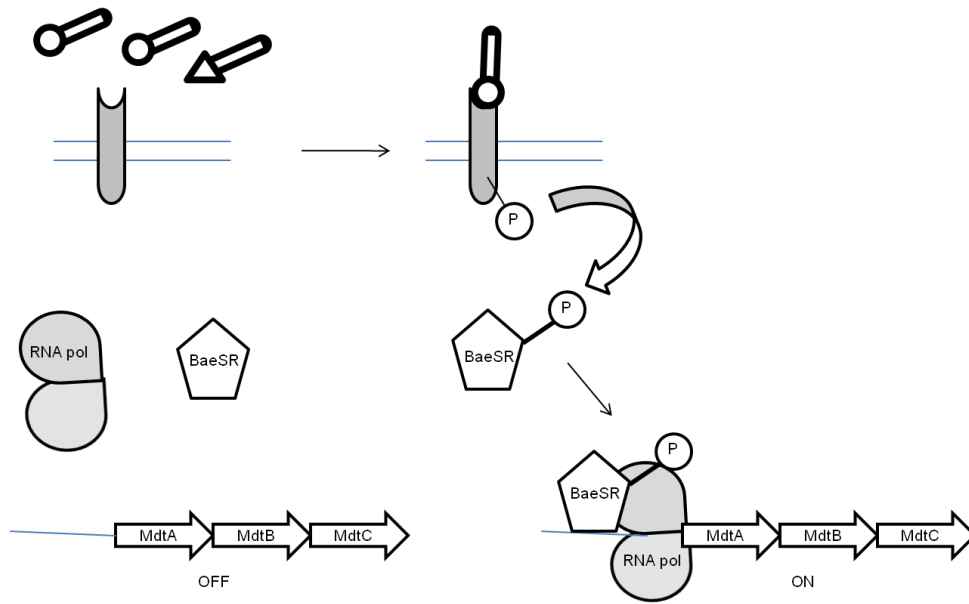


Figure 12 Schematic representation for the regulation of efflux pump genes by a two component system. The efflux pump encoded by *mdtABC* genes are under the control of the BaeSR regulator. The cell surface receptor responds to a specific stimulus and is autophosphorylated. The phosphoryl group is transferred to BaeSR, which is then activates the gene for transcription.

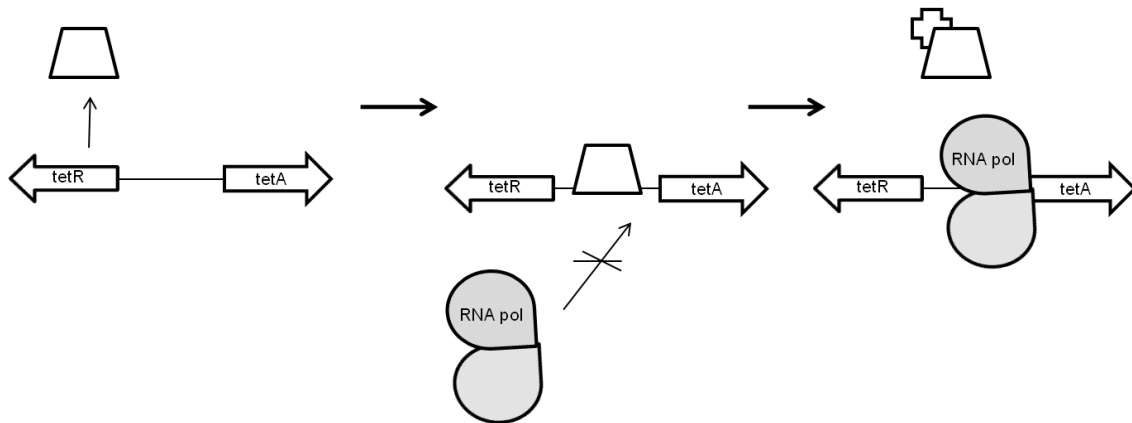


Figure 13 Schematic representation of single component regulation. The TetA transporter is under control of the TetR transcription regulator. *TetR* is divergently transcribed from *tetA* and the regulator protein occupies the operator DNA of the *tetA* gene, blocking transcription. On binding tetracycline (represented as a cross), TetR dissociates from the DNA allowing RNA polymerase to bind and transcribe the gene

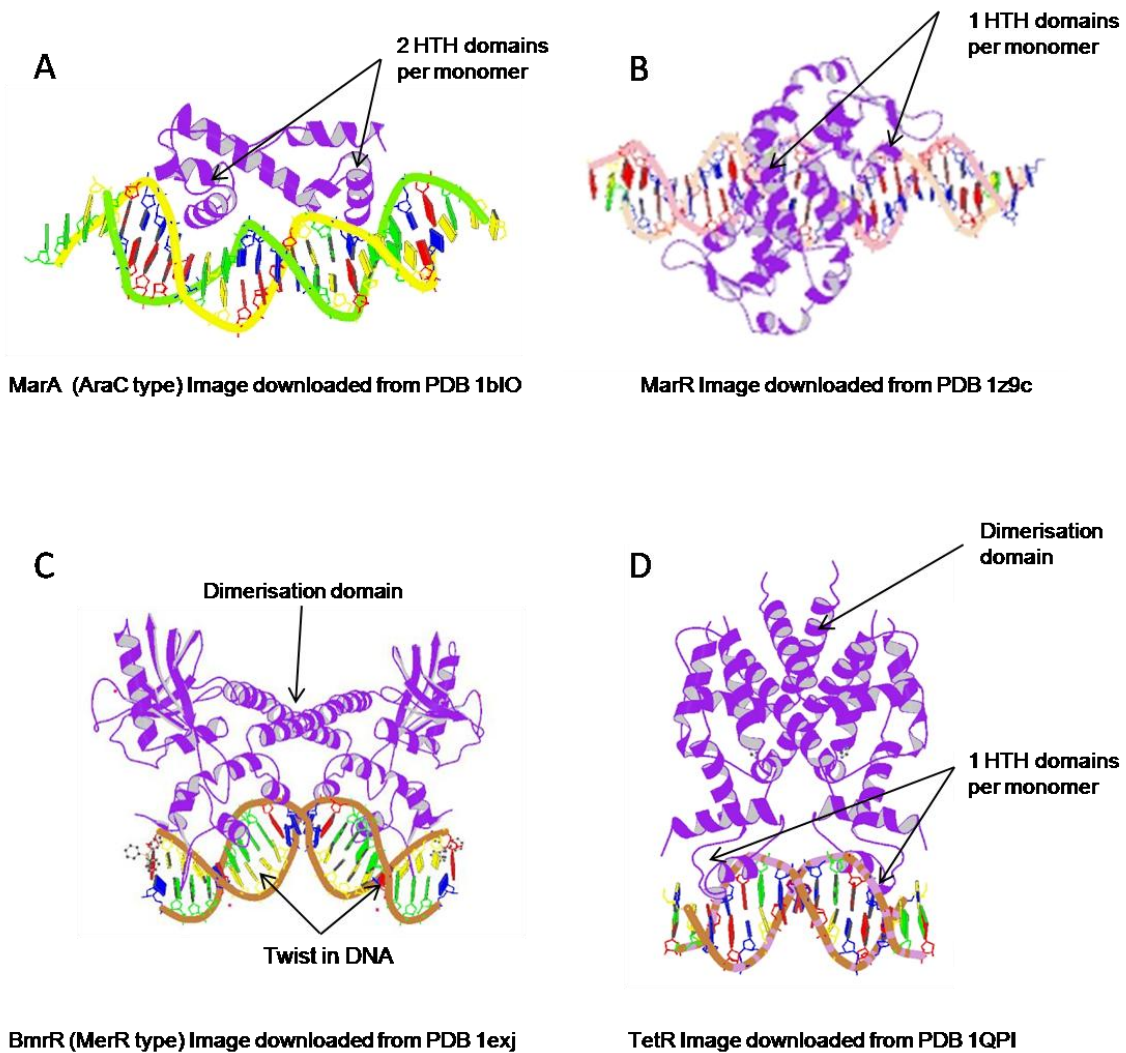


Figure 14 HTH containing bacterial regulator proteins

Regulator proteins often function as part of a complex regulatory pathway that is interdependent on several other activator and regulator proteins.<sup>70</sup> For example, regulation of the the AcrAB–TolC system by AcrR (a TetR family protein) is classed as a single component system but the expression of AcrR is governed by activator proteins MarA / SoxS / Rob (AraC class).<sup>71</sup> These activators are themselves negatively repressed by the transcriptional regulator MarR (an example of the MarR class), generating a complex regulator pathway.<sup>72,73</sup>

Each of the four classes (AraC, MerR, MarR and TetR) utilise a Helix-Turn-Helix (HTH) domain located at either the *N*- or *C*-terminus of the regulator protein to bind the major groove of DNA (Figure 14). The (HTH) motif is seen in 95% of transcriptional regulatory proteins in prokaryotes characterised to date.<sup>74</sup> The four groups are named after the first protein characterised and subsequent proteins are placed in the relevant group by

homology. AraC type proteins are classed by the homology to a 99 amino acid segment of AraC protein.<sup>75</sup> This is a large class of proteins with more than 100 members and two subgroups have been identified, namely proteins that function as dimers (regulators of sugar catabolism) or monomers (bacterial stress / antibiotic response regulators). Monomeric regulators possess two HTH domains within one protein unit to enable the regulator to bind DNA next to the promoter region, recruiting operator DNA and activator induces a 35° bend in the DNA (Figure 14A). Examples of the latter class include MarA from *E. coli* and MtrA from *N. gonorrhoeae*. The function of MtrA will be discussed further in conjunction with MtrR, a TetR type transcriptional regulator in *N. gonorrhoeae* and the subject of this thesis.

As mentioned above, the AraC activators are under the control of the negative regulator MarR. MarR family proteins contain one 'winged' HTH domain and bind DNA as dimers (Figure 14B).<sup>76</sup> It is postulated that binding of a ligand to the regulator causes a conformational change, enlarging the distance between the two HTH motifs so that the dimer is no longer able to bind DNA, thus freeing the DNA for transcription.<sup>77</sup>

MerR proteins are found in Gram negative and Gram positive bacteria and act as metal sensing proteins.<sup>78</sup> Binding of this regulator to the operator DNA induces a bend in the DNA preventing transcription of the gene, as can be seen in (Figure 14C). When a metal binds the MerR : DNA complex, a change in the conformation of MerR causes a flattening of the DNA enabling transcription to take place.<sup>79</sup>

The final family of proteins discussed here is TetR, which also functions as a dimer. TetR transcriptional regulators are found in numerous species of bacteria including *E. coli*, *M. tuberculosis* and *P. aeruginosa*. The key protein of this thesis, MtrR, is an example of a TetR protein and this class of protein is discussed in greater detail below.



## 1.3.2 The TetR family of transcriptional regulators

### 1.3.2.1 Structural studies on TetR family proteins

The TetR family derives its name from the eponymous protein that has been most fully characterised genetically and biochemically.<sup>49</sup> All TetR proteins possess a high degree of sequence homology in the N-terminal HTH motif but a low homology, typically less than 20% in the ligand binding domain. The numbering of the helices starts at the N-terminus and to differentiate between protein units in the dimer, designations are followed by an apostrophe for the second unit Figure 15.

There is a high degree of similarity in the type of amino acid present. Helix 2 and 3 contain predominantly hydrophobic residues with the latter helix exhibiting a preference for F, Y, L or W. The only conserved charged residues in the HTH motif of TetR proteins are located at position 43 (predominantly R or K). As previously mentioned, there is little sequence similarity in the C-terminal ligand binding domain but a number of crystal structures have elucidated features common to all TetR proteins. One such feature is a highly flexible ligand binding domain, which is important for the recognition of a wide range of substrates.

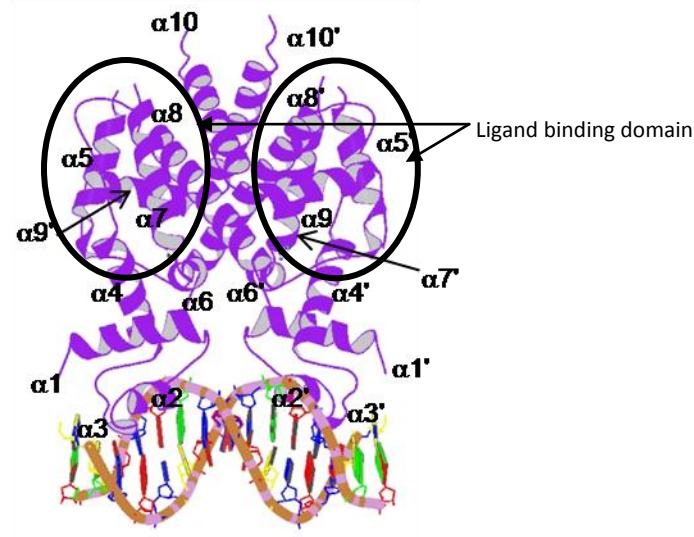


Figure 15 Dimeric structure of TetR protein in complex with its palindromic operator sequence<sup>80</sup> (PDB Code 1QPI downloaded and annotated in Powerpoint)

The dimerisation domain predominantly involves helices 8, 9 and 10. It has been demonstrated that helices 4, 5, 6 and 7 make key contacts with ligands, and in response to binding a substrate the aforementioned helices alter their conformation. This alteration causes a reordering of hydrogen bonding and salt bridges that is transmitted throughout the protein, ultimately causing the distance between helix a3 and a3' to increase above 39Å. When the distance between the two HTH motifs is greater than 39 Å, the protein can no longer bind in the major groove of DNA and hence the DNA protein complex dissociates.

Crystallographic studies revealed that TetR binds DNA as a dimer and the HTH makes contact with the DNA perpendicular to the longitudinal DNA axis, as summarised in Figure 16.<sup>80</sup> Conserved residues in 42 aligned TetR proteins suggested key residues that are involved in direct contact with DNA.<sup>81</sup> These are position 22 on helix 2, position 33-35 and 37-39 on helix 3 and 43 on helix 4 (positions are mirrored in the second subunit).

Despite the similarities in the contact points between TetR type proteins and DNA, there are large differences in the exact mode of DNA recognition. For example, QacR from *S. aureus*, introduces a 3° bend in DNA, whereas TetR induces a 17° bend. Also, 2 dimers of QacR binds one promoter DNA sequence, a ratio observed for SmeT from *Stenotrophomonas maltophilia*, AcrR from *E. coli* and TtgR from *Pseudomonas putida*.



Figure 16 Schematic representation of the TetR dimer bound to the operator DNA. Monomer A binds the -4 to -7 region on the main strand of DNA, and makes contact with the +4 to +2 positions on the complimentary strand. The symmetric dimer binds the main strand from +2 to +7 and the complimentary from -4 to -7.<sup>88</sup>

### 1.3.2.2. Functional studies of TetR proteins: Electrophoretic mobility shift assays

Crystallographic studies only give a snap shot of the molecular mechanism involved in gene regulation and so other techniques have been employed to show that ligand binding induces protein dissociation from promoter DNA. For TtgR,<sup>82</sup> ActR,<sup>83</sup> TetR and SmeT,<sup>84</sup> polyacrylamide gel electrophoretic mobility shift assays (EMSA) have been undertaken. The principle of the experiment is that oligonucleotides complexed to protein migrate slower than uncomplexed oligonucleotide in a non-denaturing polyacrylamide gel. In the experiment, the oligonucleotides are labelled with either <sup>32</sup>P (to enable detection by scintillation) or biotin (colourmetric detection via a streptavidin-horse radish peroxidase conjugate) and the DNA protein complex is run in the presence and absence of ligand.

EMSA has been used by several groups to determine the length of operator DNA recognised by TetR proteins.<sup>85</sup> The effect of ligands on the protein : DNA complex for TetR type proteins has also been studied using this method and interesting results were obtained in a ligand screen for the biofilm repressor IacR, from *Staphylococcus epidermidis*. Previous reports in the literature had indicated that aminoglycosides are able to induce biofilm formation, implying they release IacR from its operator DNA. EMSA studies with aminoglycosides showed that only gentamycin was able to completely release the regulator from its DNA, whereas spectomycin lead to approximately 50% of the DNA being released and kanamycin failed to exert any effect. This result shows that despite TetR type proteins possessing large drug binding

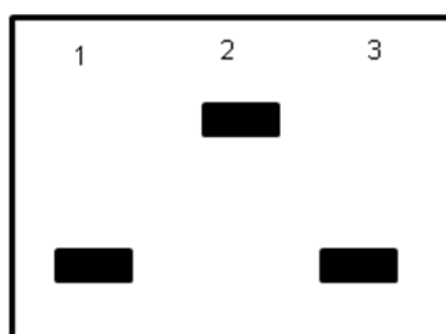


Figure 17 Principle of EMSA; lane 1 DNA only, lane 2 protein and DNA, lane 3 ligand inducer + protein and DNA. Only the DNA is visualised in the experiment so if the movement of the DNA is retarded in the gel, it is assumed that the DNA is in complex with protein.

pockets, highly specific interactions are necessary to induce the conformational change necessary to release the protein from DNA. A similar analysis of effector molecules on the TtgR : DNA complex showed that a wide range of flavones effect derepression, but the isoquinoline alkaloid berberine did not, highlighting the structural specificity of ligand binding in TtgR. EMSA studies with MtrR will be discussed in section 3.5.6.

### 1.3.2.3. *Functional studies of TetR proteins: Isothermal Titration Calorimetry*

EMSA only provides an 'on' or 'off' picture for protein : DNA binding and the effects of ligands on protein : DNA complexes. In order to gain biophysical information such as binding affinities, enthalpy and entropy changes other techniques have been used. One such technique is ITC that has the advantage of providing full thermodynamic parameters ( $\Delta H$ ,  $\Delta S$ ,  $K_d$ ,  $N$ ) from one binding experiment in solution, without the need of labels. Disadvantages to using microcalorimetry to investigate protein ligand binding are: i) it is a labour intensive technique and ii) relatively large volumes of protein are required. Despite these drawbacks ITC has been used to investigate protein : DNA and protein : ligand interactions in TetR proteins. A brief overview of these studies are provided and results using ITC to characterise MtrR : DNA and MtrR : ligand interactions are detailed in subsequent chapters of this thesis.

The length of oligonucleotide recognised by TetR type proteins and the ratio of protein : DNA binding has been investigated by ITC. Calorimetric analysis revealed TetR binds its operator as a dimer and interacts with a 16 bp palindrome with a short central spacer, whereas both QacR and IacR binds 28 bp operator regions and TtgR binds a 40 bp nucleotide sequence. In each case binding to DNA is endothermic and in the micro molar range, and TtgR, IacR and QacR bind as a pair of dimers.<sup>86</sup>

Several research groups have applied ITC to characterise ligand binding and specificity. TtgR is the regulator of the TtgABC efflux pump from *Pseudomonas putida* DOT-T1E soil organism that recognises a range of plant secondary metabolites (Figure 18). Increasing the number of hydroxy groups increases the affinity by more than a factor of 2 (**15** compared to **16**). Furthermore the double bond in the B ring appears to increase ligand binding as this is absent in **14**, which binds with much lower affinity than **15**. These experiments highlight how ITC analysis gives insights into the structural characteristics of a ligand that are required for high affinity binding.<sup>87</sup>

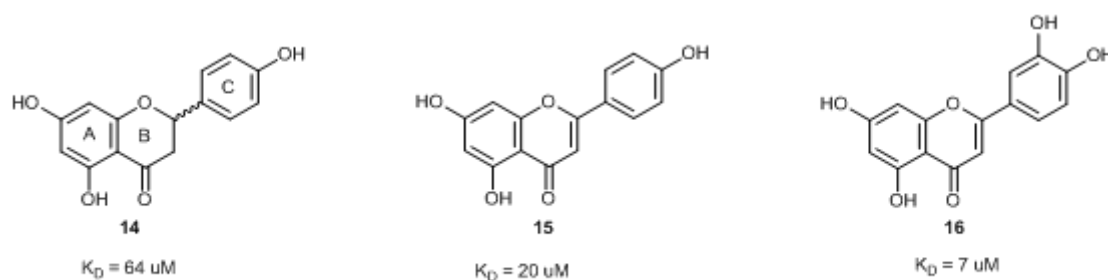


Figure 18 Ligands for TtgR identified by ITC; Naringenin (14), Apigenin (15) and luteolin (16)

Ligand binding studies with BmrR, the regulator of a lipophilic transporter system encoded by the *bmr* locus in *Bacillus subtilis*, revealed that not only does the regulator recognise diverse ligands but also that charge in the ligand binding domain is important.<sup>88</sup> Typically LBD's in TetR type proteins are characterised by hydrophobic interior surfaces with buried charged residues to stabilise ligand binding. ITC analysis of the binding of berberine and rhodamine revealed that a glutamic acid residue in the ligand binding domain is beneficial to rhodamine but not berberine binding. Berberine is a natural product and more likely to be a natural substrate than rhodamine but the ability for the protein to recognise structures represented by rhodamine is indicative of the evolutionary capability for multidrug binding proteins to recognise diverse substrates. Similar investigations describe structurally related divalent cations as substrates for the QacR protein from *Staphylococcus aureus*.<sup>89</sup>

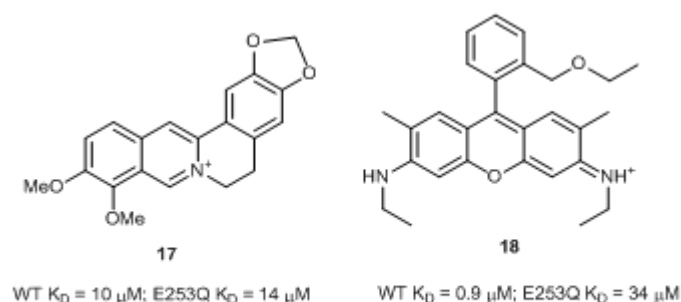


Figure 19 Substrates for BmrR; berberine (17) and rhodamine (18)

The results with TetR proteins support the hypothesis that efflux pump repressors recognise substrates for the cognate efflux pump. The structural and biochemical insights are extremely useful when studying the function of homologous TetR proteins that do not yet have a solved three dimensional structure, for example MtrR from *N. gonorrhoeae*. The available literature on MtrR shall now be discussed.

## 1.4 MtrR from *N. gonorrhoeae*

### 1.4.1 Genetic origin and structure of the mature protein

The multiple transferable resistance regulator (MtrR) is the product of the *mtrR* gene, located 250 bp upstream from the genes for the *mtrCDE* efflux pump and divergently transcribed from the efflux pump operon.<sup>90</sup> The mature regulator protein binds a 22 – 27 base pair region upstream of the *mtrC* gene as a dimer of dimers, consistent with other TetR proteins, as discussed above, protecting the efflux gene from being transcribed.<sup>91</sup>

MtrR contains 210 amino acids that shows 30 % identity to TetR, 34% to AcrR and TtgR and 27% to CmeR. Despite the low sequence homology, there is considerable similarity in the ternary structures of TetR proteins, as highlighted in the overlay diagram of TetR

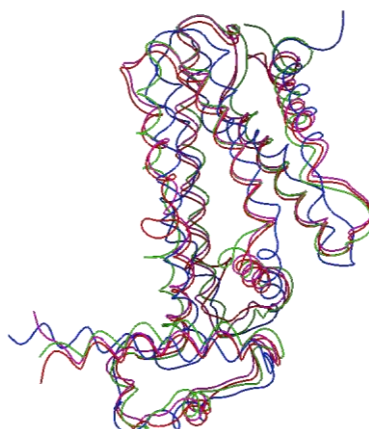


Figure 20 Overlay of  $\alpha$ -traces of MtrR homology model (red) with AcrR (green), CmeR (blue) and TtgR (pink). Image produced using MOE.

proteins (only monomers are shown, Figure 20). Homology modelling using AcrR as a template, produced a model for MtrR that provides visual support for the similarity between MtrR and TetR proteins of known 3D structure.

#### 1.4.2 Effect of oligonucleotide mutations on MtrR function

The 'normal' resting state for the MtrR protein is on the promoter region (meaning it is bound to DNA) for the *mtrCDE* operon, however, in clinical isolates of *N. gonorrhoeae* that exhibit elevated levels of resistance to antimicrobial agents several mutations in both the coding region and the promoter region for MtrR are observed. Four mutations in the MtrR gene lead to four amino acid substitutions in the mature protein: E202G, H105Y, A39T, G35D.<sup>92</sup> Substitution of glutamic acid at position 202 for glycine is postulated to disrupt dimerisation of MtrR monomers, whilst the presence of tyrosine instead of histidine at the 105<sup>th</sup> position was isolated from penicillin resistant strains of *N. gonorrhoeae* but no molecular effect of this substitution is reported in the literature.<sup>93</sup> The effect of the H105Y mutation will be discussed in more detail in Chapter 2. Mutations in the N-terminal HTH region (A39T, G35D) disrupt DNA binding by replacing hydrophobic amino acids with polar amino acids. Amino acid mutations in

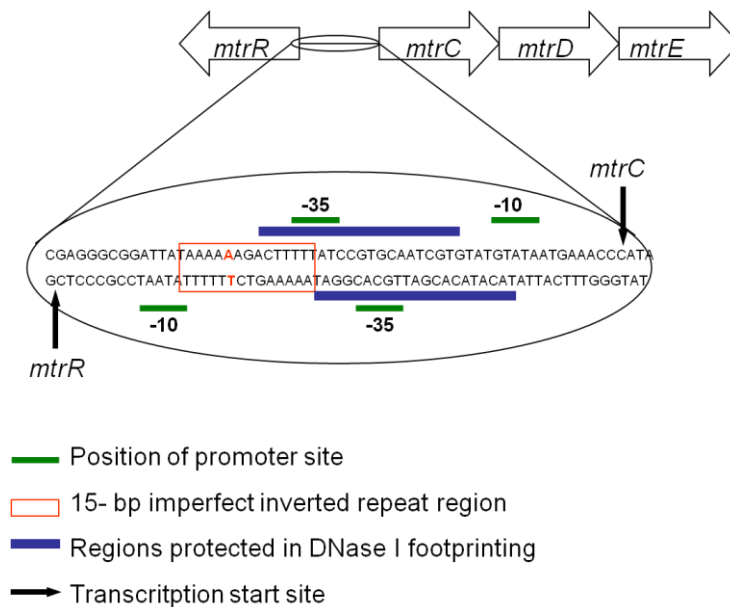


Figure 21 Location of the MtrR binding site upstream of the *mtrCDE* operon and the location of alterations in the promoter sequence that lead to high level antimicrobial resistance. The diagram is not to scale.

the primary sequence of MtrR cause modest (< 10 fold) increases in resistance to antimicrobial agents and detergents whereas mutations in the promoter sites for *mtrR* and *mtrC* and in the MtrR DNA binding region provides > 1000 resistance towards the detergent TritonX-100 (13).<sup>94</sup> The extremely high level of resistance seen is due to unregulated expression of the MtrCDE efflux pump because the mutation in the promoter region permanently abrogates protein binding. Mutations observed in clinical isolates are deletion of thymidine base or a single mutation (A→G) in the MtrR promoter region or an A → G mutation between the *mtrR* and *mtrC* start codons, which greatly increase antimicrobial resistance.

### 1.4.3 MtrR regulatory network

Although the best characterised role of MtrR in the gonococcus is transcription control of *mtrCDE*, there are an increasing number of reports in the literature that reveal a much more global regulatory capacity for MtrR.<sup>95</sup> Whole genome micro-array RNA analysis from *N. gonorrhoeae* showed MtrR to directly repress 47 and activate 22 genes.<sup>90</sup> Five of the gene cassettes implicated in the transcription analysis have been characterised in detail and the pathways listed in the literature are summarised in Figure 22.

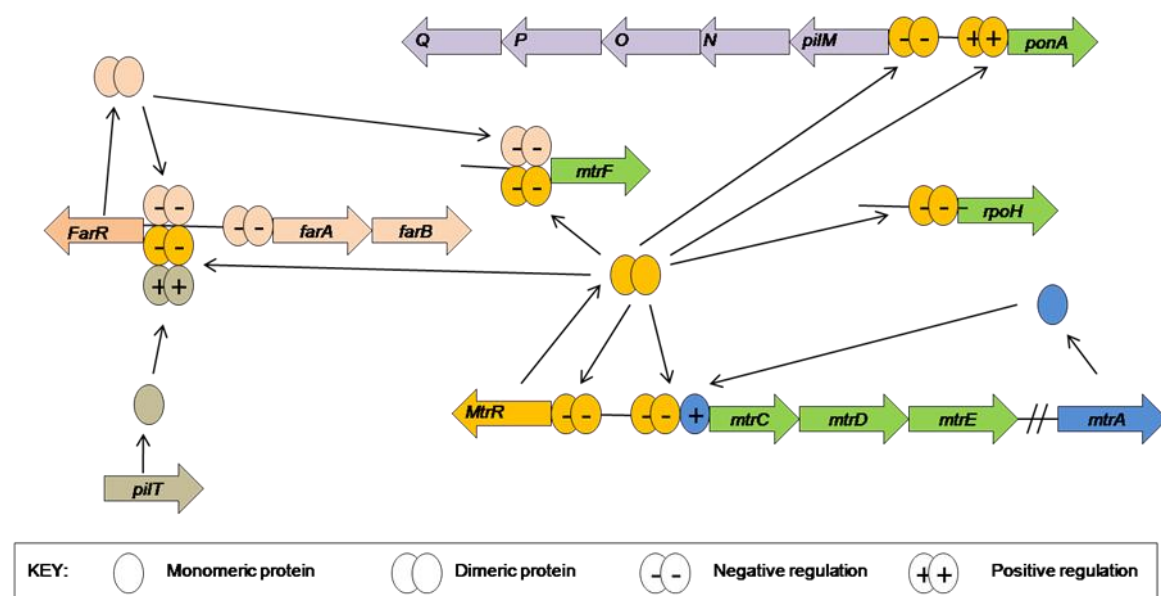


Figure 22 Schematic representation of genes that have been shown by whole genome microarray analysis to be directly regulated by MtrR.



MtrR regulates its own expression, as well as negatively regulating expression of *mtrCDE*, *rpoH* (a stress response factor),<sup>90</sup> *pilM* (part of the pilMNOPQ secretion system),<sup>96</sup> the transport protein *MtrF*,<sup>97</sup> and *FarR*, the regulator of the FarAB efflux pump.<sup>98</sup> MtrR has also been shown to positively regulate the expression of *ponA* that encodes for penicillin binding protein-1. Each gene regulated by MtrR is implicated in antimicrobial resistance in *N. gonorrhoeae* and the majority of genes are negatively repressed, that is the regulator must leave the operator DNA in order for transcription to take place implying MtrR operates by a conserved mechanism.

It is clear from genome analysis in *N. gonorrhoeae* that MtrR has multiple functions in the gonococcus. MtrR belongs to the TetR family of transcriptional regulators and is known to repress expression of the multidrug efflux pump MtrCDE. The ability for MtrR to interact with different genes leads to the hypothesis that MtrR acts as a protein sensor for a wide range of exogenous chemicals that are toxic to the bacterium. It is hypothesised that in response to binding the antimicrobial agent, MtrR dissociates from the operator / promoter upstream of the resistance gene, enabling gene transcription to take place.

## 1.5 Project hypothesis and aims

The molecular mechanisms underlying the function of MtrR have not yet been addressed in the literature and this thesis aims to answer the following key questions:

1. Does MtrR bind substrates (small molecule antibiotics and antimicrobial peptides) of the MtrCDE efflux pump?
2. Does binding of a ligand cause dissociation of MtrR from its operator DNA?

The ability for small molecule antibiotics tetracycline, spectinomycin and penicillin G to bind MtrR is reported in Chapter 2, with particular emphasis on how penicillin G interacts with MtrR.

Chapter 3 focuses on the interactions between MtrR and the human antimicrobial peptide LL-37. The structure of LL-37 is divided into small peptides to probe how the length and structure of the peptide effects binding to MtrR. The ligand binding domain of MtrR is characterised by use of a photoactivated peptide probe. The effect of ligand binding on the MtrR : DNA is investigated using EMSA.

Conclusions from the studies are drawn in Chapter 4. Suggestions for the development of the work are also made, together with a summary of other studies conducted during the course of this research project.

Chapter 5 provides experimental detail for the thesis.

## 2 MtrR interaction with peptide antibiotics

### 2.1.1 Introduction

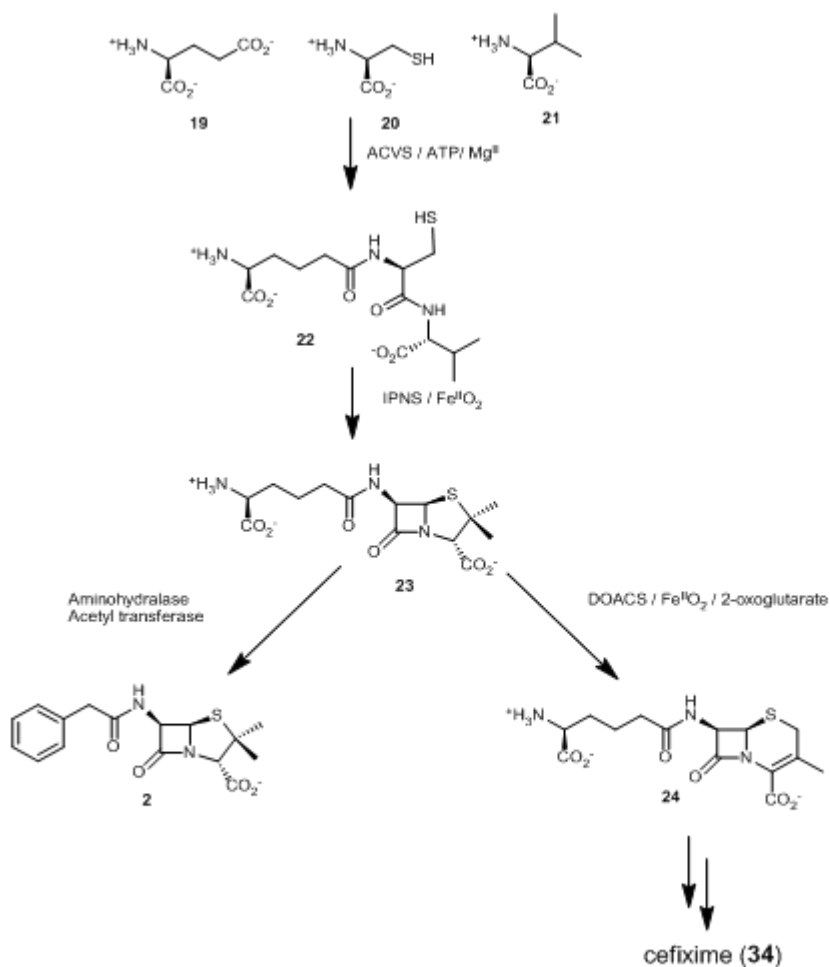
The *mtr* locus encodes the multidrug efflux pump MtrCDE and its cognate repressor MtrR, that are necessary for high level antibiotic resistance in *N. gonorrhoeae*. The transcriptional regulator MtrR has also been implicated in the regulation of specific resistance determinants necessary for high level penicillin resistance as highlighted in Figure 22 in Chapter 1.<sup>99</sup> Herein, we propose that MtrR binds diverse antibiotics, causing activation of the resistance genes controlled by MtrR. During the course of investigations to establish evidence for this hypothesis, an unexpected enzymatic activity of MtrR was discovered, and the characterisation of this new activity is reported in this chapter.

An overview of recent literature relating to  $\beta$ -lactam antibiotics and  $\beta$ -lactamases is also provided, in particular focussing on the characterisation of novel  $\beta$ -lactamases. The results of a biophysical study on how MtrR binds  $\beta$ -lactam antibiotics using isothermal titration calorimetry (ITC) and mass spectrometry are reported and discussed.

### 2.1.2 $\beta$ -Lactam antibiotics

The serendipitous discovery of penicillin by Fleming and the subsequent large scale preparation by Florey and Chain heralded the beginning of the modern antibiotic age.<sup>100</sup> The term antibiotic was proposed by Waksman to describe “a substance derived from microorganisms which has the capacity of inhibiting growth and even destroying other microorganisms.”<sup>101</sup> In this thesis, the Waksman definition is adopted with the proviso that “derived” includes synthetic compounds as well as antibiotics of sole microbiological origin.

Benzyl penicillin (**2**) represented the first antibiotic of the  $\beta$ -lactam class and more than 40 structurally diverse  $\beta$ -lactam antibiotics are marketed today, the core ring structure of which is the product of non-ribosomal peptide synthesis pathways in fungi and soil bacteria (Scheme 1).<sup>102</sup> Key chemical characteristics of these compounds are non-proteinogenic amino acids (e.g. L-aminoadiapic acid **19**), D-amino acids (D-valine), methylated nitrogen (NMe) and small heterocyclic rings.

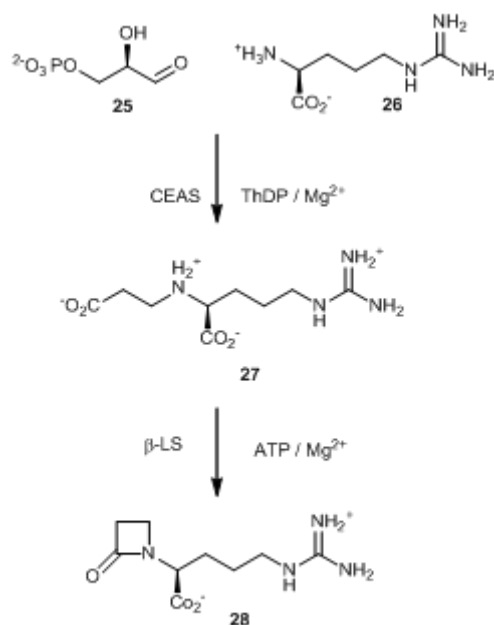


**Scheme 1 Biosynthetic origin of penicillins (6) and cephalosporins (34)**

Assembly of the isopenicillin N core structure of penicillin and cephalosporin antibiotics highlights many of the unique features of the non-ribosomal peptide synthesis (NRPS) pathway. ACV synthase catalyses the formation of a tripeptide **22** (L-β-aminoadipyl-L-cysteinyl-D-valine) from three L amino acid, valine, cysteine and aminoadipic acid. The 4,5-fused ring system is then formed in one step by isopenicillin-N-synthase (IPNS), a non-haem, Fe(II), dioxygen dependent enzyme. The core ring system is then subject to further enzymatic modification to give clinically useful secondary metabolites. The ring system can undergo oxidative ring expansion by an Fe(II) dependent enzyme deacetylcephalosporin synthase (DAOCS) to give the cephalosporin class of antibiotic, or the peptidyl side chain is modified by aminohydrolase / acetyl transferase to give penicillin derivatives.<sup>103</sup>

Early investigations into the biosynthesis of benzyl penicillin (**2**) led to the discovery of 6-aminopenicillanic acid, the core structure that was then elaborated through chemical synthesis to give semi-synthetic penicillins, e.g. Penicillin V (**29**) Carbencillin (**30**) and Nafcillin (**33**) (Table 2). These semi-synthetic drugs had better bioavailability and were more resistant to  $\beta$ -lactamases.<sup>104</sup>

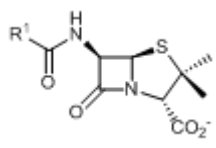
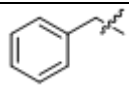
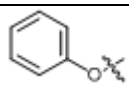
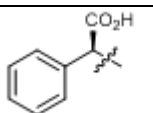
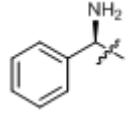
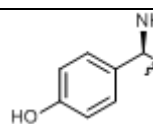
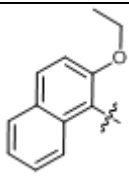
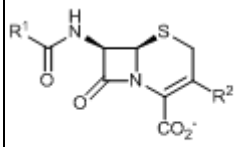
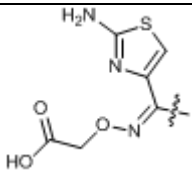

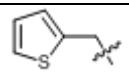
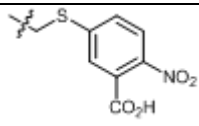
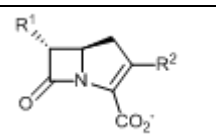
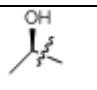
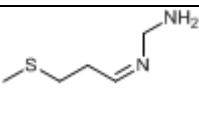
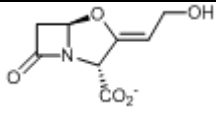
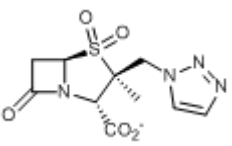
Further screening of microorganisms was undertaken to find novel entities to act as anti-infectives and these efforts led to the discovery of clavulanic acid (**36**) from *Streptomyces clavuligerus*.<sup>105,106</sup> Clavulanic acid (**37**) had very low antibacterial effects but was shown to be a potent inhibitor of  $\beta$ -lactamases. The first  $\beta$ -lactam containing secondary metabolite identified from a natural source that contained an oxazolidine ring rather than a thiazolidine or dihydrothiazine ring was **37**.<sup>107</sup> Other interesting structural features of this inhibitor are the lack of acylamino substitution at C-6 and a  $\beta$ -hydroxyethylidene function at C-2. The  $\beta$ -lactam ring of clavulanic acid is formed by  $\beta$ -lactamase synthase enzyme, that unlike IPNS is an ATP /  $Mg^{2+}$  dependent enzyme (Scheme 2).<sup>108</sup> An analogous enzyme catalyses the formation of the  $\beta$ -lactam ring in carbapenems. As with the formation of the 5 and 6-membered heterocycles of penicillin and cephalosporins, the oxazolidine ring is constructed by an oxidative cyclisation  $Fe^{2+}$ -dependent dioxygenase called clavulanic acid synthase (CAS).<sup>109,110</sup>



Scheme 2 Biosynthetic origin of the  $\beta$ -lactam ring in clavulanic acid

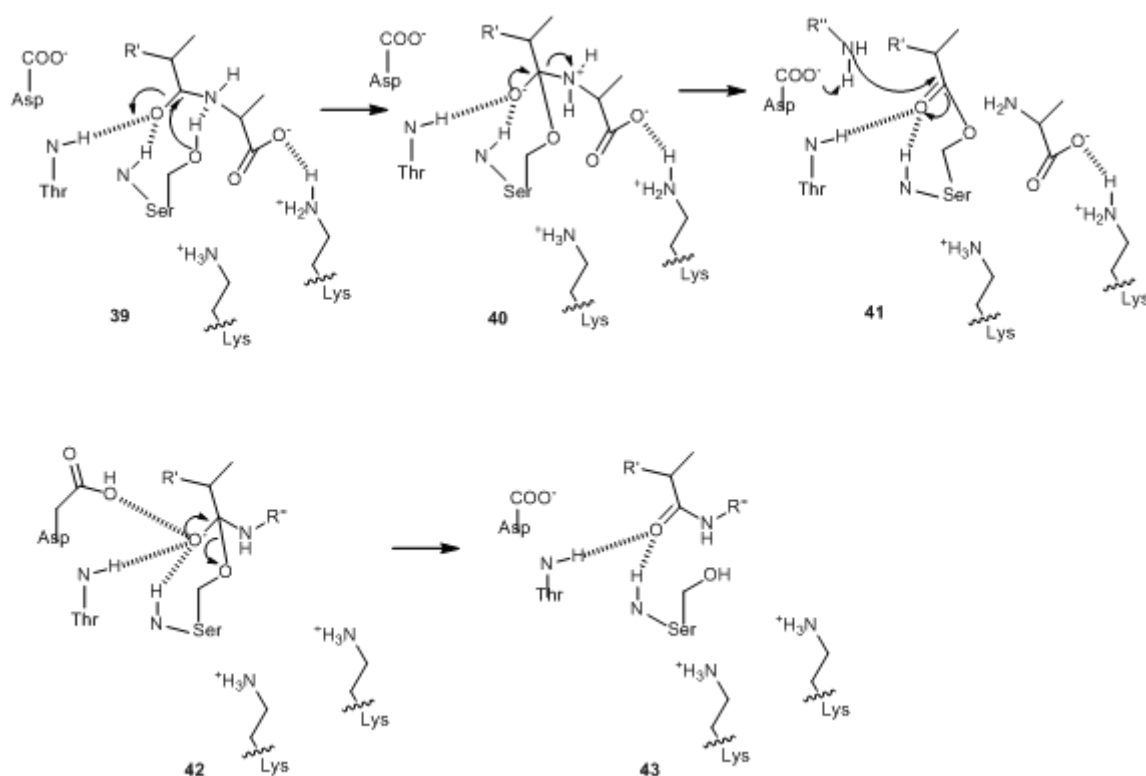
Table 2 summarises the  $\beta$ -lactams referred to in this thesis. Compounds **29** to **33** are semi-synthetic derivatives of benzyl penicillin. The introduction of amino, alcohol or carboxy functionality improves bioavailability and stability in acidic media. The bulky naphthalene moiety renders the antibiotic too large for the  $\beta$ -lactamase active site and so is  $\beta$ -lactamase resistant. Developments to the cephalosporin class have also been made in attempts to overcome resistance mechanisms that are discussed in the following section. Antibiotics **37** and **38** are compounds that exhibit low antibacterial activities but are potent inhibitors of  $\beta$ -lactamases. The mode of action of these antibiotics and the resistance developed by bacteria are discussed in the following section.

Table 2  $\beta$ -lactam antibiotics used in this study

Class	Core structure	Subgroup	R <sup>1</sup>	R <sup>2</sup>	Name
Penicillin		Extended spectrum		---	Penicillin G (2)
				---	Penicillin V (29)
				---	Carbenicillin (30)
		$\beta$ -lactamase sensitive		---	Ampicillin (31)
				---	Amoxicillin (32)
$\beta$ -lactamase resistant		---	Nafcillin (33)		
Cephalosporin		3 <sup>rd</sup> generation			Cefixime (34)
		Chromogenic substrate			CENTA (35)
Carbapenem		$\beta$ -lactamase resistant			Imipenem (36)
Clavam		$\beta$ -lactamase inhibitor	---	---	Clavulanic acid (37)
Penicillin sulfone			---	---	Tazobactam (38)

### 2.1.3 Cellular target and bacterial resistance to $\beta$ -lactams

$\beta$ -Lactam antibiotics target the enzymes that catalyse the final peptidyl-cross linking step in the synthesis of peptidoglycan (Scheme 3).<sup>4</sup> The targeted enzymes are transpeptidases (also termed DD-peptidases or penicillin binding proteins) and contain a nucleophilic active site serine. The active site serine attacks the penultimate D-Ala amino acid of the stem peptide (39), which releases the last amino acid from the donor peptide and forms a covalent acyl-enzyme complex (40). In transpeptidases, the carbonyl of the D-Ala amino acid is linked via an ester linkage with the active site serine, then undergoes attack from a primary amine of the third amino acid of a second stem peptide (41). The resultant peptide bond is formed between the two stem peptides, forming a link between the glycan strands (42).<sup>111</sup>



Scheme 3 Mechanism of transpeptidase



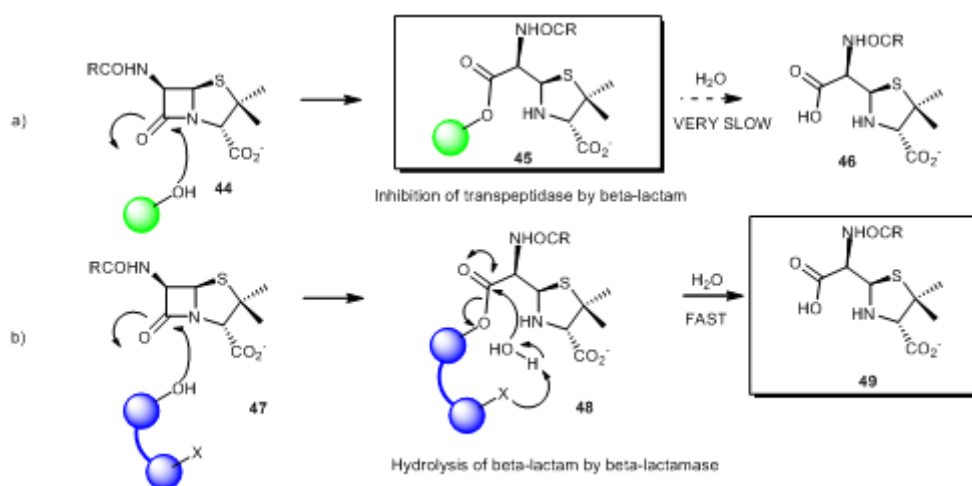


Figure 23 Schematic representation of a) inactivation of transpeptidase (green) by penicillin; b) hydrolysis of penicillin by  $\beta$ -lactamase (blue).

$\beta$ -lactams mimic the acyl-D-Ala–D-Ala peptide in acting as covalent inhibitors of transpeptidases thus inhibiting cell wall synthesis.<sup>112</sup> The  $\beta$ -lactam localises in the binding pocket by attractive electrostatic interaction involving hydrogen bonding from the backbone amide protons of the protein to the  $\beta$ -lactam carbonyl, consequently activating the carbonyl to nucleophilic attack and this protein-substrate complex stabilizes the incipient tetrahedral species so as to enable general base catalysis for serine addition to the  $\beta$ -lactam (**44**, Figure 23). The tetrahedral intermediate formed by the ring opening of  $\beta$ -lactam (**45**) closely resembles that of the natural substrate and penicillin remains in the active site. The rate of deacylation of the intermediate is low because PBPs lack amino acids near the active site that can act as a general base to activate the nucleophilic water molecule.<sup>113</sup>

The mechanism of  $\beta$ -lactam hydrolysis by serine  $\beta$ -lactamases is closely related to the mechanisms of transpeptidase inhibition. The acyl-intermediate **48** can be hydrolysed by an activated water molecule. The identity of the activating amino acid (identified by X in Figure 23) is different in each class of  $\beta$ -lactamases and is still a matter of debate in the literature, as discussed below. The rate of hydrolysis is fast compared to PBP's and the ring-opened  $\beta$ -lactam product **49** is ineffective as a PBP inhibitor thus no longer poses a threat to bacterial viability.  $\beta$ -lactamases are proposed to have developed in bacteria as a response to environmental challenges, originally in nature but now in also in response to man-made  $\beta$ -lactam antibiotics used in human and veterinary medicine. The common

ancestral root of these two families of enzyme is suggested on the basis of the substrates catalysed, the tertiary structure of the protein and the composition of the active site residues.<sup>114</sup> The different classes of  $\beta$ -lactamases will now be discussed.

#### **2.1.4 Classification of $\beta$ -lactamases**

There are currently more than 470  $\beta$ -lactamases known and they can be broadly divided into three categories; metal ion dependent enzymes, serine hydrolases and those of unknown catalytic site.<sup>6</sup> The final group only contains a few members but is particularly relevant to this thesis and will be discussed in more detail in section 2.1.5. Both PBP and  $\beta$ -lactamases are present in the periplasmic space of Gram-negative bacteria. In Gram-positive organisms (which lack the outer membrane) the PBP are located on the outer surface of the cytoplasmic membrane and the  $\beta$ -lactamases are either excreted or bound to the cytoplasmic membrane.<sup>114</sup>

The metal and serine dependent enzymes are further classified in terms of the sequence homology, substrates hydrolysed, the inhibitors of the enzyme and the mechanism of action.<sup>115</sup> The prevailing molecular classification system developed by Bush contains four families, A, B, C and D.<sup>116</sup> Class A, C and D contain active site serine residues in the hydrolysis mechanism, while class B contain zinc dependent enzymes.<sup>117</sup> Class B enzymes are not discussed further in this thesis as they are not relevant to the discussion of MtrR.

Serine  $\beta$ -lactamases contain two groupings of amino acids, the active site and the recognition domain. The former contains a minimum of five amino acids: the serine, the general base for the serine, the oxyanion hole (two amino acids), and the cationic recognition site for the carboxylate. The latter domain contains amino acids that aid binding of the  $\beta$ -lactam antibiotic by favourable hydrophobic and hydrophilic interactions.

Class A enzymes hydrolyse penicillin but not cephalosporins, and are inhibited by clavulanic acid (37). The key catalytic motif is Ser 70-Lys 73-Lys 234-Ser 130-Glu 166 where Ser 70 is the nucleophilic residue. NMR studies have revealed that Glu 166 is widely accepted as a general base in the deacylation step and Lys 73 provides stabilisation of the intermediate.<sup>118</sup>

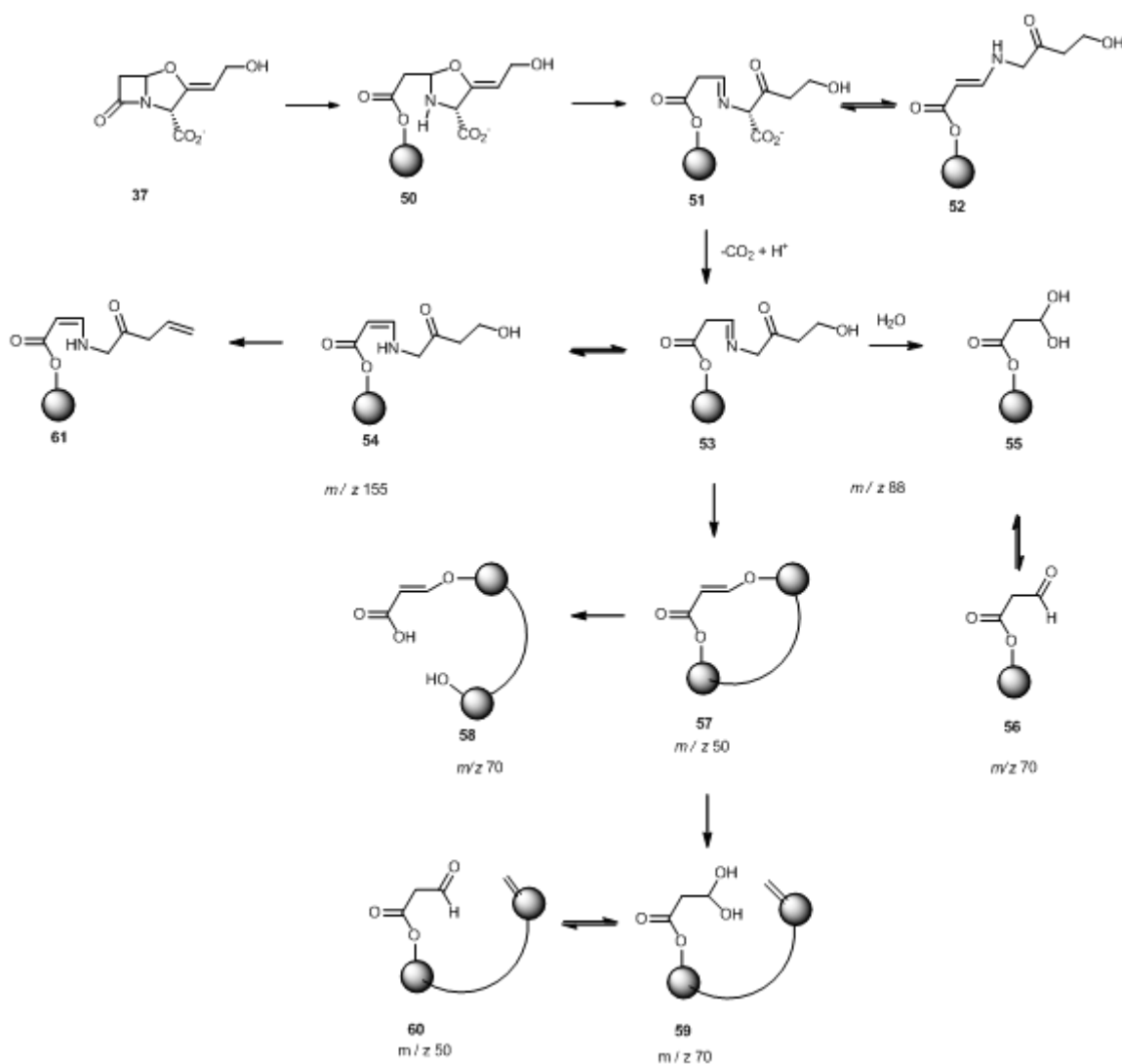
Class C  $\beta$ -lactamases are resistant to clavulanic acid and are capable of hydrolysing cephalosporins, including the clinically relevant third generation cephalosporins. A flexible loop (termed the  $\Omega$  loop) in the enzyme is responsible for the ability to turn-over sterically demanding cephalosporins, such as **34**.<sup>119,120</sup> Tyr 150 has been shown to be the activating amino acid in the acylation and deacylation steps.<sup>121</sup>

Class D are also known to be oxacillinases due to their ability to degrade 5-methyl-3-phenylisoxazole-4-carboxy side chain penicillin class, exemplified by oxacillin and cloxacillin. Mechanistic investigations of class D proteins have revealed structural differences compared to other serine hydrolases, notably a short  $\Omega$  loop and no similarity to previously identified activating amino acids outside the catalytic triad. Crystallographic studies revealed that the active site lysine is carboxylated and the resulting carbamic acid takes part in the acylation / deacylation steps as a general base.<sup>122</sup>

#### **2.1.4 Mechanism determination by mass spectrometry**

The mechanism of action for the inhibition of class A  $\beta$ -lactamases by clavulanic acid and tazobactam has been studied in depth by several research groups.<sup>104</sup> Rizwi *et al* observed an intermediate with an enamine chromophore in the inhibition of *S. aureus*  $\beta$ -lactamase and this supported by the work of Charnas, who used <sup>14</sup>C-radiolabelling experiments to determine the mechanism of clavulanate inhibition.<sup>123</sup> It had also been suggested that a lysine residue was involved in cross linking to the enzyme bound clavulanate. Subsequent X-ray crystallography<sup>124</sup> provided proof of the acylation of the enzyme by clavulanate but no lysine residue was determined to be spatially close enough to facilitate cross linking, leading Ser 130 to be implicated instead. Furthermore, the resolution of the structure determination was not sufficient to distinguish between **51** and **52**.<sup>125</sup>

A subsequent mass spectroscopic study by Brown *et al* enabled the full mechanism to be determined.<sup>126</sup> The successful approach utilised intact protein ESI MS to determine the adducts formed when *S. aureus*  $\beta$ -lactamase reacted with clavulanic acid, and digestion of the modified protein using Endopeptidase C and trypsin followed by HPLC ESI MS analysis of the proteolytic peptides enabled the location of the acylation to be determined (Scheme 4).<sup>127</sup>



**Scheme 4** Degradation pathway for clavulanic acid

The acyl-enzyme intermediate **50**, is the first product in the clavulanate reaction pathway, followed by decomposition of the oxazolidine to give imine **51**. This can be decarboxylated to give intermediate **53**. Imine **53** can degrade via a number of different pathways. Firstly imine **53** that can either be cross linked by a spatially near serine to give a vinyl ether **57** or it is converted to a hemiacetal **55** and then to aldehyde **56** by hydrolysis. The cross linked vinyl ether **57** can be hydrolysed to give either dehydroalanine and a hemiacetal (**59**) or the ester linkage is hydrolysed to give (**58**). Raman spectroscopic study of the intermediate **52** formed from hydrolysis of clavulanic acid by wild-type class A  $\beta$ -lactamase SHV-1 showed a mixture of **52**, **53** and **54**, whereas a SHV-1 mutant that contains E166A exists predominantly as the *trans*-enamine **52**. As discussed earlier E166 contributes to the inhibition of  $\beta$ -lactamase. This highlights the importance of secondary sphere amino acids in active site labelling.

The mechanism proposed by Brown *et al* is supported by the results of other groups. Sulton and co workers identified that the same pathway occurred in the inhibition of a class A  $\beta$ -lactamase from *E. coli*. In enzymes that contain a S130G mutation, however, the enzyme is still acylated but only one adduct is seen in the intact protein mass spectrum at + 70 Da, arising from hydrolysis of enamine **56**. A further adduct with  $m/z$  136 was observed in the inhibition of  $\beta$ -lactamase from *M. tuberculosis*. This fragment most likely arises from dehydration of **55**.<sup>128</sup>

HPLC ESI MS experiments with tazobactam have revealed a similar degradation pathway to that of clavulanic acid, with common protein adducts at +70 and +88 Da.<sup>129</sup>

### 2.1.5 Non-classical $\beta$ -lactamases

There are examples of  $\beta$ -lactamases in the literature that fall outside the groupings discussed above.<sup>104</sup> Recently mitochondrial Glyoxalase 2-1 from *Arabidopsis thaliana* was shown to hydrolyse nitrocefin, cefotaxime and imipenem with  $k_{cat} = 1.20 \pm 0.04 \text{ s}^{-1}$ ,  $0.20 \pm 0.01 \text{ s}^{-1}$  and  $0.20 \pm 0.01 \text{ s}^{-1}$  respectively, 10 – 100 times lower than most reported metallo- $\beta$ -lactamases.<sup>130</sup> The Glx 2-1 contains the conserved HXHXD metal binding domain, typical of metallo- $\beta$ -lactamases but the nearest homologue is the L1 metallo- $\beta$ -lactamase from *Stenotrophomonas maltophilia*, with which it shares only 10% sequence identity. The role of penicillin in plant cells is unknown and the cellular localisation of Glx 2-1 poses interesting evolutionary questions as to how the protein evolved  $\beta$ -lactamase function. One theory is that the  $\beta$ -lactamase function of Glx2-1 is a result of gene duplication and diversification and as a result is a redundant by-product of genetic evolution.

Penicillin binding proteins (PBPs) are the cellular target of penicillin type antibiotics and do not display  $\beta$ -lactamase function, instead they catalyze transpeptidation, or exhibit carboxypeptidase and endopeptidase function.<sup>131</sup> The Tp47 PBP from *Treponema pallidum* exhibits  $\beta$ -lactamase activity (for benzylpenicillin  $K_{cat} = 271 \pm 6 \text{ s}^{-1}$ ) but detailed mechanistic studies have revealed the enzyme activity does not correspond to a known mode of action. PBPs contain three conserved motifs namely SVTK, TEN and KTG as revealed through structural investigations.<sup>132</sup> Site directed mutagenesis of the Ser in the SVTK motif, and Lys in the KTG motif did not affect  $\beta$ -lactamase activity. The crystal structure of the enzyme revealed a four domain structure, with a mixture of  $\alpha$ -helical

and  $\beta$ -sheet structure. Further investigation of the same enzyme by a different research group who used a series of stopped-flow experiments, lead to the conclusion that the hydrolysed  $\beta$ -lactam product penicilloic acid acts as an inhibitor for the active site of the enzyme. The observation that the hydrolysed antibiotic blocks the enzymatic function of the PBP accounts for the clinical observation that *T. pallidum* is still susceptible to penicillin. The active site of the enzyme remains unknown.<sup>133</sup>

*Helicobacter* cysteine-rich protein A (HcpA) is another protein reported as having  $\beta$ -lactamase function yet despite crystallographic data, no active site or mode of action has been postulated.<sup>134,135</sup> This novel  $\beta$ -lactamase adopts a modular structure consisting of four  $\alpha/\alpha$ -motifs, unique amongst reported penicillinase enzymes.  $K_{cat}$  is low, less than  $1.06 \text{ min}^{-1}$  for both penicillin and cephalosporin type antibiotics, but  $K_m$  for ampicillin (**31**) and amoxicillin (**32**) is  $145 \mu\text{M}$  and  $155 \mu\text{M}$  respectively indicating that the substrate is a good fit for the enzyme active site. The extra presence of OH and NH functionality on **31** and **32** may account for the higher  $K_m$  compared to benzylpenicillin (**2**,  $K_m = 48 \mu\text{M}$ ), suggesting hydrogen bonding stabilises the substrate : enzyme complex.

## 2.2 Results and discussion

### 2.2.1 Introduction

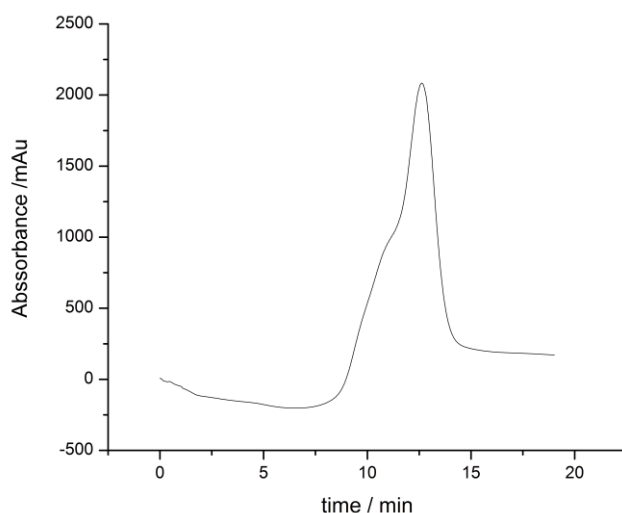
*N. gonorrhoeae* exhibits high level resistance to  $\beta$ -lactam antibiotics by a combination of the resistance mechanisms discussed above, namely i) the production of  $\beta$ -lactamases, ii) decreased influx due to mutations in porin and PilQ proteins, iii) decreased affinity for penicillin in PBP proteins, iv) increased efflux of  $\beta$ -lactam antibiotics by the MtrCDE efflux pump.

The regulation of resistance mechanisms ii-iv are under the control of the transcriptional regulator MtrR. MtrR is a member of the TetR family of transcriptional regulators and as such contains a flexible ligand binding domain. It is hypothesised that in order for MtrR to activate the described resistance determinants, the regulator must be able to bind  $\beta$ -lactam antibiotics. The following chapter describes research into how MtrR interacts with  $\beta$ -lactam type antibiotics.

### 2.2.2. Origin, overexpression and purification of MtrR.

All ligand binding studies performed in the course of this research used recombinant MtrR. Initial protein overexpression in BL21-AI cells used a pET21a plasmid carrying the

gene for MtrR, sourced from a stock of cells previously prepared in the group. The protein was expressed with an N-terminal His-TAG and purified by affinity chromatography using a 1 mL or 5 mL HITRAP column (Figure 24). Further purification was carried out by anion exchange chromatography and gel filtration. The identity and purity of the recombinant protein were assessed by SDS-PAGE (Figure 27) and mass spectrometry (Figure 26). A MASCOT (Matrix Science protein database) search using the data from trypsin digest of MtrR revealed that only tryptic peptides corresponding to MtrR were present and this result confirms that no other proteins were co-purified with MtrR. In order to ensure that any activity observed between MtrR and various  $\beta$ -lactam antibiotics was solely due to MtrR and not any co-purified  $\beta$ -lactamase, the gene for *mtrR* was digested from the pET21a plasmid and inserted into a pET28a plasmid. The later plasmid carried a kanamycin resistance marker and there is no *bla* gene present eliminating the possibility of co-purifying a  $\beta$ -lactamase.



**Figure 24** UV trace showing the absorption profile HIS-tag purification of MtrR. 40 mL crude MtrR lysate (20 mM Tris, 300 mM NaCl, 10 % glycerol, pH 8.2) was loaded onto 5 mL HITRAP column. HIS-Tagged protein was eluted using an imidazole gradient 0-100 % B over 20 minutes (Buffer A: Tris 20 mM, NaCl 300 mM, 10 mM imidazole, pH 8.2; Buffer B Tris 20 mM, NaCl 300 mM, 1 M imidazole, pH 8.2). Purification carried out at 5 mL buffer / minute.

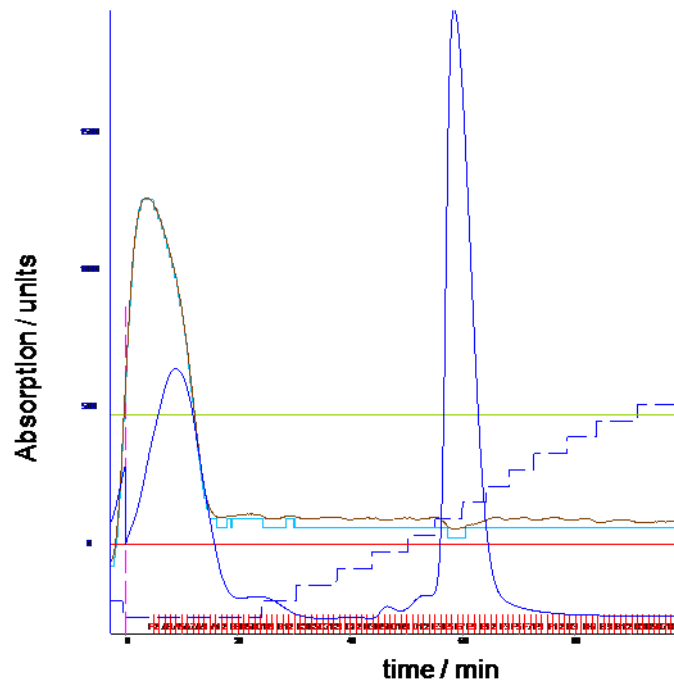


Figure 25 Gel filtration of MtrR. 5 mL MtrR loaded onto 16 / 40 sephadex column and eluted with 1.5 column volumes buffer (Tris 20 mM, NaCl 300 mM, pH 8.2). MtrR eluted between 58 and 64 minutes.

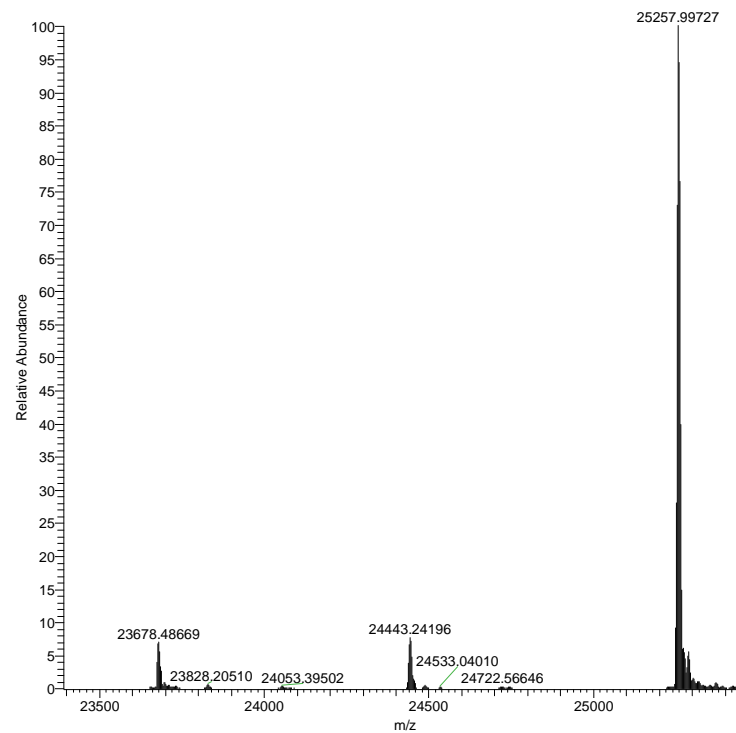


Figure 26 Deconvoluted ES<sup>+</sup> mass spectrum of MtrR



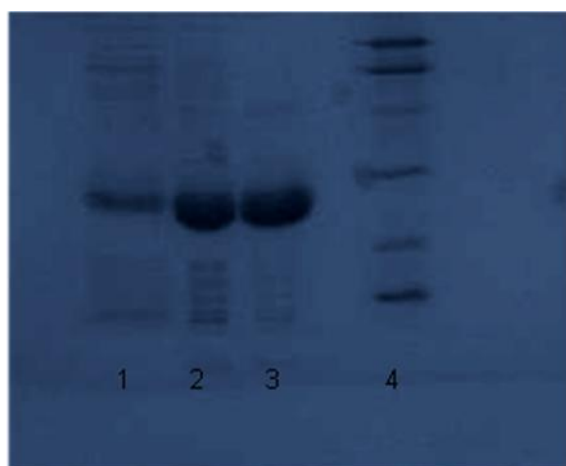


Figure 27 SDS-PAGE (12% acrylamide) analysis of MtrR purification. Lane 1 - crude overexpressed MtrR, Lane 2 - post HisTAG purification, Lane 3 - post Gel purification

Despite MtrR being a soluble protein it is considerably unstable on storage at 4 °C in aqueous buffer for more than 2 days and if stored at -20 °C in aqueous buffer containing 10 % glycerol, a considerable amount of protein precipitates on thawing. These observations are supported by the literature.<sup>136</sup> Consequently, binding studies were carried out on the same day that the protein was dialysed into the final analysis buffer, and to ensure enough protein was available for binding studies, the protein was frequently produced.

### 2.2.2. MtrR and antibiotics ITC binding study

The MtrCDE efflux pump has been shown to confer resistance to gonococci in the presence of tetracycline (**11**), benzyl penicillin (**2**) and spectinomycin (**10**).<sup>137</sup> In order to find evidence that substrates for the MtrCDE efflux pump also bind MtrR the antibiotics were used as ligands in ITC binding studies with the regulator protein.

In this investigation, **11**, **2** and **10** (1 mM) were injected into a MtrR solution (70 μM) using a VP-ITC (Microcal®). For each antibiotic control experiments involving the injection of antibiotic into buffer only were also carried out. The data from the control was subtracted from the experiment containing MtrR to remove any background effects. The observed data for tetracycline and spectinomycin could be fitted to a standard one site model using Origin® software (Figure 28), the calculated thermodynamic parameters of which are summarised in

Table 3. Both antibiotics interact with MtrR but appear to do

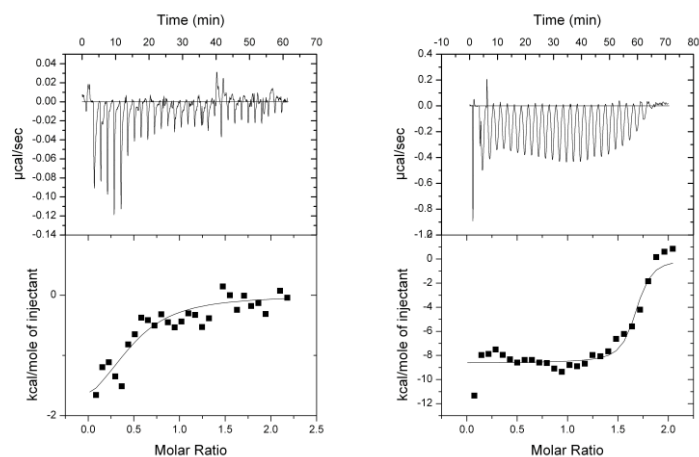


Figure 28 ITC data for (A) tetracycline (1mM) and (B) spectinomycin injected into MtrR (70  $\mu$ M). Upper panel displays raw data, lower panel shows the data fitted to a OneSite model.

Table 3 Thermodynamic parameters calculated from the raw ITC data by fitting to standard OneSite model.

Antibiotic	N	$\Delta H / \text{kJ mol}^{-1}$	$\Delta S / \text{kJ mol}^{-1} \cdot \text{K}$	$K_d / \mu\text{M}$
Tetracycline	$0.4 \pm 0.1$	$-9.5 \pm 3$	17	$4 \pm 0.1$
Spectinomycin	$1.65 \pm 0.02$	$-36 \pm 9$	3	$0.09 \pm 0.001$

so via different mechanisms. The ratio of 0.4 for **11** binding to MtrR suggests that one ligand binds to one MtrR dimer (1 : 2). MtrR appears capable of binding more than one spectinomycin (**10**) molecule as  $N > 1$ .

In contrast to the results obtained by injection of tetracycline (**11**) and spectinomycin (**10**) into MtrR, injection of penicillin G (**2**) gave an intriguing result (Figure 29 A). The steady reduction in baseline is indicative of an enzymatic reaction whereas the decreasing

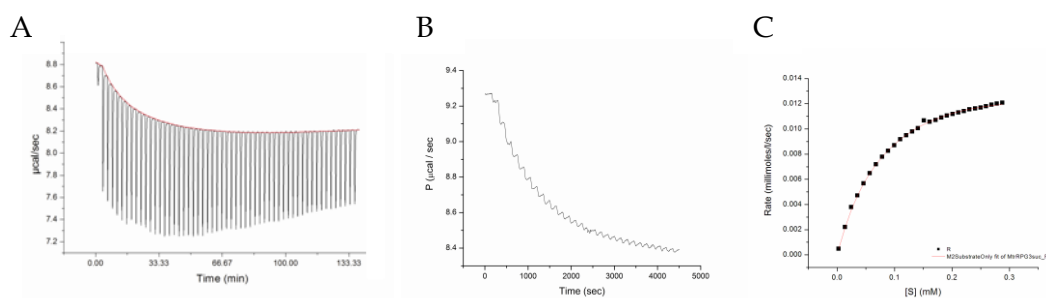


Figure 29. (A) Raw ITC data for the injection of penicillin G (1 mM) into a solution of MtrR (70 mM) in Tris buffer; (B) phosphate buffer (C) Data fitted to a Michealis-Menton model.

power output is representative of a binding event. To further investigate the interaction between MtrR and **2** further, the experiment was repeated but phosphate buffer was used instead. Sodium phosphate buffer has a much lower heat of ionisation ( $\Delta H = 3 \text{ kJ mol}^{-1}$ ) than Tris buffer ( $\Delta H = 45 \text{ kJ mol}^{-1}$ ) causing buffer effects to be minimised with the former reagent. Despite the high heat of ionisation for Tris buffer, it is the preferred buffer for MtrR as Tris buffer confers stability during dialysis, preventing the loss of protein during buffer exchange.<sup>138,143</sup> The raw data for the reaction in phosphate buffer gave a profile indicative of an enzymatic event (Figure 29 B) and the data could be fitted using the standard Michealis-Menton model supplied with the calorimeter's Origin data analysis software (Figure 29 C). The calculated kinetic constants are  $K_m = 106 \pm 0.002 \mu\text{M}$  and  $k_{\text{cat}} = 0.02 \pm 1.3 \times 10^{-4} \text{ s}^{-1}$ . The calculated parameters are low but comparable to other enzymes with unexpected  $\beta$ -lactamase activity, e.g. HcpB from *Helicobacter pylori* exhibits a  $K_{\text{cat}} = 0.74 \text{ min}^{-1}$  (section 2.1.6).<sup>139</sup>

The results from the ITC binding study confirm that **11** and **10** are ligands for MtrR. The result of the penicillin binding study was unexpected and in order to find further evidence to support this, the ITC reaction was repeated and the solution from the ITC cell was analysed by ESI mass spectrometry.

Analysis by  $\text{ES}^+$  mass spectrometry of the MtrR / penicillin from the ITC cell provided evidence for the presence of the penicillanoic acid  $m/z = 353$  and the complete destruction of all the starting penicillin G,  $m/z = 335$  (Figure 30). Identical analysis of a control sample, in which penicillin G was added to a buffer solution not containing MtrR, showed a considerable amount of unchanged **2** ( $R_t = 18.4 \text{ min}$ ) and only a limited amount of the penicilloic acid (**62**,  $R_t = 17.8 \text{ min}$ ) in contrast to the ITC solution where two peaks of approximately equal intensity are seen at 17.8 and 18.6 minutes. The peak at 15.36 minutes is for MtrR. The identity of penicillin (**2**) and penicilloic (**62**) acid were confirmed by accurate mass measurements.<sup>140</sup>

The mass spectrometry results along with the ITC findings provide evidence to support the hypothesis that MtrR acts as a  $\beta$ -lactamase. Having established this, attention turned to investigating the specificity of the MtrR activity.

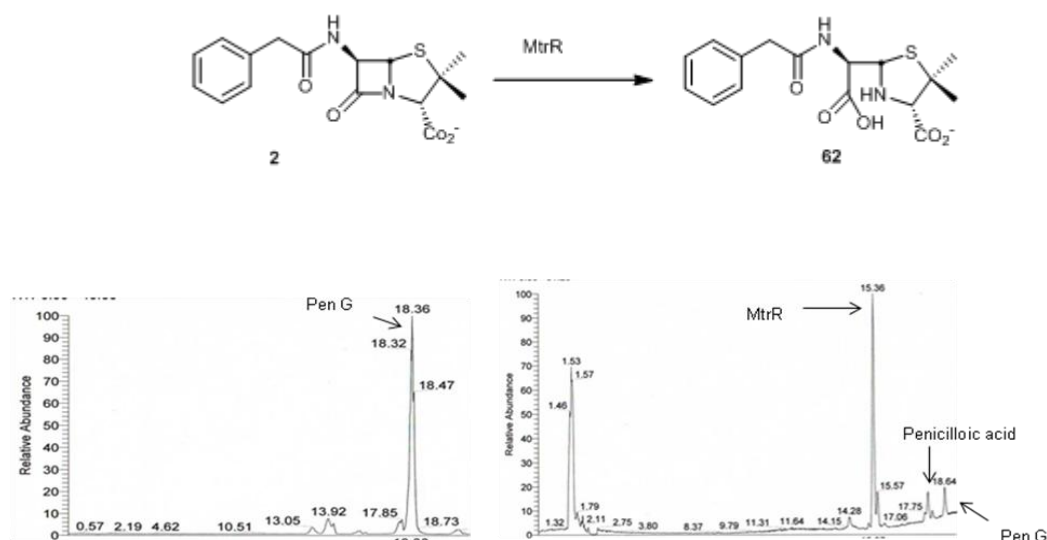


Figure 30 ES<sup>+</sup> ion chromatogram a) Control: Penicillin G in phosphate buffer, 2 hours b) MtrR and Penicillin solution post ITC

### 2.2.3 Specificity of ligand binding

As discussed in section 2.1.2 a range of penicillin type antibiotics have been developed to counter resistant strains. The modified side chains in semi-synthetic antibiotics not only improve the pharmacokinetics but also provide the antibiotic with different modes for protein binding, for example the introduction of alcohol, and amine functionality in amoxicillin enhances protein binding due to favourable hydrogen bonds while the presence of the large naphthyl group in nafcillin (**33**) has the effect of making the drug too large to fit into the active site of the protein.

Using a range of  $\beta$ -lactams it was postulated that insights into the type of active site of the enzyme could be gained. The semi-synthetic penicillins ampicillin (**31**), amoxicillin (**32**) and penicillin V (**29**) were all substrates for MtrR exhibiting kinetic parameters similar to benzyl penicillin (**2**) (Figure 31). As expected **33** was not hydrolysed by MtrR, showing instead weak binding to MtrR, as determined by a standard ligand binding ITC experiment. This ability of MtrR to promote the turnover of PenG, PenV and ampicillin to the corresponding penicillanoic acid but not nafcillin led to the suggestion that it has acquired a  $\beta$ -lactamase function. The cephalosporin **35** is turned over at a much slower rate, which indicates that MtrR operates more as a Class A rather than a Class C  $\beta$ -lactamase.

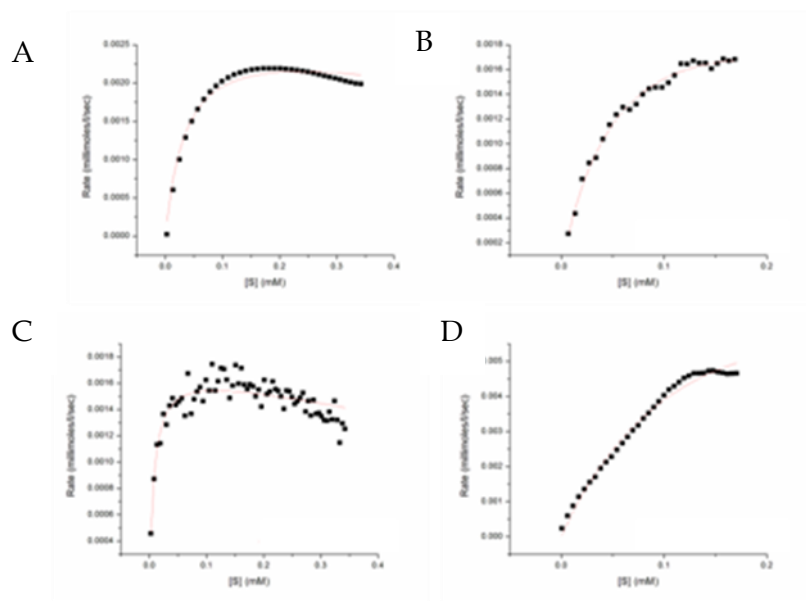


Figure 31 (A) to (D) fitted using michelis-menton model (A) Penicillin V  $k_{cat} = 0.03 \text{ s}^{-1}$ ,  $K_m = 101 \text{ } \mu\text{M}$  (B) Ampicillin  $k_{cat} = 0.04 \text{ s}^{-1}$ ,  $K_m = 64 \text{ } \mu\text{M}$ ; (C) CENTA  $k_{cat} = 2 \times 10^{-4} \text{ s}^{-1}$ ,  $K_m = 44 \text{ } \mu\text{M}$ ; (D) Amoxicillin  $k_{cat} = 0.02 \text{ s}^{-1}$ ,  $K_m = 96 \text{ } \mu\text{M}$

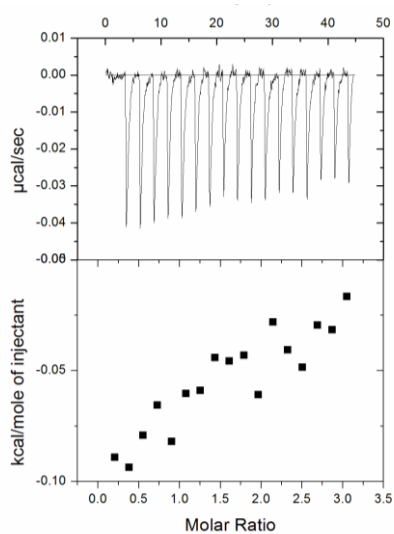
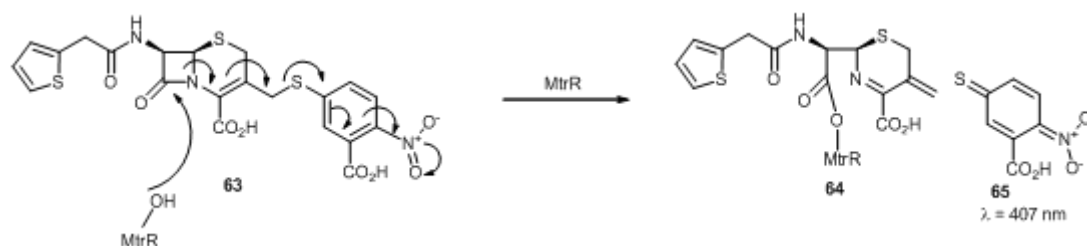


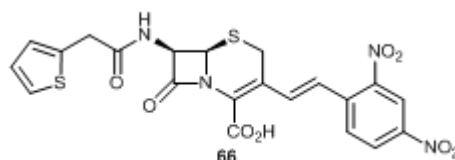
Figure 32 Injection of nafcillin (1 mM) into MtrR (70  $\mu\text{M}$ )

CENTA is a chromogenic reagent in that, on cleavage of the  $\beta$ -lactam ring the aryl thiolate chromophore (65) is released, thus allowing the hydrolysis of the substrate to be monitored using UV spectroscopy at 407 nm (Scheme 5).<sup>141</sup> CENTA is considerably more stable than nitrocefin (67), the previously commercially available chromogenic  $\beta$ -lactamase substrate. No hydrolysis was detected after incubation at pH 8

in 10 mM 300 mM Tris buffer or 50 mM phosphate buffer whereas nitrocefin had a half-life of 380 min. A further favourable characteristic of CENTA over nitrocefin is the aqueous solubility of CENTA, up to 60 mg / mL at pH 7 in sodium phosphate buffer.<sup>50</sup>

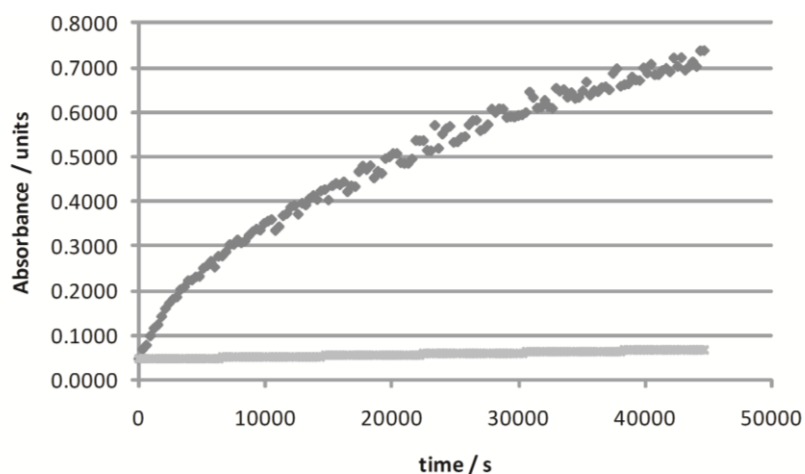


**Scheme 5** Expulsion of chromophore on ring opening of  $\beta$ -lactam ring in CENTA



**Figure 33** Nitrocefin, a chromogenic  $\beta$ -lactamase substrate

The effect of the addition of a 200  $\mu$ mol solution of CENTA to MtrR (70  $\mu$ M) was monitored in a UV-spectrophotometer over a period of 700 min and compared to a negative control, with no MtrR present (Figure 34). The release of the nitro thiolate is clearly seen in the increase in absorbance at 407 nm. It is clear that this is due to action by MtrR, in that no considerable change is seen the control sample.



**Figure 34** Monitoring of the cleavage of CENTA (0.2 mmol) by MtrR (70  $\mu$ M) (dark grey diamonds) at 407 nm. A control sample of CENTA only (light grey) showed very little change over the period of monitoring.

The ITC, mass spectrometry and UV analysis provide evidence that MtrR can act as a  $\beta$ -lactamase. In order to gain insights into the mechanism of hydrolysis a mass spectrometric study was designed, using the  $\beta$ -lactamase inhibitors clavulanic acid and tazobactam, as covalent probes.

## 2.2.4 Mechanism investigations

Firstly, ITC analysis of clavulanic acid injected into MtrR demonstrated that an exothermic binding event takes place ( $\Delta H = -80 \pm 1 \text{ kJ mol}^{-1}$ ,  $N = 0.7 \pm 0.02$ ). Moreover, subsequent addition of **2** to this mixture showed no evidence for further binding or penicillin hydrolysis, consistent with an inactivated enzyme (Figure 35). Analysis of the resultant solutions by MALDI-MS revealed that the peak for MtrR had shifted from  $m/z = 25251$  for the purified protein to  $m/z = 25327$  for the product. The mass difference of 70 Da is consistent with the acylation of protein by clavulanic acid in the mechanism proposed by Brown *et al* (scheme 5).

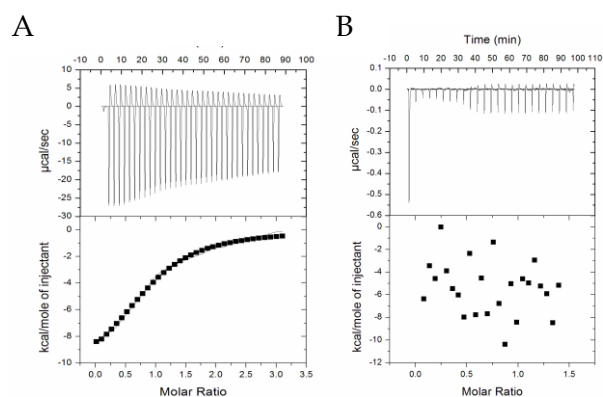


Figure 35 (A) Acylation of MtrR by clavulanic acid to MtrR  $\Delta H = -80 \pm 1 \text{ kJ mol}^{-1}$ ,  $K_d = 30 \mu\text{M}$ ,  $N = 0.7 \pm 0.02$  (B) no interaction on injection of penicillin G into MtrR

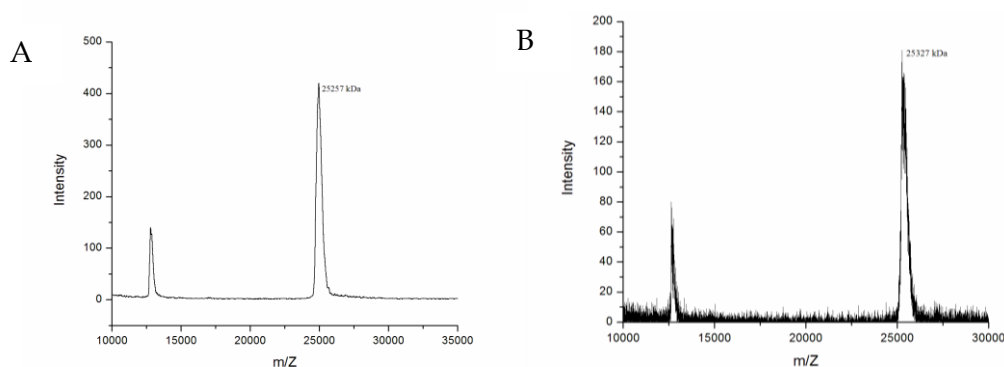


Figure 36 (A) native MtrR,  $m/z$  25257 (B) MtrR after incubation with clavulanic acid,  $m/z$  25327 ( $\Delta = 70 \text{ Da}$ ). The  $[M+H]^{2+}$  ion can be observed in both spectra  $\sim 12000$

In an attempt to resolve the modified proteins by SDS-PAGE, a 15  $\mu$ l aliquot of each inhibitor - protein sample was loaded onto a 12 % polyacrylamide gel. The samples were denatured by heating to 90 °C for 5 minutes prior to loading onto the gel and it was hypothesised that this may have hydrolysed the covalent adducts, resulting in only native protein being present. The SDS-PAGE was repeated without heating at 90 °C but, no difference in mass between labelled and unlabelled protein was observed. If only the lower mass adducts are stable to the electrophoresis conditions, a mass difference of only 50 units may not be observed. With MALDI MS evidence for a new protein species, attention turned to localising the site of addition in MtrR. It was envisaged that subjecting the inhibitor - protein complex to proteolytic digestion followed by mass spectrometric analysis of the resultant peptides would facilitate the identification of the residues of MtrR that are labelled by the inhibitors.

Clavulanic acid (1 mM) was mixed with MtrR (70  $\mu$ M) and incubated at either room temperature (approx. 22 °C) or at 37 °C for a minimum of one hour. The resulting solutions were then directly loaded onto a reverse phase HPLC column coupled to an FT-ICR mass spectrometer operating in ES+ mode. Following deconvolution, a series of peaks corresponding to covalently labelled adducts of MtrR could be identified (Figure 37). Repetition using the sulfone inhibitor tazobactam (**38**) gave similar results (Figure 38) Significantly these showed increases in mass consistent with reports in the literature, as discussed above, for labelling with tazobactam and clavulanic acid. Addition of 52 Da corresponds to cross linked protein (**57**). An increase of 70 Da indicated addition of C<sub>3</sub>H<sub>3</sub>O (**56**, **68** or **59**) and 88 Da corresponds to hemiacetal **55**. The observation of a + 155 Da adduct in the clavulanic acid containing sample indicates that **51** is unstable and rapidly undergoes decarboxylation. The +136 Da adduct arises from dehydration of **53** and this adduct is proposed to be stable and responsible for inhibition of the enzyme.<sup>142</sup> The adduct at 113 cannot be explained by chemical fragmentation of clavulanic acid but the same adduct has been observed in the literature.<sup>143</sup> Table 4 summarises the observed adducts and peaks marked with an asterisk in Figure 37 could not be identified. The evidence provided by the mass spectrometric study shows that MtrR is covalently



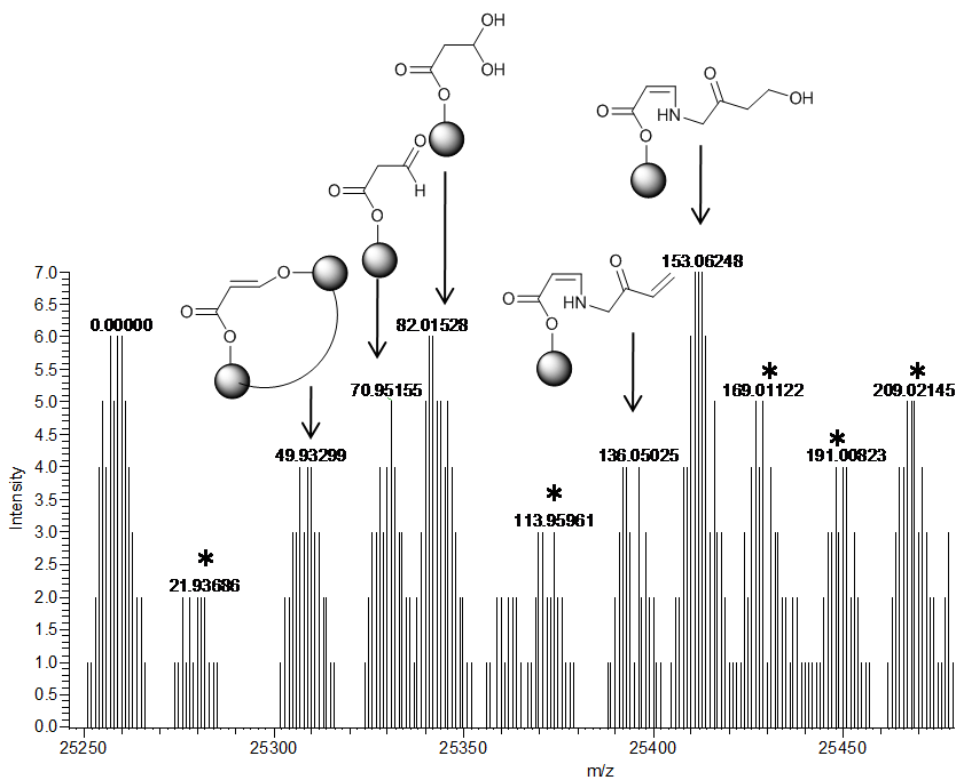


Figure 37 Representative mass spectrum for MtrR incubated with clavulanic acid with proposed identities where possible, asterisk denotes unknown addition

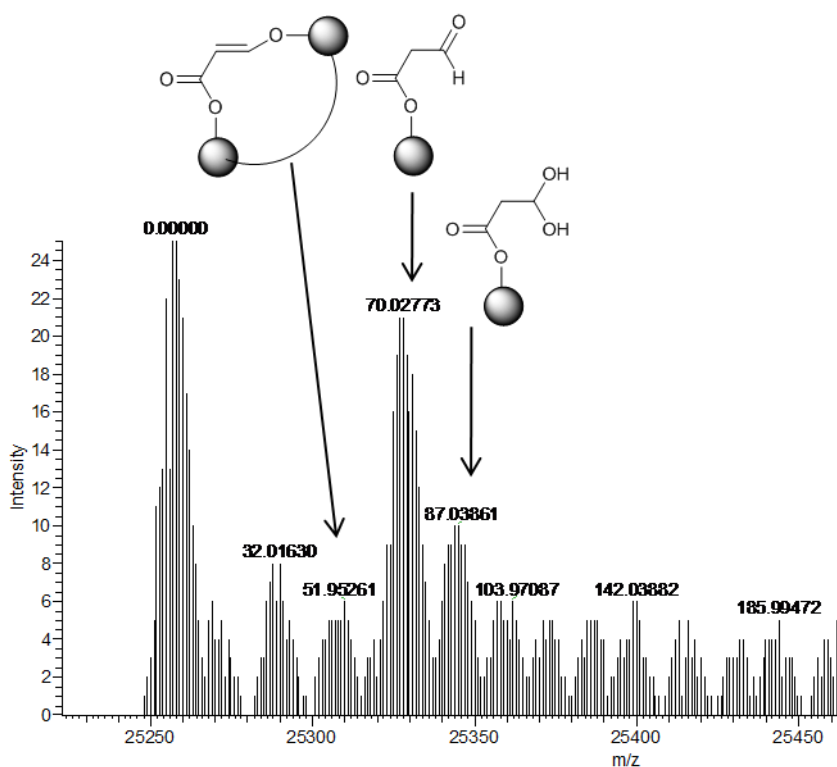


Figure 38 Representative mass spectrum for the incubation of Tazobactam with MtrR

modified by clavulanic acid and tazobactam and attention next turned to localising the site of modification.

### **2.2.5 Localisation of modified residues using trypsin digests and mass spectrometry**

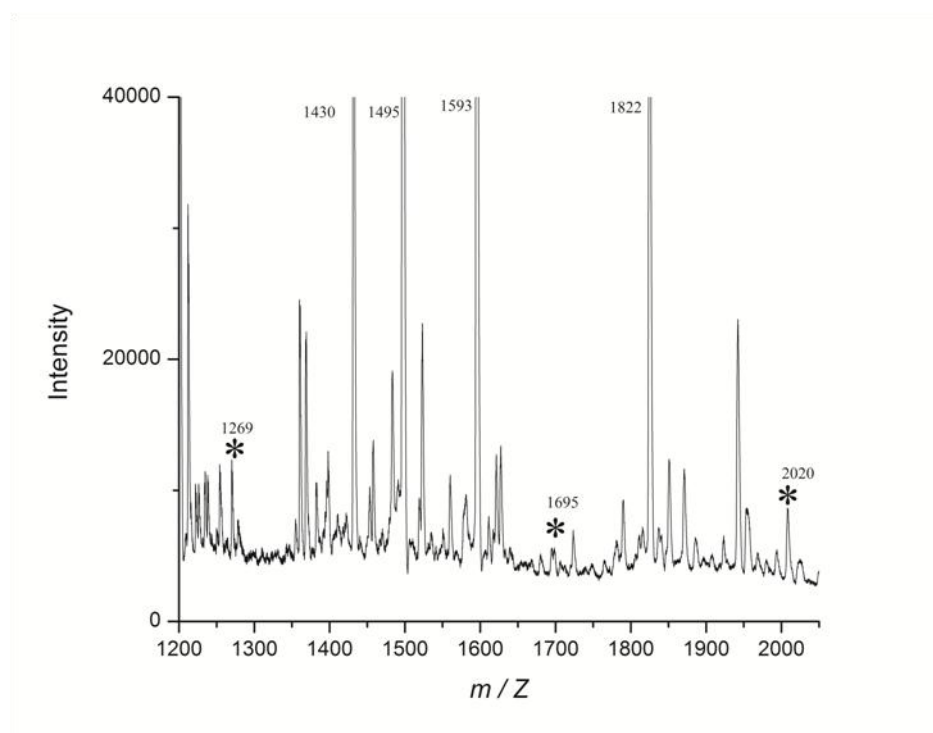
Having demonstrated that the  $\beta$ -lactamase activity of MtrR could be inhibited by clavulanic acid and that this inhibition led to covalent labelling of the enzyme it was of interest to determine the location of this modification. Amino acids modified by covalent labelling can be determined by mass spectrometric analysis of peptides produced as a result of proteolytic cleavage of the modified protein of interest. The modified protein can be digested using trypsin or endoproteinase Glu-C (endo GluC).<sup>144</sup> Trypsin cleaves peptide bonds C-terminal to lysine and arginine, whereas endoproteinase Glu-C cleaves only after glutamic acid residues. The lower frequency of proteolysis by endo GluC can produce less complex tryptic peptide maps but due to experience with trypsin digests within the group trypsin was chosen as the enzyme of choice for this work. The digest can be performed on protein extracted from an SDS-PAGE gel or soluble protein, or precipitated from buffer by acetone.

An initial control experiment using unlabeled MtrR and trypsin was conducted to check the sequence coverage of the digest. MALDI MS analysis of tryptic peptides generated by incubation of MtrR with trypsin (~ 1:30) for 12 hours at 37 °C, showed high sequence coverage with the only missing peptide being 116-124, which does not contain any serine or threonine residues and so trypsin was an ideal choice for analysis in this project. To ensure that the MtrR used in these assays was not contaminated by any  $\beta$ -lactamase, the peak list generated by MALDI analysis of the tryptic peptides was exported to the MASCOT database. The search did not identify any peptides belonging to *E. coli* and one can therefore conclude that the sample of MtrR used was 100% pure.

Two methods for the trypsin digest were attempted. Firstly, protein was extracted from an SDS-PAGE gel and digested overnight with trypsin. Mass spectrometric analysis did not indicate the presence of modified protein. In a second attempt, the protein was precipitated in acetone and re-suspended in trypsin solution. Following digestion, overnight at 37 °C, and freeze-drying, the resultant peptides were dissolved in 0.01% (v/v) aq HCO<sub>2</sub>H and analysed by MALDI MS (Figure 39).

In order to determine whether any modified peptides were present, the data set was compared a control digest of MtrR only and to an *in silico* digest of clavulanate labelled MtrR generated using SequenceEditor (Bruker Daltonik GmbH) software. The known inhibitor adducts (+52, +70, +88, +136, +155) were optionally added to all serine / threonine residues and two partial cleavages were allowed to enable all possible modifications to be predicted. The theoretical digest data set and the observed data set were manually compared and three modified peptides were identified (starred peaks Figure 39). The modified peaks are absent in the control sample of MtrR that was not treated with clavulanic acid prior to proteolysis with trypsin (Figure 40).

To confirm that these peaks were modified and were not artefacts of MALDI analysis, the trypsin digest was repeated and the tryptic peptides analysed by ESI MS (Aruna Prakash). The same peptides were identified using both mass spectrometric techniques thus it can be concluded that the observed modified peptides are real and reproducible.



**Figure 39 MALDI spectrum of trypsin digest of MtrR labelled with clavulanic acid. \* = modified tryptic peptide of MtrR**

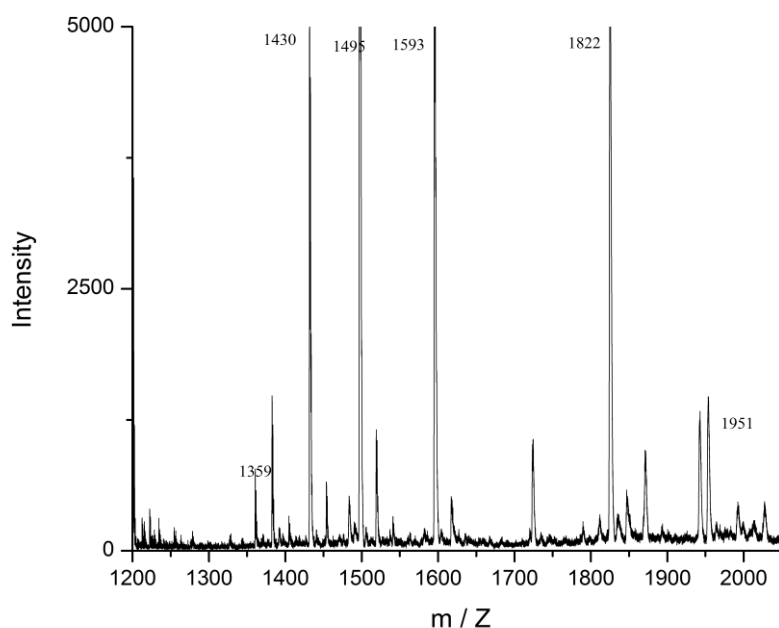


Figure 40 Mass spectrum for the trypsin digest of native MtrR.

Table 4 Summary of trypsin digest data acquired using MALDI and ES<sup>+</sup> techniques

MALDI	Accurate mass	ESI ( $\Delta_{\text{Obs-Theo}} / \text{ppm}$ )		Modified MtrR peptide	Modification
		Clavulanic acid (37)	Tazobactam (38)		
1269	1269.63748	0.257	-0.231	HTLLHFFER	+70
1695	1695.81189	1.429	0.202	CEHTEQNAAVIAAR	+70
2020	2020.00996	-2.624	Not observed	TKEHLMMLAALET FYR	+70

In order to further characterise the peptides, mass spectrometric sequencing was attempted on the modified peptides. The peptide at  $m/z = 1269$  was isolated in the ion trap on a MALDI spectrometer and fragmented using enhanced laser power (Figure 41). A more detailed account of MALDI MS/MS techniques is given in section 3.2.3.2. The abundance of ions in the low mass range (0 – 400  $m/z$ ) together with the observation of several dipeptide ions (LL-28, LH-28, HF-28) and the observation of a tripeptide carrying

the modified threonine residue (T\*LL,  $m/z = 369$ ) enables the proposed peptide sequence to be suggested with confidence. Attempts to sequence the other modified peptides were unsuccessful. Furthermore, sequencing experiments using electrospray mass spectrometry in electron capture dissociation mode have so far been unsuccessful.

The observed results indicate that MtrR is labelled on three threonine residues. This result is fascinating as it was also expected for the labelling to occur at serine, as in classic  $\beta$ -lactamases. Two of the labelled threonine residues (Thr 91 and Thr 127) are in the ligand binding domain of MtrR whereas Thr11 is at the *N*-terminal DNA binding domain. In order to understand the spatial arrangement of the modifications a homology model of MtrR was built using the protein modelling programme MOE (Chemical Computing group).

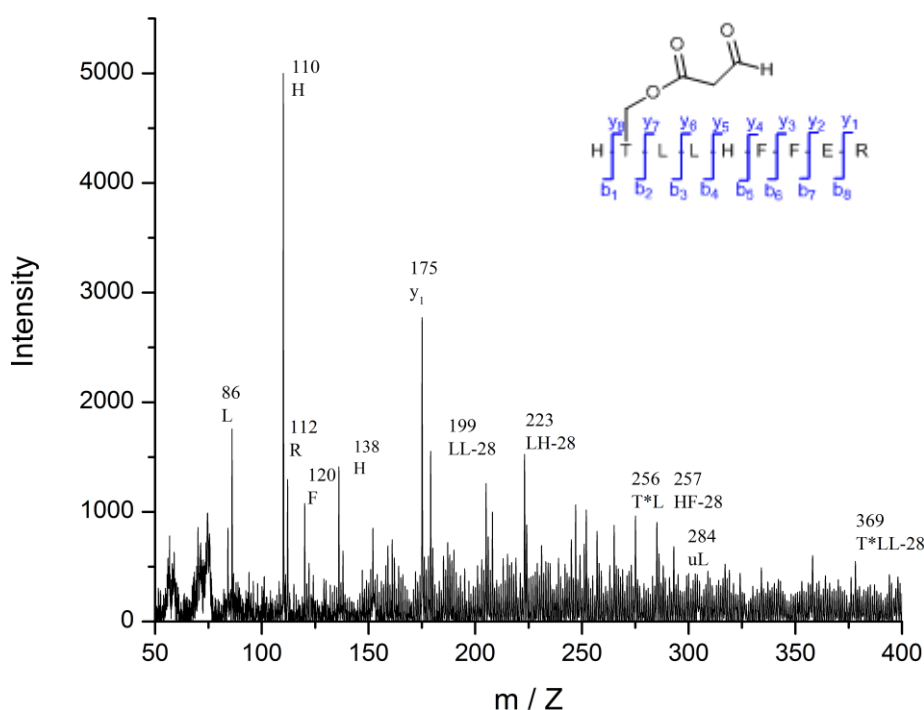


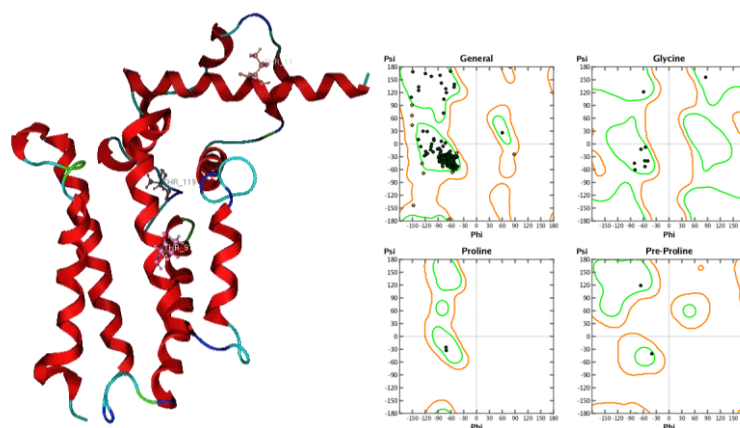
Figure 41 LIFT data for HT\*LLHFFER, where T\* is the modified residue. Detailed MS/MS data is shown in appendix 7.1

### 2.2.6 Visualisation of results using a homology model of MtrR

In order to construct the homology model, MtrR was aligned against TetR family proteins of similar sequence. The highest similarity is to AcrR from *E. coli* (overall

homology 34 %). A ten membered database of conformers is produced and the lowest energy conformer is the predicted structure for MtrR (Figure 42 A). The accuracy of a homology model can be determined by a Ramachandran plot, and the plot of phi vs psi angles in MtrR reveals no outliers, with all angles within predicted limits (Figure 42 B).

Using the homology model it is clear that Thr 11 is at the N-terminus of the protein on helix1, Thr91 is on helix 5 and Thr 119 resides in helix 6. There are 15 threonine residues in MtrR and with only 3 labelled, it is suggested that this is due to specific interactions. It would be expected that serine to be labelled in preference to threonine due to the large number of serine  $\beta$ -lactamases that are known. The methyl group  $\beta$  to the nucleophilic oxygen of threonine may hinder the access of the water nucleophile in the deacylation



**Figure 42 A: Homology model of MtrR (monomer) with labelled threonine residues represented in ball and stick format; B Ramachandran plot for the MtrR homology model showing no outliers indicating the model is biological feasible**

step. This steric hindrance could therefore account for the low  $K_{cat}$  observed and the addition of inhibitors at Thr and not Ser.<sup>145</sup> The labelling of threonines and not serines indicates a novel mechanism of action for hydrolysis of  $\beta$ -lactams. Despite threonine occurring only 1.1% less often than serine in proteins, the occurrence of active site containing hydrolases and proteases is much less common (based on current understanding gained through x-ray crystal structures and functional protein characterisation).<sup>146</sup> Examples of active site threonine enzymes are Ntn hydrolases, for example gammaglutamyl transferase, penicillinase acylase, and glutaminase-asparaginase (PGA).<sup>147</sup> Crystal structures of bacterial L-asparaginases have also revealed threonines in the active site.<sup>148</sup>

TetR family proteins exist as homodimers and it has been shown for TetR proteins that bind two ligands per dimer (one ligand per subunit), the binding site in each subunit are

slightly different. The crystal structure of phloretin bound to TtgR shows that the contacts between the ligand and the protein are not identical in both subunits of the dimer. One can therefore speculate that labelling of Thr127 and Thr 91 is due to different orientations of clavulanic acid in the ligand binding domain of MtrR. Despite Thr11 being located on the N-terminal helix of MtrR, the homology model predicts that Thr11 is within hydrogen bonding distance ( $< 15\text{\AA}$ ) of H105, and Thr 91 is also close to H105 (Figure 43). This distance is interesting as a naturally occurring H105Y mutation has been reported in the literature in clinical isolates of *N. gonorrhoeae* that exhibit high level penicillin resistance. It was therefore postulated that a H105Y mutant protein would exhibit a higher  $k_{\text{cat}}$  than the parent H105 protein (the protein used thus far in this project). Furthermore, there are reports of tyrosine participating in catalytic triads of class C  $\beta$ -lactamases and in threonine proteases such as L-asparaginase supporting the case for the preparation of mutant H105Y protein for use in catalytic studies.

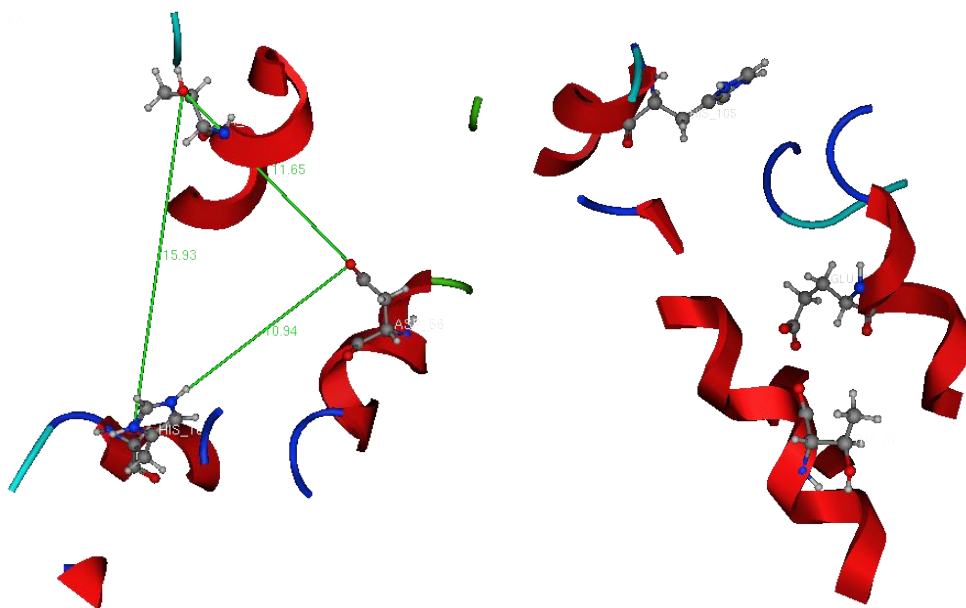


Figure 43 Possible active sites containing labelled threonine residues in MtrR. LEFT : Thr11, His 105, Asp 56; RIGHT: Thr 91, His 105, Glu 70

### 2.2.7 Site directed mutagenesis studies

The mutant MtrR proteins prepared were H105A, H105F and H105Y. The construction of the mutant plasmids was carried out by Bing Zang, a collaborator in the School of Biological and Biomedical Sciences, Durham University. The mutant proteins were

overexpressed and purified using standard techniques and mass spectrometry confirmed the correct mutation was present.

ITC analysis of the mutant proteins with MtrR unfortunately did not yield positive results. There was no discernable pattern in  $K_{cat}$  or  $K_M$  of the mutant proteins, as summarised in Table 5. The highest  $K_{cat}$  was observed in H105F mutant and the lowest in H105Y, a result which contradicts the literature reports that H105Y increases resistance to penicillin.

The results from the site directed mutagenesis study were confusing as they do not support the hypothesis that the H105Y mutation is necessary of high penicillinase activity. Other reports in the literature have suggested that the introduction of tyrosine at 105 disrupts dimer formation in MtrR, however, this is not the case as residue 105 is in the ligand binding domain and not in the protein dimerisation domain (helices 8 -10). The physiological role of the H105Y mutation, is therefore still a matter for investigation.

105 <sup>th</sup> Amino acid	Drug	Kcat /s <sup>-1</sup>	Km / mM
H	Penicillin G (2)	0.0191	0.167
Y		0.00666	0.075
F		0.0567	0.00963
A		0.0175	0.0067

Table 5 Effect of mutation at 105<sup>th</sup> position of MtrR.

### 2.2.9 *In vivo* analysis of $\beta$ -lactamase action of MtrR

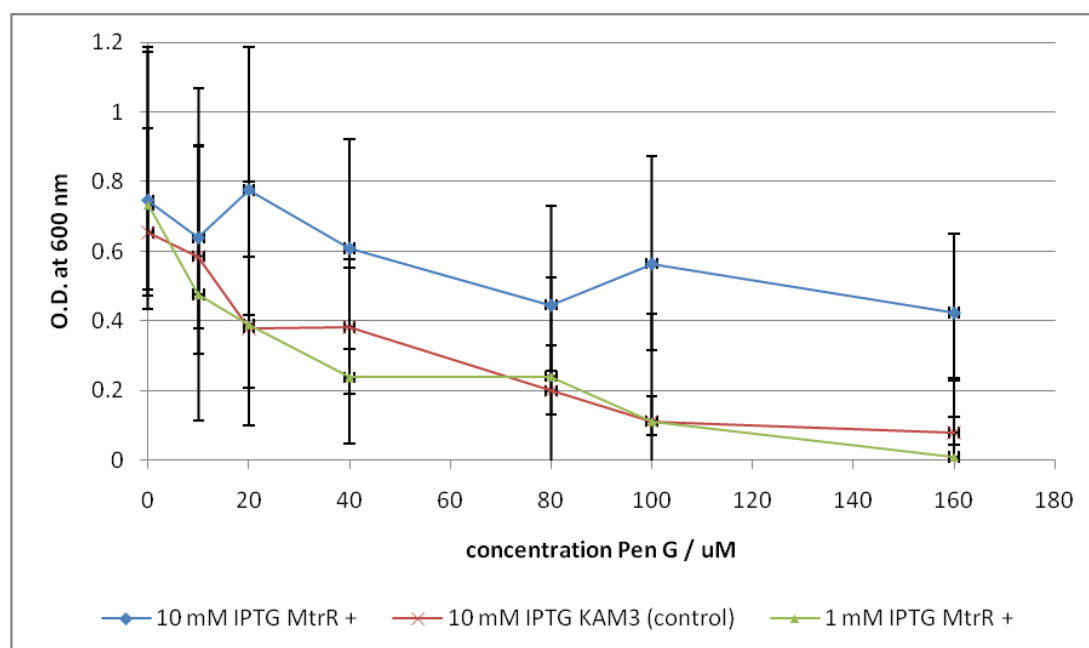
Undeterred by the lack of conclusive data to localise the active site, attention was turned to examining the ability of MtrR to confer resistance to penicillin *in vivo*. With no access to clinical stocks of *N. gonorrhoeae*, a model system was sought that could enable the survival benefit (if any) incurred by expression of MtrR in the presence of benzyl penicillin to be determined.

Mazzariol *et al* showed that deletion of *acrB* transport in a strain of K12 *E. coli*, resulted in a two fold reduction in MIC towards 2.<sup>149</sup> The resultant strain was termed KAM3 and this type of cell has been used to assess the effects of specific proteins on the survival characteristics of bacteria.<sup>150</sup> KAM3 cells are capable of low level production of AmpC  $\beta$ -



lactamase but a double knockout mutant ( $\Delta acrBampC$ ) displayed the same MIC as the single *acrB* mutant implying the background expression of AmpC does not effect the resistance profile of *E.coli*.<sup>151</sup> The KAM3 system is therefore suitable for assessing the effect of MtrR as a  $\beta$ -lactamase expression on cell survival. The strategy employed involved transformation of 'empty' (no plasmid) cells with a plasmid encoding MtrR, inducing production of MtrR followed by dosing the cells with **2** and monitoring growth using UV-Vis spectroscopy and single cell analysis using flow cytometry.

KAM3 *E. coli* were transformed with a pET28 plasmid containing the insert for *mtrR*. Expression of MtrR was induced by IPTG for 2 hours, while a control sample was not induced. Cell cultures were centrifuged, washed and resuspended in fresh LB broth for growth curve analysis to ensure that no IPTG remained. Susceptibility of the *E. coli* strain to penicillin G was followed by the monitoring of bacterial growth for 16 hours in a 96-well plate format using a UV-vis plate reader. Whilst low concentrations of MtrR, as regulated by IPTG (1 mM), afforded minimal benefit, enhanced MtrR (10 mM IPTG) expression led to superior survival rates (Figure 44).



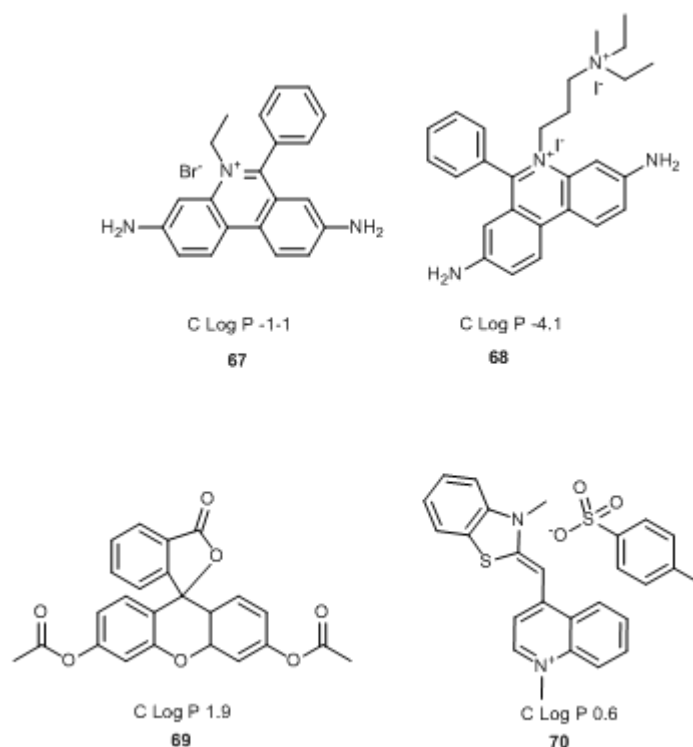
**Figure 44** Survival curve for KAM3 *E. coli* +/- MtrR

40% of cells expressing MtrR survived compared to MtrR negative or cells induced with 1 mM IPTG. The observation that increased survival is related to increased IPTG implies that there is a link between the amount of MtrR produced and the resistance of the cell to penicillin (**2**).

### 2.2.10 Flow cytometry

The use of growth curve monitoring to determine the antimicrobial effects of a compound, as described above, is a standard microbiological technique but this method only describes the whole population. In order to assess cell viability at the level of the single cell, a complimentary technique such as flow cytometry is required. The following section provides a brief overview of the literature on cell viability assays by flow cytometry. This summary is followed by a description of the experiments carried out using this technique in this thesis, and a discussion of the results.

Since the first flow cytometric susceptibility tests (FCST) in the 1980's flow cytometry has developed as an important tool for investigating bacterial susceptibility to antimicrobial agents.<sup>152,153</sup> The principle of the experiment is that the cells are stained with two dyes, each with a distinctive fluorescence emission profile and membrane permeabilities. The degree of membrane permeability is determined by the different levels of fluorescence from each dye. Numerous dyes exist but they can be classified by membrane permeability and the mechanism responsible for switching on the fluorescence. Phenanthridium nucleic acid, cell impermeant dyes such as propidium iodide (PI), ethidium bromide (EB) and ethidium homodimer 1 are typically used to assess plasma membrane integrity as these dyes can only enter membrane permeabilised cells. Inside the cell these compounds bind to DNA resulting in enhanced fluorescence. Thiazole orange is a nucleic acid stain that is able to enter cells with intact plasma membranes, whereas fluorescein diacetate (FDA) is able to cross intact membranes and is a probe for functional esterase enzymes in a cell.



**Figure 45 Viability stains for flow cytometry; ethidium bromide (67), propidium iodide (68), fluorescein diacetate (69), thiazole orange (70)**

The membrane permeabilities for the dye compounds are indicated by the ClogP values, whereby the more negative the ClogP value, the less able the compound is to traverse the membrane. Interrogating each cell with a laser and monitoring the emitted fluorescence enables the extent of staining in each cell to be determined and thus allows for the viability of the cell to be ascertained.<sup>154</sup>

Enzyme based probes that translocate across 'healthy,' intact membranes are also useful probes to ascertain cell viability. Fluorescein diacetate (FDA) can cross cell membranes and then the acetate groups are cleaved by non-specific esterases to yield the green fluorescent probe, detected spectroscopically by measuring the emission at 520 nm ( $\lambda_{\text{ex}} = 488 \text{ nm}$ ). An FDA viability assay was used by Wanandy *et al* for the flow cytometric determination of MIC's of various antibiotics for *E. coli*, *S. aureus* and *P. aeruginosa*.<sup>155</sup>

Flow cytometric viability assays do not always result in a clear live *vs* dead result, as often the bacterial population contains mixed populations resulting in intermediates often described as being in an 'unknown' metabolic state. A detailed study by Berney

and co-workers concluded that different uptake of the SYTO9® nucleic acid stain is due to changes in the composition of the outer membrane in response to UV radiation or treatment with EDTA.<sup>156</sup> Likewise, uptake of SYBR green® nucleic acid stain is higher in exponentially growing bacteria than in stationary phase bacteria. We could use the differences in membrane permeability to our advantage to determine, in detail, the effect of MtrR expression on penicillin resistance.

At the end of the growth curve monitoring experiment, each microwell culture was divided into three aliquots and stained with either 70 or 68 or both (final concentrations of 100 µg /mL) Three discrete populations could be observed, reflecting dead (68), membrane compromised (68 +70), and membrane intact live cells (70). Consistent with a protective effect, populations expressing MtrR have a significantly higher proportion of undamaged cells with an intact membrane (Figure 46).

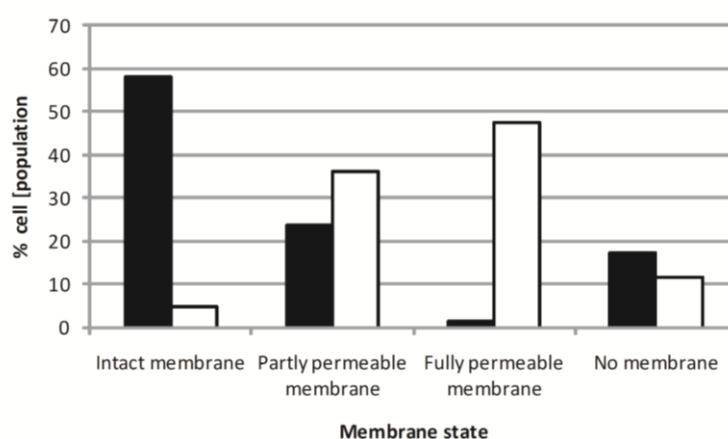


Figure 46 Cell viability as determined by flow cytometric assay. Black bars represent cells expressing MtrR, white bars represent control (MtrR negative) cells

### 2.2.11 Subcellular localisation of MtrR

In order to achieve a protective effect against a  $\beta$ -lactam antibiotic it would be necessary for MtrR to be present at the site of  $\beta$ -lactam action. This occurs in the periplasm and thus requires MtrR to be able to pass through the inner membrane. To investigate whether MtrR exists in the periplasm and the cytoplasm, localisation experiments were conducted and are described below.

Methods for extracting periplasmic protein include treatment of cells with lysozyme-EDTA,<sup>157</sup> or chloroform<sup>158</sup> and osmotic shock.<sup>159</sup> Recent literature shows that the osmotic

shock is reliable for the specific extraction of periplasmic protein without damaging the cytoplasmic membrane.<sup>160,161</sup> This technique involves suspending cells in a hypertonic solution containing 20 % sucrose and 1 mM EDTA at 4 °C or room temperature, followed by suspension in a hypotonic, aqueous buffer. The induced osmotic pressure disrupts the outer membrane causing release of solutes from the periplasmic space. Despite the gentle sucrose buffer method, it is possible that during such a procedure the cytoplasmic membrane is also damaged causing release of cytoplasmic components.<sup>162</sup> If the cytoplasmic membrane is damaged then a cytoplasmic protein such as GroEL could be detected by a specific antibody in the sucrose extract fraction and subsequent washes. Another source of error during an osmotic shock experiment is the forced translocation of protein through mechanosensitive protein channels.<sup>163,164</sup> Gentle pipetting and addition of Gd<sup>3+</sup> salts have been shown to block MscL channels in *E. coli*.<sup>68</sup>

In order to investigate the cellular localisation of MtrR, pET28a–KAM3 cells expressing MtrR were cultured and the periplasmic protein extracted by suspending the cells in ice cold 20 % sucrose solution, in the presence or absence of Gd<sup>3+</sup>. Following Western blotting using an MtrR antibody (Gift from W. M. Shafer, Emory University School of Medicine, Atlanta, USA) bands clearly showing the presence of MtrR could be observed in the periplasmic extracts. Addition of Gd<sup>3+</sup> a known inhibitor of the MscI channel (a mechanosensitive protein translocation mechanism across the inner membrane of *E. coli*) had no effect, indicating that the presence of MtrR in the periplasm is not triggered by the stresses arising from mechanical actions during the experiment such as pipetting and

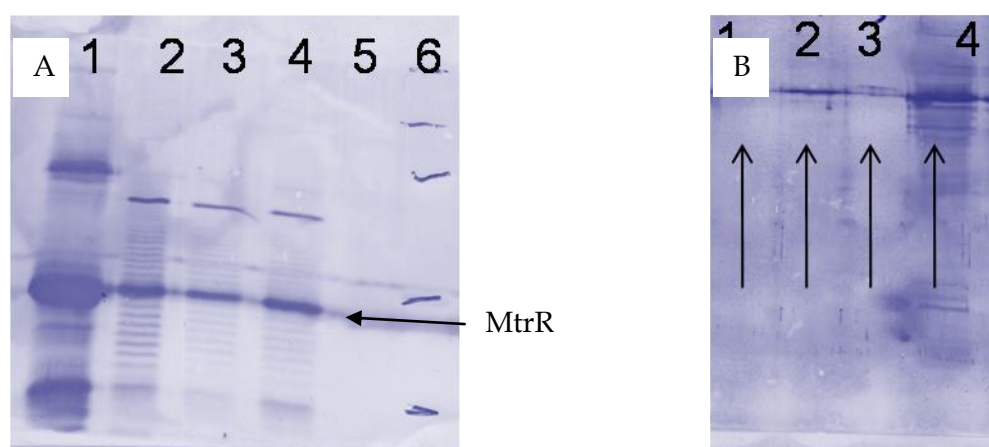


Figure 47 (A) MtrR antibody: Lane 1 Sonicated cells; Lane 2 Osmotic shock + Gd<sup>3+</sup>; Lane 3 Osmotic shock + Gd<sup>3+</sup>; Lane 4 Wash + Gd<sup>3+</sup>; Lane 5 blank; lane 6 MW markers (B) GroEL antibody: Lane 1: Osmotic shock + Gd<sup>3+</sup>; Lane 2 Osmotic shock + Gd<sup>3+</sup>; Lane 3 Wash + Gd<sup>3+</sup>; Lane 4 sonicated cells.

centrifugation. Moreover, a second control experiment using an antibody to the cytoplasmic GroEL protein failed to reveal any protein in the periplasmic extract confirming that the inner membrane remained intact during the sucrose treatment. A second control using an antibody for maltose binding protein failed to detect any protein in any fraction of the osmotic shock experiment.

### 2.3 Summary

The investigation into how small molecule antibiotics interact with MtrR can be summarised as follows:

1. ITC analysis confirms that tetracycline (**11**) and spectinomycin (**10**) are ligands for MtrR.
2. An unexpected binding isotherm was observed for the injection of penicillin G (**2**) into MtrR.
3. Subsequent analysis of the interaction between MtrR and **2** revealed a catalytic process, with  $k_{\text{cat}} = 0.02 \text{ s}^{-1}$  and  $K_{\text{m}} = 107 \text{ }\mu\text{M}$ .
3. MtrR is capable of turning over  $\beta$ -lactamases with small side chains (ampicillin **31**, amoxicillin **32**, penicillin V **29**) but not bulky side chains (nafcillin **33**) and very slowly with cephalosporins (CENTA).
4. Labelling studies with clavulanic acid identified three threonine residues, that were identified using MALDI and ES<sup>+</sup> mass spectroscopic techniques.
5. Modelling studies showed that the amino acids near the labelled threonines could form an active site and were spatially near to H105. Site directed mutagenesis to prepare a H105Y mutant did not reveal any conclusive results.
6. MtrR was shown to confer a survival advantage to hypersusceptible *E. coli* cells and flow cytometric analysis of the *E. coli* cells +/- MtrR showed that ~ 60 % of the MtrR positive cells had intact membranes, compared to ~ 5 % of the MtrR negative cells
7. Subcellular localisation studies showed that MtrR could locate in the periplasm

### 2.4 Conclusions

The experiments presented here confirm that MtrR can recognise substrates of the MtrCDE efflux pump. The ability of MtrR to act as a  $\beta$ -lactamase was a surprising result

but ITC, mass spectroscopic and microbiological assays confirmed this secondary function. The penicillinase activity may be due to an evolutionary process or a shadow of a previous function of MtrR. Further work to investigate this role are detailed in the further work section.

## 3 Peptide probes for MtrR

### 3.1 Introduction

This chapter details the work undertaken to identify peptide ligands for MtrR and to explore whether ligand binding can induce MtrR to dissociate from the operator region DNA for the MtrCDE efflux pump. The peptides synthesised are derived from human antimicrobial peptide LL-37, and a summary of the literature on LL-37 is provided first, followed by the results of the synthesis of the peptide probes used in this project. Results are also presented from the assays designed to investigate the bioactivities of the peptides.

### 3.2 Antimicrobial peptides as substrates for microbial efflux pumps

The hypothesis of this thesis is that the transcriptional regulator MtrR recognises substrates for the multidrug efflux pump, MtrCDE, and ligand binding to MtrR leads to the initiation of pump synthesis. Consequently if the function of MtrR could be modulated such that efflux pump synthesis can be permanently turned off or permanently tuned on (both states would fatally compromise the viability of the gonococcus) then a novel class of antimicrobial compound could be developed. To facilitate this long term aim, it is necessary to construct a detailed understanding of how MtrR binds substrates for the efflux pump.

The multidrug efflux pump MtrCDE from *N. gonorrhoeae* recognises a wide range of substrates including antimicrobial peptides (AMPs), as shown in Figure 11.<sup>165</sup> AMPs are produced by higher level organisms in response to bacterial challenge and are discussed in greater detail in section 3.3. Despite forming an ancient defence mechanism, not all bacteria have evolved efflux pumps that can extrude AMPs. For example deletion of the transport proteins AcrB or MexB from the AcrAB–TolC (*E. coli*) or the MexAB–OprM (*P. aeruginosa*) efflux pump systems respectively has no effect on the MIC value indicating that the efflux pumps do not confer a survival advantage to antimicrobial peptides. This is in contrast to *N. gonorrhoeae*, where deletion of the *mtrD* from the gene cassette causes a substantial reduction in MIC for three peptides tested.

The ability of the MtrCDE efflux pump to export large peptides makes the gonococcal pump unique amongst RND transporters. Assuming that substrates for the efflux pump are also substrates for the transcriptional regulator, MtrR, that controls efflux pump



synthesis then the translocated peptides should also bind MtrR and the following sections discuss research that explores this proposal.

**Table 6 Gram negative efflux pump specificity for antimicrobial peptides from different pathogenic organisms.**

Organism	Strain	MIC Peptide $\mu\text{g}/\text{mL}$			Reference	
		LL-37 (12)	PG-1 (71)	PC-8 (72)		
<i>E. coli</i>	WT	8	ND	ND	166	
	$\Delta\text{acrB}$	8	ND	ND		
<i>P. aeruginosa</i>	WT	16	ND	ND		
	$\Delta\text{oprM}$	16	ND	ND		
<i>N. gonorrhoeae</i>	WT	6.25	2.5	100		165
	$\Delta\text{mtrD}$	0.75	0.3	25		

The sequences of the peptides used in Table 7:

LL-37: LLGDFFRKSKEKIGKEFKRIVQRIKDFLRNLLVPRITES; PC-8: RGGRLARYARRRFAVAVGR,



Understanding how MtrR binds such large and diverse compounds will expand the current level of knowledge regarding substrate binding in TetR type proteins. This chapter introduces the concept of antimicrobial peptides and focuses on the human cathelicidin LL-37; an important host defence agent against gonococcal infection but also a substrate for the MtrCDE system in *N. gonorrhoeae*.

In the results and discussion sections, evidence will be presented that supports the hypothesis that MtrR binds LL-37. Understanding how LL-37 binds the regulator protein is gained by adopting a chemical approach: peptide fragments of LL-37 are synthesised and tested for protein binding capabilities. Bioactivities of the synthesised peptides are determined and peptide fragments with antimicrobial effects are also substrates for the MtrCDE pump. The peptide binding site in MtrR is explored by using a photoactivated activity based protein profiling technique. Electrophoretic mobility shift assays (EMSA)

with LL-37 and derivatives indicate that the peptides do not activate MtrR, raising questions concerning the physiological outcome of peptide binding to MtrR.

### **3.3 Antimicrobial peptides<sup>167</sup>**

#### **3.3.1 Introduction**

Antimicrobial peptides are host defence peptides that have been detected in a wide range of species including amphibians, mammals, bacteria and fungi.<sup>168</sup> There are currently more than 1300 antimicrobial peptides known<sup>169</sup> and these host defence peptides are generally cationic, with between 12-100 amino acids and possess a wide range of structural motifs.<sup>170</sup> Linked to structure is the function of the AMP and an equally wide range of bioactivities have been reported, including antibacterial, antiviral and antifungal properties. In addition there are an increasing number of reports of the immunomodulatory properties of AMP.<sup>171</sup> Humans produce two classes of AMP, defensins<sup>172</sup> and cathelicidins. Whilst humans secrete several peptides from the defensin class, only one example of a cathelicidin peptide is produced. This human cathelicidin, LL-37, is an important peptide as it not only exerts antimicrobial properties but also modulates the immune system and as reported above, the gonococcal efflux pump confers resistance to the peptide.

#### **3.3.2 Cathelicidins**

Cathelicidins are a large family of antimicrobial and immunostimulatory peptides.<sup>173</sup> Whilst most commonly found in mammalian species recent evidence indicates that these proteins are of much older origins with a suggestion that they have evolved from the cystatins, ancient cysteine protease inhibitors.<sup>174</sup> Cathelicidin peptides are characterised not by the structure of the antimicrobial peptide but rather by the form in which they are produced and stored within the cell. All members of this family are synthesised as a preproprotein, Figure 48, comprising a signal peptide, a highly conserved *N*-terminal prosequence termed the cathelin domain and a highly variable *C*-terminal peptide domain in which the antimicrobial activity is found. This last component, the cathelicidin peptide, ranges in size from 12-80 amino acids.<sup>175</sup> Mirroring this lack of primary structure homology, diverse secondary structures have been found. These can be broadly grouped into three classes. The most common are the linear antimicrobial peptides with an  $\alpha$ -helical amphipathic structure, the other groups being i) peptides rich

in amino acids such as arginine, tryptophan and proline, and ii) peptides that have  $\beta$  sheet structures stabilised by disulfide bonds, exemplified by PG-1, a porcine defence peptide.<sup>176</sup> PG-1 is a 18 residue peptide, rich in arginine, amidated at the C-terminus and with disulphide bonds between Cys 6 and Cys 15, and Cys 8 and Cys 13. The disulphide linkages hold the natural product in a strict  $\beta$ -hairpin shape and NMR studies in membrane-like environments have shown that PG-1 monomers dimerise in a head to tail fashion leading to the formation of ion conducting pores in membranes that are responsible for the antimicrobial action of the peptide.<sup>177</sup> PG-1 is considered in more detail in Chapter 4. The remainder of this introduction focuses on the human cathelicidin LL-37, providing a foundation for the subsequent experimental results.

**MKTQRDGHSLGRWSLVLLIIGLVMP LAIIAQVLSYK**  
**EAVLRAIDGINQRSSDANLYRLLDLDPRPTMDGDPD**  
**TPKPVSFVTKETVCPRTTQSPEDCDFKKGDLVKRC**  
**MGTVTLNQARGSFDISCDKDNKR FALLGDFFRKSKE**  
**KIGKEFKRIVQRIKDFLRNLPRTES**

Figure 48. Sequence of the CAMP gene product Signal peptide (red), Cathelin domain (blue); Antimicrobial Peptide LL-37 (green).

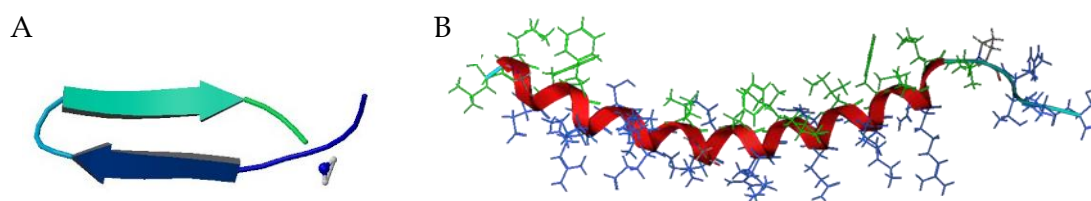


Figure 49 A: PG-1; B: LL-37

### 3.3.3 Human antimicrobial peptide LL-37

The antibacterial and immunomodulatory properties of LL-37 have been widely studied and reviewed elsewhere.<sup>178</sup> Rather than provide an exhaustive catalogue of all the bioactivities of LL-37, the primary aim of this review is to focus on developments in the understanding of how LL-37 acts at a molecular level. The human cathelicidin LL-37 is generated from the proprotein form hCAP18 encoded by the CAMP gene.<sup>179</sup> Following excision of the signal peptide, this proprotein is stored in neutrophil granules and epithelial cells until activated through cleavage by the serine protease, proteinase 3.<sup>186</sup> The actual release of LL-37 is proposed to occur at the cell surface as, on stimulation of

the neutrophil, hCAP-18 locates to the plasma membrane potentially through an interaction with an hCAP-18 specific receptor.<sup>180</sup> In addition to that stored in neutrophils, significant quantities of hCAP-18 are found in human plasma as a complex with lipoproteins.<sup>181</sup> Interestingly, Zaiou has shown that, after cleavage of LL-37, the cathelin domain has antimicrobial properties highlighting how evolution has maximised the antimicrobial function of hCAP18.<sup>182</sup>

As suggested by the name, LL-37 is a 37 residue peptide of sequence, LLGDFFRKSKEKIGKEFKRIVQRIKDFLRNLPRTES, that adopts an  $\alpha$ -helical structure in lipid membranes, micelles, and ions such as hydrocarbonate, sulphate and to a lesser extent chloride, but is a random coil in pure water.<sup>183</sup> Although LL-37 is described as the sole human cathelicidin, other cleavage sites exist leading to different mature peptides. Greatest similarity is seen in ALL-38 found in seminal plasma which contains an additional N-terminal alanine residue arising through cleavage from hCAP18 by gastricsin at the adjacent site to that used to liberate LL-37.<sup>184</sup> Similarly, patients with rosacea, a condition associated with an upregulated immune response, have been shown to possess high levels of FA29, an N terminal fragment of LL-37, as a result of hCAP18 being processed by Stratum corneum tryptic enzyme.<sup>185</sup> Conversely, a number of shorter peptides, derived from LL-37 including **102**, **114**, **120** and **121** are found in human sweat and skin cells.<sup>186</sup> These arise through processing of either hCAP18 or LL-37 by serine proteases in the skin and provide enhanced antimicrobial activity when compared with full length LL-37. This enhanced ability to provide a protective barrier against bacteria etc is accompanied by a reduced immunological function and suggests that this post-translational processing is part of the innate regulation of the multiple functions of LL-37.

### **3.3.4 Bioactivity**

LL-37 has been shown to have a multitude of roles in the body. Originally identified for its antibacterial effects LL-37 also has other antimicrobial properties including antifungal and antiviral activities and the inhibition of biofilm formation.<sup>187</sup> It has also been associated with modulation of the expression profiles of elements of the immune system, regulation of the inflammatory response, stimulation of wound healing, chemotaxis, apoptosis, angiogenesis and cancer tumourgenesis.<sup>188,198</sup> Many of these immunomodulatory functions appear to occur at concentrations below the levels required for antimicrobial activities suggesting that the immune response may arise

from interactions with more specific receptor proteins and have led to LL-37 being labelled an “alarmin”.<sup>189</sup> Reflecting this spectrum of activity, hCAP18 is constitutively expressed in range of inflammatory and epithelial cells particularly in parts of the body exposed to the outside environment, including the airway, gut and urinary tract and also in the circulatory system.<sup>190,191</sup> There is tight regulation of *in vivo* levels of LL-37 through a complex network of signalling pathways. This is important because failure to produce microcidal concentrations of the antimicrobial peptide can result in increased susceptibility to pathogens,<sup>192,193</sup> whereas over-production of LL-37 can lead to inflammatory disorders such as the skin diseases of psoriasis and atopic dermatitis.<sup>194</sup> A large number of external stimuli of LL-37 expression or release have been reported, for example, the presence of bacterial metabolites butyrate and lithocholic acid (LCA) leads to enhanced gene expression. Butyrate enhances histone acylation at the cathelicidin promoter site thus enabling AP.1 (activator protein 1) to bind to the cathelicidin promoter augmenting gene expression,<sup>195</sup> whereas LCA binds nuclear receptors that causing recruitment of the transcriptional factor PU.1, which is key to CAMP gene transcription.<sup>196</sup> Similarly, the yeast strain *Malassezia sympodialis* and bacterial products such as LPS and LTA also enhance LL-37 levels.<sup>197</sup> However, this is primarily due to the foreign lipids activating TLR-like receptors on macrophages, monocytes, and neutrophils, which then release prototypic proinflammatory cytokines, e.g., IL-1, IL-6 and TNF $\alpha$  that trigger release of LL-37 to the extracellular milieu.<sup>198</sup> Conversely, levels of LL-37 can be lowered either through the simple action of bacterial proteases or through more complex, and as yet not well understood, interference in the expression of hCAP-18 expression including a self-regulation pathway.<sup>199</sup> Importantly, proteolytic degradation appears to be one way in which the physiological role of LL-37 is regulated in a location-specific fashion. Notably there are a number of truncated forms of LL-37 found in the skin samples which exhibit reduced immunomodulatory function but retain an antimicrobial effect. Interestingly, both LL-37 and **184**, an LL-37 fragment, isolated from psoriatic skin, induce IL-8 release and hence a pro-inflammatory response, suggesting that, in homeostasis, proteases are utilised to prevent an erroneous immune response to enhanced secretion of LL-37.<sup>200</sup>

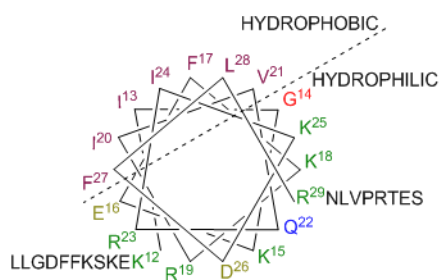


Figure 50 Helical wheel diagram for LL-37 showing the region 12-29 as an amphipathic helix (constructed using [http://www-nmr.cabm.rutgers.edu/bioinformatics/Proteomic\\_tools/Helical\\_wheel/](http://www-nmr.cabm.rutgers.edu/bioinformatics/Proteomic_tools/Helical_wheel/).) N- (residues 1-11) and C- (residues 30-37) termini residues are unstructured.

### 3.3.5 Structure

As can be seen from a classical helical projection, Figure 2 LL-37, is a classical amphiphilic  $\alpha$ -helical peptide. Whilst, at low concentrations ( $< 10^{-5}$  M) it is a largely unfolded monomeric peptide, at higher concentrations it adopts an  $\alpha$ -helical oligomeric structure. This switch can simply be attributed to the hydrophobic effect involving shielding of the hydrophobic face from the bulk medium. The enhanced  $\alpha$ -helical content observed for LL-37 in salt media, particularly that correlating to physiological conditions, is a further reflection of this phenomenon.<sup>182</sup> Reflecting the diverse and important functions of LL-37, there has been considerable effort to understand how these functions are related to peptide sequence and structures. One challenge to this has been to access sufficient quantities of the peptide. Historically these have been obtained from clinical isolates or through chemical synthesis. Recently, various ingenious biotechnological solutions have been developed.<sup>201</sup> Whilst most of these recombinant proteins are produced bearing residual residues derived from the cleavage domain, Ramamoorthy has described a GST fusion construct that affords the unmodified peptide albeit with relatively low levels of cleavage efficiency.

At the simplest level, the structure of LL-37 can be divided into three portions with each section having specific characteristics. The N-terminal unit is a relatively disordered non-polar / hydrophobic section; the central bulk of the peptide is  $\alpha$ -helical, stabilised by a set of ion-pairs spaced  $n/n+3$ , whilst the C-terminal end is best described as a short hydrophilic tail unit. Recent NMR studies of LL-37 in micelles support this view but reveal that there is some flexibility within this central helical core according to the nature of the membrane. In DPC a helix-break-helix motif was found, whereas in SDS and D8PG the structure is better described as a bent helix.<sup>202,203</sup> Significantly this 'bend' region of discontinuity corresponds to area of high glycine content in related primate orthologs.<sup>204</sup> This increased flexibility may relate to the change in role between relatively

unstructured (in solution) congeners which are primarily antimicrobial in activity to the more constrained and aggregated LL-37 in humans which has enhanced immunomodulatory function.<sup>205</sup>

The multifunctional roles of LL-37 *in vivo* has led to intense research into understanding the function of the peptide in terms of physio-chemical properties, for example  $\alpha$ -helicity, charge, hydrophobicity and hydrophilicity. Attempts to modulate these properties in order to separate and modulate the antimicrobial and immunomodulatory / inflammatory responses have led to the generation of a large number of truncated sequences involving both native as well as modified sequences. These peptide derivatives of LL-37 are summarised in Table 7. The correlation between helicity and antimicrobial activity has been reinforced by a number of studies. For example, *N*-terminal peptide **98**, which has a low calculated-helicity of 0.57, has little or no antibacterial activity, whereas the LL-37 central **100** and C-terminal fragment **96**, which have helicity values of 8.32 and 5.51 respectively, retains significant antimicrobial activity. Significantly only fragments **119** and **120**, which most closely resemble LL-37, showed consistently high activity against a range of micro-organisms and retain this activity at high salt concentrations or in the presence of human serum.<sup>206</sup> The designed LL-37 analogue **148** has a calculated helicity eight times greater than that of the natural product (**148** = 44.4; **12** = 5.08) and also exhibits a potent bioactive profile. However, this correlation is not universal as peptides **111** and **112** that have helicities of 0.96 and 0.83 respectively, are more antibacterial than LL-37 towards *E. coli* and MRSA. The high activity is likely to be due to the charge of the peptides (+6 for **111** and +7 for **112**). The presence of the two phenylalanine residues exposed at the *N*-terminus of **111** accounts for the 2 fold increase in anti-*E.coli* activity relative to **112** as aromatic amino acids are known to aid peptide insertion into the bilayer.<sup>207,208</sup>

ID	Sequence	H <sup>a</sup>	% <sup>b</sup>	+ <sup>c</sup>	C $\alpha$ <sup>d</sup>	Rel. Bioactivity <sup>e</sup>			Ref
						LPS <sup>f</sup>	AM <sup>g</sup>	CYT <sup>h</sup>	
12	LLGDFFRKSKEKIGKEFKRIVQRIKDFLRNLPRTES	0.6	54	6	5.08	1	1	1	221
73	LLGDFFRKSKEKIGKEFKRIVQ	0.7	55	4	0.99	< 0.1	ND <sup>i</sup>	ND	221
74	LGDFFRKSKEKIGKEFKRIVQR	0.9	59	5	1.01	< 0.1	ND	ND	221
75	GDFFRKSKEKIGKEFKRIVQRI	0.9	59	5	0.8	< 0.1	ND	ND	221
76	DFFRKSKEKIGKEFKRIVQRIK	1	64	6	0.8	< 0.1	ND	ND	221
77	FFRKSKEKIGKEFKRIVQRIKD	1	64	6	1.23	< 0.1	ND	ND	221
78	FRKSKEKIGKEFKRIVQRIKDF	1	64	6	1.91	< 0.1	ND	ND	221
79	RKSKEKIGKEFKRIVQRIKDFL	1	64	6	2.9	< 0.1	ND	ND	221
80	KSKEKIGKEFKRIVQRIKDFLR	1	64	6	3.81	< 0.1	ND	ND	221
81	SKEKIGKEFKRIVQRIKDFLRN	0.9	64	5	5.6	< 0.1	ND	ND	221
82	KEKIGKEFKRIVQRIKDFLRNL	0.8	59	5	7.98	< 0.1	ND	ND	221
83	EKIGKEFKRIVQRIKDFLRNV	0.6	55	4	8.01	< 0.1	ND	ND	221
84	KIGKEFKRIVQRIKDFLRNVP	0.5	50	5	11.37	0.25	ND	ND	221
85	IGKEFKRIVQRIKDFLRNVP	0.5	50	5	10.99	0.2	ND	ND	221
86	GKEFKRIVQRIKDFLRNVPRT	0.5	50	5	7.44	0.16	ND	ND	221
87	KEFKRIVQRIKDFLRNVPRT	0.7	55	4	5.37	0.2	ND	ND	221
88	EFKRIVQRIKDFLRNVPRTES	0.6	55	3	3.89	< 0.1	ND	ND	221
89	KIGKEFKRIVQRIKDFLRNLPRT	0.6	52	5	7.45	0.5	ND	ND	221
90	KIGKEFKRIVQRIKDFLRNLPRT	0.5	50	6	7.57	0.37	ND	ND	221
91	IGKEFKRIVQRIKDFLRNLPRT	0.5	50	4		0.6	ND	ND	221
92	KIGKEFKRIVQRIKDFLRNLPRT	0.6	52	6	7.58	0.34	ND	ND	221
93	IGKEFKRIVQRIKDFLRNLPRT	0.4	48	5	7.26	0.37	ND	ND	221
94	GKEFKRIVQRIKDFLRNLPRT	0.6	52	4	5.41	0.41	ND	ND	206
95	LLGDFFRKSKEKIGKEFKRIV	0.7	52	5	0.94	ND	0.75	↓	209
96	GKEFKRIVQRIKDFLRNLPRT	0.6	52	6	5.51	ND	1.5	↓	210
97	FKRIVQRIKDFLRNLPRTES	0.4	52	5	3.37	ND	1	↓	210
98	LLGDFFRKSKEK	0.8	58	2	0.57	NE <sup>k</sup>	NE	NE	210
99	IGKEFKRIVQRIKDFLRNLPRTES	0.5	52	4	6.96	ND	0.5	NS	210
100	FKRIVQRIKDFLRNLPRT	0.2	50	5	8.32	ND	2	↑	210
101	FKRIVQRIKDFLR	0.5	54	5	4.29	ND	1	↑	210
102	LLGDFFRKSKEKIGKEFKRIVQR	0.8	57	6		ND	< 0.1	↓	212
103	KRIVQRIKDFLRNLPRTES	0.6	55	4	3.14	ND	< 0.1	↓	212
104	SKEKIGKEFKRIVQRIKDFLR	0.9	62	5	2.75	ND	0.1	↓	212
105	KRIVQRIKDFLR	0.7	58	4	0.79	ND	< 0.1	↓	212
106	KEFKRIVQRIKDFLRNLV	0.5	56	5	3.11	ND	1.2 <sup>l</sup>	NS	214
107	GDFFRKSKEKIGKEFKRIVQRIKDFLRNLPRTES	0.8	57	6	6.08	2.86	0.3	↓	214
108	LLGDFFRKSKEKIGKEFKRIVQRIK	0.7	56	6	1.3	ND	4	NS <sup>m</sup>	214
109	LLGDFFRKSKEKIGKEFKRI	0.8	55	4	0.98	ND	NE	NS	207
110	LLGDFFRKSKEKIGKE	0.9	56	2	1.01	ND	NE	NS	207
111	GDFFRKSKEKIGKEFKRIVQRIK	1	61	6	0.96	ND	4	NS	207
112	RKSKEKIGKEFKRIVQRIK	1.3	68	7	0.84	ND	2	NS	207
113	EKIGKEFKRIVQRIKDFLRN	0.8	60	4	3.67	ND	2	NS	207
114	KRIVQRIKDFLRNLPRTES	0.6	55	4	3.14	ND	NE	NS	207
115	VQRIKDFLRNLPRTES	0.4	53	2	0.52	ND	NE	NS	207
116	EKIGKEFKRIVQRIK	1	60	4	0.79	ND	> 2	NS	207
117	GKEFKRIVQRIKDFLRN	0.7	59	4	2.57	ND	2	NS	207
118	EFKRIVQRIKDFLRN	0.6	60	3	1.65	ND	> 2	NS	207
119	RKSKEKIGKEFKRIVQRIKDFLRNLPRTES	0.9	61	7	6.61	ND	8	↓	207
120	KSKEKIGKEFKRIVQRIKDFLRNLPRTES	0.9	60	6	6.79	ND	8	NS	207
121	EFKRIVQRIKDFLRNLV	0.4	53	3	2.62	ND	< 0.1	↓	211
122	FRKSKEKIGKEFKRIVQRIKDFLRNLV	0.7	59	7	4.67	ND	ND	NS	211
123	KIGKEFKRIVQRIKDFLRNLPRTES	0.6	54	5	7.28	ND	ND	NS	211
124	LLGDFFRKSKEKIGKEFKRIVQRIKDFL	0.6	54	5	2.27	1	ND	ND	212
125	LLGDFFRKSKEKIGKEFKRIVQRIK	0.7	56	6	1.3	1	ND	ND	212
126	LLGDFFRKSKEKIGKEFKR	0.9	58	4	1.00	4.5	ND	ND	212
127	RKSKEKIGKEFKRIVQRIKDFLRNL	1	64	7	4.75	1	ND	ND	212
128	RKSKEKIGKEFKRIVQRIK	1.3	68	7	0.84	3.5	ND	ND	212
129	IGKEFKRIVQRIKDFLRNLPRTES	0.5	52	4	6.96	0.9	ND	ND	212
130	IGKEFKRIVQRIKDFLRNL	0.5	53	4	5.18	1	ND	ND	212
131	IGKEFKRIVQRIK	0.7	54	4	0.82	4	ND	ND	212
132	RIVQRIKDFLRNLPRTES	0.5	53	3	2.39	ND	ND	ND	212
133	NLPRTES	0.4	50	0	0	ND	NS	ND	212
134	KRIVQRIKDFL	0.5	50	1	0	ND	< 0.1	ND	185
135	IVQRIKDFLR	0.3	50	2	0.34	ND	NS	ND	185



136	LLGDRRF	0.4	43	1	0.01	ND	NS	ND	185
137	NLVPR	0	40	1	0	ND	NS	ND	185
138	RKSKEKIGKEF	1	40	0	0.11	ND	NS	ND	185
139	KRIVQRIKDF	0.8	60	3	0.31	ND	<0.1	ND	185
140	RIVQRIKDFL	0.3	50	2	NC <sup>a</sup>	ND	<0.1	ND	185
141	LLGDFFRKSKEKIGKEF	0.8	3	60	0.99	ND	NS	ND	185
142	LLGDF	-0.9	-1	17	0	ND	NS	ND	185
143	LRNLVPRTES	0.4	1	50	0	ND	NS	ND	185
144	LLGDF	-0.6	-1	20	0	ND	NS	ND	185
145	IGKEFKRIVQRIKDFLRNLV <b><u>RPLR</u></b>	0.5	50	6	10.55	0.27	ND	ND	221
146	IGKEF <b><u>ERIV</u></b> QRIKDFLRNLVPRTE	0.5	50	2	6.49	0.16	ND	ND	221
147	IGKEFKRIV <b><u>ERIKDFLRNLV</u></b> <b><u>RPLR</u></b>	0.6	50	3		0.27	ND	ND	221
148	IGKEFKRIV <b><u>ERIKDFLRNLV</u></b> <b><u>RPLR</u></b>	0.7	50	6	44.49	0.52	1.5	ND	221
149	IGKEFKRIV <b><u>ERIKDFLRNLV</u></b> <b><u>RPLR</u></b>	0.8	50	4	43.23	0.17	ND	ND	221
150	IGK <b><u>L</u></b> FKRIVQRIKDFLRNLVPRTES	0.3	48	5	2.7	0.2	ND	ND	221
151	IGKEFKRIV <b><u>QLIKDFLRNLV</u></b> <b><u>RPLR</u></b>	0.3	48	3	8.07	0.22	ND	ND	221
152	IGK <b><u>L</u></b> FKRIV <b><u>QLIKDFLRNLV</u></b> <b><u>RPLR</u></b>	0.1	44	4	5.08	0.35	ND	ND	221
153	IGKEFKRIV <b><u>ERIKDFLRNLV</u></b> <b><u>RPLR</u></b>	0.8	52	2	20.23	0.15	ND	ND	221
154	LLGDFKRIVQRIKDF	0.3	47	3	0.37	0.16	0.25	NE	210
155	<b><i>GFKRIVQRIKDFLRNLV</i></b>	ND	ND	ND	ND	ND	2	NE	210
156	FKRIVQRIKDFLRNLV	0.2	50	5		ND	1	↓	210
157	RLFDKIRQVIRKF	0.5	54	4	2.08	ND	<0.1	ND	211
158	KRIVQRIKDFLR	0.7	58	4	0.79	ND	<0.1	ND	211
159	<b><i>GFKRIVQRIKDFLRNLV</i></b>	0.2	47	4	2.85	ND	0.5°	↑	210
160	<b><i>GFKRIVQRIKDFLRNLV</i></b>	0.2	47	4	ND	ND	NE°	↓	210
161	<b><i>GFKRIVQRIKDFLRNLV</i></b>	0.2	47	4	ND	ND	NE°	↓	210
162	<b><i>GKIKRIVQRIKDFLRNLV</i></b>	0.4	50	4	5.16	ND	0.75°	↓	210
163	<b><i>GKEXRIVQRIKDFLRNLV</i></b>	ND	ND	ND	ND	ND	NE°	↑	210
164	<b><i>GKEWRIVQRIKDFLRNLV</i></b>	0.3	50	4	6.63	ND	0.2°	↓	210
165	<b><i>GKQFKRIVQRIKDFLRNLV</i></b>	0.2	50	5	3.18	ND	0.56°	↓	210
166	<b><i>GKFKREFQRIKDFLRNLV</i></b>	0.6	55	3	6.26	ND	1°	↑	210
167	<b><i>KLFRIVQRIKDFLRNLV</i></b>	0	44	5	7.74	ND	0.75	↑	217
168	KEFKRIV <b><u>KRIKDFLRNLV</u></b>	0.8	56	9	1.13	ND	2	NS	217
169	<b><i>KLFRIVKRIKDFLRNLV</i></b>	0.3	44	8	3.77		0.5	↑	217
170	<b><i>LLGDFFRKSKEKIGKEFKRIVQRIKDFLRNLVPRTES</i></b>	NC	NC	NC	ND	ND	ND	ND	212
171	FRKSKEKIGK <b><u>LFRIVQRIKDFLRNLV</u></b>	0.4	52	7	10	ND	ND	↓	211
172	FRKSKEKIGK <b><u>FRIVQRIKDFLRNLV</u></b>	0.3	52	7	1.22	ND	ND	NS	211
173	LLGN <b><u>FRKSKEKIGKQFKRIVQRIKDFLRNLVPRTES</u></b>	0.2	54	11	2.9	ND	2.3 <sup>p</sup>	ND	218
174	RKKW K <b><u>RIVQRIKDFLRNLVPRTES</u></b>	0.7	58	7	3.79	ND	2.5 <sup>a</sup>	ND	219
175	RKTPFWK <b><u>RIVQRIKDFLRNLVPRTES</u></b>	0.4	50	6	6.64	ND	2.5 <sup>a</sup>	ND	219
176	<b><i>GSLGDFFRKSKEKIGKEFKRIVQRIKDFLRNLVPRTES</i></b>	0.6	54	6	5.7	ND	1	ND	
177	<b><i>PLGDFFRKSKEKIGKEFKRIVQRIKDFLRNLVPRTES</i></b>	0.6	53	6	5.6	ND	1	ND	
178	<b><i>ALLGDFFRKSKEKIGKEFRIVQRIKDFLRNLVPRTES</i></b>	0.6	53	6	5.7	ND	1	ND	
179	<b><i>EFRIQRIKDFLRNLV</i></b>	NC	NC	NC	NC	ND	<0.1	↓	220
180	<b><i>EWRWVQRWKDWLRNLV</i></b>	0.1	53	3	NC	ND	0.25	NS	220
181	Ac- <b><i>EFRIQRIKDFLRNLV</i></b>	0.5	52	2	ND	ND	0.25	↓	220
182	Ac- <b><i>EFRIQRIKDFLRNLV</i></b>	NC	NC	NC	NC	ND	<0.1	↓	220
183	Ac- <b><i>EWRWVQRWKDWLRNLV</i></b>	0.2	53	2	NC	ND	0.25	↑	220
184	<b><i>FALLGDFFRKSKEKIGKEFRIVQRIKDF</i></b>	0.4	48	3	1.11	ND	ND	ND	186
185	DISCDKDNKRF <b><u>ALLGDFFRKSKEKIGK</u></b>	0.9	59	3	2.08	ND	ND	ND	186
186	DISCDKDNKRF <b><u>ALLGDFFRKSKEKIGKE</u></b>	1	61	2	2.11	ND	ND	ND	186
187	<b><i>ALLGDFFRKSKEKIGKEFKRIVQRIKDFLRNLVPRTE</i></b>	0.6	51	6	5.85	ND	ND	ND	228
188	LLGDFFRKSKEKIGKEFKRIVQRIK <b><u>DWLRNLVPRTES</u></b>	0.6	54	6	ND	ND	NS	ND	228

Table 7: LL-37 analogues and derivatives. Bold and underlined indicate non-native amino acids, bold italic indicates D-amino acid, a = hydrophilicity, b = % hydrophobic, + = charge, Ca = calculated  $\alpha$ -helicity, rel. Bioactivity = activity of peptide relative to LL-37

The overall structure of the peptide is a key contributing factor to the bioactive profile of LL-37 and its derivatives. By using NMR techniques to identify disordered regions on binding of peptides to micelles it is possible to show that the predominance of hydrophobic residues in the N-terminal region and the hydrophilic amino acids at the C-terminus make terminal sections of LL-37 unstructured in lipid micelles and therefore not essential for antibacterial activity.<sup>213,214</sup> Wang was able to use this approach to identify a 'core' antibacterial peptide from LL-37, **100**. This showed MIC values against *E.coli* K12 of 20  $\mu\text{M}$  (cf **12** 40  $\mu\text{M}$ ). This highly active is found in many of the degradation products of LL-37 (e.g. **119**, **120**, **109**) notably those detected in human skin and excreted in sweat, that show higher antimicrobial activity than LL-37 but with lower immunostimulatory properties suggesting that this is one way in which the activity of LL-37 may be regulated in vivo.<sup>215</sup>

Further reduction in size of this 'core' region led to the smallest  $\alpha$ -helical fragment of LL-37, **105** to retain antimicrobial effects (40  $\mu\text{M}$  vs *E.coli* K12). Curiously, whilst **105** has reduced host cell toxicity when compared with the one residue longer 'analogue' **101**, further reduction in size to **133**, **134** and **138** lead to almost complete loss of antimicrobial activity.<sup>205</sup> As suggested by these observations, the location and specific nature of the amino acids in the central region of LL-37 appears crucial for the function of the peptide. For example, whilst fragment **100** has increased antimicrobial activity compared to LL-37, it also has significant cytotoxicity compared to **101**. This is rationalised by the presence of hydrophobic residues at the C-terminus that enable the peptide to insert more easily into membranes than analogue **101**.<sup>216</sup> Nagoaka has demonstrated that incorporating Leu at positions 16 and 25 gives the peptide **167** maximum amphiphaticity (average hydrophilicity = 0).<sup>217</sup> Further modification to the core sequence to give peptide **169**, incorporating Lys in place of Asp-26, Gln-22 and Asn-30 increased the cationicity and hydrophilicity whilst maintaining the ratio of hydrophilic: hydrophobic residues. These alterations led to an even more effective antimicrobial peptide that killed 100% of MRSA at 0.1  $\mu\text{M}$ . For comparison, at the same concentration, peptide **106** and LL-37 1 achieved 50% and 30% cell-death respectively.<sup>217</sup> The antibacterial effects of analogue **173**, where acidic side chain are replaced by amides, is not reduced by the presence of plasma protein apolipoprotein A-I indicating that charge, as well as the previously discussed hydrophilic effects, are important in minimising inhibition of the natural product.<sup>218</sup>

Other reports have described peptides that combine elements of the core region with designed peptide motifs. Whilst a combination of the core region with a short LL-37 N terminal sequence led to an inactive peptide coupling of a synthetic antifungal hexapeptide with the C terminal fragment of LL-37 (**148**) provided a conjugate with activity greater than the equivalent length LL-37 fragment **91**. Although the greater degree of helicity induced by this modified *N*-terminus could be responsible for the increase in activity, a better correlation was observed for net charge and hydrophobicity.<sup>219</sup>

In addition to the cell lytic activity, LL-37 has proven to be effective in binding to and thus neutralising LPS and consequently has considerable potential in the treatment of endotoxic shock and sepsis associated with bacterial infections. In order to seek a viable therapeutic agent, there have been a number of attempts to dissect this activity from both the immuno-stimulatory role and general host cell toxicity of LL-37.<sup>220</sup> A common strategy involves initial removal of the *N*-terminal sequence, which is believed to contribute most to the immuno-regulatory function, and then a selective modification of the central core. Consistent with such a suggestion, Nell and co-workers found that the *N*-terminal region (1-12) was not essential for LPS binding, as demonstrated by peptide **91**, whereas removing C-terminal residues (30-37) significantly decreased LPS binding, for example peptides **73** to **83**. Further analysis reveals that a hydrophilicity value of 0.5 and minimum charge of +4 favours LPS binding (peptides **89**, **91**, **94**).<sup>221</sup>

Incorporation of D-amino acids in the peptide can also impact on the function of the natural product. Whilst the enantiomeric peptide **170** retains much of the activity of *L*-LL-37 in stimulating the immune system, suggesting that overall shape, if not helical sense, is important to activity,<sup>209</sup> the selective incorporation of D amino acids into the sequence drastically reduced toxicity towards human cells whilst retaining antimicrobial activity.<sup>212</sup> Structural analysis revealed that, although the introduction of these enantiomeric amino acids maintained an amphipathic structure with an equivalent number of charged side chains on the hydrophilic face, the hydrophobic surface of the peptide was significantly disrupted. This is likely to arise from the D-amino acids distorting the alignment of the peptide backbone causing hydrophobic defects in the amphipathic structure of the peptide.

Analysing the bioactivity profiles of LL-37 and its 118 derivatives in terms of these physio-chemical properties not only aids the design and synthesis of new therapeutic agents but also provides insights into the molecular mode of action of the natural product. Although immunological function can be linked to hydrophobicity and antimicrobial activity to charge and  $\alpha$ -helicity there is still considerable difficulty in predicting a bioactive peptide with minimal unwanted side effects. Only 15 (3 analogues and 12 native fragments) of the reported 118 derivatives have an antimicrobial activity higher than the parent natural product.

### **3.3.6 Molecular mode of action of LL-37**

The previous section highlighted the effect of amino acid substitutions in, and truncations to, the sequence of LL-37 on the observed bioactivity of the peptide. This section will focus on the origins of these effects of LL-37 and various derivatives. In the simplest classification, the biological profile of LL-37 can be dissected into three groups reflecting how LL-37 interacts with membranes; with cellular proteins and with DNA.

LL-37 is a fascinating diversion from most  $\alpha$ -helical AMPs because it does not exhibit high species specificity with in vitro experiments revealing binding to both microbial and mammalian membranes.<sup>222,223</sup> In general, antimicrobial peptides have evolved to target bacterial rather than mammalian cells due to a fundamental difference in the composition of the cell membrane.<sup>224,225</sup> The outer surface of Gram negative bacteria is covered in lipopolysaccharides, and Gram positive bacteria present a surface of teichoic acids resulting in both classes of bacteria having negatively charged cell surfaces. In contrast, most mammalian cell membranes have an outer leaflet comprised of zwitterionic phosphatidylcholine (PC) and sphingomyelin phospholipids (SM), whilst the inner leaflet is composed of phosphatidylserine (PS) leading to an essentially neutral surface. The negative charge associated with bacterial cells means that cationic AMP's are primarily attracted to the pathogenic membrane rather than that of mammalian cells. Consistent with such a model, NMR, epifluorescence and impedance spectroscopic studies revealed that LL-37 readily inserts in monolayers derived from anionic DPPG or Lipid A whereas little penetration occurred into zwitterionic mono-layers derived from DPPC or DOPC.<sup>226</sup> One notable exception is human erythrocytes which contain negatively charged sialic acid units on external glycoproteins rendering these cells are

vulnerable to lysis by cationic peptides and thus accounting, in part, for the observed cytotoxicity of LL-37 derived peptides, e.g. 100, 101 However, *in vivo* host cell cytotoxicity of LL-37 is minimised for two reasons. Firstly, the high concentration of sterols, notably cholesterol and spingomyelin, in the outer leaflet of mammalian cell membranes decreases the ability for LL-37 to insert into the lipid bilayer<sup>227</sup> and, secondly, because serum and apolipoprotein-1 binds the antimicrobial peptide with  $K_d = 0.6-2.4 \mu\text{M}$  effectively reducing the concentration of free peptide.<sup>228,229</sup>

Three general mechanisms have been proposed for how antimicrobial peptides such as LL-37 disrupt membranes and hence exert their antimicrobial effects. These are the barrel-stave model, the carpet model and toroidal mechanism (Figure 51).<sup>230</sup> The barrel-stave model requires that membrane bound peptides recognise each other, oligomerise forming structured transmembrane pores through the membrane through which essential cellular components can escape. Alternatively, in the 'carpet model', peptides coat the phospholipid membrane surface until a threshold concentration is reached when the peptide either permeates the membrane in a detergent like manner or leads to the formation of toroidal holes. In the former, the peptides bind parallel to the membrane surface such that the positively charged amino acids of the peptide can maintain constant contact with the membrane. At this threshold concentration the peptide exerts disruptive forces on the membrane leading to curvature in the membrane lamellae, causing defects and ultimately disintegration of the lipid bilayer. The toroidal-pore mechanism follows a similar initial pathway also involving curvature of the membrane. In this case, self-association of the membrane associated peptides leads to the formation of toroidal (doughnut like) holes in the membrane.<sup>231</sup>

For LL-37 the carpet model appears to be more plausible. Recent studies suggest that on binding to a lipid surface the peptide adopts a helical conformation with a parallel alignment to the membrane surface.<sup>232</sup> NMR studies have demonstrated that, whilst the peptide can diffuse into the bilayer such that the hydrophobic face of the helix interacts with the hydrophobic interior, the orientation to the surface is maintained. Moreover, LL-37 does not re-orientate even under conditions that might favour the adoption of the aggregates need for a transmembrane spanning mode.<sup>233</sup> In addition, LL-37 is suggested to associate to membranes in an oligomeric state in which the (relatively unstructured and non-helical) *N*-terminal amino acids form hydrophobic bundles which facilitate the insertion into the bilayer.<sup>234</sup>

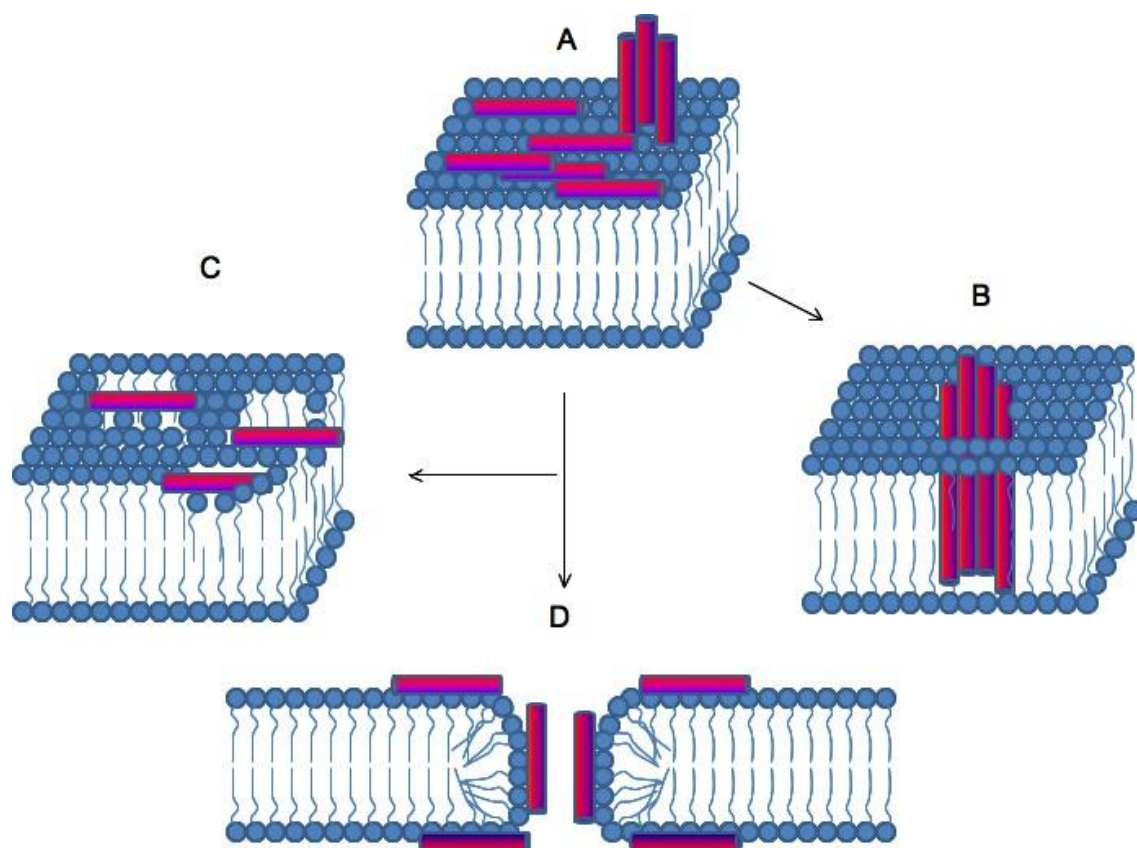


Figure 51 Postulated mechanisms for insertion of LL-37 into membranes. Peptides adsorb to the membrane as either monomers or aggregates (A). Barrel stave mechanism: Peptides insert perpendicular to the bilayer forming a large cylindrical pore lined with peptide oligomers (B). Carpet mechanism: Peptides coat the membrane surface until a critical concentration when either the membrane is disrupted in a detergent like manner (C) or binding to the phospholipid headgroups induces such a high degree of membrane curvature that toroidal pores are formed (D)

Consistent with this, the formation of amyloid-type structures has been observed during the interaction of peptide 179 with a lipid bilayer surface.<sup>224</sup>

Distinguishing between the toroidal-pore and detergent models has proved to be more difficult and appears to be highly dependent on the exact nature of the membrane lipids. For example in DPC micelles NMR studies revealed that, whilst LL-37 induces significant membrane curvature consistent with the peptide maintaining contact with the lipid headgroup as the membrane opens, no evidence could be found for the destruction of the membrane into small fragments indicating a non-pore mechanism. In

contrast, in the case of the fungal membrane found in *Candida albicans*, LL37 induced rapid phase separation and ultimately disintegration of membrane into discrete vesicles resulting in the formation of large pores or channels in the cytoplasmic membrane that allow molecules <40 kDa to diffuse out of the cell.

### **3.3.7 Interactions of LL-37 with mammalian cellular proteins**

As discussed above, although LL-37 can cause significant and selective disruption of microbial membranes, it is also able to interact with the mammalian cell membrane and stimulate a wide range of cell receptors and transcriptional factors. Significantly, it is through stimulating such targets that the human natural product exerts its immunomodulatory effects.<sup>239</sup> For example, DNA array analysis reveals that LL-37 stimulation caused differential expression of over 450 genes in a complex network of signalling pathways.<sup>241</sup> However, despite the wide range of responses caused, there is still surprisingly little known of the precise molecular basis for these responses and a number of potential pathways have been proposed.<sup>235</sup>

The simplest models are those most closely related to the antimicrobial mode of action and rely on the disruption of the lipid bilayer to modulate the function of a membrane bound receptor proteins. Either, AMP binding triggers a chain of events leading to the displacement of a signalling molecule which then activates its cognate receptor or insertion of the AMP into the lipid structure triggers an allosteric change to the receptor structure thus modifying the activity. Evidence for both possibilities have been described. The transactivation of the epidermal growth factor receptor (EGFR) is a key component in the wound healing activity of LL-37 and transactivation of this receptor is an example of the first mode of function.<sup>236,237,238</sup> In this, insertion of LL-37 into the membrane activates a metalloprotease on the cell membrane. This results in the cleavage of the extracellular domain of the membrane bound heparin binding EGF family. The resultant soluble growth factor can locate, bind to and initiate phosphorylation of EGFR, thus activating signalling pathways which ultimately leads to enhanced keratinocyte migration to the wound site and cell proliferation respectively.<sup>239,240</sup> Importantly, EFGR is upregulated in cancer cells and so stimulation of this receptor by LL-37 can lead to cancer cell proliferation.<sup>241</sup> In a related model, it has been proposed that insertion of the peptide into the membrane increases membrane fluidity resulting in leakage of intra-cellular signalling components.<sup>242</sup> For example, insertion of LL-37 into the membrane has been suggested to result in the release of ATP and Ca<sup>2+</sup> that can then

stimulate the P2X7 receptor, an ATP activated ion channel having an important role in inflammation.<sup>243,244</sup> However, other studies have shown that the effect of exogenous ATP but not LL-37 on P2X7 can be inhibited suggesting that LL-37 has a more direct interaction.<sup>245</sup> This alternative mode of activation, relying on a direct allosteric effect triggered by insertion of LL-37 deep into the membrane bilayer has also been proposed to be key to the downregulation of the TLR4 dependent inflammatory response. Surprisingly, such membrane perturbations must be quite specific as unlike P2X7 and TLR4 the related P2Y and TLR2 receptors are not sensitive to LL-37.<sup>246</sup>

In a more classical small molecule receptor interaction model, it has been suggested that LL-37 can function as an alternative ligand for certain receptor proteins. In particular, this mechanism has been proposed for the interaction of LL-37 with the G protein coupled receptor FPRL-1 leading to direct initiation of a signalling cascade, which is currently of interest in cancer research.<sup>247</sup> In support of this, recent inhibitor studies, using simple hydrophobic peptides, WRWWW and WYMV, revealed evidence for direct interaction of LL-37 with FPRL1.<sup>248</sup> The former peptide successfully inhibits LL-37 induced kinase induction in fibroblasts.<sup>249</sup> Furthermore F2L (Ac-MLGMIKNSLFGSV-ETWPWQVL; average hydrophilicity = - 0.7, % hydrophilicity = 29 %) inhibits LL-37 induced chemotactic migration in human vascular epithelial cells suggesting the peptides occupy similar binding sites.<sup>250</sup>

The final model proposed for LL-37 induced action is an indirect process arising from scavenging of other signalling molecules of either host or external origin. For example, LL-37 is effective at negating excessive inflammation in wounds as part of the immune response by binding bacterial products such as lipopolysaccharide and lipoteichoic acid thus preventing activation of the Toll Like Receptors (TLRs). The positive charge associated with LL-37 enables the peptide to bind LPS/LTA preventing the bacterial saccharides from binding to lipopolysaccharide binding proteins or its receptor. In support of this idea, complex formation between the LL-37 and bacterial product can be enhanced by truncation of both the N and C termini to produce peptide **79**, which has a greater positive charge.<sup>251</sup>

More detailed mechanisms at the molecular level for the action of LL-37 are still a matter for debate and, as indicated above, remain very much target protein / system specific. In all these models, as with antimicrobial activity, it appears likely that it is the  $\alpha$ -helical



and hydrophobic nature of LL-37 that is key. In support of this, analogues which retain similar helicity, although not necessarily helical sense e.g. enantiomeric (all D, 101) LL-37, exhibit similar effects whilst relatively unstructured orthologues do not.<sup>84</sup> Such concepts are more challenging for the receptor binding model and one suggestion that accounts for the hydrophobicity and  $\alpha$ -helicity of LL-37 and the all D-amino acid analogue is that the cell receptors contain a 'promiscuous' binding domain or hydrophobic binding groove that recognises lower order structural features of a ligand.<sup>252,253</sup> These structural features are exploited in the design of high affinity, engineered small protein ligands for LL-37 responsive receptors.<sup>254,255,256</sup> These results are consistent with the concept of LL-37 acting as hydrophobic signalling molecule as part of an ancient response mechanism.

### **3.3.8 Interactions with DNA**

As discussed above, LL-37 achieves membrane selectivity through preferential binding to the negatively charged microbial membrane lipids. The other common negatively charged biomolecules are nucleic acids and although the association of LL-37 with DNA is a relatively unexplored area but there is growing evidence that these interactions can influence both transport, immunomodulatory and antimicrobial effects.<sup>257</sup> For example, psoriasis is an autoimmune disease characterised by an upregulation in the production of LL-37 and an overactive immune response. Lande has rationalised these observations by showing that, through binding to LL-37, self-DNA can form condensed aggregates capable of translocation to plasmacytoid dendritic cells where they stimulate interferon production through interactions with the toll like receptor (TLR9).<sup>258</sup> Whilst electrostatic attraction is likely to be a key factor, structure remains important as a scrambled analogue GL-37 was not able to bind the DNA.

Similarly through binding to LL-37 plasmid DNA a similar binding of LL-37 to DNA (and F-actin) is associated with increased severity of microbial infection in patients with cystic fibrosis.<sup>259</sup> This binding appears to require poly valency in the anionic component as treatment of these LL-37 : DNA bundles with human DNase I or poly-aspartic acid releases the antimicrobial peptide and such methods may provide a new regime for treatment of chronic airway infections.<sup>260,261</sup>

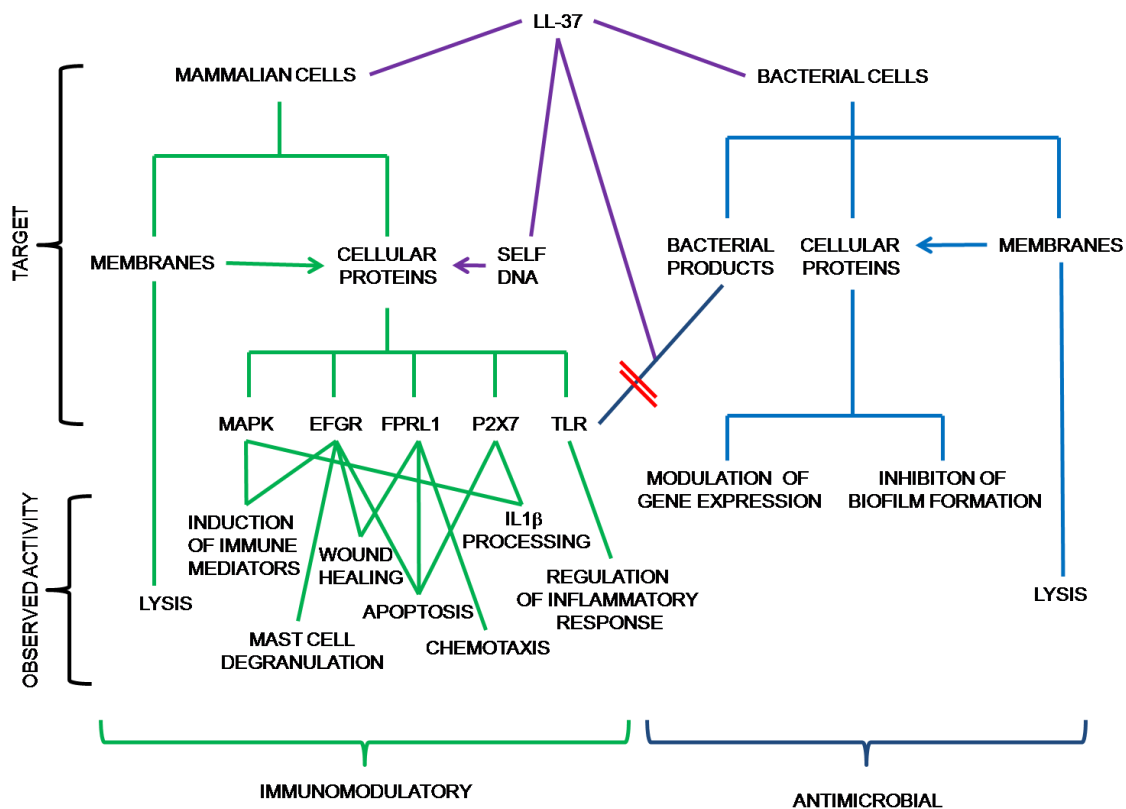


Figure 52 Web of *in vivo* LL-37 interactions<sup>167</sup>

### 3.3.9 Conclusions

It is clear from analysing the mode of action of LL-37 that the antimicrobial and immunomodulatory effects of the peptide are interlinked and dependent on the key properties of charge, helicity and amphiphaticity. The interplay between LL-37, mammalian and microbial systems, and the complex pathways influenced by this natural product are summarised in Figure 52.

Reflecting the growing challenge of microbial resistance to conventional small molecule antibiotics there is a growing number of reports describing attempts to isolate and optimise the antimicrobial and other activities from the various responses revealed by LL-37 and other AMPs. A major motivation for such an approach is that AMPs, unlike conventional antibiotics are less likely to lead to a general resistance process than any small molecule class of antibiotic. However a number of challenges remain notably cost, *in vivo* stability and selectivity.<sup>130,262</sup> LL-37 has potential roles in many therapeutic areas; as an antibacterial agent including the inhibition of biofilm formation, and also in the treatment of inflammation, cancer, HIV, and fungal infections.<sup>263,264,265</sup> The specific challenges in the application of LL-37 in these contexts reside in the need to simplify the

structure (reducing production costs) and reduce host-cell toxicity whilst maintaining stability to general proteolysis and enhancing activity and selectivity. To this end several AMP databases and prediction software programmes have been developed for use by chemists and biologists.<sup>266</sup>

The multifarious activity profile of LL-37 makes it a fascinating natural product to study. Despite intense research into the physiological role of LL-37 since its discovery in degranulated granulocytes in 1996 there is still much to understand and investigate. The production of derivatives and analogues of the antimicrobial peptide sequence has revealed a wealth of knowledge regarding how the structure affects the function of the peptide but unravelling the molecular mechanisms that underpin how LL-37 acts remains a challenging problem. The ability to tune the physio-chemical properties, notably amphipathicity, helicity and charge, of LL-37 so that its activity can be altered makes the peptide an ideal foundation for the development of new therapeutic agents.

With the knowledge gained from the reported structure-activity relationships LL-37, and the reports that LL-37 is a substrate for the MtrCDE efflux pump, this chapter presents work done to characterise the interaction of LL-37 with MtrR. The following sections summarise techniques applied in the course of this research project to analyse how LL-37 and chemically synthesised derivatives interact with MtrR and the MtrCDE efflux pump.

### **3.4 Interaction studies**

In order to investigate how LL-37 and synthetic peptides interact with MtrR, isothermal titration calorimetry (ITC) was used. Isothermal titration calorimetry provides a label free experiment for the determination of thermodynamic parameters for protein : ligand interactions, *viz.* the association constant ( $K_a$ ), stoichiometry ( $n$ ), free energy ( $\Delta G^\circ$ ), enthalpy ( $\Delta H^\circ$ ) and entropy ( $\Delta S$ ) of binding<sup>267</sup>. ITC studies have revealed valuable information about the ligand specificity and the strength of interactions for ligand : TetR protein interactions as discussed in the introduction. To further characterise peptide : MtrR binding a photoactivated binding study strategy was instigated. The principles of activity based protein profiling are discussed below.

### 3.4.1 Activity based protein profiling

ITC gives a wealth of information regarding the thermodynamics of binding but no direct structural information about the site of binding. Consequently other methods are needed to provide structural information and these can include X-ray crystallography and Activity Based Protein Profiling (ABPP).<sup>268</sup> These are complementary techniques as a crystal structure is not always available and so ABPP then becomes the method of choice for mapping the binding pocket of a protein. ABPP can also supplement other structures generated from X-ray studies as ABPP is a solution state technique whereas the information gained from the crystal structure represents only the solid state structure, in which the protein may adopt a different conformation. Two key processes occur in an ABPP experiment - firstly ligand capture and second analysis. There are three different methods that have been developed to enable ligand capture are shown in Figure 53.

Typically, the ABPP probes contain a functional group that reacts with the nucleophilic residue of the protein (Figure 53). If the probe carries a purification tag, *e.g.* biotin, the protein of interest can be pulled out of the protein pool by affinity chromatography

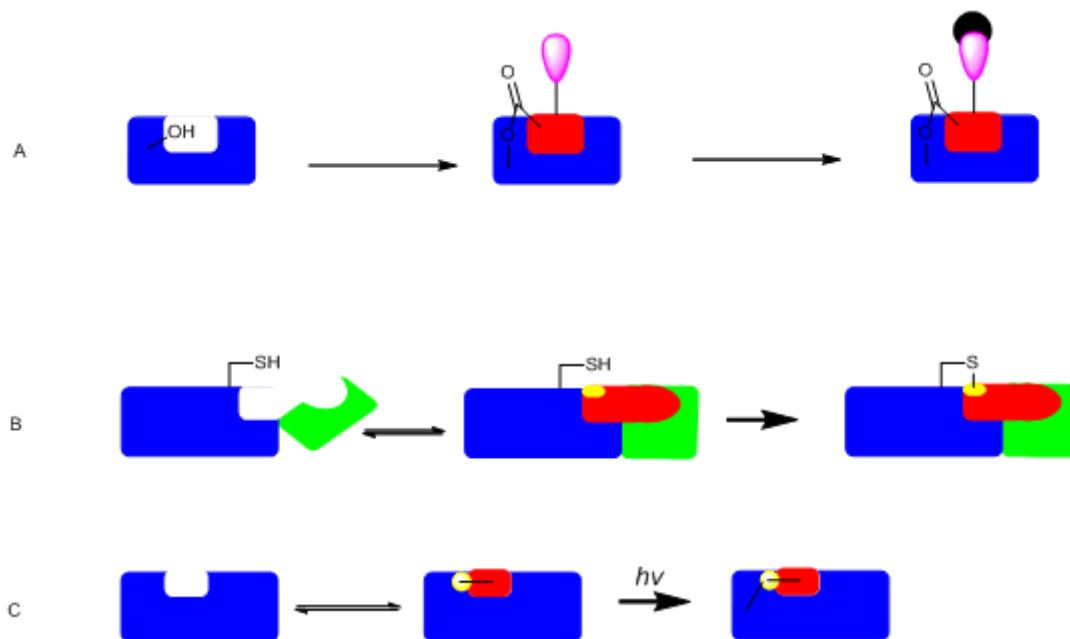


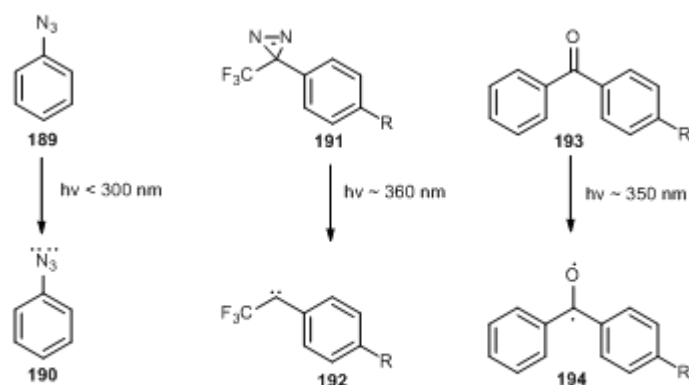
Figure 53 Different approaches to activity based protein profiling (ABPP): A) Reactive nucleophilic amino acid side chain reacts with ligand to form a covalent adduct. The ligand modified protein can then be separated from other proteins by using affinity chromatography. B) A reactive cysteine near the ligand binding site cross links the ligand trapping the protein in the ligand bound form (Proximity Induced Covalent Capture). C) A high affinity ligand bearing a photoactivateable cross linking group is held in the ligand binding site by non-covalent interactions until irradiation with UV light causes the photoactivated group to react with the protein forming a covalent bond.

(streptavidin is used as the binding partner for biotin). During this project experiments were carried out on recombinant purified protein so using ABPP probes for use *in vivo* or with mixtures of proteins will not be discussed further. For target proteins that can be expressed using recombinant techniques but do not contain an active site nucleophile, a reactive cysteine can be engineered into the protein for reaction with an electrophilic centre on the ligand (*e.g.* Michael acceptor B, Figure 53). Once the ligand is located in the active site, the reactive amino acid can form a covalent bond with the probe trapping the protein in the ligand bound state. This technique is termed Proximity Induced Covalent Capture (PICC). The third type of ABPP is affinity controlled, photoreactive ligand capture (C, Figure 53).<sup>269</sup> In this technique the ligand binds in the ligand binding site and then the sample is irradiated with a UV source, activating a reactive group in the probe to crosslink the protein.

MtrR contains a large ligand binding site that is composed of six  $\alpha$ -helices, as is seen in all members of the TetR family of proteins. In order to probe the binding of peptide ligands to MtrR by PICC, several mutations would be required in order to cover the large surface area of the ligand binding site. The mutations may affect the stability of the protein and the introduction of extra cysteines may alter the structure of the protein as there are already four cysteines present in the wild type protein. For these reasons, PICC was discounted as an appropriate method to map the ligand binding site of MtrR and instead an affinity controlled, photoreactive ligand capture approach was followed. The following section details literature reports of photoreactive ligand capture peptide probes that influenced the design of photoreactive ligand capture experiments implemented in this thesis.

#### ***3.4.1.1 Photoactivated activity based protein profiling***

The aryl azides (**189**), benzophenone (**190**) and diazirine (**193**) moieties have been developed as photophores that generate reactive intermediates on irradiation with UV light, which can insert into a nearby C-H bond of a protein (Figure 54).<sup>270</sup> Both the benzophenone and diazirines have the advantage that they are activated with light > 350 nm, which is not damaging to biomolecules. Aryl azides, however, are activated with light < 300 nm, which can effect the integrity of biomolecules. The nitrene (**190**) generated by irradiation of **189** is also highly promiscuous compared to radicals **192** and **193** therefore aryl azides were discounted as an option in this study.



**Figure 54** Photophores for protein labelling and the reactive intermediates generated on irradiation with UV light specific for each photophore.

The carbene produced by irradiation of **191** has been shown to insert more selectively than **190**, but **192** is more prone to side reactions and insertion with solvent molecules than the carbonyl diradical of the benzophenone system (**194**).<sup>271</sup> Diazirine carbenes react more quickly than carbonyl diradicals and so to increase the likelihood of a specific insertion in to an unactivated protein C-H bond the benzophenone moiety (**194**) was chosen as the photophore of choice for this project. The photochemistry and application of the benzophenone photolabel will now be described in more detail.

#### 3.4.1.2 Benzophenone containing photoactivated ABPP

Absorption of a photon at  $\sim 350 \text{ nm}$  results in the promotion of an electron from the non-bonding  $sp^2$ -like  $n$  orbital on oxygen to an antibonding  $\pi^*$  orbital of the carbonyl (Figure 55).<sup>272</sup> The oxygen  $n$ -orbital thus has electrophilic character and interacts with a nearby weak C-H  $\sigma$ -bond resulting in proton abstraction. The resulting ketyl and alkyl radicals recombine to give a new C-C bond. The lifetime of the diradical is 100 times longer than the singlet state and the excited state will relax to the ground state if no suitable proton is available for abstraction. The ability for the excited state to return to that stable ground state is one of the main advantages over diazirine and aryl azides in photolabelling experiments as the benzophenone moiety can go through several cycles of excitation before inserting into a C-H bond, whereas the carbene of the diazirine and nitrene of an azide must react immediately when formed.<sup>273,274</sup>

ABPP peptide probes containing a benzophenone moiety have been used to investigate several protein families such as metalloproteases,<sup>275</sup> RAS,<sup>276</sup> and G-coupled protein receptors as highlighted in Figure 56.<sup>277</sup> The photolabel can be placed in the sequence of

the peptide by use of Fmoc-benzoyl phenylalanine as the amino acid building block, or on an amino acid side chain or at the N-terminus. The benzophenone peptide probes designed in this thesis are described in section 3.5.5.3.

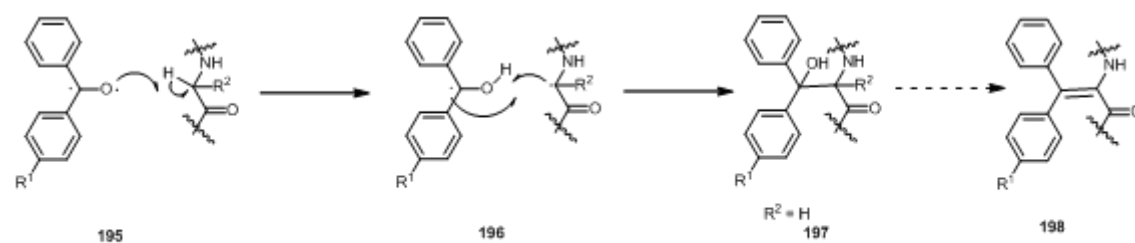


Figure 55 Photochemistry of the benzophenone system

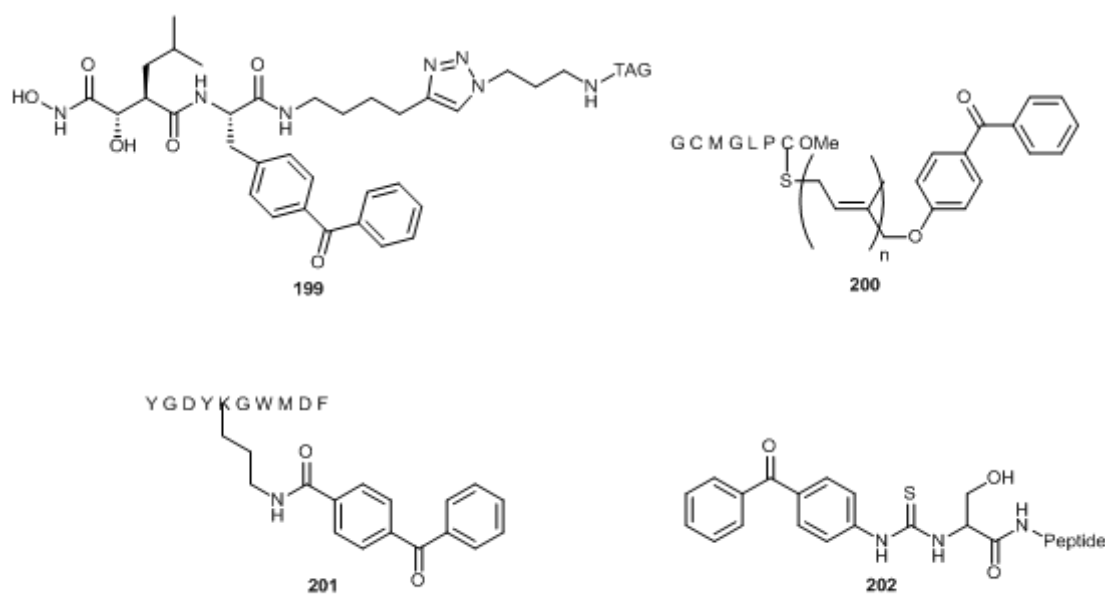


Figure 56 Structures of benzophenone containing peptide ABPP probes. Incorporation of benzoyl phenylalanine amino acid in metalloprotease probe (199); RAS peptide probe carrying a benzophenone modified farnesyl side chain (200); C) Probe for cholecystokin receptor (a G-coupled receptor) with a modified lysine side chain (201); D) N-terminally modified inflammatory protein-1R (MIP-1R) probe for chemokine receptor 1 (a G-coupled receptor) (202).

### *3.4.1.3 Techniques for analysing ABPP experiments*

The ABPP probes bound to the protein were analysed using mass spectrometry. The insertion of the peptide into the protein can be confirmed by MALDI or electrospray mass spectrometry. The location of the modification can be located by proteolytic digestion of the complex, followed by either MALDI or electrospray analysis of the peptides. Sample preparation for MALDI analysis is quick and no chromatography is necessary enabling rapid determination of modified peptides, by either comparison to control samples or database searches. For example, 1  $\mu\text{L}$  of the trypsin peptide solution containing buffer can be mixed with  $\sim 1 \mu\text{L}$  of MALDI matrix (for peptides typically this is  $\alpha$  cyano-4-hydroxycinnamic acid) and provide enough sample for several analyses by MALDI. MALDI analysis typically yields singly charged peptides whereas electrospray yields doubly charged peptides. Samples analysed by electrospray are subject to HPLC to separate out the constituent peptides to facilitate identification. LC-MS analysis requires more time than MALDI, but typically a greater mass accuracy can be achieved on electrospray systems such as Fourier Transform Ion Cyclotron (FT-ICR) or quadrupole devices than on MALDI instruments and so greater confidence can be placed in the observed masses.<sup>278</sup>

Once novel peptides have been identified, these can be further interrogated by MS / MS experiments to locate the position of modification. The LIFT technique can be used on a MALDI instrument, whereby the peptide of interest is selected in an ion trap, the laser power increased to a sufficient level to fragment the peptide along the peptide backbone to give predominantly b and y ions (Figure 57). Several techniques have been developed on electrospray instruments for sequence determination and these include collision induced dissociation (CID) and electron capture dissociation (ECD). In CID, the selected ion is held in a trap with an inert gas and collisions between the peptide and the gas molecules induces peptide fragmentation, principally yielding b and y ions (Figure 57).



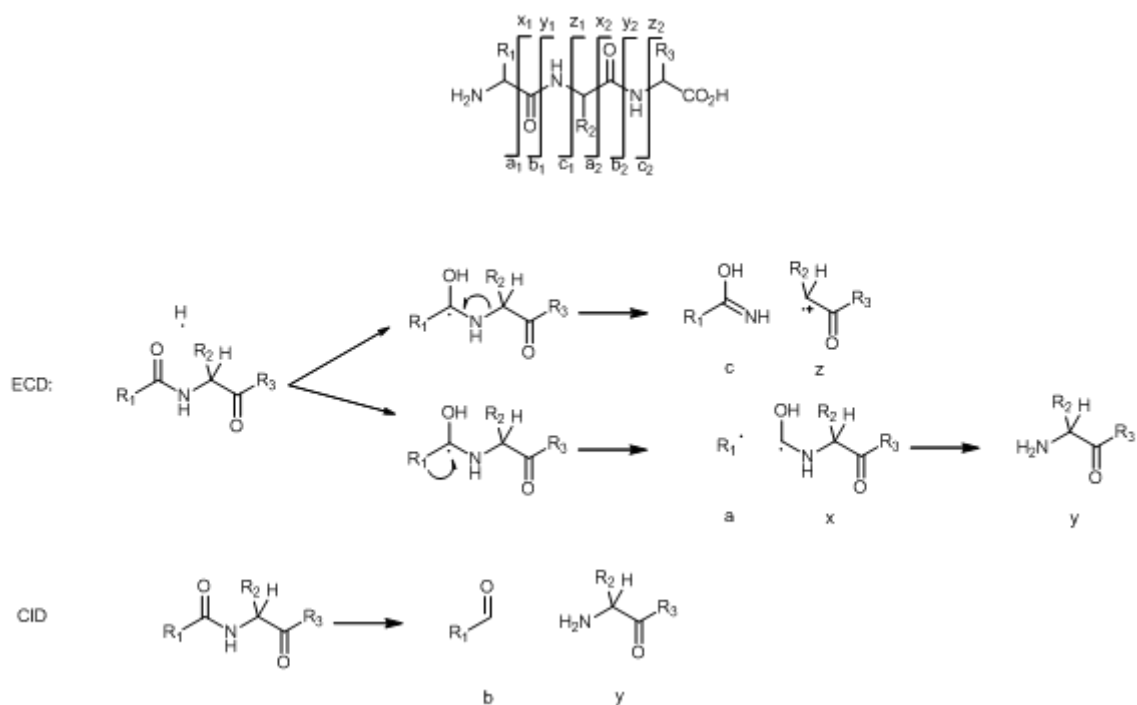


Figure 57 Generation of fragment ions in peptide MS/MS

Analysis using an FT-ICR instrument allows for ECD analyses to be carried out that generates  $C_\alpha$ -N cleavages enabling  $c$  and  $z$  fragments to be generated, with smaller amounts of  $b$  and  $y$  ions. The complementary nature of MALDI and ESI techniques allows a vast amount of sequence data to be generated that can locate where an ABPP has inserted into a protein.

## 3.5 Results and discussion

### 3.5.1 Introduction

The hypothesis of this thesis is that in order for MtrR to dissociate from the operator DNA of the MtrCDE genes, ligands bind to MtrR. The substrates for MtrCDE efflux pump are putative ligands for MtrR. LL-37 is a candidate ligand for the regulator as it has been shown to be transported by MtrCDE and cellular studies have shown the LL-37 can translocate to the nucleus and target DNA so it is possible for LL-37 to migrate to where MtrR is bound to DNA. The following chapter begins with preliminary studies that confirm LL-37 as a ligand for MtrR. The design and synthesis of peptide fragments of LL-37 is discussed followed by a range of studies used to characterise the function of the peptides.

### 3.5.2 LL-37 MtrR ITC study

In order to probe the nature of the interaction between the human antimicrobial peptide LL-37 and MtrR, ITC was used. Recombinant MtrR was obtained from over-expression in *E. coli* as detailed in chapter 2. The protein was dialysed overnight into the ITC analysis buffer (Tris 20 mM, NaCl 300 mM, pH 8.2), and the same buffer was used to solubilise LL-37 (gift from Dr Peter Henklein, Institute for Biochemistry, Charité University Berlin).

The ITC trace shows that LL-37 (1  $\mu\text{M}$ ) binds weakly MtrR (70  $\mu\text{M}$ ) (Figure 58). The initial endothermic reaction is due to the oligomers of LL-37 dissociating in solution, an enthalpy that is larger than the binding interaction between the regulator protein and the peptide. Attempts to decrease the heat of dilution by altering the injection volume of the ligand were unsuccessful. Decreasing the injection volume from 10  $\mu\text{L}$  to 4  $\mu\text{L}$  did not produce enough signal to see a binding isotherm. Analysis of such data can be supported by reference to the literature, and particularly to host-guest complexation in cavitands as such interactions have been used to model protein ligand interactions. In the supramolecular host-guest interaction, an amphiphilic ligand inserts into a hydrophobic cavity inside a cyclodextran, mimicking the insertion of amphiphilic peptide into a protein.<sup>279</sup> Similar binding profiles to the LL-37 MtrR interaction were seen for the binding of organic carboxylates to 15-metallocrown-5 complexes.<sup>280</sup> With confirmation that LL-37 is a ligand for MtrR, we initiated a chemical strategy to investigate how LL-37 binds MtrR by dividing the peptide into sections and analysing each section for protein binding.

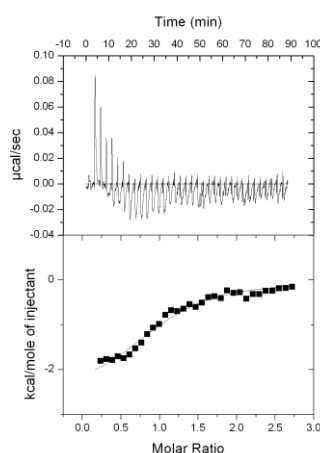


Figure 58 ITC of LL-37 and MtrR.  $N = 1.1$ ,  $K_a = 1.1 \times 10^{-5}$ ,  $\Delta H = -2577 \pm 190 \text{ kJ mol}^{-1}$ ,  $\Delta S = 14.5 \text{ kJ mol}^{-1} \text{ K}$

It has been proposed that regulation of TetR protein can function by one of three mechanisms: disruption of the dimerisation domain, occupation of the ligand binding pocket or competition for operator DNA. Each mechanism arises from a particular property of a peptide:  $\alpha$ -helicity determines the ability to prevent dimerisation, hydrophobicity governs the ability to insert into hydrophobic pockets and charge is the mediating factor in competing for DNA. In order to understand how LL-37 binds MtrR and if binding to MtrR affects the function of the transcriptional regulator, a range of derivatives of LL-37 were designed. The following section details the design, synthesis and evaluation of LL-37 derivatives binding to MtrR.

### 3.5.2 Peptide synthesis plan

LL-37 is a large molecule (MW > 4000 Da) and the overview of the peptide in section 3.3 showed that its different functions are due to key motifs within the structure of the peptide. We reasoned that the binding to MtrR (Figure 58) may be due to a key binding motif that we hoped to access through structure function studies. The ability for only a small motif of a large effector molecule to cause activation or repression of protein function is exemplified by the activation of nuclear cell receptors. The androgen receptor (AR) is a nuclear transcription factor involved in ligand inducible gene regulation of male sexual development, prostate growth and bone metabolism. The naturally occurring cellular coactivators of AR are large ~ 600 amino acid proteins that contain an LXXL or FXXLF helix motif that binds to a hydrophobic groove on the AR surface.<sup>281</sup> It has been shown that activation of the AR can be achieved when the helical motifs (LXXL or FXXLF) is contained in much smaller (~ 20 amino acid) peptides.

In order to probe whether  $\alpha$ -helicity is important for LL-37 to bind to MtrR, peptides **99** and **101** were selected. Peptide fragment **101** of LL-37 is known in the literature to be the minimum  $\alpha$ -helical peptide required to maintain antimicrobial activity (see section 3.3.5) and as part of this thesis we investigated the correlation between  $\alpha$ -helicity of the ligand and MtrR binding.



Figure 59 Regions of LL-37 to be synthesised to probe the different properties that effect binding to MtrR

Table 8 Physiochemical properties of the planned fragments of LL-37.

Sequence	Hydrophilicity	Charge	Predicted $\alpha$ -helicity
LL-37 ( <b>12</b> )	0.6	6	5.0
FLRNLPRTES ( <b>203</b> )	0.1	1	0.01
FKRIVQRIKDFLR( <b>101</b> )	0.7	4	4.29
IGKEFKRIVQRIKDFLRNLPRTES ( <b>99</b> )	0.5	4	6.96
LLGDFFRKSK ( <b>204</b> )	0.4	3	0.63

Hydrophilicity is calculated using the Innovagen property calculator ([www.innovagen.se](http://www.innovagen.se)) with hydrophilicity values taken from Hopp and Woods.<sup>282</sup>  $\alpha$ -helicity is predicted using the AGADIR online calculator ([www.agadir.crg.es](http://www.agadir.crg.es))

The peptide sequences to the N and C-terminus of the central peptide (**101**) display different hydrophobicities and charges. To investigate the effect of hydrophobicity on binding to MtrR, we designed peptide **203**. The low hydrophilicity (0.1, Table 6) suggests that this peptide would be suitable for inserting into the hydrophobic binding pocket of MtrR.

In contrast to the C-terminal peptide, the N-terminal 12 residues (**204**) display a hydrophilic profile. The acidic and basic amino acids present in the peptide sequence may enable the peptide to bind (via salt bridges) to the DNA binding domain of MtrR and thus act as a competitor for DNA thereby enabling a further mechanism for peptide binding to MtrR to be investigated. The N-terminal domain **92** has also been shown to be necessary for **12** to form oligomers and so peptide **99** was synthesised to investigate whether removal of the oligomerisation domain increases binding to MtrR.

The peptides synthesised in this thesis were constructed using Fmoc solid phase peptide synthesis (SPPS) Figure 60. The principle advantages of Fmoc SPPS over Boc SPPS, are the conditions required to remove the *N*-terminal protecting group and cleave the peptide from the resin. The *tert*-butyloxycarbonyl group requires treatment with trifluoroacetic acid, whereas the *N*<sup>α</sup>-Fluorenylmethoxycarbonyl protecting group is removed by mild bases, e.g. piperidine and morpholine, that abstract the acidic fluorenyl proton ( $pK_a \sim 22$ ). Repetitive treatment with TFA during peptide synthesis increases the risk of peptide degradation during synthesis, which is avoided during Fmoc SPPS.<sup>283</sup>

A further advantage of Fmoc chemistry is that the leaving group has a chromophore thus the deprotection reaction can be monitored by UV absorption spectroscopy at 290 nm. There are two advantages from monitoring the cleavage of the *N*-terminal blocking group, namely the speed of the deprotection gives an indication of the extent of chain aggregation during peptide synthesis and secondly the amount of the piperidine-fluorene adduct can be quantified, thus the resin loading can be determined.

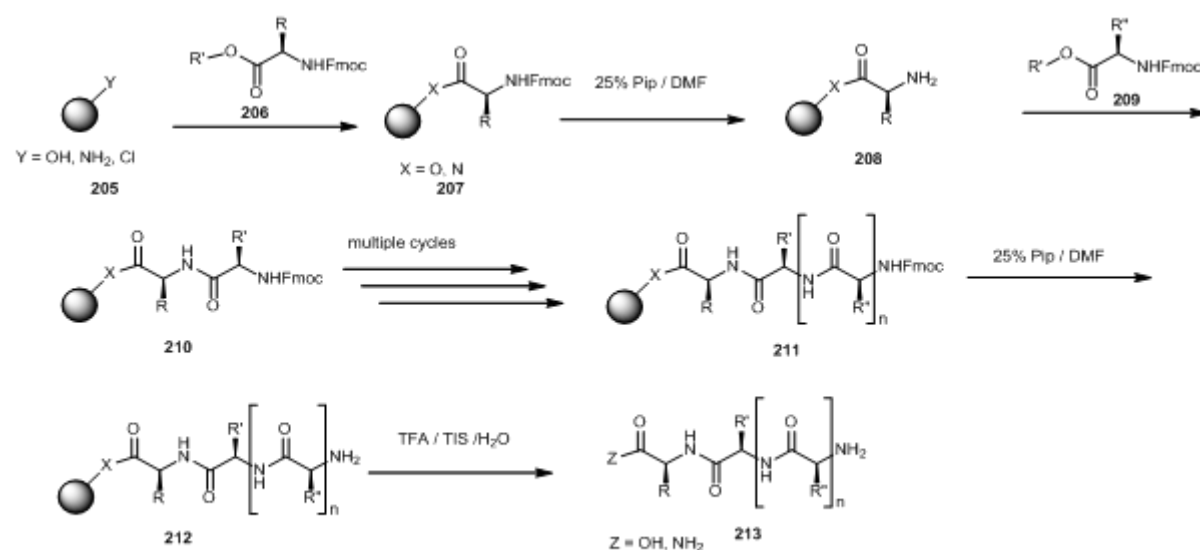


Figure 60 Principles of Fmoc solid phase peptide synthesis; Resin 205 is acylated with side chain protected amino acid (207) that is activated by a coupling agent (denoted R'). The *N*-terminal Fmoc group of 207 is removed with 25 % piperidine / DMF to give free amine (208). The acylation and deprotection steps are repeated until the peptide with the desired chain length is reached (211). Fmoc deprotection followed by acidolysis yields unprotected peptide 213.

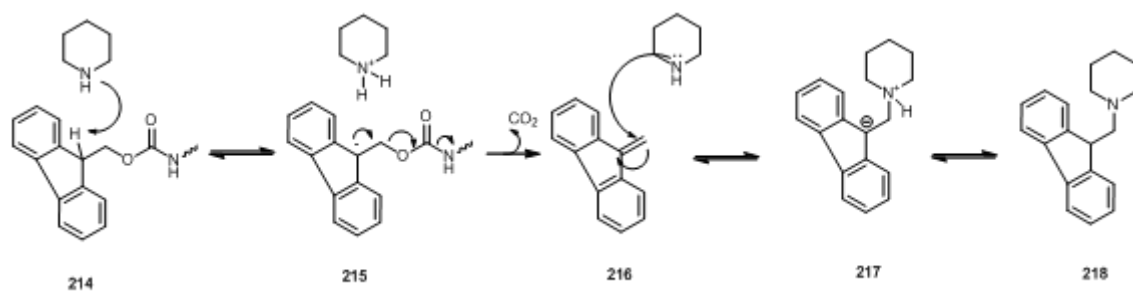


Figure 61 Mechanism of Fmoc removal by piperidine

The resins used in the course of this project contained a polymer matrix composed of either copoly(styrene - 1 % divinyl benzene) or a polyethylene glycol polystyrene mix. Resins composed of **219** swell better in DMF than **220** and have been reported to increase the yields of long peptides so resin **219** was used to synthesise peptides > 20 amino acids in length. The linkers attached to the resin are shown in Figure 62. Linkers that are cleaved in 95% TFA include Wang (**221**) and Rink amide (**222**) were used for the most of the peptides synthesised. For the preparation of side chain protected peptides **223** was used as the peptide is cleaved from the resin using TFE / DCM.

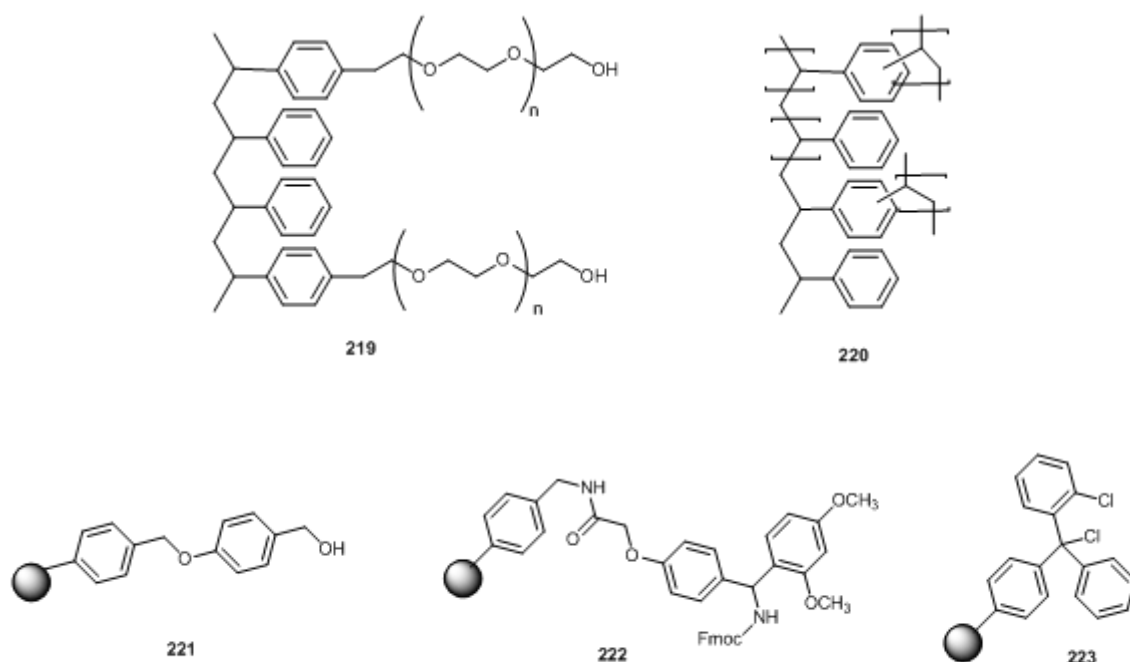


Figure 62 Polymer structures of resins used in this project Tentagel - polyethyleneglycol resin (**219**) and polystyrene-divinylbenzene (**220**); Linkers attached to resins used were Wang linker (**221**) Rink amide linker (**222**) and chloro trityl (**223**).

Resins were purchased ready loaded or derivitised at the beginning of each synthesis. Attachment to Rink amide resin (**222**) is carried out using standard amino acid coupling protocols described below, whereas attachment to **221** requires special conditions. Three methods have been developed for the esterification of alcohol functionalised resin, that use either a symmetric anhydride, mixed anhydride or activated carboxylic acid strategy (Figure 63). The symmetric anhydride method was applied in this project. Advantages of the chosen method are its simplicity, no special agents are required unlike the MSNT (**217**) method. The symmetric anhydride is not as sensitive to water as the MSNT method and acylation occurs faster than with the mixed anhydride dichlorobenzoyl chloride (**218**) method. For example to achieve a loading above 70%, an 18 hr reaction time is needed for the DCB method, compared to 1 hour for the symmetric anhydride method.

284285

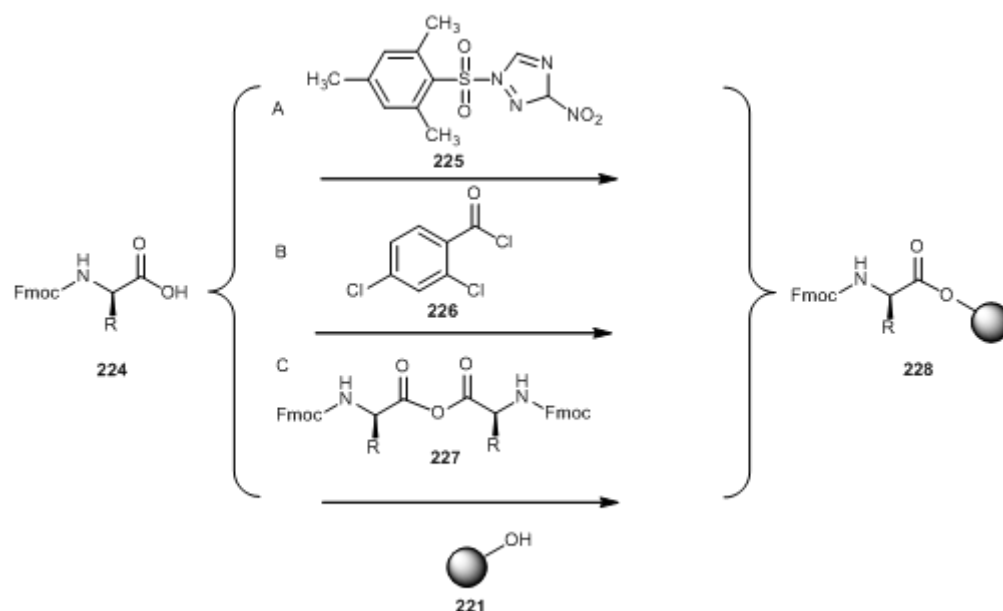


Figure 63 Esterification of Wang resin using A) MSNT method, B) DCB C) symmetric anhydride

### 3.5.3 Results of peptide synthesis

#### 3.5.3.1 Automated synthesis

The synthesis of **203** was carried out on an ACT348Ω synthesiser, using Wang resin previously derivitised outside of the machine using the symmetric anhydride method. The symmetric anhydride of Fmoc-Ser(tBu)-OH was prepared and after addition to the Wang resin (substitution 0.25 mmol /g) the Fmoc loading was determined to be 88%.

The unreacted resin -OH groups were capped with *N*-acetyl-imidazole.<sup>286</sup> The resin was transferred to an ACT 348 synthesiser but the synthesis failed to yield any product, despite each coupling done twice using PyBOP (**230**), an analogue of BOP (**229**), that unlike its predecessor does not evolve toxic HPMA in the course of the reaction.<sup>287</sup> PyBOP possesses good reactivity and was considerably cheaper than the more reactive uronium salts but HBTU (**231**) and HATU (**232**).

A large number of side products were detected in the crude product and several deletion peptides could be identified by MALDI mass spectroscopic analysis (Figure 65). The truncated peptides that were observed corresponded to [M-V]<sup>+</sup> [M-R]<sup>+</sup> [M-P]<sup>+</sup> [M-2R]<sup>+</sup>. Also present were peptides carrying the Pbf protecting group as a result of the slow cleavage of Pbf that can occur in peptides with more than one Pbf protecting group.<sup>288</sup>

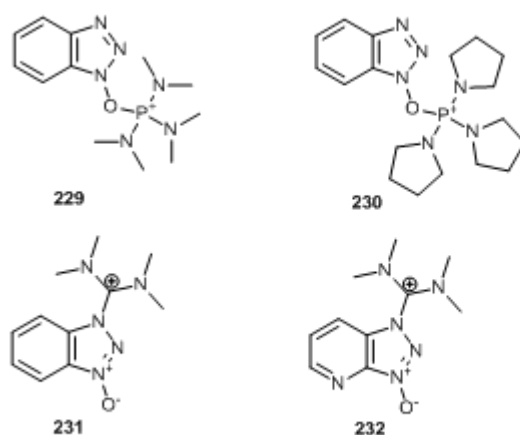


Figure 64 Structures of selected coupling agents: BOP (**229**), PyBOP (**230**), HBTU (**231**) and HATU (**232**)

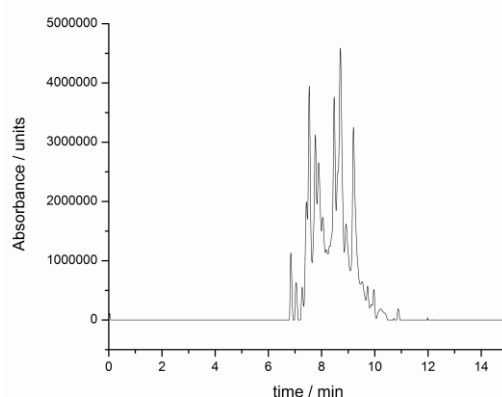


Figure 65 HPLC trace for automated synthesis of 203. HPLC gradient: 5-95% MeCN over 40 min



Deletion peptides were also encountered in the automated peptide synthesis of **204**. The purity of the crude product was lowered by the presence of piperidides. Consistent with literature reports, the excess treatment with piperidine during Fmoc deprotection may lead to the formation of  $\alpha$  and  $\beta$  piperidides (**235** and **236**) at aspartic acid residues carrying tBu protection on the side chain.<sup>289</sup> Repetition of the synthesis on an ACT357 synthesiser using deprotection reagent 20% piperidine / 0.1 % HOBT in DMF suppressed piperidide formation and gave an 8% yield. The peptide synthesis was optimised by manual synthesis, as discussed below.

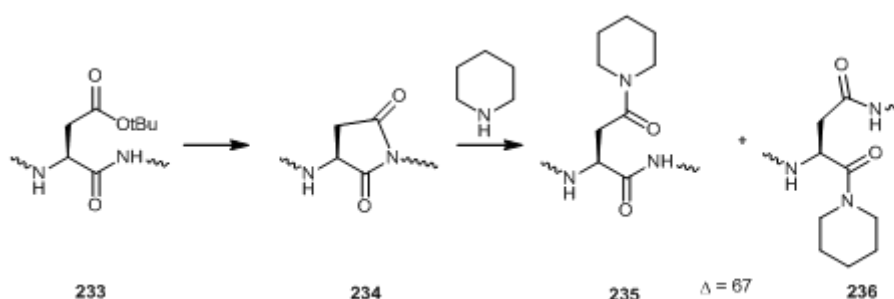


Figure 66 Piperidide formation in conventional SPPS

Similarly, the problems encountered in the synthesis of the short peptides were mirrored in the synthesis of fragment **99**. Furthermore, the activator solution for the automated peptide synthesis experiments was made fresh at the beginning of each experiment, but despite efforts to keep the solution in the dark, it is known that PyBOP solutions can degrade by over 57% within 48 hours. The degradation of **230** may account for the poor yield from the ACT synthesis.<sup>290</sup> The yield of the crude product was very low (2%) indicating that couplings failed to reach completion and this led to a re-evaluation of the conditions used as discussed in the following section.

### 3.5.3.2 Manual synthesis

Changing from an automated to a manual synthesis approach enabled each coupling to be monitored by the Kaiser or chloranil test. A sample of resin was removed from the reaction vessel after 1 hour of coupling and if the test was negative, the coupling was

repeated. The synthesis of **195** was repeated manually using the same coupling conditions but on a less substituted resin, 0.28 mmol / g *vs* 0.87 mmol / g with the aim of decreasing the steric crowding close to the resin surface. Couplings were performed with **230** and each coupling done twice, with each coupling monitored by using the Kaiser test. The Kaiser test cannot be performed on proline due to the lack of a primary amino group and so the chloranil test was used instead couplings that showed blue beads indicative of a free amine and therefore an incomplete coupling reaction were identified at the R34 to T35, V32 to P33 and L31 to V32 (Figure 67).<sup>291</sup> Coupling to  $\beta$ -branched amino acids is described in the literature as a “difficult” coupling and to overcome these slow couplings alternative strategies were sought.<sup>292</sup>

The aminium coupling agent HATU (**232**) has been shown to be more reactive than PyBOP (**230**). The increased reactivity for the aminium agents is due to the ammonium ion being a better leaving group than the phosphonium ion.<sup>293</sup> This more reactive coupling agent (**232**) was used to facilitate couplings at threonine, valine and proline in a repeat of the synthesis of **203**. The couplings proceeded quicker (completed in 30 min as judged by Kaiser test) and the crude HPLC was cleaner than the ACT synthesis (Figure 65). After preparative HPLC a single peak was isolated but mass spectrometry showed that the isolated peak contained a considerable amount of a side product which was 27 mass units higher than expected and inseparable by HPLC. Accurate mass in ESI mode coupled with ECD experiments indicated that modification occurred at the N- or C-terminus. The mass adduct corresponds to addition of CHO, possibly during the acid cleavage step.

Application of the combined PyBOP / HATU strategy to the synthesis of **100** increased the crude yield from 2 mg to 10 mg but the product still contained piperidide adducts. The synthesis of **99** was carried out manually with the PyBOP / HATU strategy and although side products were detected, enough material was isolated (2 mg) to supply biological studies.

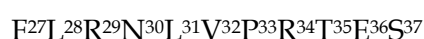


Figure 67 Numbering of residues in peptide 203 is based on the numbering in the parent peptide (12)

To further optimise the synthesis of **100**, HBTU (**231**) was also tried as a coupling agent based on a recommendation by Dr J Fox (Alta Bioscience). Repeating the synthesis with **231** as the sole coupling agent, yielded the desired peptide in higher purity than with the combined PyBOP/HATU synthesis but still in low yield (15%).

### 3.5.3.3 Microwave synthesis

In an attempt to further increase the yield of the peptide synthesis, we next turned to a microwave assisted synthesis. Recent studies have shown that microwave heating not only enhances the coupling efficiency by reducing the coupling time from 1 hour to 5 minutes, but can also overcome problems of chain aggregation in long or hydrophobic peptides (higher yield, cleaner HPLC spectrum).<sup>294</sup> It has been proposed that the *N*-terminal amine and peptide backbone are polar thus they try and align with the alternating electric field of the microwave, helping to break up aggregated chains. In a comparative study of a 20-mer amino acid (VYWTSPFMKLIHEQCNRADG-NH<sub>2</sub>) synthesised on a conventional and microwave peptide synthesiser, the conventional synthesis gave only a 68% crude yield with several deletion products, whereas the microwave synthesis gave 84% in an unoptimised system. Recently, Galanis and co workers showed that microwave heating is also efficient at facilitating solid phase peptide synthesis where water is the solvent.<sup>295</sup> The reasons for the improvements in yield and purity in microwave peptide synthesis have been challenged by Kappe, who has shown that conventional heating is as efficient as microwave heating at improving the yield of solid phase peptide synthesis.<sup>296</sup> Nevertheless, in our hands we found microwave assisted chemistry most advantageous.

Application of microwave heating to the synthesis of **203** made a huge difference to the speed of the synthesis, the yield and the purity. Coupling reactions were conducted for 5 minutes instead of 1 hour, with the exception of arginine, which was incorporated in 20 minute coupling. All deprotections and couplings were conducted at 70 °C. Couplings were only done once, and the purity of the synthesis was checked periodically by HPLC. After the addition of P and V, no deletion or side products were obtained. Similar successes were achieved with peptides **100** and **204**, where microwave synthesis gave the desired product in high crude yield, 35% and 28% respectively. All the peptides synthesised are summarised in Table 9.

### 3.5.3.4 Summary

Table 9 Summary of synthesised peptides and yields (NA = not attempted)

Peptide	Sequence	Yield (%)		
		ACT	Manual	Microwave
203	FLRNLVPRTES	2	15	25
100	FKRIVQRIKDFLR	0	Mixture	35
99	IGKEFKRIVQRIKDFLRNLVPRTES	0	4	NA
204	LLGDFFRKSK	8	10	28
237	IKDFLRNLVPRTES	0	12	NA
238	RIVQRIK	7	NA	30
239	KIGKEKFRIVQR	4	16	NA
240	KEKIGKEKFRIVQR	4	18	NA

### 3.5.4 ITC binding studies involving synthetic peptide fragments and MtrR

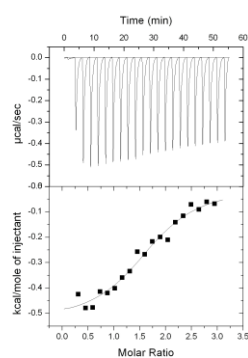
#### 3.5.4.1 Screening of synthetic peptides by ITC

With the successful preparation of peptide fragments of LL-37, attention next turned to investigating how these peptides interact with MtrR and to compare the results to the ITC experiment with LL-37.

The recombinant MtrR used in the ITC experiments was purified by affinity chromatography, gel filtration and anion exchange chromatography, as discussed in Chapter 2. In contrast to the penicillin binding studies, the protein was dialysed into 20 mM Tris, 300 mM NaCl, pH 8.2 prior to the ITC experiment. The ligand was dissolved in the same buffer as used for the protein. A typical ITC experiment involved 10  $\mu$ L injections of a 1 mM solution of peptide every 2 minutes into 70  $\mu$ M of protein. In each case, a control experiment was performed whereby the peptide of interest was injected into buffer alone. The data acquired from the buffer only experiment was subtracted from the experiment with protein and the modified data was fitted using the One-Site Model provided in the Origin software.

The first synthetic peptide that was checked for binding to MtrR was **99**, as the effect of the *N*-terminal region could then be assessed by resulting raw data was fitted with the one site model. The 10  $\mu$ M dissociation constant ( $K_d$ ) and 20 kJ mol<sup>-1</sup> · K change in entropy ( $\Delta S$ ) values are very similar to the  $K_d$  and  $\Delta S$  for LL-37. The major difference between the two experiments is observed in the shape of the raw data. The initial endothermic event is missing in the truncated peptide indicating that residues 1-10 are responsible for the aggregating potential of the peptide. Furthermore, although the observed heat change for **99** does not return to the base line at the end of the experiment, literature suggests that such data is still sufficient for fitting to a model.<sup>297</sup> The increase in entropy suggests that interactions are non-specific, and the increased entropy arises from desolvation of the hydrophobic surfaces when the peptide associates with the protein.<sup>298</sup> Interestingly, the *N*-terminal peptide (**204**) does not bind at all.

IGKEFKRIVQRIKDFLRNLPRTES (99)



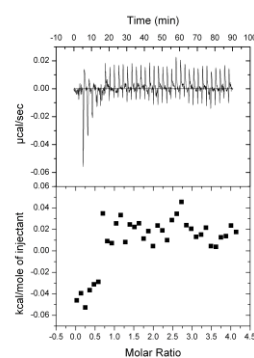
$$\Delta H = -2.5 \pm 0.2 \text{ kJ mol}^{-1}$$

$$\Delta S = 20.5 \text{ kJ mol}^{-1} \cdot \text{K}$$

$$K_d = 10 \pm 1 \text{ } \mu\text{M}$$

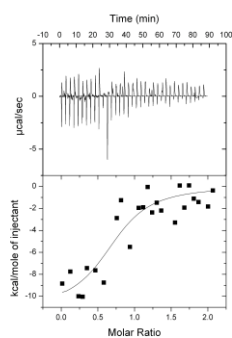
$$N = 2 \pm 0.09$$

LLGDFFRKSK (204)



Data does not fit One Site Model

FKRIVQRIKDFLR (100)



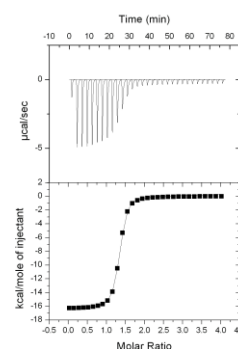
$$\Delta H = -42 \pm 8 \text{ kJ mol}^{-1}$$

$$\Delta S = -12.8 \text{ kJ mol}^{-1} \cdot \text{K}$$

$$K_d = 5 \pm 0.7 \text{ } \mu\text{M}$$

$$N = 0.8 \pm 0.1$$

FLRNLPRTES (203)



$$\Delta H = -69.7 \pm 0.2 \text{ kJ mol}^{-1}$$

$$\Delta S = -26.5 \text{ kJ mol}^{-1} \cdot \text{K}$$

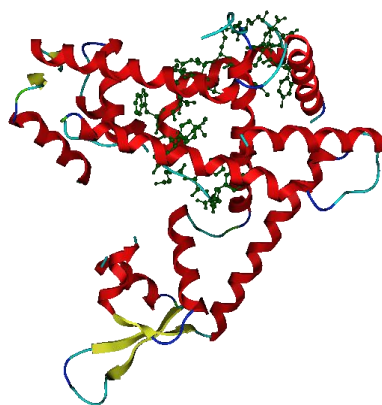
$$K_d = 30 \pm 0.8 \text{ nM}$$

$$N = 1.3 \pm 0.02$$

Figure 68 Summary of ITC experiments for LL-37 fragments binding to MtrR

In contrast to the long peptides, the shorter C-terminal (**203**) and central peptide (**101**) bind with  $K_d$  of 30 nM and 5  $\mu$ M respectively (Figure 68). The binding constants are indicative of tight binding and analysis of the  $\Delta H$  and  $\Delta S$  values provides further insight into the binding event. The enthalpy change ( $\Delta H$ ) is a measure of the heat change of the system thus the more negative the  $\Delta H$  the more favourable non-covalent interactions that are formed. Typically, these involve hydrogen bonds between polar groups and van der Waals interactions.<sup>299</sup> The negative entropy for **203** and **101** indicates that there is a large degree of reordering of the protein when the ligand binds. The central peptide is known to adopt an  $\alpha$  helical structure whereas the C-terminal peptide **203** has no overall structure in solution thus when **203** binds MtrR there is a much larger change in entropy than when the **101** binds MtrR. By homology to other TetR proteins, MtrR is predicted to have a large binding pocket formed by several  $\alpha$ -helices. It is known that on ligand binding, the ligand binding domain of TetR proteins undergoes a conformational change and this is transmitted through the breaking of existing, and the formation of new, salt bridges and hydrogen bonds to the DNA binding domain. The observation that the **203** produces a greater change in  $\Delta S$  and  $\Delta H$  than the **99** indicates a tighter binding ligand.

The ability for a segment of a large peptide to bind stronger than the parent molecule is illustrated by the 53 amino acid regulatory peptide ArmR. ArmR binds the regulatory protein MexR with  $\Delta H = -60 \text{ kJ mol}^{-1}$  and  $\Delta S = 78 \text{ kJ mol}^{-1} \cdot \text{K}$ , whereas the C-terminal region of ArmR (residues 41 - 53) exhibits  $\Delta H = -42 \text{ kJ mol}^{-1}$  and  $\Delta S = -21 \text{ kJ mol}^{-1} \cdot \text{K}$ .<sup>300</sup> The observed change in the sign of entropy from positive to negative suggests strong binding due to a net reorganising of the protein structure to a more stable conformation. The dissociation constants of 290 nM for the full peptide and 190 nM for the truncated peptide underscore the increased binding affinity that is achieved on truncating the regulatory peptide. The regulatory peptide ArmR is a natural molecule produced by *P. aeruginosa* whereas LL-37 is an antimicrobial peptide that has previously not been shown to bind a regulatory protein before and so the ITC data presented here provides new insights into ligands for DNA binding proteins.



**Figure 69** MexR-ArmR (peptide in green). The peptide binding site extends across the ligand binding domain in MexR (a MarR family protein) .Image produced in MOE from PDB file 3ECH.

There are three postulated mechanisms for peptide derepression of transcriptional regulators. The functional dimer can be disrupted through insertion into the dimerisation domain, the peptide can bind to the DNA binding region of the regulator or the peptide can insert in the the ligand binding domain.<sup>300</sup> The results of the ITC suggest that full length LL-37 and the shortened 27 amino acid fragment predominantly interact with MtrR via non-specific hydrophobic interactions but the ITC results alone are not enough to discount insertion into the ligand binding domain. More conclusive thermodynamic evidence was obtained to support the theory that the shorter peptides insert into the ligand binding domain. The negative  $\Delta H$  and  $\Delta S$  for the FLRNLPRTES (203) peptide is indicative of a high affinity peptide.

#### **3.5.4.2 Conclusion**

The ITC results show that decreasing the number of residues from 37 in the parent peptide to 11 in FLRNLPRTES substantially increases binding of the peptide to MtrR. This result is rationalised by comparison to the literature on peptidic ligands for DNA binding proteins. In order to gain more insights into the molecular mechanism of peptide binding to MtrR, the site of binding was investigated next and efforts to elucidate the ligand binding site in MtrR are discussed in the following section.



### 3.5.5 Photoactivated peptide substrates

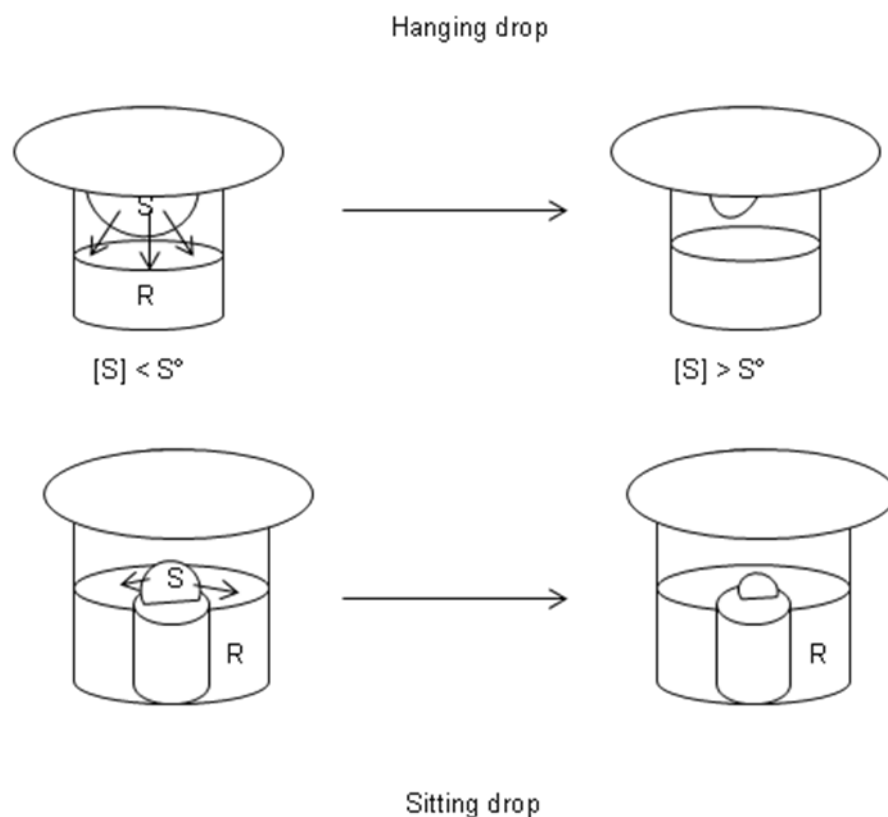
#### 3.5.5.1 Introduction

With the successful identification of **203** as a high affinity ligand for MtrR, attention turned to localising the peptide binding site. At the outset of this research project there was no structure information on MtrR and so two strategies were instigated to enable insights at the molecular to be gained. This involves X-ray crystallography and affinity based protein profiling (ABPP). A brief overview of the X-ray crystal trials attempted in this research project will be summarised below. ABPP was described above and results presented here provide insights into molecular recognition by MtrR.

#### 3.5.5.2 X-ray crystallographic trials

As reported in Chapter 1, the 3D structure of TetR proteins has provided valuable information regarding DNA and ligand binding mechanisms. Attempts to crystallise MtrR in this research project are described herein.

Crystal screening trials were set up using an Innovadyne Screenmaker robot that enables 96-well plates to be prepared on a nanolitre scale. The ability to screen a large number of conditions for crystal growth is essential as nucleation of a crystal requires the protein to be brought to a point of supersaturation, when the concentration of the protein exceeds its intrinsic solubility  $S^0$ .<sup>301</sup> The point of  $S^0$  is unique for each protein and dependent on temperature, pressure and solvent. Consequently crystallisation screening experiments are conducted at room temperature and 4 °C and with a range of buffer conditions. Supersaturation can be induced by decreasing the volume of the solvent drop in which the protein is dissolved and this is termed the vapour diffusion method. Two different ways exist to set up vapour diffusion method experiments (Figure 70) and each method was attempted in this study.



**Figure 70** Vapour diffusion methods for crystallisation. In the hanging drop method, the sample is suspended above a reservoir of buffer (R). The lower vapour pressure of the reservoir draws water from the sample to reduce its volume and thus the protein concentration increases above  $S^\circ$ , resulting in precipitation or crystallisation. In the sitting drop, the sample is located in a well next to the reservoir but otherwise the method is the same as for hanging drop.

Ten 96-well plate screening trials were set up (using the robot) in the sitting drop format and twenty 12 well hanging drop plates were set up (manually) to screen a range of commercially available buffer systems (Wizard I and II, Cryo I and II, Crystal Screen HT). The concentration of protein used was 10 mg / mL. Attempts to concentrate the protein above 10 mg/ mL lead to precipitation of the protein. Disappointingly, only precipitated protein or clear droplets were observed in the screening trials after 1 day, 1 week and 1 month of setting up the plates.

The observed precipitation of MtrR during buffer exchange processes in the purification of the protein and also when concentrated over  $\sim 10$  mg /mL and also in the crystallisation trials indicates that the protein is not very stable. Consequently, when the concentration of protein increases in the droplets in the crystal screening trials, instead of nucleation occurring (a slow process requiring a highly ordered lattice to form), numerous tiny nuclei formed and precipitated from the solution. Due to the failure of

the crystal screening trials, an alternative approach was sought and the use of photoactivated activity based protein profiling is detailed in the next section.

### 3.5.5.3 Photoaffinity peptides

As reviewed in section 3.4.1, ABPP can reveal the site of ligand binding and the use of peptides as active ligands has been shown to be a useful strategy. The literature on benzophenone containing ABPP probes revealed that the photolabel can be placed at any point along the peptide sequence. The insertion of the benzophenone moiety can affect the affinity of the peptide for the protein, however, the ligand binding domain of MtrR is predicted to be large so the effect of adding a benzophenone group to the peptide should be tolerated. At the outset of this project, there was no structural information regarding the ligand binding domain of MtrR and so as a proof of concept experiment, the photolabel was placed at the *N*-terminus of the peptide. The chemistry required to insert the photolabel at the *N*-terminus is facile and would allow for the photolysis and mass spectrometric conditions to be optimised.

Peptide **203**, was synthesised on Rink amide resin using microwave assisted manual synthesis using 250 mg of resin was used with a substitution of 0.61 mmol /g. The benzophenone label was introduced after deprotection of the *N*-terminal residue. 4-carboxyl-benzoyl-benzoic acid (**241**) was activated with HATU / DIPEA in DMF for 5 min prior to addition to the *N*-terminal deprotected peptidyl resin (**242**). The coupling reaction was carried out at 70 °C for 15 minutes, which is 10 minutes longer than for a standard coupling reaction as carboxylic acids on aromatic systems are slower to react than standard amino acids. The product

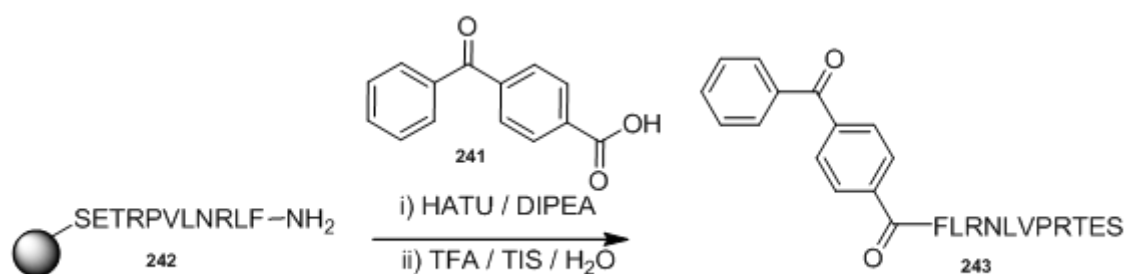


Figure 71 Synthesis of benzophenone labelled peptide

was cleaved from the resin using TFA /TIS /H<sub>2</sub>O. LC-MS analysis of the crude material revealed two major products, with  $m/z = 770$  [M+H]<sup>2+</sup> and  $m/z = 762$  [unknown] (Figure 72). The desired product and unknown side product were isolated by preparative mass directed HPLC and the identity of the desired product was confirmed by accurate mass measurement.

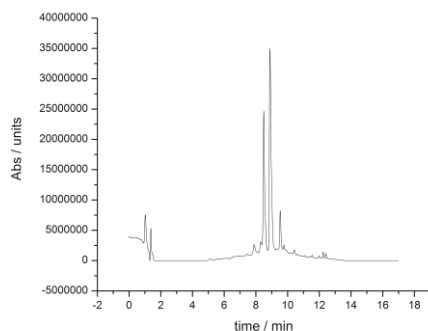
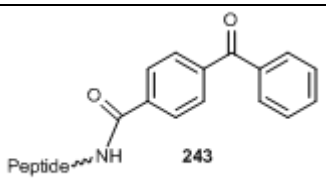
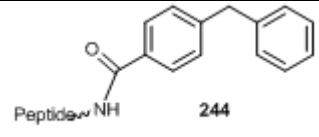
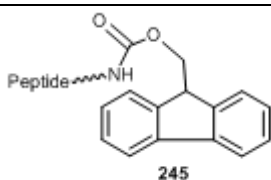
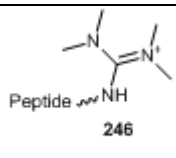


Figure 72 HPLC trace of crude 243 (Gradient 5→95% MeOH, 20 min)

The accurate mass measurement for the unknown side product indicates that structure 244 is present ( ). Other side products that were considered included Fmoc-peptide 245, that might be formed due to incomplete treatment with piperidine and *N*-terminal guandidated peptide 246, which would be due to excess HATU in the coupling mixture but neither of these adducts gave the desired mass. The primary sequence of the unknown product was solved by sequencing the peptide using an FT-ICR mass spectrometer in ECD mode. The z11 fragment confirms that sequence of the peptide is 203 and that the modification is at the *N*-terminus. The difference between the MH<sup>+</sup> signal and the z11 signal corresponds to the c<sub>1</sub> ion and the accurate mass for the c<sub>1</sub> ion corresponds to peptide 244. Comparison to the peptide sequencing data for 243 shows that the C-terminal data is identical for both peptides and the only difference is at the *N*-terminal region. The origin of the impurity is not known. The starting material 4-carboxylic acid benzophenone was bought from Sigma–Aldrich and its purity as the desired compound was confirmed by NMR and LC-MS.

Table 10 Side products in the preparation of 243

Peptide $C_{59}H_{100}N_{19}O_{16}$	Composition	$[M+H]^+$	$[M+H]^{2+}$
 <p>243</p>	$C_{73}H_{108}N_{19}O_{18}$	1540.8033	770.4017
 <p>244</p>	$C_{73}H_{110}N_{19}O_{17}$	1524.832711	762.164
 <p>245</p>	$C_{74}H_{111}N_{19}O_{18}$	1553.835451	776.177
 <p>246</p>	$C_{64}H_{111}N_{21}O_{16}$	1429.851768	714.925

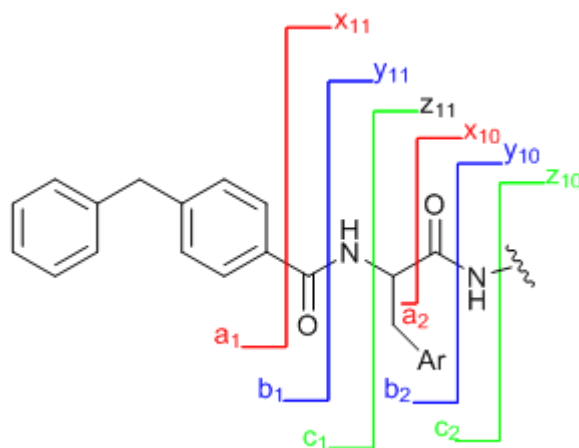


Figure 73 Diagram showing fragmentations possible at the N terminus of peptide 244 in MS / MS experiments. The colour indicates ion pairs.  $a_n$ ,  $x_n$  ions arise from C-C bond cleavage.  $b_n$ ,  $y_n$  ions are due to fragmentation at a C-N bond.  $c_n$ ,  $z_n$  ions are due to breakage of N-C bonds.

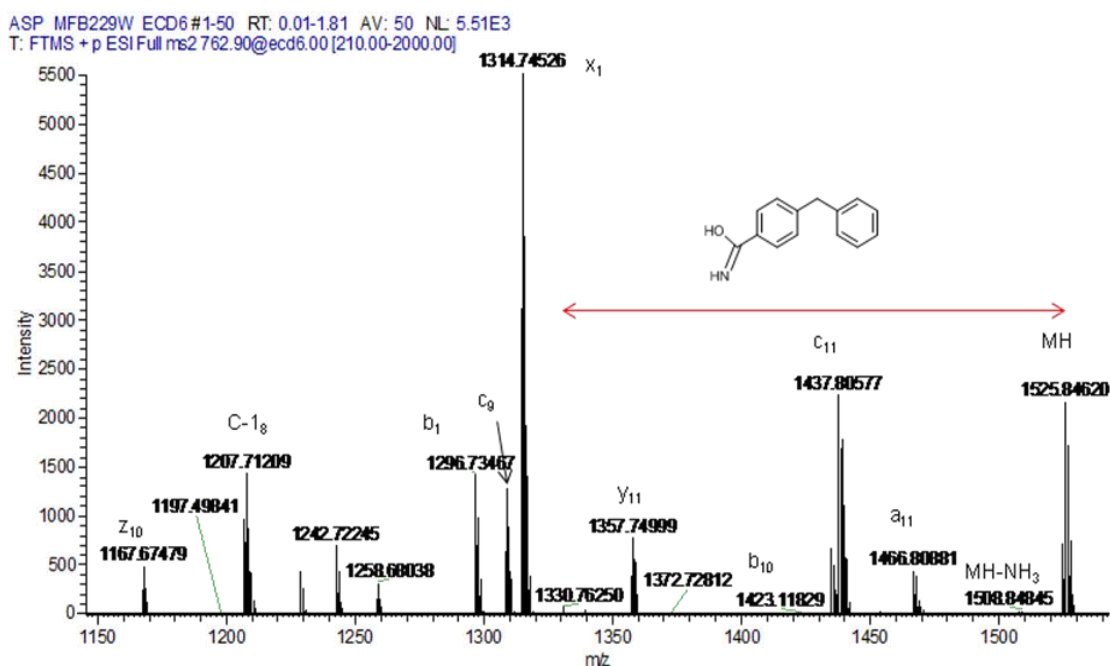


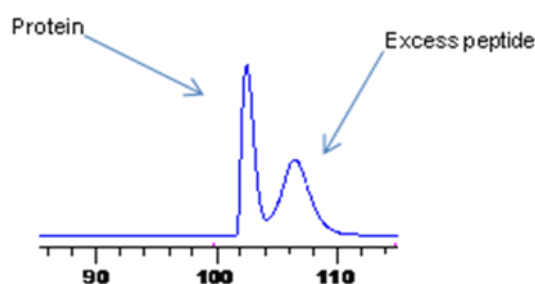
Figure 74 ECD mass spectrum for the characterisation of the side product from the labelling of 195

The *N*-terminal labelling of peptide **203** with 4-benzophenone-4-carboxylic acid (**241**) gave a 50 : 50 mixture of the desired product **243** and an unwanted side product **244**. Using mass directed prep. HPLC, the desired product was isolated in 30 % yield. With the photoactive peptide in hand, the photoaffinity binding study with MtrR was attempted next.

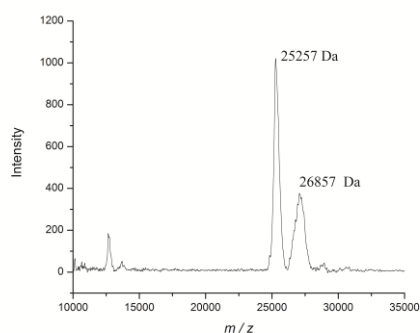
A variety of incubation procedures and UV sources are listed in the literature for the conversion of benzophenone to the corresponding ketyl diradical.<sup>302</sup> Initial experiments involved incubating the photoactive peptide with the protein for 2 hours at room temperature. Incubation of protein and ligand is normally undertaken at 4 °C but due to the low stability of MtrR when stored at 4 °C, incubation of the peptide ligand with the protein was conducted on a rotary shaker at room temperature. The solubility of the benzophenone peptides in Tris buffer was lower than for the parent peptides and to effect dissolution, addition of 5 % MeCN was necessary. Irradiation was conducted at 355 nm for 30 minutes using a Jobin-Yvon Fluorolog FL-3-22/ Tau-3 Spectrofluorimeter. Irradiation was also conducted at room temperature and to prevent localised heating of the protein : peptide solution the cuvette was shaken periodically. A 20 µL sample was removed from the irradiated sample every 15 minutes for one hour to monitor the

conversion process. Very low intensity signals were seen that corresponded to modified protein peaks after 2 hours, but the absolute identity of the species could not be determined. Trypsin digest of the irradiated protein did not yield any modified peptides relative to an MtrR only control that was treated in the same way.

The low yield from the insertion was proposed to arise from insufficient power arising from the UV source and so the UV source was changed to an Nd:YAG laser. The incubation time was also reduced to 1 hour. Following irradiation at 355 nm using a Nd:Yag laser for 15 min at room temperature, an initial analysis of the reaction showed the presence of a new peak but the resolution was low. To remove low molecular weight contaminants, the reaction mixture was injected onto a 5 mL desalting column and the excess peptide was separated from the protein (Figure 75). MALDI mass spectrometry analysis of the protein peak, showed the presence of unmodified MtrR ( $m/z = 25257$ , Figure 76) and modified protein ( $m/z = 26857$ , Figure 76) with a mass difference of 1600 Da.



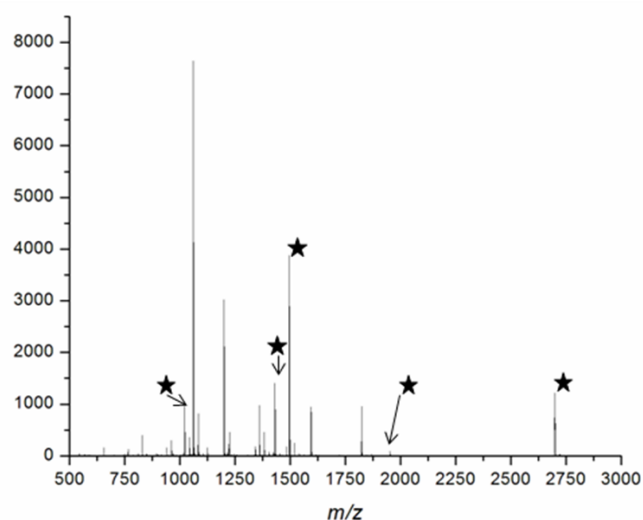
**Figure 75** Separation of excess peptide from protein after photo-irradiation. Injection of 1 mL photobinding solution onto 5 mL HITRAP Desalting column, fractions eluted with Tris 20 mM, NaCl 300 mM, pH 8.



**Figure 76** Appearance of modified protein after irradiation of photopeptide with MtrR for 15 min at 355 nm using an Nd:Yag laser.

Analysis of the excess peptide peak confirmed the presence of the benzophenone labelled peptide ( $m/z = 1540.742$ ) indicating that not all the benzophenone peptide reacted with the protein. With firm evidence to show that the benzophenone peptide inserts into the peptide, attention next turned to localising where the benzophenone had inserted into MtrR. As discussed in the introduction, the site of insertion can be located by mass spectrometric analysis of tryptic peptide derived from the modified protein. MtrR contains several trypsin cleavage sites (lysine and arginine) and there are well developed protocols for the use of trypsin digests in the group so this enzyme was chosen for this investigation.

The modified protein was precipitated in acetone, and subjected to trypsin digest overnight. As a control, MtrR that had been incubated and irradiated in the absence of photolabelled peptide was also digested. An initial comparison of the tryptic peptide data from the MALDI mass spectrometry analysis showed the presence of 5 modified peptides (Figure 77). Subsequent analysis by ESI mass spectrometry confirmed the presence of the peptides (Table 11).



**Figure 77 MALDI mass spectrum for tryptic digest of 243. Modified peptides are indicated with a star.**

The identity of the peptides was deduced by comparison of the observed data to an *in silico* digest. The sequence for MtrR containing all potential modifications was inputted into SequenceEditor (Bruker) and 'digested'. The peptide ligand used in this experiment is also a substrate for trypsin so the different cleavage products of the peptide were also considered. The settings applied allowed for 2 missed cleavages, which is important in



this experiment because when a peptide is bound in a protein it can be protected from cleavage by trypsin.<sup>78</sup> The modified sequences from MtrR are highlighted in Figure 78.

Table 11 Tryptic peptides deduced from mass spec data

m/Z	Peptide origin		Method
	MtrR	Peptide 6	
1017.53	KTK	FLR	MALDI, ES <sup>+</sup>
1430.77	TKTEALK	FLR	MALDI, ES <sup>+</sup>
1452.75	HQAIWR	FLR	ES <sup>+</sup>
1481.65	EK	FLRNLVPR	MALDI, ES <sup>+</sup>
1506.82	KTKTEALK	FLR (-NH <sub>3</sub> -2H <sub>2</sub> O)	ES <sup>+</sup>
1805.97	HTLLHFFER	FLR (-2H <sub>2</sub> O)	ES <sup>+</sup>
1841.67	HTLLHFFER	FLR	MALDI
2620.32	HQAIWR	FLRNLVPR (-NH <sub>3</sub> )	MALDI, ES <sup>+</sup>
2720.16	HTLLHFFER	FLRNLVPRTES(-H <sub>2</sub> O)	ES <sup>+</sup>

MRKT**KTEALK**TKEHLMMLAALETFYRKGIARTSLNEIAQAAGVTRGALYWH  
 FKNKEDLFDALFQRICDDIENCIAQDAADAEGGSWTVFR**HTLLHFFER**LQ  
 NDIHYFHNILFLKCEHTEQNAAVIAIARK**HQAIWREK**ITAVLTEAVEN  
 QDLTEAVENQDLADDDKETA VIFIKSTLDGLIWRWFSSGESFDLGKTA  
 PRIIGIMMDNLENHPLCRRK

Figure 78 Sequence of MtrR with labelled peptides highlighted

To confirm the identity of the modified peptides MS / MS experiments were conducted on a Bruker TOF / TOF MALDI spectrometer. Parent ions were isolated and subject to increased laser power in order to fragment the peptide. The observed sequence data was then compared to an *in silico* generated fragmentation. The theoretical peptide fragment data for the peptides was generated using the MS-Protein software (UCSF Protein Prospector).<sup>303</sup> Comparison of the experimental data with theoretical peptide fragment data enabled the identity of two peptides (HTLLHFFER and KTKEALK) to be confirmed, the identity of the third peptide HQAIWR was confirmed by comparison of the observed and calculated accurate mass for the peptide. The modified HQAIWR peptide was not able to be isolated in the MALDI analysis due to the low abundance of the parent ion.

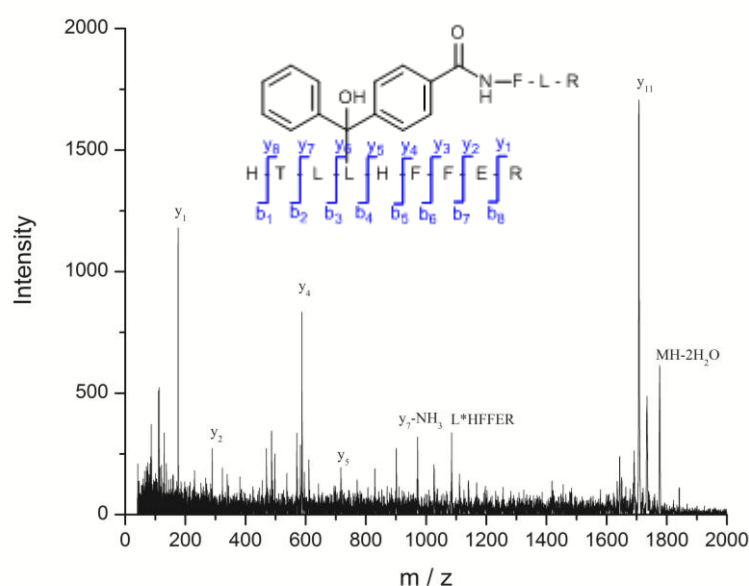
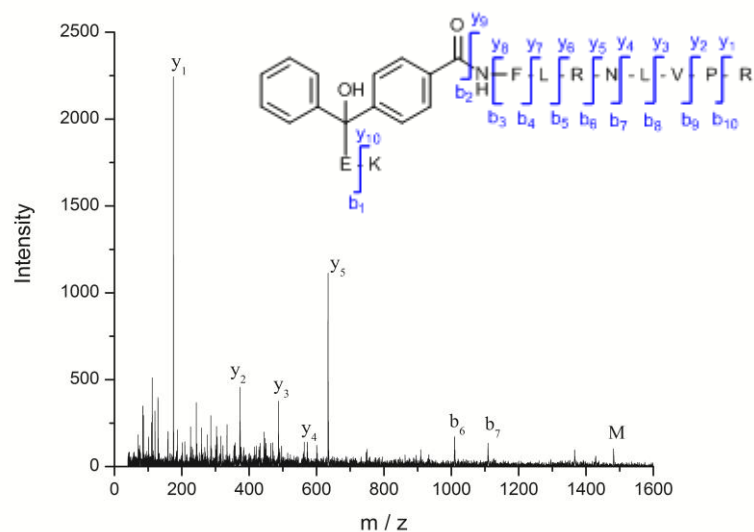
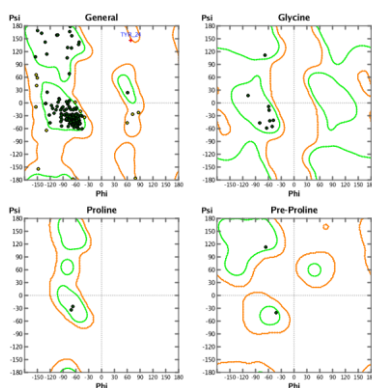


Figure 79 LIFT spectrum for the characterisation m / Z 1841 (benzophenone-FLR modified HTLLHFFER). The observation of y5 and y7 ions either side of the proposed site of modification provide evidence that the insertion occurred at the leucine indicated. The internal fragment peptide L\*HFFER (where \* indicates the benzophenone modification) provides further proof for the proposed sequence. Full mass list is given in appendix 7.2



**Figure 80 LIFT spectrum for m/z 1481 (benzophenone-FLRNLVPRTES modified EK)**

The trypsin digest data enabled three peptides of MtrR to be identified that are modified by the benzophenone peptide. The peptides HQAIWREK, HTLLHFFER and KTKEALK correspond to helices 6, 5 and 1. Figure 78 highlights the modified sequences but does not provide an easy way to visualise the relationship in space between the modified helices. In order to understand the localisation of the labelling in a 3D format, a homology model was constructed using MOE (Chemical Computing Group). The MtrR amino acid sequence was searched against the PDB database and MOE identified a family of proteins with similar fold / topologies, as described by the 'hydrophobic fitness score' ( $Z$ ); the higher the value of  $Z$ , the greater the accuracy of the alignment. The greatest homology was seen with AcrR. MtrR was aligned to the found sequences and 10 homology models built using the Amber-99 force field. The 10 models represent different energy conformations with different side chain rotomers. The final homology model is the lowest energy conformer. The validity of the homology model can be checked by analysing the psi and phi bond angles, as displayed in the Ramachandran plot in Figure 81. All the angles are within accepted limits and so the homology model represents a biologically feasible conformation.



**Figure 81** Ramachandran plot for the MtrR homology model. No outliers are observed indicating the model is reliable.

The model produced by MOE corresponds to a single MtrR protein, not to the biological unit (dimeric MtrR). In order to provide a dimeric model of MtrR, the symmetry mate for AcrR (homologous to MtrR) was found using the crystallography software Coot (this analysis was performed by Dr. Ehmke Pohl).<sup>304</sup> MtrR was then mapped to the symmetry mate to provide a dimeric model (Figure 82).

The modified residues are highlighted on an homology model of MtrR (Figure 82). Helix 1 is at the bottom of the ligand binding domain and helices 5 and 6 are part of the ligand binding domain. Labelling of helices 5 and 6 is expected as ligands have been shown to have contact with these helices in other TetR proteins. The location of insertion on hydrophobic helices is indicative of specific interactions between the peptide and protein. In an attempt to gain greater insight into the ligand binding process, the peptide was docked into the dimeric homology model using MOE. The aim of this docking process was to correlate the observed labelling with a particular mode of peptide binding to MtrR.

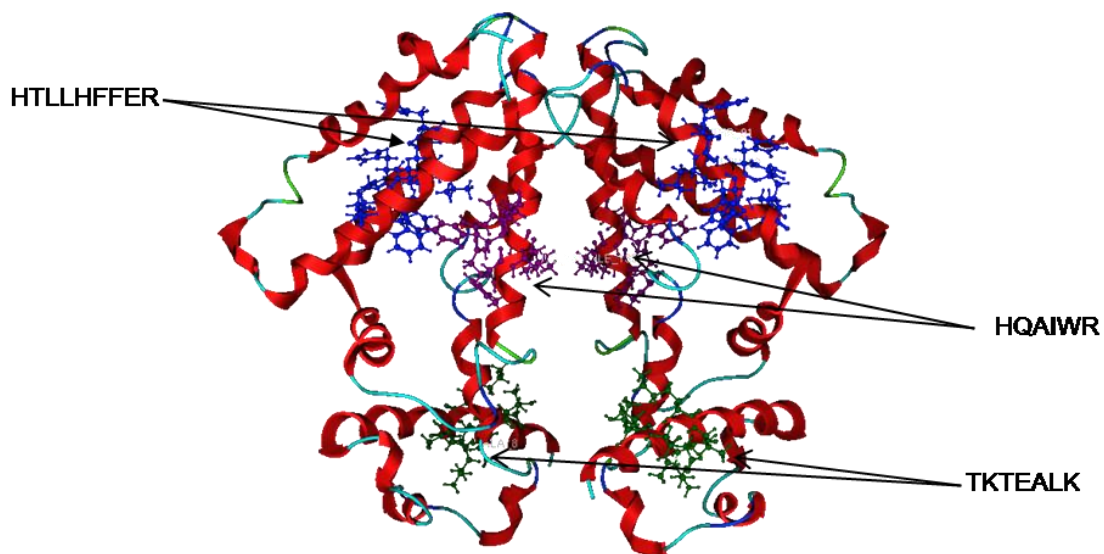


Figure 82 Annotated homology model of MtrR with peptides identified by mass spectrometry studies highlighted. Peptides are highlighted on both subunits as it is not possible to determine the origin of the peptides in the mass spectrometry experiments undertaken.

Before the peptide can be docked to MtrR, potential binding sites on MtrR must be identified using the 'Site Finder' programme in MOE. The 'Site Finder' applies geometric methods ( $\alpha$  spheres) to identify hydrophobic pockets that are not "too exposed" to solvent and then ranks the sites found by the number of hydrophobic contacts within an  $\alpha$  sphere.<sup>305</sup> The largest site found corresponded to the tunnel composed of the two ligand binding domains in MtrR, consistent with other TetR proteins, eg EthR.<sup>306</sup> As a control, the site finder programme was run on TetR protein and isolated the site occupied by TIP peptide indicating the reliability of the method.

Peptide **243** was then docked into the found binding site. Ten lowest energy conformers were generated and two orientations found that account for the labelling observed in the mass spectrometry study. The eight discarded conformers show the peptide bound with the benzophenone moiety extending away from the protein so insertion is not possible (appendix 7.3).

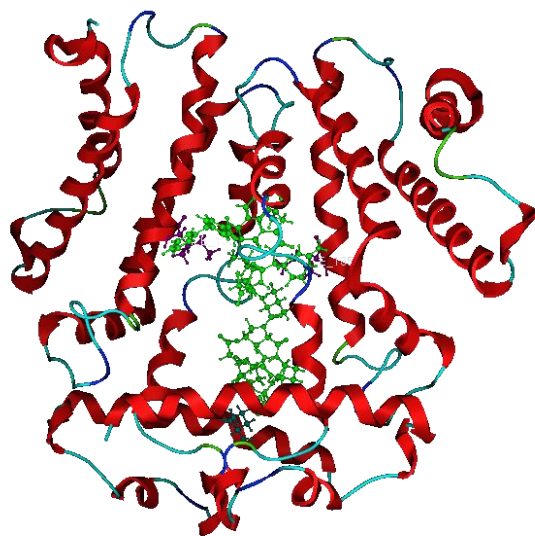


Figure 83 MOE docking result for peptide 243 bound to MtrR. The benzophenone moiety is orientated close in space to Ile 135 (shown in purple), contained on the HQAIWR peptide isolated from the trypsin digest analysis.

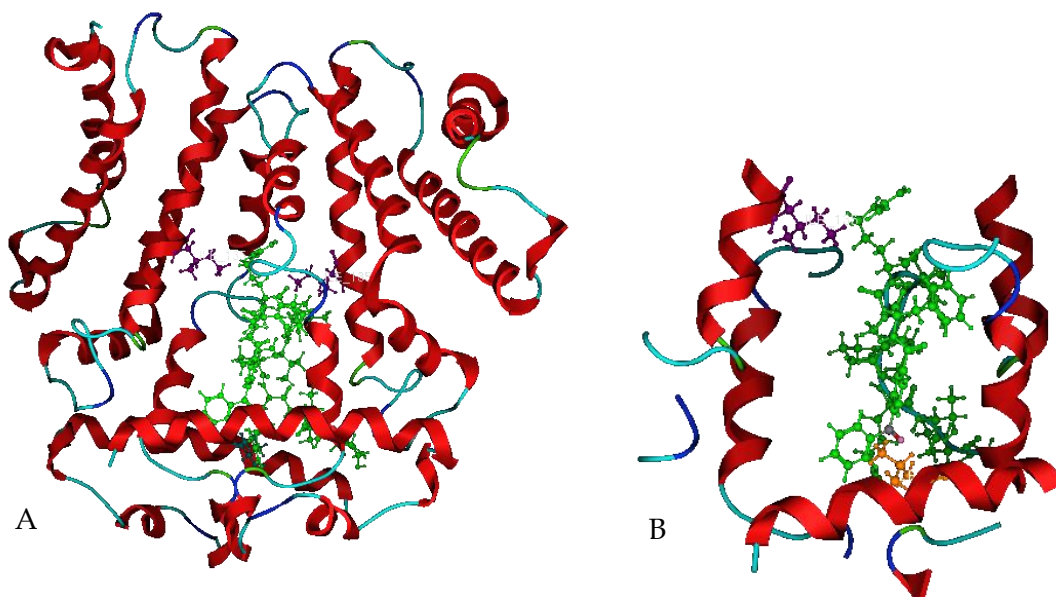


Figure 84 A: MOE docking result for peptide 243 bound to MtrR. The benzophenone is orientated close in space to Leu 9 (KTKEALK, helix 1), contained on KTKEALK isolated from the trypsin digest analysis. B: Close up of interaction between benzophenone (green) and Leu 9 (orange)

A Gaussian surface representation of the MtrR dimer (Figure 85) highlights the hydrophobic Ile135 residue (shown in red) in the peptide binding site. This also highlights the accessibility of the residue towards ligand binding.

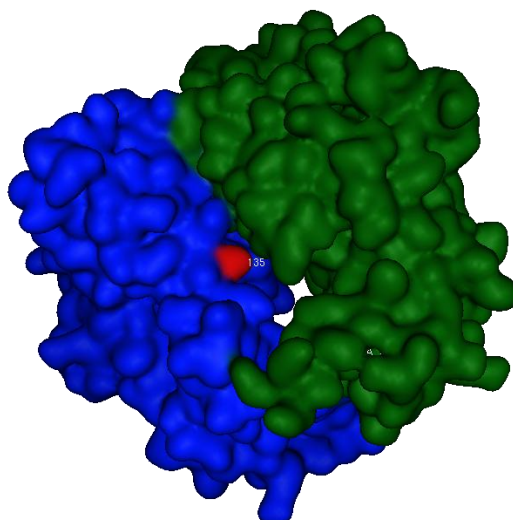


Figure 85 Surface map of MtrR showing the benzophenone labelled Ile 135 in red.

A secondary site found by the site finder function in MOE identified the outer most helices as a potential site and this also supports the mass spectrometric data for labelling at L 93 of helix HTLLHFFER. The location of this binding on the edge of the protein and not in the main ligand binding domain may arise from non-specific labelling of the protein due to favourable hydrophobic interactions on the protein surface as the labelled at Ile 135 corresponds to an opening in the protein surface enabling ligand entry to the ligand binding domain (Figure 85).

#### 3.5.5.4 Summary

The work described above using an affinity controlled photoactivatable peptide ligand of MtrR, can be summarised as follows:

- The LL-37 C-terminal peptide FLRNLVPRTES (**203**) was labelled with benzophenone - 4 - carboxylic acid (**241**) in a single step on the solid phase.
- Conditions were developed and optimised to facilitate photoactivated insertion of the benzophenone labelled peptide (**243**) into MtrR.

- Trypsin digest of the labelled protein followed by MALDI and ES<sup>+</sup> mass spectrometric analysis identified five non-native peptides that corresponded to insertion of the probe into three helices of MtrR.
- MS / MS experiments were used to confirm the identity of two of the insertion products.
- *In silico* analysis of the peptide binding to MtrR provides evidence to support the mass spectrometric results.

#### **3.5.5.5 Conclusion**

The use of benzophenone labelled peptide provides the first characterisation of the ligand binding domain from MtrR. The observed insertion products can be rationalised by comparison to an *in silico* modelling study that shows two putative peptide binding sites. The central and larger of the two binding sites, is capable of binding the benzophenone labelled peptide in two possible conformations. The different orientations of the peptide account for the observed labelling of helices 1 and 6. A secondary binding site composed of three parallel  $\beta$ -helices accounts for labelling of helix 5.

### **3.5.6 Electrophoretic gel mobility shift assays**

#### **3.5.6.1 Introduction**

The ITC and photoaffinity binding studies involving peptide **203** showed that the peptide is a ligand for MtrR and so attention next turned to investigating the effect of ligand binding on the MtrR : DNA complex. The widely accepted mechanism for the activation of genes by a TetR type protein assumes ligand induced dissociation of the regulator protein from DNA. The following section details efforts to investigate this hypothesis.

A common *in vitro* technique used to assess protein : DNA complexes and the effect of a ligand on protein : DNA complex is the electrophoretic mobility shift assay (EMSA) as discussed in section 1.3.2.2. The results in the literature show that EMSA provides a reliable method for investigating the effects of ligand on protein : DNA complexes. The



operator region for MtrR has been previously identified in the literature so the studies in this project began by ensuring the MtrR : DNA protein complex could be observed before the peptide ligands were screened to probe the effects of the synthetic peptides on the MtrR : DNA complex.

### 3.5.6.2 MtrR:DNA complex

The DNA sequence that MtrR binds was identified by DNA footprinting assays, as discussed in Chapter 1 and biophysical evidence to support the microbiological evidence was provided by Hoffmann *et al* who showed using a fluorescence polarisation assay that a 27-mer oligonucleotide (5'-TTTTTATCCGTGCAATCGTGTATGTAT) bound MtrR with a  $K_d$  0.9 nM. The interaction of MtrR with its operator DNA was undertaken by ITC to provide greater chemical insight into the nature of the protein : oligonucleotide complex. MtrR and dsDNA (sequence see Figure 86) were dialysed into the same buffer (Tris 20mM, NaCl 300mM, Glycerol 10%, DTT 1mM, pH 8.0) and dsDNA was injected into MtrR. The observed data was fitted using the standard OneSite Model provided in the ITC analysis software by Microcal.

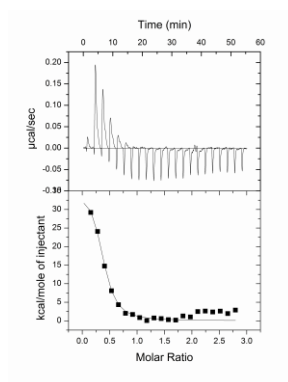


Figure 86 ITC data for the injection of dsDNA (1 mM) into MtrR (70  $\mu$ M)

(F: 5'-TTTTTATCCGTGCAATCGTGTATGTATAATG-3' (247)

R : 3'-AAAAATAGGCACGTTAGCACATACATATTAC-5' (248)

**Table 12 Summary of thermodynamic parameters for the interaction of TetR type proteins MtrR, IacR and QacR with their respective DNA operator regions**

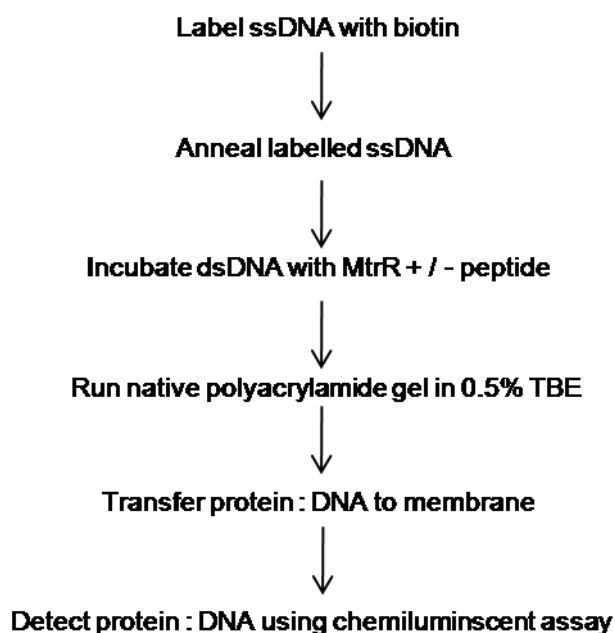
Protein : DNA	$K_d$ / nM	$\Delta H$ / kJ mol <sup>-1</sup>	$\Delta S$ / kJ mol <sup>-1</sup> .K	Ref.
MtrR	56 ± 1	156 ± 11	158	This study
MtrR	0.9	ND	ND	136
IacR	5 ± 0.1	57 ± 0.8	84	86
QacR	46 ± 3	64 ± 5.7	359	88

The calculated thermodynamic parameters are compared to the values obtained by Hoffmann *et al* for MtrR and also to 2 other TetR proteins (Table 12). The ten fold discrepancy in  $K_d$  between the values obtained in this study and by Hoffman is likely to be due to the different oligonucleotide sequences used.<sup>136</sup> Hoffmann used a 27-mer dsDNA sequence that was 4 residues shorter at the 3' end than in this study. The large  $\Delta H$  can be attributed to the presence of four more charged residues in the DNA binding domain of MtrR relative to IacR and QacR therefore increasing the potential for salt bridges and thus increasing  $\Delta H$ .

### 3.5.6.3 Development of EMSA conditions using synthetic peptide as ligands

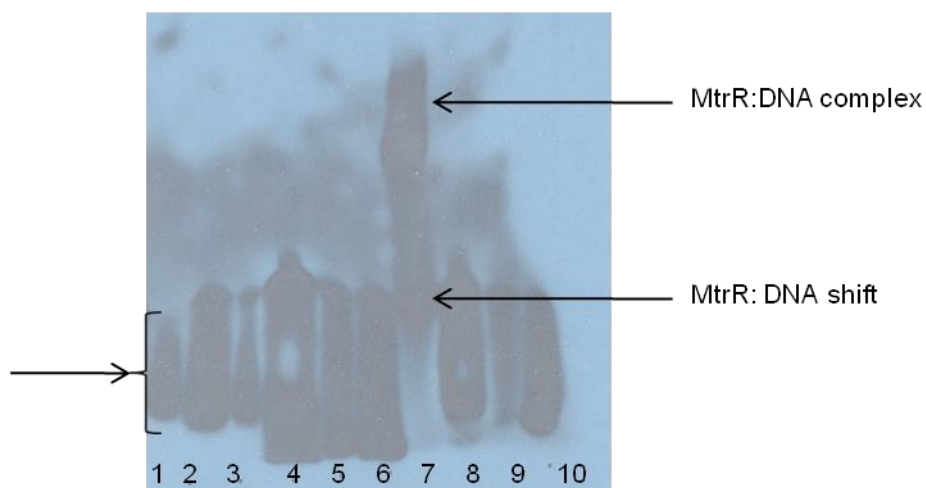
Following the ITC binding study between MtrR and DNA, the conditions for the EMSA study between MtrR, DNA and peptide were developed. These experiments were conducted in collaboration with Dr Ines Borges-Walmsley.

The strategy of the EMSA assay is outline in Scheme 6. Biotin was chosen as the visualisation tag as biotinylated DNA can be detecting using a chemiluminescent method and thus avoids the safety issues surrounding the use of <sup>32</sup>P labelled DNA. Following the labelling reaction, the single stranded DNA is annealed. dsDNA is then incubated with protein in the presence or absence of peptide ligand for 10 – 20 minutes. It is at this point that the protein : DNA complex may form and so to support complex formation the native gel is run in Tris borate buffer (TBE) rather than SDS which can disrupt protein : DNA binding. Following gel electrophoresis, the protein and DNA are transferred to a nylon membrane and then the DNA can be detected by a chemiluminescent assay (Scheme 6).



Scheme 6 Work flow for EMSA assay

The oligonucleotide sequences in Figure 87 were labelled at the 3' end using the commercially available biotin 3' end DNA labelling kit (Pierce). The forward and reverse strands (1  $\mu\text{M}$ ) were incubated separately with 0.5  $\mu\text{M}$  biotin-11-UDP and 2U/ $\mu\text{L}$  terminal deoxyribonucleotidyl transferase (TdT). After stopping the reaction with EDTA, the labelled DNA was extracted and the single strands annealed using either a hotblock or PCR machine. The melting temperature for the DNA sequence is 59.9  $^{\circ}\text{C}$  (as determined by the MWG online calculator) and so equal volumes of forward and reverse strand DNA were mixed together, heated to 90  $^{\circ}\text{C}$  in a hot block and slowly cooled to room temperature. Alternatively, the DNA was annealed in a PCR machine. The labelled DNA was not purified at any stage prior to the EMSA as literature states that purification is not necessary.



**Figure 87: Concentration screen to determine concentration of MtrR required to observe a gel shift. Lanes 1-7: 3'-labelled dsDNA (1 nM) incubated with 0, 0.0125, 0.25, 0.375, 0.62, 0.75 and 1  $\mu$ M MtrR. Lanes 8-10: 3'-labelled forward DNA, 3'-labelled reverse DNA, 3'-labelled annealed DNA.**

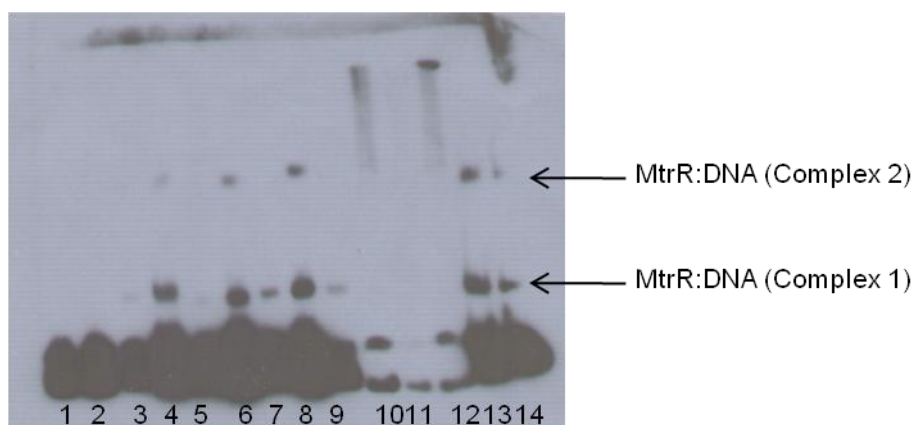
**DNA sequence used:**

**Forward: 5'-TTT TTA TCG GTG CAA TCG TGT ATG TAT AAT (249)**

**Reverse: 3'-AAA AAT AGC CAC GTT AGC ACA TACATA TTA (250)**

The annealing was not 100% successful in forming double stranded DNA as can be seen in Figure 87. The absence of a lower band in lane 7 together with the retarded band is indicative of the MtrR : DNA complex.

With evidence that 1  $\mu$ M MtrR causes a gel shift of labelled ds DNA (5 nM), an experiment was designed to assess the effect of peptide **203** on the complex. If the peptide acts as an inducer of MtrR, the protein should be released from the DNA. A screen of different concentrations of **203** was undertaken (Figure 88). The peptide did not appear to dissociate MtrR from the operator DNA. In experiments using 1  $\mu$ M MtrR two shifts were observed, whereas when 0.5  $\mu$ M MtrR was used only one shift (a faint band) was observed. The high shift may be due to a 4:1 MtrR : DNA complex and the lower shift due to a 2:1 MtrR : DNA complex, although this is only speculation. At high concentrations of peptide, the peptide : DNA : protein complex does not enter the gel, as no dsDNA is observed in lane 9, 10, 11 or 12.



Lane	1	2	3	4	5	6	7	8	9	10	11	12	13	14
MtrR ( $\mu\text{M}$ )	-	-	0.5	1	0.5	1	0.5	1	0.5	1	0.5	1	1	1
DNA (nM)	5	5	5	5	5	5	5	5	5	5	5	5	5	5
Peptide ( $\mu\text{M}$ )	-	-	0	0	1	1	25	25	50	50	1000	1000	-	-

Figure 88 Result of EMSA using peptide 203 (0 - 1mM) , biotin-labelled mtrDNA (5 nM) and MtrR (0.5 or 1  $\mu\text{M}$ ) and table detailing reagents used.

### 3.5.6.4 Conclusions

The synthetic peptide **203** did not displace MtrR from its operator DNA. Despite ITC evidence showing that this peptide binds MtrR it appears not to act in the hypothesised manner as a ligand that causes derepression of the gene. Furthermore, EMSA experiments using the natural product LL-37 (personal communication Dr Ines Borges-Walmsley) also indicate that LL-37 does not cause the protein to dissociate from the DNA. These results indicate that either the peptides function via an unexpected mechanism, possibly binding to MtrR not complexed to the DNA thus preventing MtrR from locating on the operator DNA. More studies are necessary to determine the role of peptides in the activation of the *mtrCDE* genes via MtrR depression of the *mtrCDE* operon. Unfortunately there was no time to explore other techniques such as NMR, cell and *in vitro* methods to assess the ability of ligands to induce protein based depression of

genes are reported in the literature. A cell based assay was used to show that a TetR ligand peptide isolated from a PHAGE display library could induce derepression of the *lacZ* gene by binding to TetR.<sup>307</sup> Expression of the inducer peptide was as a thioredoxin fusion and rather than attempting to express the C-terminal section in vivo as a fusion protein, a chemical biology solution was sought.

### 3.5.7 Investigating antimicrobial properties of LL-37 and derivatives

#### 3.5.7.1 Introduction

Undeterred by the negative result from the EMSA assays, two further questions remained regarding the bioactivities of the synthetic derivatives of LL-37, *viz.* antimicrobial activity and the ability for MtrCDE to export the peptides. The following section outlines microbiological methods to determine the antibacterial effects of peptides and then the results from this study are discussed.

An experiment was designed that allowed the antibacterial effects and substrate specificity for the MtrCDE pump to be screened in the same experiment. It was not possible to work with strains of *N. gonorrhoeae* (a Category II pathogen) during this research project, so an *E. coli* system was used that contained the genes for the MtrCDE efflux pump. Precedent exists in the literature for using an antibiotic susceptible strain of *E. coli* (KAM3 strain) to probe the effects of  $\beta$ -lactamase and efflux pump genes on antimicrobial susceptibility.<sup>308</sup> It was envisaged that the inclusion of the *mtrC*, *mtrD*, *mtrE* and genes into KAM3 *E. coli* cells would create a system to test whether the synthesised peptides are substrates for the MtrCDE efflux pump. The antibacterial effect of the peptides would be tested at the same time, as control cells with no gonococcal gene inserts would show whether the peptides are capable of killing susceptible bacteria.

The KAM3 *E. coli* cell strains containing the *mtrC*, *mtrD* and *mtrE* and genes were constructed by Li Zhang from the Walmsley research group.<sup>309</sup> The genes for the inner membrane protein, MtrD, the outer membrane protein MtrE and the membrane fusion protein, MtrC, were cloned into the pACYC-duet expression vector that allows for simultaneous expression more than one protein. Four KAM3 strains were prepared that contained 0, 1, 2, or 3 membrane protein genes: *mtrD*, *mtrCD*, *mtrCDE* and plasmid only

(strain previously described in Chapter 2).<sup>310</sup> The strains are designed to reveal the importance of the different components of the tripartite efflux pump and analogue systems have been reported in the literature for testing the resistance conferred by the efflux pump to a variety of antimicrobial compounds. Expression of MtrD alone does not lead to increased resistance without the membrane fusion protein MtrC. The expression of *mtrCD* can increase resistance towards antimicrobial agents as the toxic compounds can be removed from the cytoplasm to the periplasm. High levels of resistance can be achieved by expression of *mtrCDE* as the toxic compound can be transported across the outer membrane. Previous studies by the Walmsley group using pACYC containing strains have shown that the *mtrCDE* expressing *E. coli* gave results comparable to growth curve monitoring in *N. gonorrhoeae* cultures indicating the utility the model *E. coli* system.<sup>309</sup> Glycerol stocks of the four pACYC strains were kept at -80 °C and colonies grown on agar plates as required for culturing of cells for growth assays.

#### **3.4.2 Antimicrobial assays using synthetic peptides as probes**

Screening of the peptide antibiotics against the various strains of *mtrCDE* expressing bacteria requires multiple readings to obtain repeats of the data in order to validate it. Whilst this can be achieved manually this requires considerable time and resources. For example, if four strains of *E. coli* are to be screened against one antimicrobial agent using a manual growth curve assay, three test tubes are required per concentration, which is 18 tubes per strain and a total of 72 test tubes are required. Consequently, an automated method was sought to simplify and expedite data collection. In the literature, several methods to assess antimicrobial susceptibility have been reported that use 96-well plates and UV-vis spectrophotometric plate readers.<sup>311</sup> For example, bacterial susceptibility to small molecule antibiotics and antimicrobial peptides has been evaluated using 96-well plate technologies since Brewster reported a reliable 96-well plate method for bacterial enumeration.<sup>312,313</sup> Brewster showed that there is a direct correlation between optical density as measured at 600 nm and bacterial cell survival so that observing a decrease in the optical density indicates a decrease in the number of viable bacteria. The optical density can then be used instead of the traditional plate assays to count the number of bacteria present, as measured in colony forming units (cfu). It was also shown, that the length of time for the culture to reach an O.D of 600 nm, set as the threshold value for survival, is indicative of the number of viable cells present. These methods have been developed by other researchers and applied to peptide antibiotics. For example Ericksen

*et al* used the length of time for the threshold value to be reached to determine the MIC's of a range of defensin peptides.<sup>314</sup> Otvos used the relationship between O.D and cell viability to generate a general method for the determining the antimicrobial effects of cationic peptides by monitoring growth at 600 nm, then taking the final O.D value at 600 nm at the end of the growth curve monitoring (16 hrs) and plotting O.D. versus peptide concentration to determine cell MIC values.<sup>315</sup> IC<sub>50</sub> values can also be determined using the Otvos method and an IC<sub>50</sub> is defined as the antibiotic concentration where the activity crosses the half-line between uninhibited growth and medium only at  $\lambda = 600 \text{ nm}$ .<sup>316</sup>

Application of the 96-well method in this project enabled the four test strains (pACYC-*mtrD* KAM3, pACYC-*mtrCD* KAM3, pACYC-*mtrCDE*, pACYC-only KAM3) to be grown on the same microwell plate and at a range of concentrations (Figure 89). The outermost wells are prone to evaporation so these contained only 100  $\mu\text{L}$  of media. Each well in the microplate has a capacity of 400  $\mu\text{L}$  and so using only 200  $\mu\text{L}$  per well ensures that when the microplate is shaken in the spectrophotometer there is no cross contamination between wells.

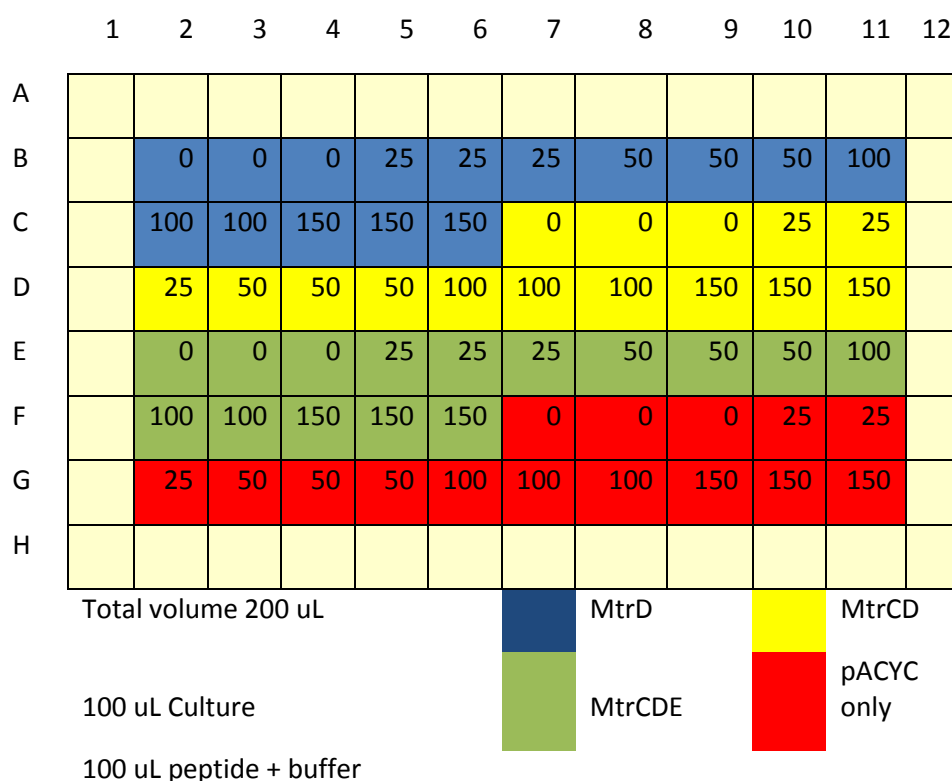


Figure 89 Preparation of microwell plate for peptide bioactivity studies



Growth was monitored for 16 hours using a UV-Vis spectrophotometer thermostated at 37 °C. The data was exported and analysed in EXCEL. To construct the survival curves, the end points of each concentration were averaged and the mean O.D. values were changed to percent survival using the equation  $([\text{mean O.D.} \times \mu\text{M peptide}] / [\text{mean O.D.} \times 0 \mu\text{M peptide}])$  and the data plotted on a graph with concentration vs O.D.

Initial experiments with peptide **203** used LB broth as the media for the growth curve monitoring but the lowest survival rate observed was 40%. It is known that antimicrobial peptides can be inhibited by salts and this effect may contribute to the low activity so Müller Hinton broth was used in the repeat of the experiment and a larger antibacterial profile was observed.<sup>317</sup> The difference between *mtrCDE* expressing cells and control cells (pACYC only) was ~ 30% compared to ~ 20% for the experiment carried out using LB. Consequently, all subsequent experiments were carried out with MH broth.

Using the conditions optimised with the C-terminal peptide the other synthesised peptides were assessed for antimicrobial activity. The addition of the benzophenone moiety to the *N*-terminus of peptide **203** decreases the susceptibility of pACYC control and MtrD expressing KAM3 cells towards the peptide (40% survival relative to 20% survival with the native peptide), but the survival of MtrCD and MtrCDE expressing cells is not affected (~ 50% in both experiments). This suggests that the aromatic group does not affect the ability for the efflux pump to transport the peptide. The MtrCDE pump is also capable of recognising peptides, as shown by the survival curve for the *N*-terminal peptide (Figure 92).

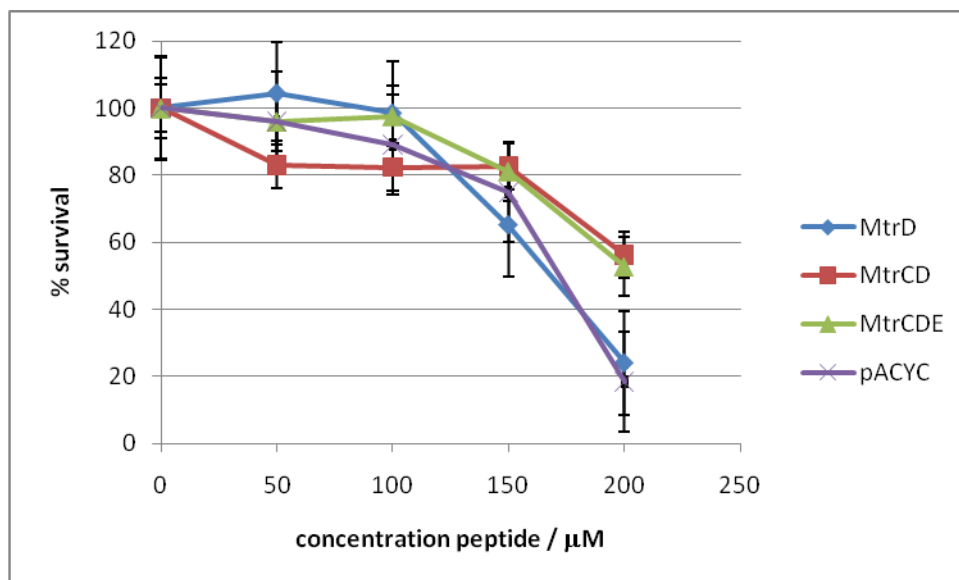
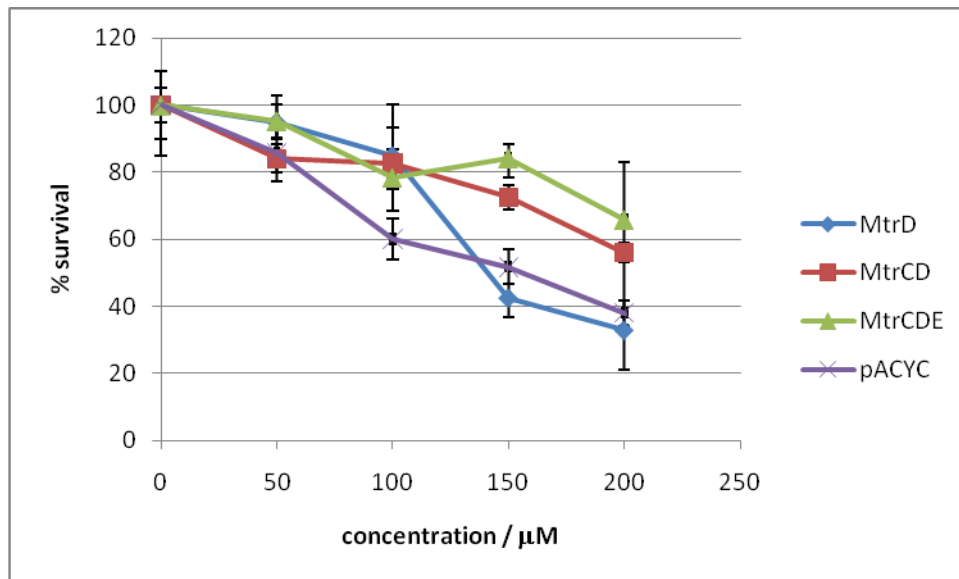


Figure 90 Survival curves for FLRNLVPRTE5 (203) in either Luria Broth (LB, upper panel) or Müller Hinton Broth (MHB, lower panel)

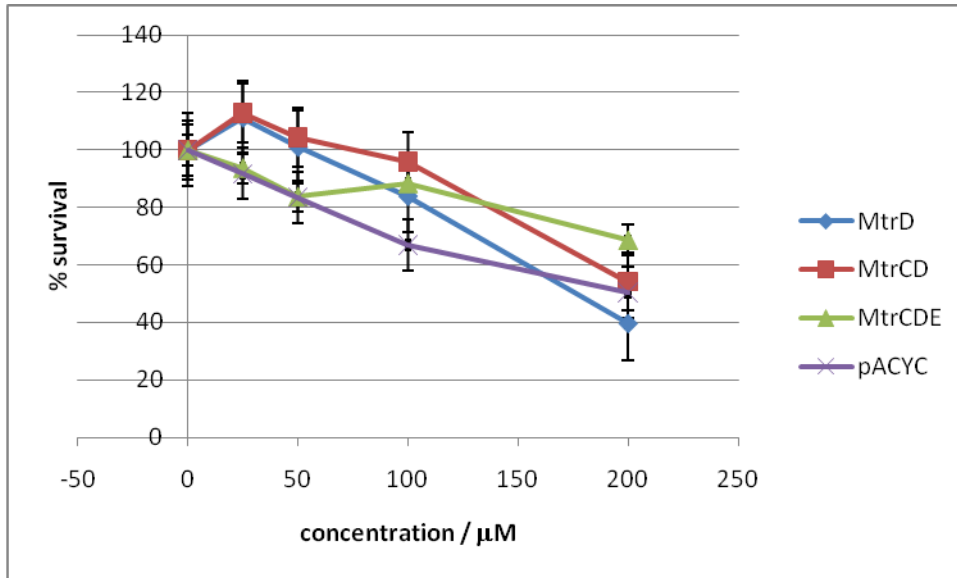


Figure 91 Survival curve for peptide 243

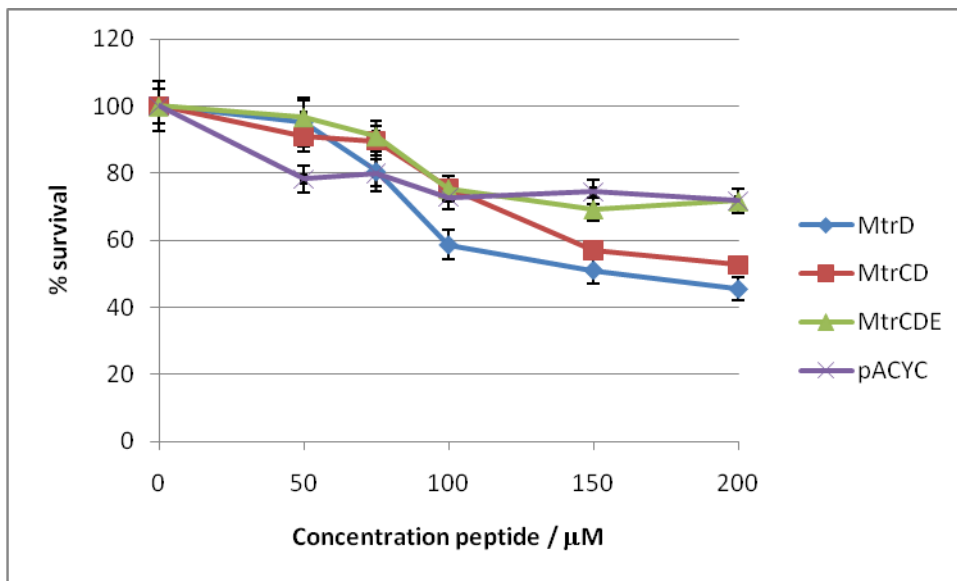


Figure 92 Survival curve for N-terminal peptide of LL-37 (204)

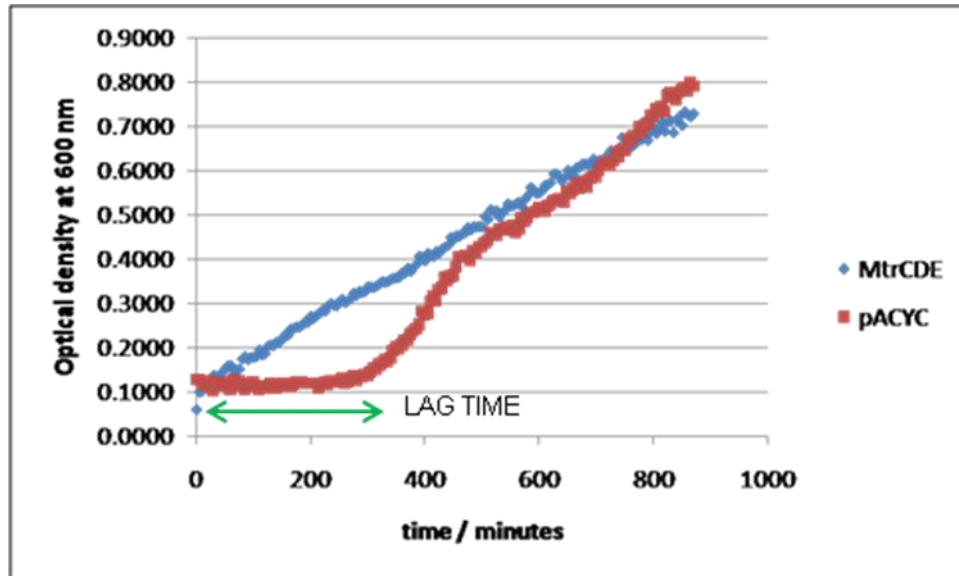


Figure 93 Growth curve data for pACYC and MtrCDE expressing KAM3 cells in the presence of peptide 204 (200  $\mu$ M)

There is only a small change in strain susceptibility to the N-terminal peptide **196**, even at high concentrations, which suggests that the peptide is not very effective at penetrating the cell membrane. Greater insight into the observation that the MtrCDE expressing strain and the pACYC control strains exhibit the same level of survival at 200  $\mu$ M is provided by looking at the optical densities with respect to time (Figure 93). The MtrCDE expressing cells are not affected at all by the peptide and grow at the same rate over the course of the experiment. The pACYC strain shows a lag time of 250 minutes when the cell density is not increasing but thereafter the strain grows at exponential rate to reach a final O.D similar to MtrCDE strain.

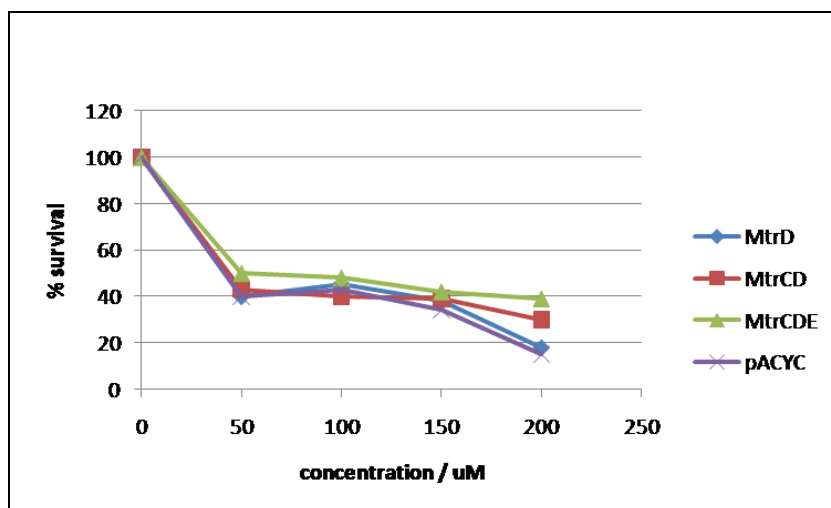


Figure 94 Survival curve for core peptide 100

The core peptide **100** is also hydrophilic but in contrast to the NT peptide **204**, the core peptide is  $\alpha$ -helical.<sup>214</sup> As a result of the defined structure the core peptide displays a potent antimicrobial effect against each of the test strains (Figure 94). A 50% increase in susceptibility is seen for each strain on increasing peptide concentration from 0  $\rightarrow$  50  $\mu$ M.

Further truncation of the core peptide to RIVQRIK (**238**) decreases activity to a level comparable to the *N*-terminal region (Figure 95).

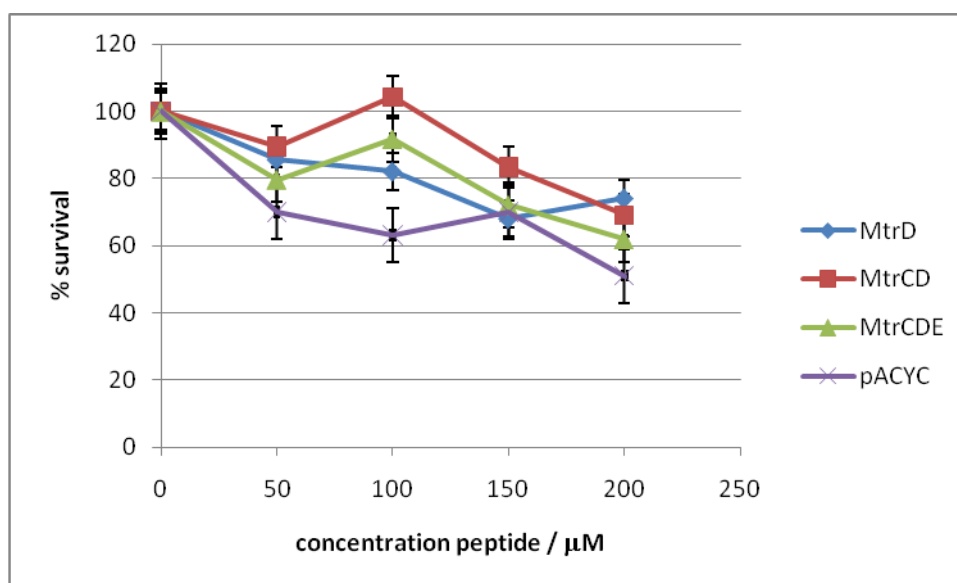


Figure 95 RIVQRIK 238

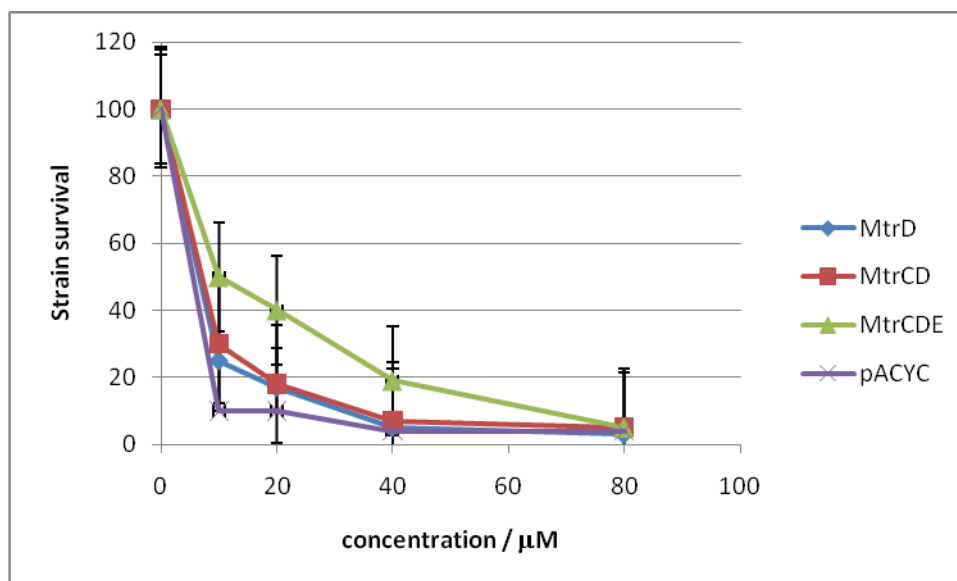


Figure 96 Survival curves for LL-37 (12) in at various concentrations and different strains of mtrCDE

These results together with the observation that the 203 peptide has an MIC against the pACYC strain comparable to the core peptide indicate that  $\alpha$ -helicity and hydrophobicity are more important structural factors that contribute to antibacterial activity than charge.

The natural product LL-37 is the most active antibacterial peptide, and due to the high activity the concentration range was lowered to 0 - 10.0  $\mu$ M range (Figure 96). The MtrCDE pump provides some resistance to the peptide, raising the MIC four fold.

The effects of the tested peptides against the pACYC strain are summarised in graph G. The only peptides to have an MIC of 200  $\mu$ M or less were the natural product and the core and C-terminal peptides. The addition of the benzophenone moiety to the C-terminal peptide reduced the antibacterial effect by a factor of 2. This can be rationalised by the addition of the hydrophobic photolabel to the peptide increases the overall hydrophobicity of the peptide significantly, causing the peptide to lodge in the membrane but not to cause structural defects sufficient to cause bacterial cell wall lysis.

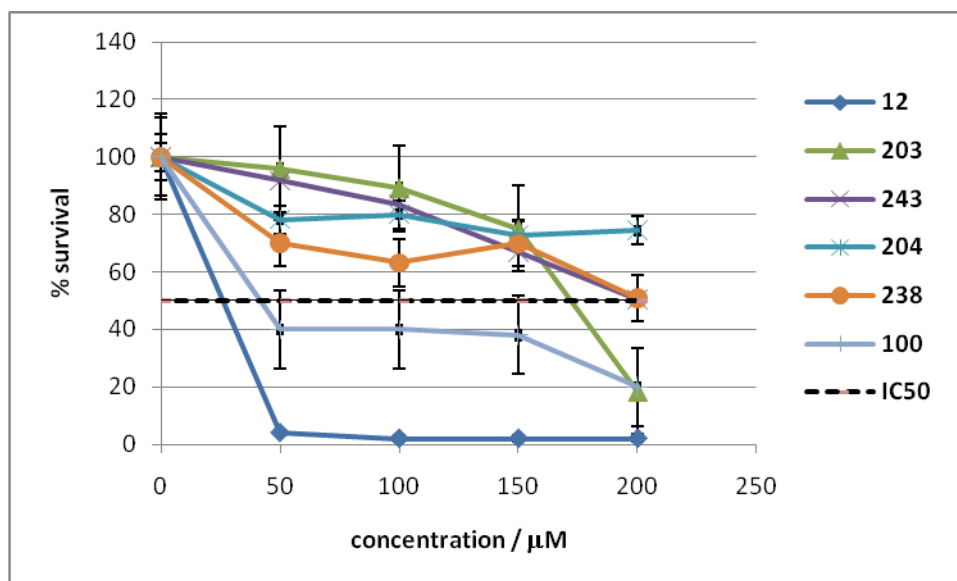


Figure 97 Comparison of MtrCDE expressing KAM3 cells grown in the presence of different peptides

Previous studies in the Walmsley group using the pACYC strains showed that the MIC for nafcillin against the pACYC strain was 153  $\mu\text{M}$  (64  $\mu\text{g} / \text{mL}$ ). The observed MIC for LL-37 in this study is 50  $\mu\text{M}$  (43  $\mu\text{g} / \text{mL}$ ) the two synthetic peptides **203** and **100** are  $\sim 200 \mu\text{M}$  indicating that despite exhibiting much MIC higher values than LL-37, they still maintain antibacterial activity.

Differences are observed in MIC values between MtrCDE expressing bacteria and pACYC stains indicating that the synthesised peptides are substrates for the MtrCDE efflux pump. In order to investigate the protective effect of expressing *mtrC*, *mtrD* and *mtrE* genes, growth curve monitoring was performed for the MtrCDE expressing strain in the presence of **203** (100  $\mu\text{M}$ ) and varying concentrations of CCCP (Figure 98), which uncouples proton motive force across the bacterial membrane, removing the energy source for the efflux pump.<sup>318</sup> If the MtrCDE efflux pump is capable of exporting the peptide, then the presence of CCCP should effect the efflux of the antibacterial peptide from the cell and hence compromise the growth rate and survival of the bacteria. It has been shown that the concentration of CCCP necessary to block efflux is strain dependent

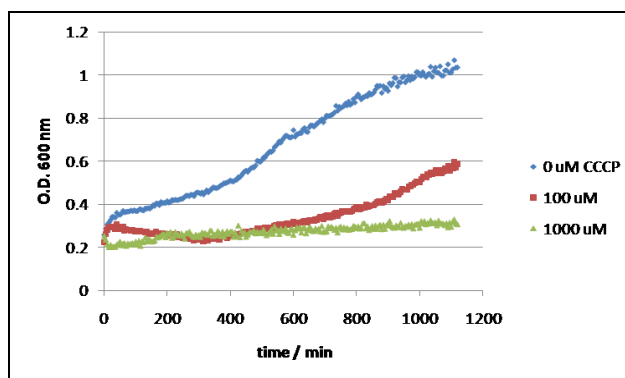
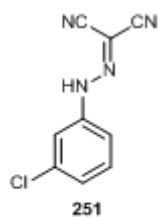


Figure 98 Effect of peptide (203, 100  $\mu\text{M}$ ) in the presence of CCCP at different concentrations on the growth of KAM3 *E. coli* cells expressing proteins for the MtrCDE efflux pump. Blue circles = 0  $\mu\text{M}$  CCCP, red squares 100  $\mu\text{M}$  CCCP, green triangles 1000  $\mu\text{M}$ .

consequently *E. coli* were grown at two concentrations of CCCP, 100 and 1000  $\mu\text{M}$ .<sup>319</sup> 200  $\mu\text{M}$  peptide concentration was chosen because Figure 98 shows MtrCDE to confer a distinct protective effect to the bacteria compared to the control strain. The effect of 100  $\mu\text{M}$  CCCP is clearly seen, with growth considerably slowed and the presence of 1000  $\mu\text{M}$  CCCP is fatal for the bacteria.

As a control to analyse the effect of CCCP, the concentration of CCCP was held constant at 100  $\mu\text{M}$  and the concentration of peptide varied. The aim of this analysis was to check that the decrease in survival of bacteria seen in Figure 98 was due to the peptide and not due to the CCCP. Figure 99 indicates that the change in susceptibility towards peptide **203** is due to the removal of the proton motive force and not due to a toxic concentration of CCCP. The general reduction in survival across all strains suggests that CCCP may compromise the viability of cells, however, only a small change in survival of the pACYC only strain relative to the strains is seen at 200  $\mu\text{M}$  concentration peptide. It would be expected that the pACYC only strain not to be greatly affected by CCCP due to the lack of active efflux in the membrane and, as expected, the percent survival at 200  $\mu\text{M}$  peptide is comparable to that in Figure 98. A considerable change is seen for MtrCDE and MtrCD expressing strains. The percent survival for the MtrCDE expressing strain is lower at 200  $\mu\text{M}$  peptide than the control strain. The presence of protein channels in the bacterial membrane may compromise the stability of the inner and outer membrane, and possibly enable more peptide to enter the cell thus decreasing cell survival to a level lower than that of the control strain.



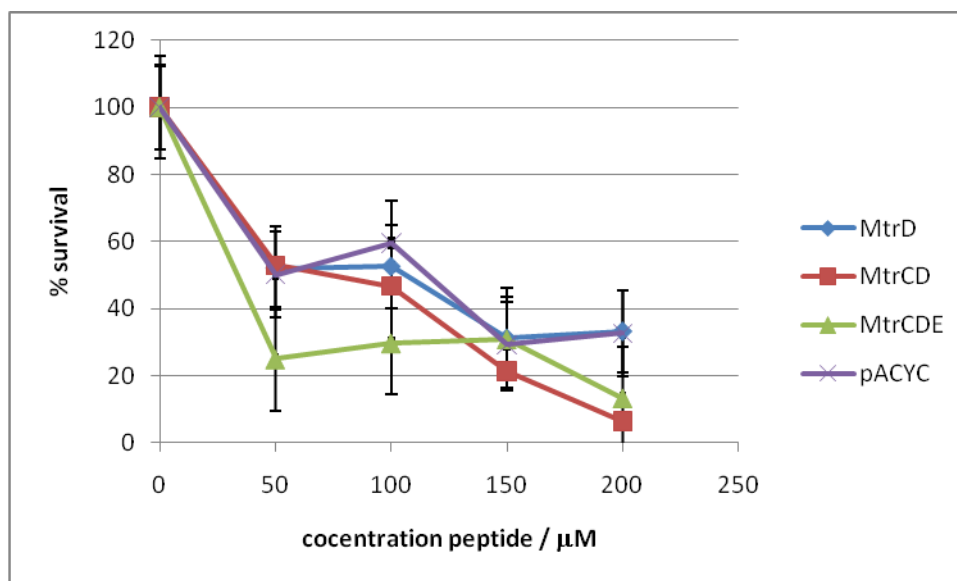


Figure 99 Effect of 100 mM CCCP on the survival of MtrD, MtrCD, MtrCDE and pACYC strains of *E. coli* in varying concentrations of peptide 203

#### 3.4.4 Summary

The studies using *E. coli* cells expressing gonococcal membrane transport proteins show that the peptides synthesised in this project are substrates for the MtrCDE efflux pump. Peptides 203 and 100 were shown to have MIC values of 200  $\mu\text{M}$  towards *E. coli* cells not expressing membrane transport proteins and this concentration is comparable to the known antibiotic nafcillin (MIC 153  $\mu\text{M}$  for KAM3 *E. coli*).

#### 3.4.5 Conclusions

In conclusion, the growth curve studies show that the synthesised peptides are substrates for the MtrCDE efflux pump and have weak antimicrobial effects at high concentrations.

## 4. Conclusions and further work

This chapter details work carried out alongside the research project described and provides suggestions for the development of the work described.

### 4.1 Conclusions

Key findings from this thesis are:

1. Tetracycline (**11**), spectinomycin (**10**), penicillin G (**2**) and LL-37 (**12**) were shown to be ligands for MtrR.
2. MtrR is capable of hydrolysing penicillin G (**2**) and this was shown to provide a survival benefit to *E. coli* cells.
3. The binding of LL-37 was analysed by synthesising fragments of the natural product and assessing each peptide individually for binding to MtrR by ITC. This approach confirmed that the N-terminal peptide (**204**) does not interact with the protein whereas the C-terminal peptide (**203**) binds MtrR with high affinity. The known antibacterial peptide **100** was shown to bind the peptide weakly.
4. Using a photoactivated analogue of **203** insights into the molecular interactions between the peptide ligand and MtrR were determined. A large peptide binding domain and a secondary peptide binding domain were isolated through a mass spectrometric assay and confirmed by homology modelling.
5. Peptide **203** was shown not to dissociate MtrR from its operator DNA. This contradicts the hypothesis that ligands for the MtrR and MtrCDE efflux pump induce derepression of the efflux pump genes. It is possible that the charged peptide associates with the DNA in the EMSA assay, stabilising rather than destabilising the interaction.
6. A microwell plate assay was developed to assess the antimicrobial effects of the synthesised peptides and also whether the peptides are substrates for the MtrCDE pump. Hydrophobic or  $\alpha$ -helical peptides are more active than hydrophilic and charged peptides.

The following section details suggestions for future elaboration of the results of this project, together with a summary of some initial studies conducted alongside the discussed research.

## 4.2 Future work

### 4.2.1 Introduction

#### 4.2.2 Development of cathelicidin peptide screening

At the beginning of section 3.2 it was shown that not only was LL-37 a substrate for the MtrCDE efflux pump, but also porcine antimicrobial peptide PG-1 (**71**) and its synthetic analogue PC-8 (**72**). PG-1 belongs to the cathelicidin family due to the way in which it is produced and stored *in vivo*. In contrast to LL-37, PG-1 adopts a  $\beta$ -hairpin structure constrained by two disulphide bonds. Initial experiments to assess the viability of PG-1 and PC-8 to act as ligands for MtrR began with the synthesis of PC-8. This proceeded well using PyBOP double coupling. Although some deletion peptides were identified arising from incomplete couplings of arginine to arginine, subsequent prep HPLC yielded the desired product in 18% yield.

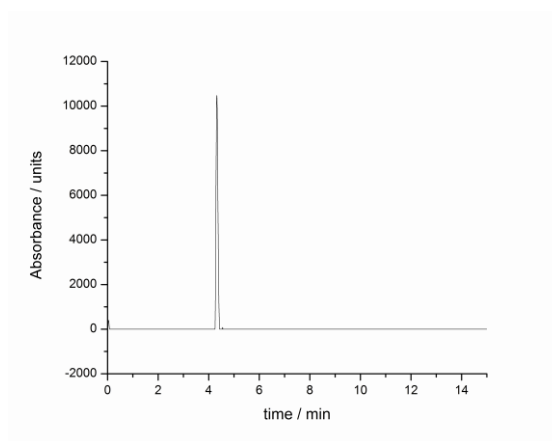
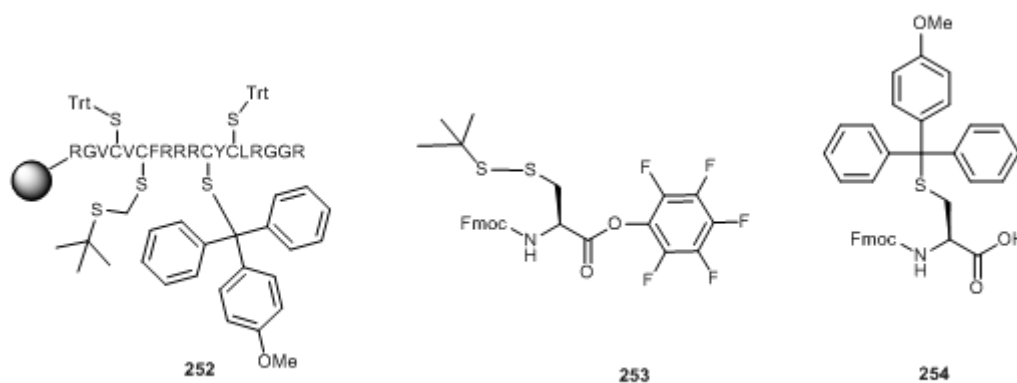


Figure 100 HPLC PC-8

Encouraged by the successful synthesis of PC-8, attention next turned to the preparation of the parent natural product PG-1. The preparation of cysteine containing peptides requires special consideration due to the number of potential side products due to the unique reactivity of the sulphur containing side chain. Preparation of multiple disulphide bonds requires prudent use of protecting groups.<sup>320</sup> Reflecting this, it was envisaged that the disulphide bond between Cys8 and Cys13 would be installed by selectively deprotecting Cys8 and Cys13 on the solid phase. TFA / TIS / H<sub>2</sub>O cleavage would then yield the side chain deprotected peptide in a  $\beta$ -turn conformation, constrained by the Cys8-Cys13 disulphide bond. This would bring Cys6 and Cys15 in close proximity to allow formation of the second disulphide bond by air oxidation. The

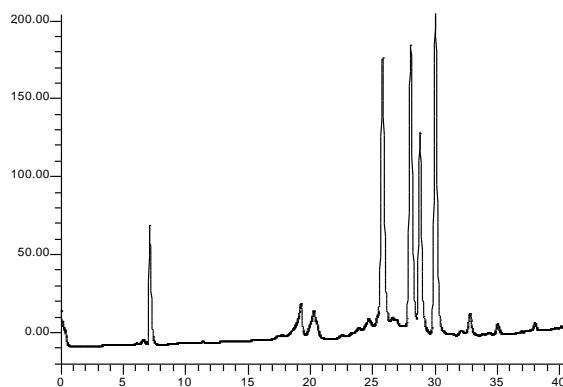


**Figure 101 Organisation of cysteine protecting groups for regioselective disulphide bond formation (252); Fmoc-Cys(tBuS)-OPfp (253); Fmoc-Cys(Mmt)-OH (254)**

protecting groups chosen to establish the disulphide bond on the solid phase were tert-butyl-S ether and monomethoxytrityl (mmt). The tBuS ether can be removed by treatment with  $\beta$ -mercaptoethanol and mmt is removed in 1% TFA.<sup>321</sup> HPLC purification of the mono-disulphide peptide provides the substrate for the second disulphide bridge formation that occurs in 100 mM Tris buffer, pH 7 over a period of hours, the reaction can be monitored by HPLC. Protection of sulphur with tBuS has been shown to activate the  $\alpha$  proton to base removal and so to avoid racemisation at the  $\alpha$  chiral centre, the amino acid is introduced as the highly reactive OPfp ester, that does not require activation with a phosphonium or uronium coupling agent.<sup>322</sup>

Unfortunately, in two attempts at the synthesis the machine completed its cycles but HPLC analysis (Figure 102) revealed multiple products and the MALDI analysis showed that contained only trace amounts of the desired peptide were present.

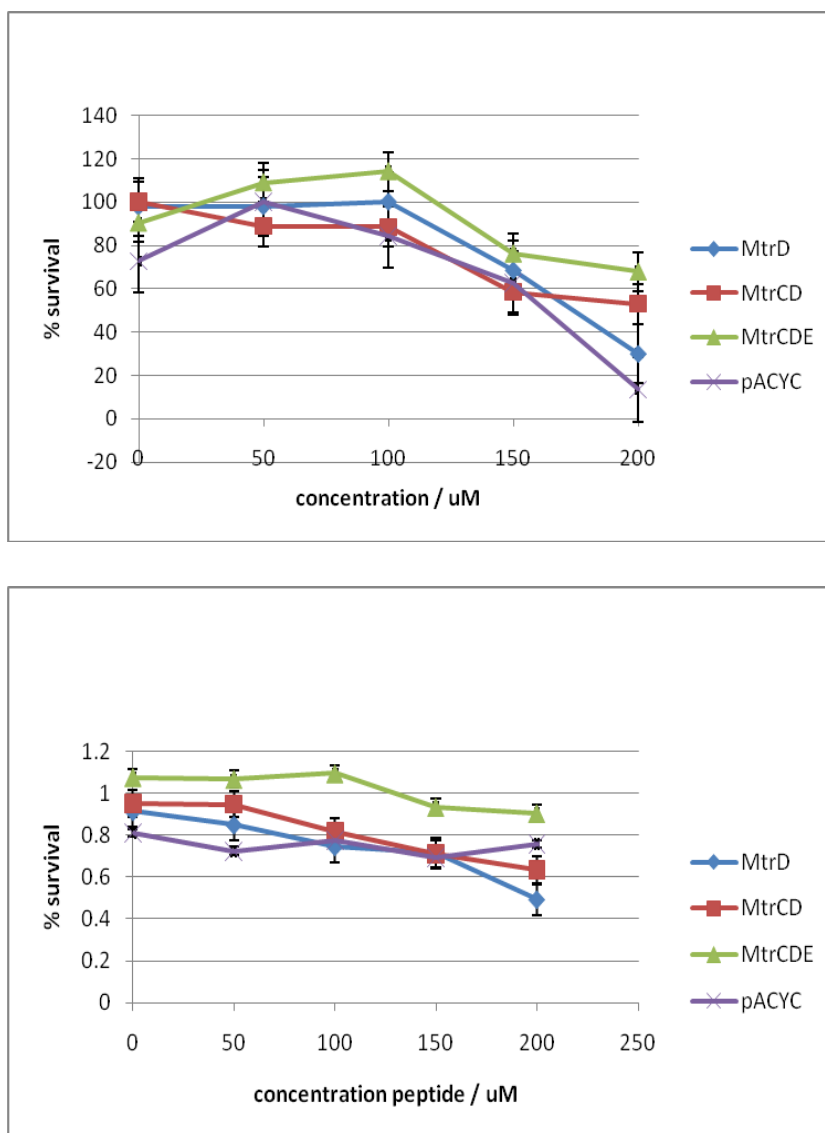
Following the failure of the initial syntheses, and owing to the high cost of the Fmoc-Cys(tBuS)-OPfp and Fmoc-Cys(Mmt)-OH, an alternative strategy was sought. Reviewing the literature revealed the possibility of constructing both disulphide bonds by air oxidation, as the conformation of the desired product represents the most thermodynamically stable arrangement of disulphide bonds.<sup>323</sup>



**Figure 102 HPLC trace of failed PG-1 synthesis**

Building on the success of the microwave synthesis of LL-37 peptides, a manual microwave assisted synthesis of **71** was attempted. Standard HBTU couplings were used, with no preactivation of Cys in the HBTU solution. The synthesis proceeded without problems and the desired product linear peptide was obtained in a crude yield of 35%. The peptide was dissolved in 100 mM Tris-HCl, pH 8.2 and stirred in an open vial for 24 hours. Mass spectrometry indicated full conversion to the disulphide product.

With both peptides in hand, ITC binding studies with MtrR were carried out. Dissappointingly, neither PC-8 nor PG-1 were observed to bind MtrR by ITC. To confirm that these peptides are substrates for the MtrCDE efflux pump, growth curve experiments were performed that confirmed literature reports of PC-8 and PG-1 as substrates for MtrCDE and that PG-1 was more active than PC-8. Further investigation with these peptides was not undertaken. Future avenues for investigation include the use of fluorescence assays or NMR (isotopically labelled or fluorine labelled peptides) to monitor protein : peptide binding and to correlate the results with the ITC studies.



**Figure 103 Bioactivity of PG-1 (upper panel) and PC-8 (lower panel)** Each of the KAM3 strains was more susceptible to PG-1 than to PC-8 and this is consistent with literature that suggests the structure of PG-1 being more able to insert into membranes than the random coil PC-8. In both sets of experiments, it is clear the MtrCDE efflux pump provides a survival advantage indicating that the peptides are transported by the efflux pump.

#### 4.2.3 Conclusion

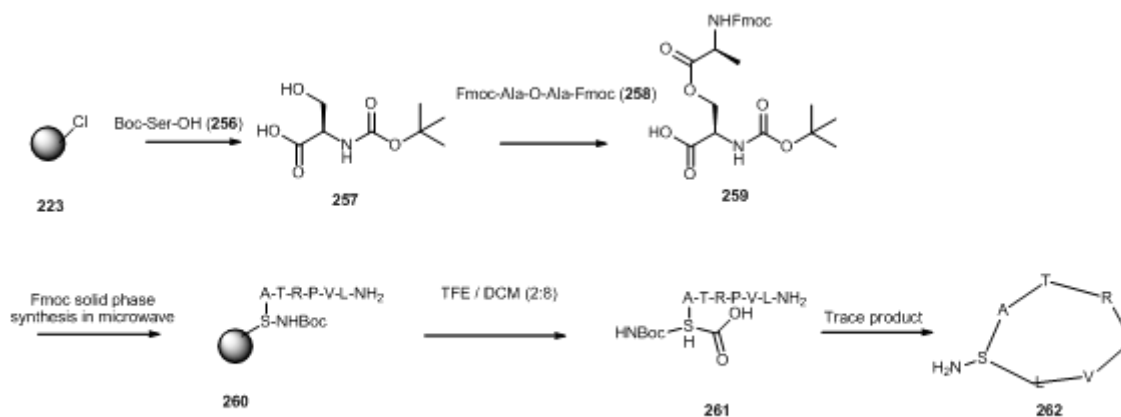
The porcine antimicrobial peptide and its linear analogue were synthesised and shown not to bind to MtrR by ITC. Antimicrobial assays showed that PG-1 (71) is more active than PC-8 (72) and both are substrates for the MtrCDE efflux pump. Further experiments are required to investigate the ligand binding capabilities of PG-1 and PC-8 to MtrR.

### 4.3 Cyclic peptides

The C-terminal peptide fragment (**203**) reported here as a ligand for MtrR and antimicrobial peptide is an interesting lead peptide for further investigation. Linear peptides are not stable *in vivo* for a long time and the predicted *in vivo* persistence of **203** is only 2 minutes.<sup>324</sup> In order to improve the lifetime and antimicrobial effects of the peptide it would be interesting to look at cyclic analogues. To this end, an initial study on the synthesis of cyclic peptides as ligands for MtrR was undertaken. Two strategies will be discussed briefly a) the solution cyclisation using a protected peptide precursor and b) the synthesis of a solid phase linker to aid peptide cyclisation on the solid phase.

#### 4.3.1 Solution phase synthesis

In order to develop the chemistry to produce cyclic analogues of peptide **203**, the sequence was simplified. The peptide was shortened to seven residues and the glutamic acid residue changed to alanine. Scheme 7 outlines the synthesis of cyclic LVPRTAS (**262**). The synthesis began with the acylation of chloro trityl resin (**223**) with Boc-Ser-OH (**256**). The side chain OH was then acylated, with Fmoc-Ala anhydride (**258**), and at this point the loading was determined by Fmoc number to be 80%. The remaining OH were capped with acetic anhydride and the remaining amino acids added using standard microwave assisted peptide couplings. The linear peptide was removed from the resin (**260**) using TFE / DCM (2:8) to maintain the side chain protecting groups (**261**). Cyclisation with PyBOP and HBTU were attempted but no product were seen. Due to time constraints, the synthesis was not optimised further but represents the foundation for future studies in the group.



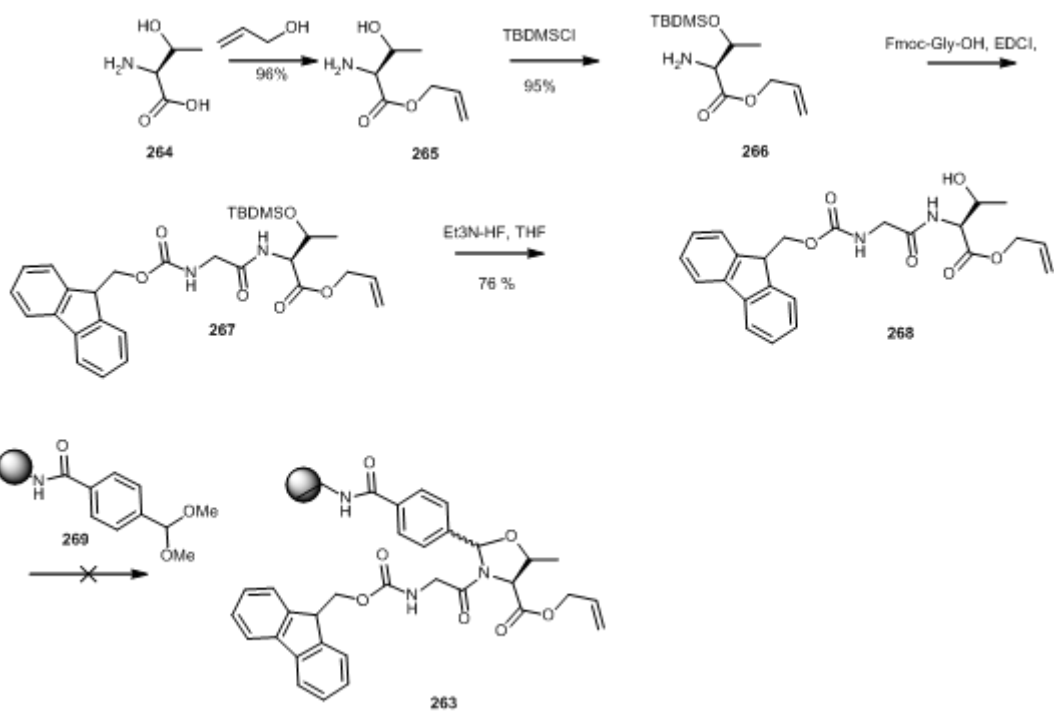
Scheme 7 Synthesis of cyclic analogue of FLRNLPRTES

### 4.3 Initial studies on the synthesis of a pseudo-proline linker for solid phase peptide synthesis

In order to aid the solid phase synthesis of cyclic peptides, preorganisation of the linear peptide in a conformation that aids cyclisation is desirable. One possible way to achieve this is to introduce a bend at the C-terminus by construction of the peptide on a pseudo-proline linker (**263**). The orthogonal protecting groups allow Fmoc chemistry to be followed by Pd catalysed removal of the allyl protecting group to enable on-resin N- to C-terminus cyclisation. On TFA cleavage of the cyclic peptide from the resin, the pseudo-proline is cleaved to give native amino acids in the peptide product.

The synthesis began with the allyl protection of the carboxylic acid of threonine and this proceeded in 96% yield. Protection of the side chain alcohol was followed by an EDCI mediated peptide coupling to Fmoc-Gly-OH. Removal of the TBDMS protecting group was initially attempted with TBAF but this led to removal of the Fmoc protecting group so the milder  $\text{Et}_3\text{N-HF}$  was used and this gave **268** in 76% yield. Disappointingly, attempts to couple the dipeptide to the linker **269** were unsuccessful. Future development of this work is necessary and a screen of the conditions for forming the oxazolidine ring (acid catalyst and temperature) is needed to identify the optimum conditions for forming **263**.





Scheme 8 Initial synthesis route to pseudo proline linker

## 5. EXPERIMENTAL

### 5.1 Chemistry

#### 5.1.2 General procedures

Dried solvents were prepared using the Innovative Technology Solvent Purification System, as per standard procedures within the department.

#### Melting point

Melting points were determined using a Thermo Scientific 9100 machine.

#### NMR spectroscopy

<sup>1</sup>H-NMR experiments were recorded in CDCl<sub>3</sub>, DMSO or d<sub>6</sub>-MeOH at 200, 300, 400 or 500 MHz on Varian Mercury 200, Varian unity 300, Varian 400, Bruker Avance 400 or Varian Ionva 500 and reported as follows: chemical shift  $\delta$  (ppm) (number of protons, multiplicity, coupling constant  $J$  (Hz), assignment). Residual protic solvent CHCl<sub>3</sub> ( $\delta_{\text{H}} = 7.26$ ) was used as the internal reference. <sup>13</sup>C NMR were recorded at 126 MHz on a Varian Ionva 500 or at 101 MHz on a Bruker Avance 400 using the NMR solvent peak as the internal reference. <sup>19</sup>F NMR was recorded on a Varian 400.

#### Mass spectrometry

Electrospray mass spectra (ES) were recorded at the University of Durham on either a Micromass LCT, Thermo Finningan LTQ FT or Micromass LCT, Q-TOF Premier. MALDI spectra were recorded on either an Applied Biosystems Voyager-DE STR, Micromass MALDI TOF MS or Bruker Autoflex TOF/TOF.

#### *Preparation of MALDI target (Synthetic peptides)*

A saturated solution of  $\alpha$ -cyano hydroxyl cinnamic acid (~ 50 mg) in 3:7 H<sub>2</sub>O containing 0.1 % TFA (1 mL) was prepared. 2  $\mu$ L of this matrix solution was mixed with 2  $\mu$ L analyte and each target well of the 96-well plate was spotted with three drops (each ~ 1  $\mu$ L) of analyte. The matrix : analyte drops were air dried before analysis.

## **Chromatography**

*Thin layer chromatography* was carried out on Merck aluminium backed silica gel 60 F<sub>254</sub> plates and visualised under UV light at 254 nm; phosphomolybdic acid in ethanol and potassium permanganate in water were used as stains.

*Flash chromatography* was carried out manually using 40 – 63  $\mu\text{m}$ , 60 Å silica gel, or using pre-loaded cartridges on a Combiflash® Rf (Teledyne Isco) system.

*HPLC* was carried out at either Cambridge Research Biochemicals using Waters system with a Jupiter column (C18, 250 x 25 mm, 5  $\mu\text{m}$  particle size) or at Durham University on either a Perkin-Elmer Series 200 HPLC with a ACE semi-prep column (C18, 250 x 10 mm, 5  $\mu\text{m}$  particle size), or on a Waters Mass Directed Prep instrument using an Xbridge analytical column (C18, 100 x 4.6 mm, 3  $\mu\text{m}$  particle size) or a preparative column (C18, 100 x 19 mm, 5  $\mu\text{m}$  particle size). Peptides were eluted in either H<sub>2</sub>O / MeCN + 0.1 % TFA or H<sub>2</sub>O / MeOH + 0.1 % formic acid.

## **IR spectroscopy**

Infra red spectra were recorded either as a solution in chloroform via transmission IR cells or as KBr discs on a Perkin Elmer Series 1600 FT-IR spectrometer.

## **Optical rotation**

Optical rotations were acquired on a Jasco P-1020 polarimeter in solution (solvent stated per experiment).

### 5.1.3 Peptide synthesis

#### 5.1.3.1 General procedures

Fmoc-amino acids and Boc-amino acids were purchased from Novabiochem (Nottingham, UK), Pepteuticals (Nottingham, UK) or CEM (Buckingham, UK). Coupling agents were purchased from Novabiochem. HPLC grade DMF was used for coupling reactions and was purchased from Fisher Scientific or Rathburn (Walkerburn, UK). Resins were purchased from Novabiochem.

Method	Coupling			Deprotection		T / °C
	Activator	t / min	Eq.	Composition	t / min	
ACT 348Ω	HOBt	60	4.9	25% Piperidine	I) 3	~ 25
	PyBOP				II) 10	
ACT 578	PyBOP	2 x 60	4.9	25% Piperidine	3	~ 25
					10	
Pioneer	PyBOP,	60	4.9	20 % piperidine /3% DBU	5	~ 25
	HATU Arg, Val, Ile)					
CEM Microwave	HBTU	5	4.9	25% Piperidine	5	70
	HBTU Arg	15	4.9			
Manual	PyBOP	60	7	25% Piperidine	3 15	~ 25
	HBTU	30	5			
	HATU	30	5			

Table 13 Peptide synthesis cycles

Method	Resin	Cleavage mixture <sup>i</sup>	Time / min	Temp. / °C
Manual and after automated synthesis	Rink amide, Wang	TFA / TIS / H <sub>2</sub> O	120 - 300	~ 25
Microwave	Rink amide, Wang	TFA / TIS / H <sub>2</sub> O TFA / TES / H <sub>2</sub> O	15 - 30	38
	Trytil	TFE / DCM	15	38

<sup>i</sup>Volume of cleavage solution was 5 x resin volume

**Table 14 Peptide cleavage conditions**

Process	Temperature / °C	Microwave power / W	Time / min
Deprotection	70 ± 5	20	3
Coupling (not Arg)	70 ± 5	20	5
Coupling (Arg)	25 ± 5	0	5
	70 ± 5	20	15
Coupling (benzoyl benzoic acid)	70 ± 5	20	10
Cleavage	38 ± 5	20	18

**Table 15 Settings used in the CEM microwave for peptide synthesis**

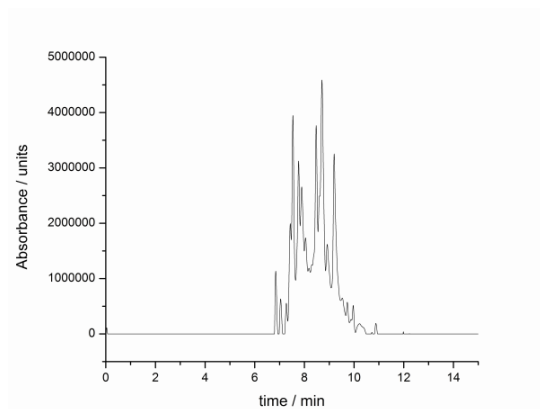
### **Fmoc loading test**

5 mg resin was removed for the Fmoc loading test. The resin was agitated in 3 mL piperidine / DMF solution for 15 min and the resin allowed was to settle prior to measuring the absorption of the solution at 304 nm.

### 5.1.3.2 Synthesis of LL-37 and derivatives

#### FLRNLVPRTES (203)

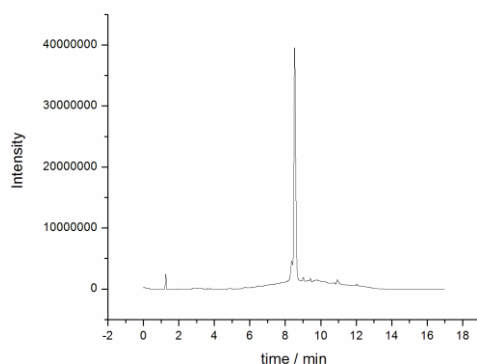
*ACT 348 synthesis:* Wang resin was (300 mg, 0.87 mmol / g) derivitised with Fmoc-Ser(tBu)-OH using the symmetric anhydride method.<sup>336</sup> Fmoc-Ser(tBu)-OH (1 g, 2.61 mmol) and DIC (163 mg, 1.3 mmol) were dissolved in dry DCM (10 mL) at 0 °C and the reaction stirred for 30 min. The reaction was concentrated and the resulting white foam dissolved in DMF (2 mL) and added to pre-swollen Wang resin contained in an SPPS tube. DMAP (3 mg, 0.03 mmol) was added and the reaction was shaken for 2 hours at room temperature. The resin was drained, washed with DMF (3 x resin volume) and 5 mg resin removed for Fmoc loading test. The resin was agitated in 3 mL piperidine / DMF solution for 15 min and the resin allowed to settle prior to measuring the absorbance of the solution at 304 nm. Resin loading was calculated to be 0.55 mmol / g. Unreacted OH functionality of the resin was blocked by reaction of 10% acetic anhydride with the resin for 60 min. The resin was washed with DMF (3 x resin volume) before being transferred to the peptide synthesiser. Standard Fmoc / tBu chemistry used as described in Table 13. The final Fmoc protecting group was removed in the synthesiser and the peptide cleaved using the standard protocol. Although the desired product was detected, separation from the side products was not possible. MS  $m/z$  (MALDI) 1330.7 [M+H]<sup>+</sup>, 1231.6 [M-V]<sup>+</sup>, 1216.6 [M-L]<sup>+</sup>, 1174.6 [M-R]<sup>+</sup>, 1017.5 [M-2R]<sup>+</sup>; HPLC (5→95% MeCN)



**Figure 104** HPLC trace for the crude product from the ACT348 synthesis of 203

*Manual synthesis:* Pre-loaded Fmoc-Ser(tBu)-Wang resin (750 mg, 0.28 mmol / g) was swollen in DMF for 15 min in a SPPS reaction vessel. Couplings were conducted with PyBOP as described in Table 13 and all couplings monitored by Kaiser test. 250 mg resin was cleaved and isolated using standard protocols. Purification gave FLRNLVPRTES (**203**) as a white powder (3 mg, 15%). MS  $C_{59}H_{98}N_{18}O_{17}$ :  $m/z$  (MALDI) 1331.1 HRMS: Calculated for  $C_{59}H_{98}N_{18}O_{17}$  1331.521 found 1331.743. HPLC (5→95% MeCN)

*Microwave synthesis:* Rink amide resin (500 mg, 0.61 mmol / g) was swollen in DMF (8 mL) and all deprotections and couplings conducted in a CEM microwave as per Table 13, 15 and 16. The peptide was cleaved and isolated using standard protocols. 250 mg of resin was used for the cleavage step. Purification gave **203** as a white powder (8 mg, 25%). MS  $C_{59}H_{98}N_{18}O_{17}$ :  $m/z$  (MALDI) 1331.1 HRMS: Calculated for  $C_{59}H_{98}N_{18}O_{17}$  1331.521 found 1331.621; HPLC (5→95% MeOH)



**Figure 105** HPLC trace for the purified product from the microwave synthesis of **203**

#### IKDFLRNLVPRTES (**237**)

*ACT 348 synthesis:* Wang resin (300 mg, 0.87 mmol / g) was derivitised with Fmoc-Ser(tBu)-OH using the symmetric anhydride method as detailed above before being transferred to the peptide synthesiser (final loading 0.55 mmol / g). Standard Fmoc / tBu chemistry used as described in Table 1. The final Fmoc protecting group was removed in the synthesiser and the peptide cleaved using the standard protocol product. No desired product was detected. MS:  $m/z$  (MALDI) 1905.9, 1790.9.

*Manual synthesis:* The resin was prepared as above (resin substitution 0.28 mmol /g). The peptide chain was assembled in an SPPS tube and all couplings were facilitated by HBTU, as per conditions listed in Table 13. 50 mg of resin was transferred to a SPPS vessel and the peptide was cleaved and isolated using standard procedures to yield **237** as a white powder (2.8 mg, 12%). MS  $C_{75}H_{127}N_{22}O_{22}$ ;  $m/z$  (MALDI) 1686.9  $[M+H]^+$ ; HPLC (5→95% MeCN)

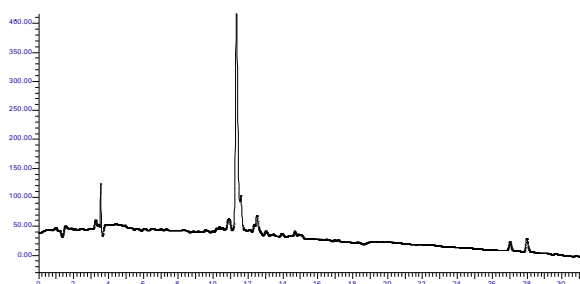


Figure 106 HPLC trace for the purified product from the manual synthesis of 237

#### FKRIVQRIKDFLR (101)

*Manual synthesis:* Rink amide resin (500 mg, 0.60 mmol /g) was swollen in DMF in a SPPS tube. The peptide was prepared manually using PyBOP as the coupling reagent and the conditions listed in table. The peptide was cleaved and isolated using standard procedures. Crude yield not determined due to many side products, inseparable by HPLC; MS (MALDI)  $m/z$  1719.0  $[M+H]^+$ , 1786.2  $[M+piperidine]^+$ , 1562.2  $[M+H-R]^+$ , 1406  $[M+H-2R]^+$ ; HPLC (5→95% MeCN)

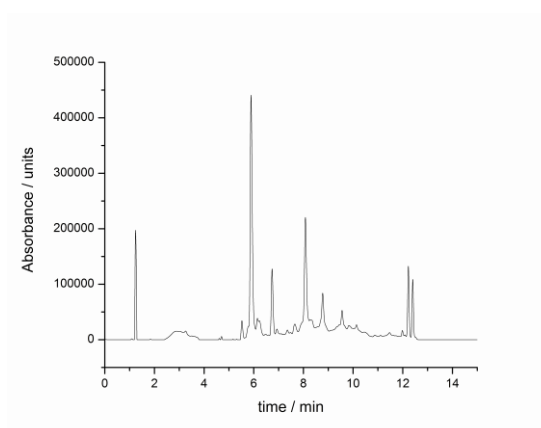


Figure 107 HPLC trace for crude product from the manual synthesis of 101



*Microwave synthesis:* Rink amide resin (500 mg, 0.60 mmol /g) was swollen in DMF in a SPPS tube. All deprotection and coupling reactions were carried out using a CEM microwave adapted for peptide synthesis. The conditions and settings are listed in Tables 14, 15 and 16. 250 mg of resin was used for cleavage, using standard protocols to give 12 mg, 4% of the final product after HPLC purification. MS  $C_{74}H_{124}N_{24}O_{16}$ :  $m/z$   $M+H^+$  (MALDI) 1619.1; (ES<sup>+</sup>) 573.99  $[M+3H]^{3+}$  HRMS: Calculated for  $C_{80}H_{136}N_{25}O_{17}$  1719.054 found 1719.064; HPLC (5→95% MeOH)

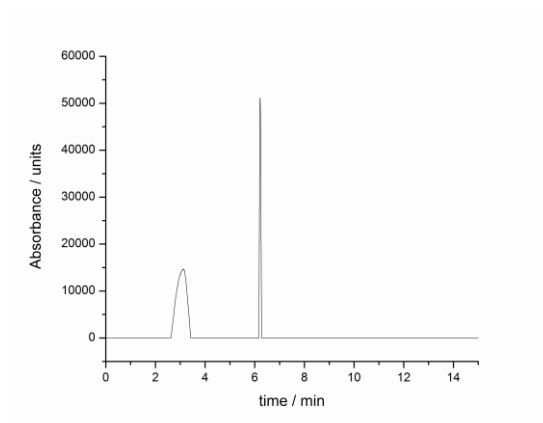


Figure 108 HPLC trace for the purified product from the microwave synthesis of 101

### RIVQRIK (238)

*Manual synthesis:* The resin was prepared as above for FKRVQRIKDFLR. The peptide chain was assembled in an SPPS tube and all couplings were facilitated by HBTU, as per conditions listed in Table 14. The peptide was cleaved and isolated using standard procedures to yield **238** as a white powder. MS  $C_{68}H_{120}N_{22}O_{16}$ :  $m/z$  (MALDI) 911.9 $[M+H]^+$ ; HPLC (5→95% MeCN)

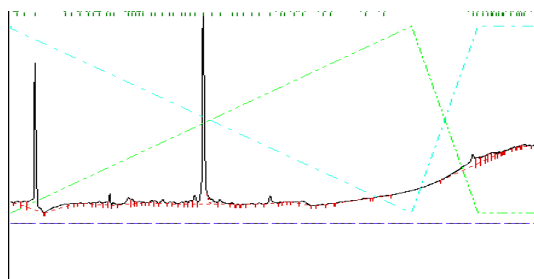


Figure 109 HPLC trace for the final product 238

## LLGDFFRKSK (204)

*ACT 578 synthesis:* Rink amide resin (250 mg, 0.67 mmol / g) was swollen in the peptide synthesiser and all couplings conducted as described in Table 1. The N-terminal Fmoc protecting group was removed on the synthesiser and the resin was transferred to a sintered glass funnel. The resin was washed with DMF (3 x resin volume) and DCM (3 x resin volume) before addition of the cleavage solution. The resin was submerged in cleavage solution for 2 hours, before the resin was drained and the filtrate evaporated to give thick oil. The crude peptide was precipitated in cold diethyl ether, decanted and air dried yielding white platelets; MS:  $C_{57}H_{91}N_{15}O_{14}$   $m/z$  (MALDI) 1210.9  $[M+H]^+$ ; HPLC (5→95% MeOH).

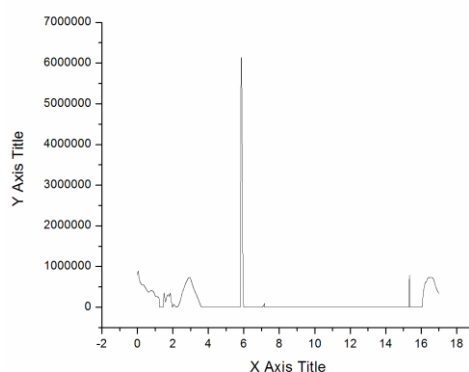
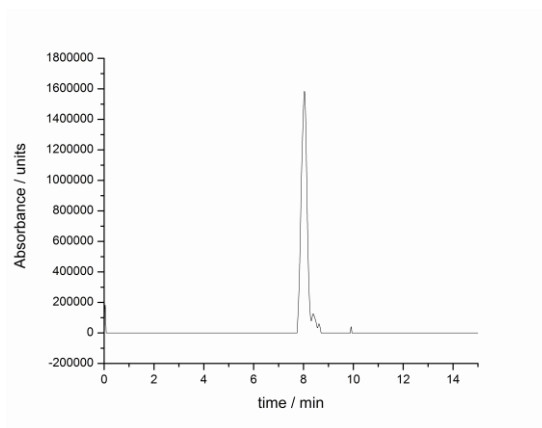


Figure 110 HPLC trace for the final product 204

## KIGKEFKRIVQRIKDFLRNLVPRTES (99)

*Manual synthesis:* Wang resin loaded with Fmoc-FLRNLVPRTES (500 mg, 0.28 mmol / g) was swollen in DMF for 15 min in a SPPS reaction vessel. Couplings were conducted with PyBOP as described in Table 14 and all couplings monitored by Kaiser test. 50 mg of resin was cleaved and the peptide isolated using standard protocols. Purification gave **99** as a white powder (2 mg, 4.5 %); MS:  $C_{143}H_{244}N_{44}O_{37}$   $m/z$  (MALDI) 3171.1  $[M+H]^+$ ; HPLC (5→95% MeCN)

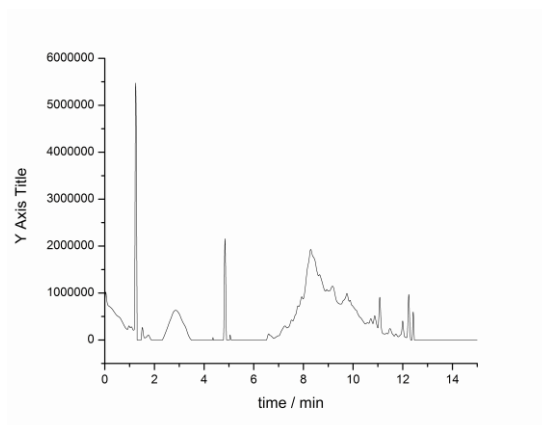


**Figure 111 HPLC analysis for the final product 99**

LLGDFFRKSKEKIGKEFKRIVQRIKDFLRNLPRTES (**12**)

*Pioneer synthesis:* Wang resin pre-loaded with Fmoc-Ser(tBuOH) was loaded dry into the synthesiser. Couplings were carried out as described in Table 1. Synthesis was aborted after addition of R<sup>18</sup> due to many side products, inseparable by HPLC. HPLC (5→95% MeCN)

*Manual synthesis:* Wang resin loaded with Fmoc- KIGKEFKRIVQRIKDFLRNLPRTES (450 mg) was swollen in DMF for 15 min in a SPPS reaction vessel. At the end of the synthesis the final Fmoc group was removed by treatment with 25% piperidine /DMF/3 % DBU before cleavage from the resin using TFA/TIS/H<sub>2</sub>O. After cleavage of the peptide from the resin, mass spec showed no desired product to be present. HPLC (5→95% MeCN)

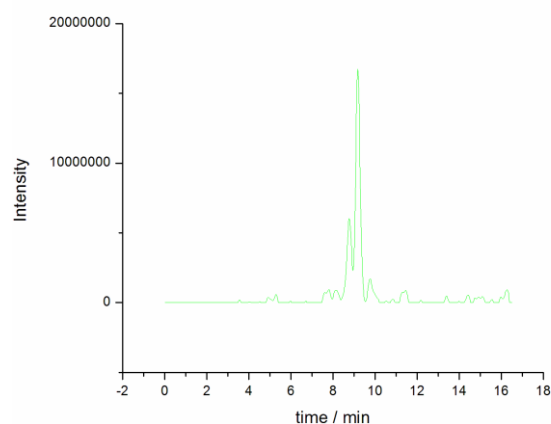


**Figure 112 HPLC trace for the failed synthesis of LL-37**

## 5.1.4. Synthesis of benzophenone labelled peptides

### 5.1.4.1 Benzophenone-FLRNLVPRTES (243)

*Microwave synthesis:* Rink amide resin carrying Fmoc-FLRNLVPRTES (200 mg) was swollen in DMF for 15 min. The N-terminal Phe residue was deblocked using 20% piperidine / DMF using the standard microwave programme. Benzophenone-4-carboxylic acid (280 mg, 1.1 mmol) was dissolved in activator solution of HATU (380 mg, 0.62 mmol) and DIPEA (2M) for 5 min before being added to the deblocked resin. The coupling was conducted in the microwave for 10 min at 70 °C. The resin was drained, washed with DMF (3 x resin volume) and fresh reagents added and the coupling repeated. The resin was drained, washed with DMF (3 x resin volume), DCM (3 x resin volume) and then the resin was cleaved using standard protocols. The crude peptide was precipitated in cold Et<sub>2</sub>O, decanted and dried (30 mg, 12%, 59% pure by HPLC). A small sample was removed for HPLC and mass spectrometric analyses. The crude material was purified using mass directed HPLC to yield a fluffy white solid (3 mg, 1.2%) *m/z* 770 (M+H)<sup>2+</sup> HRMS (1540.4584) HPLC (5→95% MeOH)



### 5.1.5 Photoactivated binding studies

*General method:* Benzophenone labelled or unlabelled (control) peptide (64 μM) was incubated with purified MtrR (64 μM) for 15 min at 4 °C. The reaction was transferred to a quartz cuvette and the photo conversion was performed using a Q-switched third harmonic YAG (Elforlight UVFQ series) operating at 355 nm for 15 min. The temporal width of the optical pulses was 5 ns and the repetition rate was 1 kHz. Typical pulse energies are 100 micro J per pulse. Immediately after irradiation, the cuvette was placed

on ice. In order to remove unreacted peptide, the solution was injected onto a 5 mL Hitrap desalting column (30 mM Tris, 300 mM NaCl, pH 8.2). The first peak eluted contained modified protein and the second peak contained only peptide. The buffer used was. The solution was analysed by SDS-PAGE, MALDI and ES<sup>+</sup> mass spectrometry.

### 5.1.6 Synthesis of PC-8

#### RGGRLAYARRRFAVAVGR (72)

*ACT 348 synthesis:* Fmoc-Arg(Pbf)-Wang resin (0.43 mmol/g substitution) was placed in the synthesiser and all deprotections and couplings carried out a per Tables 1, 2 and 3. No desired product was synthesised. HPLC (5→95% MeCN)

*ACT 578 synthesis:* PC-8 was synthesised on a 0.2 mmol scale using Fmoc-Arg(Pbf)-Wang resin, (0.43 mmol/g substitution). Fmoc deprotection step was performed with 30% piperidine in DMF. and all deprotections and couplings carried out a per tables 1, 2 and 3. The crude peptide was purified by RP-HPLC to yield # as a fluffy white solid 70 mg after freeze drying (18%, 100% pure by HPLC). MS C<sub>88</sub>H<sub>150</sub>N<sub>36</sub>O<sub>20</sub> (MALDI) 2032.31 HRMS: Calculated for C<sub>88</sub>H<sub>150</sub>N<sub>36</sub>O<sub>20</sub> found ESI- 508.80349 [M+H]<sup>4+</sup>

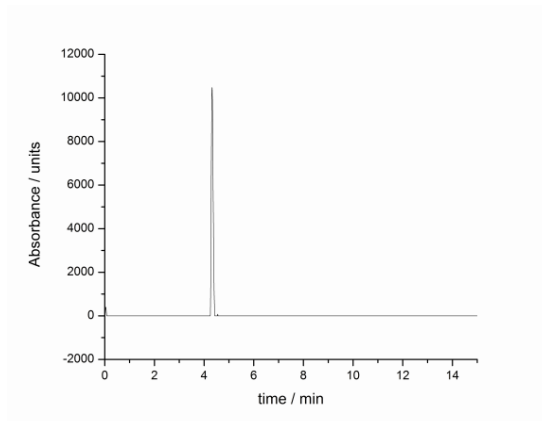


Figure 113 HPLC trace for final product 72

### 5.1.7 Synthesis of PG-1

RGGLCYCRRRFCVVCVGR (71)

*ACT348 synthesis:* Rink amide resin (100 mg, 0.62 mmol / g) was swollen in DMF (8 mL). All couplings were conducted as described in Tables 14, 15 and 16. After addition of the final R residues, the resin was removed from the synthesiser, N-deblocked using 25 % piperidine / DMF solution and the resin washed with DCM (3 x resin vol.) No desired product seen.

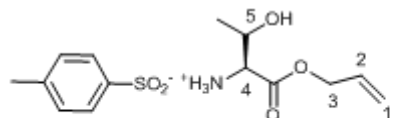
*Microwave synthesis:* Fmoc-Arg(Pbf)-Novasyn TGA® resin (300 mg, 0.32 mmol/g) was swollen in DMF in a SPPS tube suitable for a CEM microwave. All couplings used standard conditions detailed. 100 mg resin was cleaved to give the product as a white powder (32 mg, 50%); (MS (MALDI) 2003.5, 1901.99 C<sub>88</sub>H<sub>150</sub>N<sub>36</sub>O<sub>20</sub>S<sub>4</sub> 1901.98589 (ES<sup>+</sup>) 476 [M+H]<sup>4+</sup>; HPLC (5→95% MeOH).

### 5.1.8 Cyclic analogue of 203

Chlorotrityl resin (500 g, 1.3 mmol / g substitution) was swollen in DCM (8 mL) in a SPPS tube. The resin was drain and then Boc-Ser-OH (220 mg, 2 mmol) and DIPEA (0.39 mL) were added to the resin in DCM (8 mL) and shaken at room temperature for 30 minutes. The resin was drained, washed with DCM and the procedure repeated. Unreacted resin was capped using DCM / MeOH / DIPEA (8 : 15 : 5). The free OH of serine was esterified with Fmoc-Ala-O-Ala-Fmoc, preformed by stirring Fmoc-Ala-OH (2.4 g, 7.8 mmol), DIC (0.49 g, 3.3 mmol) and DMAP (10 mol %) in dry DCM for 30 min at 0 °C. The acylation with anhydride was repeated once with fresh reagents to yield **259**. The resin was transferred to a CEM microwave adapted for peptide synthesis and standard coupling procedures applied to prepare **260**. The resin was treated with TFE /DCM (8 : 2) for 45 minutes to cleave the peptide from the resin to yield **261**. m/z (ES<sup>+</sup>) 965.5 [M-Ser]<sup>+</sup> Cyclisation using in solution was attempted using PyBOP but no desired product was seen.

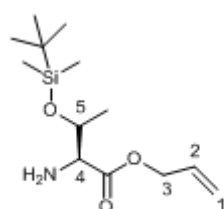
### 5.1.9 Pseudo proline synthesis

#### L-Threonine Allyl Ester<sup>325</sup> (265)



Threonine (10g, 84 mmol) was dissolved in  $\text{CCl}_4$ , allyl alcohol (7.32g, 126 mmol) and *para*-toluene sulphonic acid (126 mmol) were added and heated under reflux using Dean-Stark apparatus. When no more water was collected (15 mL), the reaction mixture was concentrated *in vacuo*. The crude product was washed with water, the organic layers collected, dried over  $\text{MgSO}_4$  and the solvent removed under reduced pressure to yield **265** as a viscous yellow oil (24.1 g, 91 %).  $[\alpha]_D = 4.4$ ,  $c = 1.5$  mg/mL, MeOH,;  $\nu_{\text{max}}(\text{film})$  3154 ( $\text{NH}_2$ ), 2979, 1748, 1215  $\text{cm}^{-1}$ ;  $\delta_{\text{H}}$  (200 MHz;  $\text{CDCl}_3$ ) 7.91 (3H, brd,  $\text{NH}_3^+$ ) 7.73 (2H, d,  $J$  8, Ar-H) 7.11 (2H, d,  $J$  8, Ar-H) 6.34 (1H, brd, OH) 5.90 (1H, m, 2-H) 5.30 (1H, d,  $J$  18, 1, 1-HH), 5.14 (1H, d,  $J$  10, 1, 1-HH) 4.52 (2H, t,  $J$  6, 3- $H_2$ ), 4.18 (1H, dd,  $J$  13, 6, 4-H) 3.94 (1H, dd,  $J$  8, 5-H) 1.24 (3H, d,  $J$  7,  $\text{CH}_3$ );  $\delta_{\text{C}}$  (125 MHz;  $\text{CDCl}_3$ ) 21( $\text{CH}_3$ ) 22 (Ar- $\text{CH}_3$ ) 54 (CH) 59 (NCH) 67 (CH) 69 ( $\text{CH}_2$ ) 119 ( $\text{C}=\text{CH}_2$ ) 126 (Ar-C) 128 (Ar-C) 131 (Ar-C) 140 (Ar-C) 141 (Ar-C) 142 (Ar-C) 172 (OC=O);  $m/z$  ( $\text{ES}^+$ ) 160.1 ( $\text{M}+\text{H}^+$ ); HRMS ( $\text{ES}^+$ ) found  $\text{MH}^+$  160.123,  $\text{C}_7\text{H}_{13}\text{O}_3\text{N}$  requires  $\text{M}^+$  160.125.

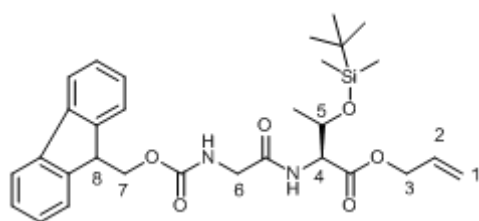
#### L-Threonine (OTBS)OAlloc (266)



Crude **265** (4g, 12 mmol) was dissolved in dry DCM (50  $\text{cm}^3$ ) and *tert*-butyl dimethyl silyl chloride (3.6g, 23 mmol) and imidazole (4.1g, 53 mmol) were added and the reaction stirred at room temperature overnight. The reaction was diluted with ethyl acetate (50  $\text{cm}^3$ ), washed with sodium hydroxide (50  $\text{cm}^3$ ) and saturated brine solution (50  $\text{cm}^3$ ). The organic layers were combined dried over magnesium sulphate and the

solvent removed *in vacuo* to yield a yellow oil (3.12g, 95%)  $[\alpha]_{\text{D}} = +16.7, c = 1.0 \text{ mg/mL}$ , MeOH;  $\nu_{\text{max}}(\text{film})$  3429, 2955, 2858, 1731 (C=O) 1216  $\text{cm}^{-1}$ ;  $\delta_{\text{H}}$  (400 MHz;  $\text{CDCl}_3$ ) 5.86 (1H, m, 2-H), 5.34 (1H, dd,  $J$  16, 1, 1-HH), 5.25 (1H, d,  $J$  9, 1, 1-HH), 4.71 (2H, d,  $J$  5, 3-H<sub>2</sub>), 4.64 (1H, dd,  $J$  13, 6, 4-H), 4.42 (1H, dd,  $J$  17, 6, 5-H), 4.25 (1H, m, 4-H), 1.24 (3H, d,  $J$  7, CH<sub>3</sub>) 0.9 (9H, s, tBu), 0.01 (6H, d,  $J$  7 Hz, 2 x Si-CH<sub>3</sub>);  $\delta_{\text{C}}$  (101 MHz;  $\text{CDCl}_3$ ) 19.7 (HCCH<sub>3</sub>), 37 (C(CH<sub>3</sub>)<sub>3</sub>), 61 (H<sub>2</sub>NC), 65 (OCH<sub>2</sub>), 71 (OCHCH<sub>3</sub>), 119 (C=CH<sub>2</sub>) 148 (CH<sub>2</sub>C=CH<sub>2</sub>) 174 (OC=O);  $m/z$  (ES<sup>+</sup>) 273.2 [M+H]<sup>+</sup>; HRMS (ES<sup>+</sup>) found MH<sup>+</sup> 273.1831, C<sub>7</sub>H<sub>13</sub>O<sub>3</sub>N requires M<sup>+</sup> 273.1825.

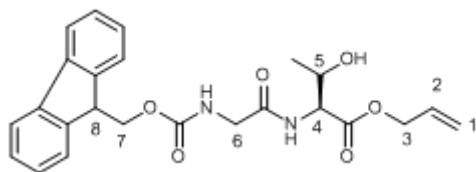
### Fmoc-Gly-Thr(OTBS)-OAlloc (267)



Fmoc-Gly-OH (216, 0.73 mmol) was dissolved in dry DCM at 0 °C. EDCI (140 mg, 0.73 mmol) and DMAP (17 mg, 0.15 mmol) were added. After 10 minutes, a solution of **2** (200 mg, 0.73) in dichloromethane was added and the reaction stirred for a further 2 hours at 0°C. The solvent was evaporated and the crude mixture purified by column chromatography (1:1 Et<sub>2</sub>O: Hexane) to give **3** as a colourless oil (320 mg, 79%) R<sub>f</sub> 0.2  $[\alpha]_{\text{D}} = 4.4$ ,  $c = 1.5 \text{ mg/mL}$ ,  $\text{CHCl}_3$ ;  $\nu_{\text{max}}(\text{film})$  3494, 3019, 2955, 2930, 1731 (C=O), 1687, 1504, 1216, 897  $\text{cm}^{-1}$ ;  $\delta_{\text{H}}$  (500 MHz;  $\text{CDCl}_3$ ) 7.78 (2H, d,  $J$  8, Ar-H) 7.61 (2H, d,  $J$  8, Ar-H) 7.32 (2H, t,  $J$  8, Ar-H), 7.28 (2H, t,  $J$  8, Ar-H), 6.6 (1H, d,  $J$  10, NH), 5.95 (1H, m, 2-H), 5.35 (1H, d,  $J$  17, 1-HH), 5.27 (1H, d,  $J$  10, 1-HH), 4.61 (2H, m, 3-H<sub>2</sub>) 4.5 (2H, t,  $J$  8, 6-H), 4.01 (2H, d,  $J$  6, 7-H<sub>2</sub>), 1.23 (3H, d,  $J$  6, CH<sub>3</sub>), 0.9 (9H, s, tBu), 0.05 (3H, s, Si-CH<sub>3</sub>), 0.01 (3H, s, Si-CH<sub>3</sub>);  $\delta_{\text{C}}$  (126 MHz;  $\text{CDCl}_3$ ) 20 (C-CH<sub>3</sub>) 28 (C-(CH<sub>3</sub>)<sub>3</sub>) 42.5 (6-CH<sub>2</sub>) 48 (C-(CH<sub>3</sub>)<sub>3</sub>) 58 (5-C) 61.5 (3-O) 63.5 (7-C), 70 (4-C) 119.6 (1-C) 120.1 (2-C) 128-136 (Ar<sub>Fmoc</sub>) 140 (OCONH);  $m/z$  (ES<sup>+</sup>) 552.73 [M]<sup>+</sup> 553.2 [M+H]<sup>+</sup> 575.4 [M + Na]<sup>+</sup>, 489.4 [M-C<sub>3</sub>H<sub>5</sub>]<sup>+</sup> HRMS (ES<sup>+</sup>) found MH<sup>+</sup> 553.2725, C<sub>30</sub>H<sub>40</sub>O<sub>6</sub>N<sub>2</sub>Si requires M<sup>+</sup> 553.2715.



### Fmoc-Gly-Thr-OAlloc (268)



**267** (200mg, 0.36 mmol) was dissolved in dry THF (5 cm<sup>3</sup>) and triethylamine trihydrofluoride (0.41 cm<sup>3</sup>, 2.3 mol) was added dropwise. After stirring overnight the reaction was complete by TLC analysis. The reaction was filtered through silica to remove excess triethylamine trihydrofluoride and the solvent removed in *vacuo*. Purification by flash chromatography (Ethyl acetate: Hexane 2:1) gave **268** as an off white oil that crystallised on standing (157 mg, 76%);  $R_f$  0.8 [ $\alpha$ ]<sub>D</sub><sup>20</sup> = 10.0;  $\nu_{\max}$ (film) 3250, 2954, 2930, 1728, 1665, 1216 cm<sup>-1</sup>;  $\delta_H$  (500 MHz; CDCl<sub>3</sub>) 7.78 (2H, d,  $J$  10, Ar-H), 7.59 (2H, d,  $J$  10, Ar-H), 7.39 (2H, m, Ar-H), 7.31 (2H, m, Ar-H) 6.87 (1H, d, NH) 5.88 (1H, m, NH) 5.45 (1H, m, 2-H) 5.27 (1H, d,  $J$  17, 1-HH) 5.21 (1H, d,  $J$  8, 1-H) 4.65 (1H, m, NH) 4.41 (2H, t,  $J$  9, 3-H<sub>2</sub>) 4.21 (1H, t,  $J$  6, 8-H<sub>2</sub>), 4.11 (1H, m, 5-H), 4.0 (2H, 6-H<sub>2</sub>) 1.24 (3H, m, CH<sub>3</sub>);  $\delta_C$  (126 MHz; CDCl<sub>3</sub>) 21 (CH<sub>3</sub>) 43 (Gly-CH<sub>2</sub>) 58 (NHCH) 62 (OCH<sub>2</sub>CH) 63 (OCH<sub>2</sub>CH) 119 (C=CH<sub>2</sub>) 120 (H<sub>2</sub>C-CH=CH<sub>2</sub>) 128-136 (Ar<sub>Fmoc</sub>) 142 (C=O) 172 (C=O) 175 (C=O);  $m/z$  (ES<sup>+</sup>) 461 [M+Na]<sup>+</sup>; Found C, 65.21; H, 5.80 C<sub>24</sub>H<sub>25</sub>N<sub>2</sub>O<sub>6</sub> requires C, 65.74; H, 5.98%

## 5.2 Biology

### 5.2.1 General Procedures

#### Bacterial culture

The following media were used for the culturing of bacteria:

*LB broth*: 10.0 g / L Tryptone, 5.0 g / L yeast extract, 5.0 g / L NaCl

*LB agar*: 10.0 g / L Tryptone, 5.0 g / L yeast extract, 5.0 g / L NaCl, 15.0 g agar

*YT broth*: 16.0 g / L Tryptone 10.0 g / L yeast extract, 5.0 g / L NaCl

*SOC media*: 2.0 g Tryptone, 0.5 yeast extract, 2.0 mL NaCl (5M), 1.0 mL KCl (1M), 1.0 mL MgCl<sub>2</sub> (1M), 1.0 mL MgSO<sub>4</sub>, 2.0 mL glucose (1M) in 100 mL H<sub>2</sub>O

*MH broth*: Purchased from Fluka and used at 23 g / L

All media were prepared using MilliQ H<sub>2</sub>O and autoclaved at 121°C for 15 min. prior to use.

#### SDS-PAGE

*Preparation of gel*: Typically a 10% acrylamide gel was prepared: The resolving gel consisted of 2.75 mL resolving buffer (1.5M Tris-HCl, 0.4% (v / v) TEMED, 0.4% (w/v) SDS, pH 9.0), 2.58 mL 40% bis-acrylamide, 4.82 mL H<sub>2</sub>O and 10% APS. The stacking gel was composed of 4.5 mL stacking buffer (0.14M Tris-HCl, 0.11% (v/v) TEMED, 0.11 (w / v) SDS, pH 6.8), 0.5 mL 40% bis-acrylamide, 50 µL 10% APS.

*Running of gel*: Electrophoresis was carried out at 180V for 1 hour in 124 mM Tris, 1M glycine, 17 mM SDS.

*Molecular mass markers*: Biorad low molecular mass markers were used.

*Gel stain*: Protein bands were stained using 20 mL of Coomassie blue colloidal stain (prepared by filtering a suspension of 70 mg Coomassie G-250 in 250 mL EtOH into phosphoric acid solution)

### **Agarose gel (for DNA)**

*Preparation of 1.0% gel:* 0.5 g agarose was dissolved in 50 mL TAE buffer (50 x TAE, 242 g Tris, 57.1 mL glacial acetic acid, 100 mL 0.5M EDTA, pH 8.0) by microwave heating. On cooling to 60 °C, 1 µL ethidium bromide was added and the gel poured into the gel tank.

*Sample loading:* 20 µL digest DNA was mixed with 4 µL 6x loading buffer (0.25 % bromophenol blue, 0.25 % xylene cyanol FF, 15 % Ficoll in H<sub>2</sub>O) and loaded into the gel.

*Running of gel:* 120 V were applied for 30 min.

### **5.2.2 Overexpression and purification of MtrR**

An LB–Agar plate was poured containing 5 µL carbenicillin or kanamycin (stock solution 100mM) and when solid was streaked with stock cells (BL21-AI containing gene for MtrR in pET21a vector or pET28). The plate was placed in 37 °C room overnight. In the morning, the plate was removed from the 37 °C room and placed in the fridge for storage. In the afternoon a colony picked and transferred to 10mL LB–overnight culture (containing 5 µL carbenicillin) and left on a flat bed shaker set at 180 rpm in the 37 °C room overnight. 1 mL of culture transferred to 250 mL of YT broth containing carbenicillin (250 µL). The flasks were shaken using a flat bed shaker set to 220 rpm at 37 °C for 3 hours. The O.D. at 600 nm was measured using a spectrophotometer previously blanked using YT broth. If the O.D. was less than 0.5 the flasks were shaken for 20 minutes longer before the O.D. was remeasured. When the desired optical density had been reached, the cells were induced with 1mM IPTG and 0.4% L-arabinose. The flasks were shaken for a further four hours at 180 rpm, at 37 °C.

The cell suspensions were transferred to centrifuge bottles and centrifuged using a JLB–10.5 rotor at 7,500 rpm for 20 minutes at 4 °C. The broth was decanted and the cell pellet dissolved in a small volume (2 mL) of lyses buffer (Tris 20 mM, NaCl 300 mM, 10% glycerol). Lysozyme was added to a final concentration of 1mM. The cell suspension was then sonicated for a total of 2 minutes (4 x 30 second bursts of sonar energy) at a power output of 12%. All sonication were carried out whilst the protein was on ice.

The lysed cells were centrifuged in a JB–25.5 rotor at 20,000 rpm for 20 minutes at 4 °C.

A HITRAP 1mL or HITRAP 5 mL FF column was washed with water (10 column volumes) and equilibrated with 5 volumes of loading buffer (10mM Tris, 300 mM NaCl, pH8.2). The cell lysate / crude protein solution was filtered through a 0.4  $\mu$ M filter and loaded onto the HITRAP column using a peristaltic pump running at 0.5 mL / min. The flow through was collected and analysed by SDS-PAGE to ascertain if all the His-tagged protein had been loaded onto the column.

The HISTRAP column was transferred to a GE healthcare AKTA Explorer FPLC. The column was washed with 2 column volumes of loading buffer and the flow through collected. A gradient of increasing buffer B (Tris 20mM, NaCl 300mM, Imidazole 500 mM, pH 8.0) from 0-100% was run over 10 column volumes and 1 mL fractions collected. The fractions were analysed by SDS-PAGE, MALDI mass spectrometry.

The elution buffer was exchanged for a non-imidazole containing buffer using either a PD-10 column (Pierce), HITRAP 5 mL desalting column or dialysis overnight.

The second purification was carried out on a MonoQ column. Protein was dialysed into Tris 20mM, NaCl 100 mM and prior to injection onto column. Buffer a = Tris 20 mM, buffer B = Tris 20 mM, NaCl 1 M, pH 8.2. Protein eluted at approximately 50% B.

The protein was purified on a gel filtration column (15/60 superdex, GE Healthcare). The purification buffer was (tris 20 mM, NaCl 300 mM, pH 8.2). The gel column was equilibrated in water (1 column volume) and buffer (2 column volumes) before the sample was injected. The sample was eluted after 50 minutes with a flow rate of 1 ml/min.

### **5.2.3 MtrR mutant proteins**

Primers for H105A, H105Y and H105F were designed using online Stratagene software. Site directed mutagenesis was undertaken by Bing Zhang. Proteins were overexpressed and purified as per MtrR above.

### **5.2.4 Construction of BL21AI and KAM3 *E. coli* containing pET28a-MtrR plasmid**

#### **5.2.4.1 Plasmid prep from BL21-AI (pET21a-mtrR)**

A single colony of BL21AI *E. coli* carrying pET21a-MtrR was picked from an agar plate and transferred to 10 mL LB media containing carbenicillin (1 mmol) and incubated overnight at 37 °C with shaking at 180 rpm. The pET21a-MtrR plasmid was isolated

from the overnight culture using a Wizard mini-prep kit. Plasmid DNA sequenced by DBS Genomics.

#### **5.2.4.2 Transformation of XL-10 with pET21a-mtrR**

100  $\mu$ L XL-10 ultracompetent (Stratagene) were incubated on ice with 4  $\mu$ L of  $\beta$ -mercaptoethanol for 2 min. 50 ng of plasmid DNA was added and the tube swirled gently. Incubated on ice for 30 min., heat shocked at 42 °C for precisely 30 sec., incubated on ice for 2 min., 0.9 mL SOC medium added and incubated at 37 °C for 1 hour. Cells were spread on LB-agar plates containing carbenicillin and plates incubated overnight at 37 °C.

#### **5.2.4.3 Excision of mtrR gene from pET21a and purification of the mtrR gene**

Buffer D (Promega) was placed in an autoclaved eppendorf. 1  $\mu$ L of XbaI and 16  $\mu$ L of MtrR plasmid were added. The eppendorfs were incubated at 37 °C overnight. Digest was analysed by running the sample on a 1.0% agarose gel. The bands containing MtrR at ~ 750 kbp and the pET 28a blank vector were visualised on a UV-transilluminator and cut from the gel using a scalpel. The gel pieces were transferred to autoclaved eppendorfs and the DNA extracted using the 'Prep-B-Gene' system (Biorad).

100  $\mu$ L DNA purification buffer (sodium perchlorate 6M, Tris 50 mM, EDTA 10 mM, pH 8) was added per 100 mg of gel. 20  $\mu$ L of Prep-B-Gene matrix (slurry of diatomaceous earth) was added to each eppendorf and vortexed briefly. The eppendorfs were incubated at 40 °C for 5 min, vortexed briefly and the process repeated until the gel pieces had dissolved. The matrix bound DNA was pelleted by centrifugation (1 min, 16,000 rpm). The supernatant was removed carefully with a pipette. The pellet was washed with DNA purification buffer (NaCl 400 mM, Tris 20 mM, EDTA 2mM, 50% EtOH) and vortexed to mix thoroughly. The DNA-matrix was pelleted by centrifugation (1 min, 16,000 rpm). The wash process was repeated with a further 750  $\mu$ L purification buffer. After removal of the liquid the pellet was air dried. The DNA was removed from the matrix by addition of 30  $\mu$ L of autoclaved H<sub>2</sub>O to the pellet followed by vortexing and incubation at 40 °C to solubilise the DNA. The eppendorf was centrifuged at 16,000 rpm for 1 min to pellet the matrix. The supernatant (DNA) was transferred to a clean eppendorf and stored at -20 °C.

#### **5.2.4.4 Ligation of *mtrR* gene into *pET 28a***

1  $\mu$ L of ligase buffer, 1  $\mu$ L ligase (T4 DNA) and 4  $\mu$ L *mtrR* DNA were placed in an eppendorf and 4  $\mu$ L of autoclaved H<sub>2</sub>O was added. Simultaneously a control sample was prepared in which 4  $\mu$ L H<sub>2</sub>O was added instead of *mtrR* DNA. Both samples were incubated at room temperature for 2 hours.

2  $\mu$ L of ligase each reaction was used to transform XL10 competent cells (2 aliquots, each 25  $\mu$ L). The cells were spread on LB-plates containing kanamycin and incubated at 37 °C overnight. Successful ligation and transformation was indicated by more colonies on the *MtrR* positive plate compared to the negative control and this was confirmed by DNA sequencing of plasmid DNA acquired by plasmid prep of 1 mL overnight cultures from two colonies (one colony from each plate).

#### **5.2.4.5 Transformation of *Kam3 (DE3)* cells with *pET28-mtrR***

An overnight culture (10 mL) of KAM3 cells (empty, no plasmid) was centrifuged at 4,500 rpm for 15 min at 4 °C. The cells were resuspended in 10 mM CaCl<sub>2</sub> (1 mL) and kept on ice for 5 min. The suspension was centrifuged for 2 min at 5,000 rpm. The supernatant was discarded and the cells resuspended in 10 mM MgCl<sub>2</sub> (1 mL) and incubated on ice for 5 min. The cells were pelleted by centrifugation (2 min, 5000 rpm) and resuspended in 10 mM CaCl<sub>2</sub> (1 mL). 150  $\mu$ L of cells were transferred to an ice cold eppendorf and incubated with 2  $\mu$ L plasmid DNA for 30 min. The cells were heat shocked at 42 °C for 2 min, then incubated on ice for 2 min. 250  $\mu$ L SOC medium was added and the cells incubated at 37 °C for 1.5 hours. The recovered cells were spread on kanamycin containing LB plates, incubated at 37 °C overnight and the plates stored at 4 °C.

#### **5.4.5 Analysis of covalent modification of *MtrR* by small molecule probes using trypsin digests and mass spectrometry**

##### *Gel method*

SDS-PAGE gel prepared and run as normal. Gel stained for minimum time necessary to reveal protein bands. The desired bands were removed from the gel using a scalpel and the gel pieces transferred to a clean eppendorf tube. Rapid destain solution (50  $\mu$ L, 40% MeOH, 25 mM NH<sub>4</sub>HCO<sub>3</sub>) was added and incubated at room temperature, with occasional vortexing, until the blue colour had faded. The decolourised gel was mashed into several pieces, washed with MeCN and dried in a stream of N<sub>2</sub>. Trypsin solution (2

$\mu\text{L}$  in 40  $\mu\text{L}$  25mM  $\text{NH}_4\text{HCO}_3$  per sample) was added and the eppendorf incubated at 37°C overnight, with shaking at 120 rpm. Peptides were extracted from the gel using 3:7  $\text{H}_2\text{O}$  : MeCN +0.1% TFA. The peptide solutions were lyophilised and stored at -20 °C until analysed by MALDI mass spectrometry.

#### *Solution method*

The protein of interest was precipitated by addition of acetone (4 x sample volume) and incubated at -20 °C for 1 hour. The precipitate was isolated by centrifugation, the solution decanted and the pellet dried in a stream of  $\text{N}_2$ . Trypsin solution (2  $\mu\text{L}$  in 40  $\mu\text{L}$  25 mM  $\text{NH}_4\text{HCO}_3$  per sample) was added and the eppendorf incubated at 37 °C overnight, with shaking at 120 rpm. The solution was lyophilised and stored at -20 °C until analysed by MALDI mass spectrometry

#### **5.2.6 $\beta$ -lactamase activity of MtrR as determined by growth curve analysis using Kam3 *E. coli* expressing MtrR**

Agar plate containing kanamycin streaked with stock KAM 3 cells containing pET28a vector carrying the gene for mtrR, or no insert, were incubated overnight at 37 °C.

One colony from each plate was used to inoculate 3 x 25 mL YT media containing kanamycin. Cultures grown at 37 °C with shaking at 150 rpm until an optical density of 0.6 was reached at which point the cultures were induced with IPTG (1 or 10 mM) and the cultures were incubated for a further two hours.

Cultures were transferred to sterile Falcon tubes and centrifuged at 45,000 rpm for 15 min at 4 °C. The supernatant was decanted and the cell pellet washed in fresh LB media. Cells were resuspended in 20 mL YT media (devoid of antibiotic) and the optical density at 600 nm was measured. 1 mL was removed from the stock cell solution and diluted n-fold until an optical density of 0.1 was reached. 100  $\mu\text{L}$  of cell solution was transferred to a prepared 96 well plate containing appropriate volumes of media and penicillin G (2). The 96-well plate was placed in FLASHSCAN and cell growth monitored for 720 minutes. Data exported and analysed using EXCEL.

FLASHSCAN settings: Microwell plate: NuncF; Cyclic measurement, 3 point reading, 1 reading every x 5 minutes.

### **5.2.7 Analysis of bacterial cultures by Flow Cytometry**

Propidium iodide and thiazole orange were purchased from Sigma Aldrich. Fluorescein diacetate was a gift from Aileen Congreve.

The contents of selected wells from the 96-well plate used for overnight monitoring of bacterial growth in the presence of a test compound, were transferred to eppendorf tubes and centrifuged using a bench top centrifuge set at maximum speed. The supernatant was decanted and the pellets washed in PBS solution. The cell pellet was resuspended in analysis buffer (PBS, 1 mM, EDTA, 0.1% sodium azide, 0.01 % TWEEN 20, pH 7.4). For dead control samples, cells were resuspended in 70% EtOH, kept on ice for 5 min, then centrifuged and washed with PBS prior to being resuspended in analysis buffer.

50  $\mu$ L of PI (17  $\mu$ M) and 50  $\mu$ L of FDA 240  $\mu$ M or TO (17  $\mu$ M) were added to the cell suspensions and incubated at room temperature for 5 min. Stained cell solutions were kept on ice until analysis.

Cells were analysed on a MoFlo (Beckman Coulter) cell sorter. Cells were interrogated with 488 nm laser and fluorescence collected through FL1 (530 / 30) and FL4 (630 / 30) band filters. Data analysed with Summit software.

### **5.2.8 Isothermal Titration Calorimetry**

ITC experiments were carried out using a VP-ITC (Microcal) Protein was dialysed overnight into the appropriate buffer. Dialysis buffer was retained for preparation of ligand solution. Standard settings used were: 70 injections (1 x 2  $\mu$ L, 69 x 10  $\mu$ L, spacing between injections = 150 sec) stirring speed of 307 rpm, T = 25°C. initial delay = 60 sec, reference power = 10. Data was analysed using Origin™. Experimental data was fitted using standard models.

### **5.2.9 Subcellular localisation of MtrR by Western blot**

2 x 10 mL cultures of pET28 KAM cells harbouring the plasmid for MtrR were centrifuged (4500 rpm, 20 min, 4 °C) 2 hours after induction with IPTG. The cells were washed with Tris 20 mM, NaCl 300 mM, glycerol 10% supplemented with 1 M Gd<sup>3+</sup> for the control, the cells were centrifuged and resuspended in ice cold hypertonic solution (20% sucrose, 30 mM Tris) in the presence or absence of 1 mM Gd<sup>3+</sup>. The cells were incubated for 10 min at 4 °C. The cells were centrifuged, supernatant collected and the



process repeated once. 15 µL of each sample was loaded in 12% acrylamide gels for SDS-PAGE (1 gel prepared for MtrR and GroEL). After electrophoresis, the gel was transferred onto a Hybond P membrane (Amersham), blotting occurred for 1 hour at 100 V using cooled, circulating transfer buffer (15 mM Tris, 125 mM glycine). The membranes were washed in Tris-buffered saline and blocked by incubation with 1% BSA in tris buffered saline for one hour. The primary antibody was added (1:1000 dilution for MtrR, 1:16000 dilution for GroEL) and the membranes incubated at room temperature for 1 hour. The membranes were washed well with TBS solution, and the secondary antibody (anti-rabbit alkaline phosphatase, 1:10000 dilution) were added and the membranes gently shaken overnight. The membranes were washed well with final buffer (Tris 100 mM, pH 9.5). Proteins were visualised by addition of colourmetric reagents NBT and BCIP. After 30-45 seconds strong bands could be seen and the reaction was stopped by addition of 100 mL MilliQ water. Membranes were air dried and scanned.

Antibodies used in this study:

Protein	Primary antibody	Dilution	Secondary antibody
MtrR	Anti-mtrR produced in rabbit	1:1 000	Alkaline phosphatase produced in goat
GroEL	Anti-GroEL produced in rabbit	1:10000	Alkaline phosphatase produced in goat
MBP	Anti-MBP produced in mouse	1:16000	Antimouse Fab alkaline phosphatase

### 5.2.10. Electrophoresis gel mobility shift assays

Oligonucleotides were purchased from MWG and used without further purification.

#### 5.2.10.1 Concentration of oligonucleotides

The concentration of oligonucleotides used in these experiments was determined by UV method:

$$\text{Concentration / mM} = (\text{Abs}_{260} \times \text{dilution factor} \times 33,000) / \text{MW oligonucleotide}$$

### **5.2.10.2 Biotin 3' end labelling of DNA**

*General procedure:* 5 x TdT reaction buffer (10 µL), unlabelled oligonucleotide (5 µL), Biotin-11-UdP, Tdt enzyme (2U / µL) 5 µL and DNAase free water (5 µL) were gently mixed in an eppendorf and incubated in a water bath at 37 °C for 30 min. EDTA (2.5 µL) was added to stop the reaction. Chloroform : isoamylalcohol (50 µL) was added, the mixture vortexed and centrifuged (2 min, 16,000 rpm). The supernatant was removed and stored at -20 °C until required.

Oligonucleotides used in this study:

(Forward-1) 5'-TTT TTA TCG GTG CAA TCG TGT ATG-3'

(Reverse-1) 3'-CAT ACA CGA TTG CAC CGA AAC-5'

(Forward-2) 5'-TTT TTA TCG GTG CAA TCG TGT ATG TAT AAT-3'

(Reverse-2) 5'-CAT ACA CGA TTG CAC CGA AAC-3'

### **5.2.10.3 Annealing of labelled oligonucleotides**

*Hot block method:* Forward (10 µL) and reverse (10 µL) oligonucleotides labelled at the 3' position were annealed by heating at 90 °C (hot block) for 5 min, then cooling slowly to room temperature

*PCR machine method:* Equal volumes of forward and reverse labelled oligonucleotides were placed in a PCR tube. The PCR machine was programmed to maintain 94 °C for 5 min and then cool 1 °C per min until 27 °C was reached.

### **5.2.10.4 Preparation of 4 % bis-acrylamide gels**

Biorad mini-gel glass plates and gel cassettes were used for setting of the gels.

Distilled water (9 mL), 10 x TBE (1.2 mL), 30% bis-acrylamide (1.6 mL), 10% APS (120 µL) and TEMED (10 µL) were mixed and pipetted into the prepared glass plates. The gel was allowed to set for 5 hours at room temperature and stored overnight at 4 °C prior to use.

### 5.2.10.5 DNA/Protein/ligand binding reactions

Table 16 Volumes of reagents used in EMSA reaction

	Component	Volume / $\mu\text{L}$
	DNAase free $\text{H}_2\text{O}$	10 - n
1	10 x reaction buffer	5
2	Poly (dI.dC)	0.5
3	MtrR	0.5
4	Peptide	0.5
5	Biotin-DNA	0.5
6	80 % glycerol	1.5
7	Loading buffer	1

$$n = \text{total volume of components } 1+2+3+4+5$$

Components 1, 2, 3, 4, 5 were added in that order to a sterile eppendorf and incubated at room temperature for 30 min. Components 6 and 7 were added immediately prior to loading of acrylamide gel.

### 5.2.10.6 Gel electrophoresis

Prior to loading the gel with the samples the gel was prerun for 2 minutes at 100 V. Loading buffer (0.5  $\mu\text{L}$ ) was added to each lane and the gel run at 100 V for a further 3 minutes. This step enables easy visualisation of the wells to aid the loading of the gel. Samples were loaded into the gel and electrophoresis occurred for 45 min at 100 V until the bromophenol blue dye had migrated  $\sim 2/3$  down the gel. The tank was surrounded by ice for the duration of the electrophoresis.

### 5.2.10.7 Electrophoretic transfer of binding reaction to membrane

Positively charged nylon membrane (Amersham) was soaked in 0.5 x TBE for 10 min. The gel was carefully removed from the glass plates and sandwiched between the nylon

membrane, filter paper and transfer sponges. The gel sandwich was placed in a transfer unit and the transfer cassette filled with cold 0.5 x TBE. The outer tank was filled with 600 mL cold H<sub>2</sub>O. The tank was placed on ice and the transfer proceeded at 380 mA (~30 to ~50 V) for 60 minutes. The membrane was removed from the transfer unit, drained on paper towel and the DNA fixed to the membrane by exposure to UV light at 312 nm on a transilluminator for 15 minutes.

#### **5.2.10.8 Detection of Biotin-labelled *mtrR* DNA by chemiluminescence**

The membrane was blocked in blocking buffer (20 mL, Pierce) for 15 min with gentle shaking. The buffer was drained and replaced with blocking buffer (20 mL) containing streptavidin-horseradish peroxidase conjugate (66.67 µL). The membrane was incubated with the antibody for 15 min with gentle shaking. The solution was decanted and the membrane washed with washing buffer (4 x 20 mL). The membrane was soaked in equilibration buffer (30 mL, 5 min) prior to addition of the substrate developer solution (2 mL luminal and 2 mL enhancer solution). The membrane was incubated with the developer solution for 5 min, without shaking. The membrane was drained on paper towel before being placed in a film cassette. The film was exposed to the membrane for 2 -10 minutes and developed using a Xenograph cartridge machine.

#### **5.2.11 Antibacterial activity of synthetic peptides as determined by growth curve analysis using Kam3 *E. coli* expressing full, or elements of, MtrCDE**

##### **5.2.11.1 FLASHSCAN method**

Agar plates containing chloramphenicol were streaked with stock KAM 3 cells containing pACYC vector carrying either *mtrD*, *mtrCD*, *mtrCDE* or no insert - as prepared by Li Zhang (PhD thesis, Durham, UK, 2009). The plates were incubated overnight at 37 °C.

One colony from each plate was used to inoculate 4 x 25 mL YT media containing kanamycin. Cultures grown at 37 °C with shaking at 150 rpm until an optical density of 0.6 was reached at which point the cultures were induced with IPTG to a final concentration of 1mM. Cultures were incubated for a further two hours.

Cultures were transferred to sterile Falcon tubes and centrifuged at 45000 rpm for 15 min at 4 °C. The supernatant was decanted and the cell pellet washed in fresh LB media.

Cells were resuspended in 20 mL YT media (devoid of antibiotic) and the optical density at 600 nm was measured. 1 mL was removed from the stock cell solution and diluted n-fold until an optical density of 0.1 was reached. 100  $\mu$ L of cell solution was transferred to a prepared 96 well plate containing appropriate volumes of media and test compound (peptide or antibiotic). 96-well plate was placed in FLASHSCAN and cell growth monitored for 720 minutes. Data exported and analysed using EXCEL.

FLASHSCAN settings: Microwell plate: NuncF; Cyclic measurement, 3 point reading, 1 reading every x 5 minutes.

---

---

## 6. References

- <sup>1</sup> H. C. Neu, *Rev. Infect. Diseases*, 1983, **5**, S1, S9-S20
- <sup>2</sup> J. Tapsall, *Sexually Transmitted Diseases*, 2006, **33**, 1, 8-10
- <sup>3</sup> A. P. MacGowen and R. Wise, *J. Antimicrob. Chemother.*, 2001, **48**, Suppl. S1, 17-28.
- <sup>4</sup> A. Zapun, C. Contreras-Martel and T. Vernet, *FEMS Microbiol. Rev.*, 2008, **32**, 361-385.
- <sup>5</sup> A. Liakopoulos, C. Neocleous, D. Klapsa, M. Kanellopoulou, I. Spiliopoulou, K. D. Mathiopoulos, E. Papafrangas and E. Petinaki, *J. Antmicrob. Chemother.*, 2009, **64**, 1, 206-207.
- <sup>6</sup> J. F. Fisher, S. O. Meroueh, and S. Mobashery, *Chem. Rev.*, 2005, **105**, 395-424.
- <sup>7</sup> G. D. Wright, *Advanced Drug Delivery Rev.*, 2005, **57**, 1451- 1470.
- <sup>8</sup> L. McMurry, R. E. Petrucci and S. B. Levy, *Proc. Acad. Nat. Sci. USA*, 1980, **77**, 7, 3974-3977.
- <sup>9</sup> L. A. Mitscher, *Chem. Rev.*, 2005, **105**, 559-592.
- <sup>10</sup> J. A. Vázquez, R. Enriquez, R. Abad, B. Alcalà, C. Salcedo and L. Arreaza, *FEMS Microbiol. Rev.*, 2007, **31**, 1, 64-70.
- <sup>11</sup> M. R. Mulvey and A. E. Simor, *Canadian Med. J.*, 2009, **180**, 4, 408-416.
- <sup>12</sup> J. Tapsall, *Canadian Med. J.*, 2009, **180**, 3, 268-269.
- <sup>13</sup> T. Deguchi and M. Yasuda, *Ann. Intern. Med.*, 2008, **145**, 5, 363-364.
- <sup>14</sup> P. M. Hawkey and A. M. Jones, *J. Antimicrob. Chemother.*, 2009, **64**, Suppl. 1, i3-i10.
- <sup>15</sup> M. C. McManus, *Am. J. Health Syst. Pharm.*, 1997, **54**, 1420-1433.
- <sup>16</sup> A. H. Delcour, *Biochemica et Biophysica Acta*, 2009, **1973**, 808-816.
- <sup>17</sup> L. Stryer in *Biochemistry*, Freeman and Company, NewYork, 4<sup>th</sup> Ed. 1995, ch. 32, pp 827 - 831.
- <sup>18</sup> F. C. Tenover, *Am. J. Med.*, 2006, **119**, 6A, S3-S10

- 
- <sup>19</sup> L. Ferrero, B. Cameron and J. Crouzet, *Antimicrob. Agents Chemother.*, 1995, **39**, **7**, 1554-1558.
- <sup>20</sup> B. Alberts, D. Bray, J. Lewis, M. Raf, K. Roberts and J. D. Watson, in *Molecular Biology of the Cell*, Garland Publishing, New York, 3<sup>rd</sup> edn, 1994, ch. 10, pp 477-480.
- <sup>21</sup> H. Nikaido, *Mol. Biol. Reviews*, 2003, **67**, **4**, 593-656.
- <sup>22</sup> L. A. Lewis, B. Choudhury, J. T. Balthazar, L. E. Martin, S. Ram, P. A. Rice, D. S. Stephens, R. Carlson, W. M. Shafer, *Infection and Immunity*, 2009, **77**, **3**, 1112-1120.
- <sup>23</sup> D. S. Stephens and W. M. Shafer, *J. Gen. Microbiol.*, 1987, **133**, 2671-2678.
- <sup>24</sup> J. T. Weadge, J. M Pfeffer and A. J Clarke, *BMC Microbiol.*, 2005, **5**, 49-54.
- <sup>25</sup> W. W. Navarre and O. Schneewind, *Mol. Biol. Reviews*, 1999, **63**, **1**, 174-229.
- <sup>26</sup> M. Olesky, M. Hobbs and R. A. Nicholas, *Antimicrob. Agents Chemother.*, 2002, **46**, 2811-2820.
- <sup>27</sup> W. M. Shafer and J. P. Folster, *J. Bacteriol.*, 2006, **188**, **7**, 2297-2299.
- <sup>28</sup> M. Olesky, S. Zhao, R. L. Rosenberg and R. A. Nicholas, *J. Bacteriol.*, 2006, **188**, **7**, 2300-2308.
- <sup>29</sup> D. M. Livermore, R. Canton, M. Gniadkowski, P. Nordmann, G. M. Rossolini, G. Arlet, J. Ayala, T. M. Coque, I. Kern-Zdanowicz, F. Luzzaro, L. Poirel and N. Woodford, *J. Antimicrob. Chemother.*, 2007, **59**, **2**, 165-174.
- <sup>30</sup> A. M. Queenan and K. Bush, *Clin. Microbiol. Rev.*, 2007, **20**, **2**, 440-458.
- <sup>31</sup> G.A. Jacoby, *Clin. Microbiol. Rev.*, 2009, **22**, **1**, 161-182.
- <sup>32</sup> S. J. Salipante and B. G. Hall, *Mol. Biol. Evol.*, 2003, **20**, **4**, 653-659.
- <sup>33</sup> I. Murray and W. V. Shaw, *Antimicrob. Agents. Chemother.*, 1997, **41**, **1**, 1-6.
- <sup>34</sup> A. Robicsek, J. Strahilevitz, G. A Jacoby, M. Macielag, D Abbanat, C. H. Park, K. Bush, and D. C Hooper, *Nature Medicine*, 2006, **12**, **1**, 83-88.

- 
- <sup>35</sup> M. D. Adjei, T. M. Heinze, J. Deck, J. P. Freeman, A. J. Williams, and J. B. Sutherland, *App. Environ. Microbiol.*, 2006, **72**, 9, 5790-5793.
- <sup>36</sup> X. Zhao, C. Xu, J. Domagal and K. Drlica, *Proc. Natl. Acad. Sci. USA*, 1997, **94**, 13991-13996.
- <sup>37</sup> C. J. R. Willmott and A. Maxwell, *Antimicrob. Agents Chemother.*, 1993, **37**, 126-127.
- <sup>38</sup> F. J. Schmitz, P. G. Higgins, S. Mayer, A. C. Fluit, A. Dalhoff, *Eur. J. Clin. Microbiol. Infect. Dis.*, 2002, **21**, 647-659.
- <sup>39</sup> R. Karunakaran and I. C. Sam, *J. Antimicrob. Chemother.*, 2007, **59**, 4, 803-804.
- <sup>40</sup> R. Lecelerq and P. Courvallin, *Lancet*, 1998, **352**, 591-592.
- <sup>41</sup> M. C. Roberts, W. O. Chung, D. Roe, M. Xia, C. Marquez, G. Borthagara, W. L. Whittington, and K. K. Holmes, *Antimicrob. Agents Chemother.*, 1999, **43**, 6, 1367-1372.
- <sup>42</sup> B. Weisblum, *Antimicrob. Agents Chemother.*, 1995, **39**, 3, 577-585.
- <sup>43</sup> L. K. Ng, I. Martin, G. Liu and L. Bryden, *Antimicrob. Agents Chemother.*, 2002, **46**, 9, 3020-3025.
- <sup>44</sup> S. T. Gregory and A. E. Dahlberg, 1999, *J. Mol. Biol.*, **289**, 827-834.
- <sup>45</sup> P. M. Duffin and H. S. Seifert, *Int. J. Antimicrob. Agents*, 2009, **33**, 321-327.
- <sup>46</sup> A. S. Mankin, *Curr. Opin. Microbiol.* 2008, **11**, 5, 414-21.
- <sup>47</sup> R. Lindberg, H. Fredlund, R. Nicholas and M. Unemo, *Antmicrob. Agents Chemother.*, 2007, **51**, 6, 2117-2112.
- <sup>48</sup> J. L. Martinez, M. B. Sanchez, L. Martinez-Solano, A. Hernandez, L. Garmendia, A. Fajado and C. Alvarez-Ortega, *FEMS Microbiol. Rev.*, 2009, **33**, 430-449
- <sup>49</sup> S. Grkovic, M. H. Brown and R. A. Skurray, *Microbiol. Mol. Biol. Rev.*, 2002, **66**, 671-701.
- <sup>50</sup> J. L. Martinez and F. Baquero, *Clin. Microbiol. Rev.*, 2002, **15**, 647-679.



- 
- <sup>51</sup> M. H. Saier Jr, I. T. Paulson, M. K. Sliwinski, S. S. Pao, R. A. Skurray and H. Nikaido, *FASEB J*, 1998, **12**, 265-274.
- <sup>52</sup> K. P. Langton, P. J. F. Henderson and R. B. Herbert, *Nat. Prod. Rep.*, 2005, **22**, 439-551.
- <sup>53</sup> I. T. Paulsen, M. H. Brown and R. A. Skurray, *Microbiological Reviews*, 1996, **60**, 6, 575-608.
- <sup>54</sup> C. F. Higgins, *Annu. Rev. Cell Biol.*, 1992, **8**, 67-113.
- <sup>55</sup> S. Murakami, R. Nakashima, E. Yamashita and A. Yamaguchi, *Nature*, 2002, **419**, 6907, 587-593.
- <sup>56</sup> X. Li, K. Poole, *J. Bacteriol.*, 2001, **183**, 12-27.
- <sup>57</sup> K. E. Hagman, C. E. Lucas, J. T. Balthazar, L. Snyder, M. Nilles, R. C. Judd and W. M. Shafer, *Microbiol.*, 1997, **143**, 7, 2115-2125 .
- <sup>58</sup> H. Nikaido, *Ann. Rev. Biochemistry*, 2009, **78**, 119-146.
- <sup>59</sup> E. H. Lee and W. M. Shafer, *Mol. Microbiol.*, 1999, **33**, 4, 839-845.
- <sup>60</sup> C. E. Rouquette-Loughlin, J. T. Balthazar and W. M. Shafer, *J. Antimicrob. Chemother.*, 2005, **56**, 856-860
- <sup>61</sup> P. F. Sparling, F. A. Sarubbi Jr and E. Blackman, *J. Bacteriol.*, 1975, **124**, 740-749
- <sup>62</sup> L. F. Guyman, D. L. Walstad and P. F. Sparling, *J. Bacteriol.*, 1978, **136**, 391-401
- <sup>63</sup> R. M. Delahay, B. D. Robertson, J. T. Balthazar, W. M. Shafer, and C. A. Ison, *Microbiology*, 1997, **143**, 2127-2133
- <sup>64</sup> C. E. Lucas, J. T. Balthazar, K. E. Hagman and W. M. Shafer. *J. Bacteriol.*, 1997, **179**, 4123-4128.
- <sup>65</sup> J. P. Folster and W. M. Shafer, *J. Bacteriol.*, 2005, **187**, 11, 3713-3720
- <sup>66</sup> L. Zhang, T. K. Janganan, V. N. Bavro, D. Matak-Vinkovic, N. P. Barrera, C. Venien-Bryan, B. Zhang, M. F. Burton, P. G. Steel, C. V. Robinson, M. I. Borges-Walmsley and A. R. Walmsley, *Mol. Microbiol.*, submitted

- 
- <sup>67</sup> W. L. Veal, A. Yellen, J. T. Balthazar, W. Pan and B. G. Spratt, *Microbiology*, 1998, **144**, 621-627.
- <sup>68</sup> J. A. Hoch, *Current Opinion in Microbiology*, 2000, **3**, 2, 165-170
- <sup>69</sup> N. Braranova and H. Nikaido, *J. Bact.*, 2002, **184**, 4168-4176.
- <sup>70</sup> C. L. Santos, F. Tavares, J. Thioulouse and P. Normand, *FEMS Microbiol. Rev.*, 2008, **33**, 2, 411-429.
- <sup>71</sup> D. M. Alberti, C. Lynch, H. Nikaido and J. E. Hearst, 1996, *Mol. Microbiol.*, **19**, 101-112.
- <sup>72</sup> T. T. Tanaka, T. Horii, K. Shibayama, K. Sato, S. Ohsuka, Y. Arakawa, K. Yamaki, K. Takagi, and M. Ohta, *Microbiol. Immunol.*, 1997, **41**, 697-702.
- <sup>73</sup> D. G. White, J. D. Goldman, B. Demple and S. B. Levy, *J. Bacteriol*, 1997, **179**, 6122-6126.
- <sup>74</sup> C. Pabo and R. T. Sauer, *Annu. Rev. Biochem.*, 1992, **61**, 1053-95.
- <sup>75</sup> R. G. Martin and J. L. Rosner, *Cur. Opinion Microbiol.*, 2001, **4**, 132-137.
- <sup>76</sup> V. Saridakis, D. Shahinas, X. Xu and D. Christendat, *J. Mol. Biol.*, 2008, **377**, 3, 655-667.
- <sup>77</sup> M. S. Wilke, M. Heller, A. L. Creagh, C. A. Haynes, L. P. McIntosh, K. Poole and N. C. J. Strynadka, *Proc. Nat. Acad. Sci. U.S.A.*, 2008, 105, **39**, 14832-14837.
- <sup>78</sup> J. L. Hobman, *Mol. Microbiol.*, 2007, **63**, 5, 1275-1278.
- <sup>79</sup> K. J. Newberry, J. L. Huffman, M. C. Miller, N. Vazquez-Lopez, A. A. Neyfakh and R. G. Brennan, *J. Biol. Chem.*, 2008, **283**, 39, 26795-26804
- <sup>80</sup> P. Orth, D. Schnappinger, W. Hillen, W. Saenger, and W. Hinrichs, 2000, *Nat. Struct. Biol.*, 2000, **7**, 215-219
- <sup>81</sup> J. L. Ramos, M. Martinez-Bueno, A. J. Molin<sup>o</sup>-Henares, W. Ter<sup>o</sup>n, K. Watanabe, X. Zhang, M. Trinidad Gallegos, R. Brennan and R. Tobes, *Microbiol. MolBiol. Rev.*, 2005, **69**, 2 326-356
- <sup>82</sup> W. Teran, T. Krell, J. L. Ramos and M.-T. Gallegos, *J. Biol. Chem.*, 2006, **281**, 11, 7102-7109

- 
- <sup>83</sup> A. R. Willems, K. Tahlan, T. Taguchi, K. Zhang, Z. Z. Lee, K. Inchinose, M. S. Junop and J. R. Nodwell, *J. Mol. Biol.*, 2008, **376**, 1377-1387
- <sup>84</sup> A. Hernandez, M. J. Mate, P. C. Sanchez-Diaz, A. Romero, F. Rojo and J. L. Martinez, *J. Biol. Chem.*, 2009, **284**, 21, 14428-14438
- <sup>85</sup> W. Y. Jeng, T. P. Ko, C. Liu, R. T. Guo, C. L. Liu, H. L. Shr and A. H. J. Wang, *Nucleic Acid Res.*, 2008, **36**, 5, 1567-1577; R. S. De Silva, G. Kovacicova, W. Lin, R. K. Taylor, K. Skorupski and F. J. Kull, *J. Bact.*, 2007, **189**, 15, 5683-5691; T. Krell, W. Teran, O. Lopez-Mayorga, G. Rivas, M. Jimenez, C. Daniels, A. J. Molinβ–Heneras and J. L. Ramos, *J. Mol. Biol.*, 2007, **369**, 1188-1199.
- <sup>86</sup> W. Y. Jeng, T. P. Ko, C. Liu, R. T. Guo, C. L. Lui, H. L. Shr and A. H. J. Wang, *Nuc. Acid Res.*, 2008, **36**, 5, 1567-1577.
- <sup>87</sup> W. Teran, T. Krell, J. L. Ramos, M. T. Gallegos, *J. Biol. Chem.*, 2006, **281**, 11, 7102-7109.
- <sup>88</sup> K. J. Newberry, J. L. Huffman, M. C. Miller, N. Vazquez-Lopez, A. A. Neyfakh and R. G. Brennan, *J. Biol. Chem.*, 2008, **283**, 39, 26795-26804.
- <sup>89</sup> B. E. Brooks, K. M. Piro and R. G. Brennan, *J. Am. Chem. Soc.*, 2007, **129**, 8389-8395.
- <sup>90</sup> C.C. Su, D. J. Rutherford and J. Denae E.W. Yu, *Biochem. Biophys. Res. Commun.*, 2007, **361**, 1, 85-90
- <sup>91</sup> T. Krell, W. Teran, O. Lopez-Mayorga, G. Rivas, M. Jimenez, C. Daniels, A.-J.Molinβ–Henares, M. Martinez-Beuno, M. -T. Gallegos and J. L. Ramos, *J. Mol.Biol.*, 2007, **369**, 1186-1198
- <sup>92</sup> W. B. Pan and B. G. Spragg, *Mol. Microbiol.*, 1994, **11**,4,769-775
- <sup>93</sup> D. E. Warner, J. P. Folster, W. M. Shafer and A. E. Jerse, *J.Infect. Dis.*, 2007, **196**, 1804-1812
- <sup>94</sup> D. E. Warner, W. M. Shafer, A. E. Jerse, *Mol. Microbiol.*, 2008, **7**, 2, 462-478
- <sup>95</sup> J. P. Folster, P. J. T. Johnson, L. Jackson, V. Dhulipali, D. W. Dyer and W. M. Shafer, *J. Bacteriol.*, 2009, **191**, 1, 287-297

- 
- <sup>96</sup> J. P. Folster, V. Dhulipala, R. A. Nicholas and W. M. Shafer, *J. Bacteriol.*, 2007, **189**, 13, 4569
- <sup>97</sup> J. P. Folster and W. M. Shafer, *J. Bacteriol.*, 2005, **187**, **11**, 3713-3720
- <sup>98</sup> E. H. Lee, C. R. Loughlin, J. P. Folster and W. M. Shafer, *J. Bacteriol.*, 2003, **185**, 24, 7145-7152
- <sup>99</sup> W. L. Veal, R. A. Nicholas, and W. M. Shafer, *J. Bacteriol.*, 2002, **184**, 20, 5619-5620
- <sup>100</sup> J. S. Rokem, A. E. Lantz and J. Nielsen, *Nat. Prod. Rep.*, 2007, **24**, 1262-1267.
- <sup>101</sup> S. A. Waksman and H. B. Woodruff, *J. Bacteriol.*, 1942, **44**, 3, 373-384
- <sup>102</sup> N. J. Kershaw, M. E. C. Cains, M. C. Sleeman and C. J. Schofield, *Chem. Comm.*, 2005, 4251-4263
- <sup>103</sup> P. L. Roach, I. J. Clifton, C. M. H. Hensgens, N. Shibata, C. J. Schofield, J. Hajdu and J. E. Baldwin, *Nature*, 1997, **387**, 6635, 827-830.
- <sup>104</sup> G. N. Rolinson, F. R. Batchelor, C. D. Butterworth, J. Cameronwood, M. Cole, G. C. Eustace, M. V. R. M. Hart and E. B. Chain, *Nature*, 1960, **187**, 4633, 236-237.
- <sup>105</sup> T. T. Howarth, A. G. Brown and T. J. King, *J. Chem. Soc. Chem. Commun*, 1976, 266-267.
- <sup>106</sup> C. Reading and M. Cole, *Antimicrob. Agents Chemother.*, 1977, **11**, 852-857.
- <sup>107</sup> A. G. Brown and I. François, in *Medicinal Chemistry: The Role of Organic Chemistry in Drug Research*, ed. C. R. Ganellin and S. M. Roberts, London, 2<sup>nd</sup> edn., 1993, ch. 14, pp 273-293
- <sup>108</sup> N. Khaleeli, R. Li and C. A. Townsend, *J. Am. Chem. Soc.*, 1999, **121**, 9233-9224.
- <sup>109</sup> M. E. Caines, J. M. Elkins, K. S. Hewitson and C. J. Schofield, *J. Biol. Chem.*, 2004, **279**, 5685-5692.
- <sup>110</sup> M. E. Caines, J. L. Sorensen and C. J. Schofield, *Biochem. Biophys. Res. Commun.*, 2009, **385**, 4512-4517.
- <sup>111</sup> C. Fenollar-Ferrer, J. Frau, J. Donoso and F. Muñoz, *Theor. Chem. Account*, 2008, **121**, 209-218.

- 
- <sup>112</sup> D. J. Tipper and J. L. Strominger, *Proc. Natl. Acad. Sci. U.S.A.*, 1965, **54**, 1133-1141.
- <sup>113</sup> S. O. Meroueh, G. Minasov, W. Lee, B. K. Shoichet and S. Mobashery, *J. Am. Chem. Soc.*, 2003, **125**, 9612-9618.
- <sup>114</sup> J. B. K. Nielsen and J. O. Lampen, *J. Biol. Chem.* 1982, **257**, 4490-4495.
- <sup>115</sup> R. P. Ambler, *Phil. Trans. R. Soc. London B*, 1989, 321-331.
- <sup>116</sup> K. Bush, *Antimicrob. Agents Chemother.*, 1989, **33**, 259-263.
- <sup>117</sup> K. Bush, G. A. Jacoby and A. A. Medeiros, *Antimicrob. Agents Chemother.*, 1995, **39**, 6, 1211-1233.
- <sup>118</sup> G. Guillaume, M. Vanhove., J. Lamotte-Brasseur, P. Ledent, M. Jamin, B. Joris and J. Frere, *J. Biol. Chem.*, 1997, **272**, 5438-5444.
- <sup>119</sup> R. A. Powers, E. Caselli, P. J. Focia, F. Prati and B. K. Shoichet, *Biochemistry*, 2001, **40**, 9207-9214.
- <sup>120</sup> G. Crichlow, M. Nukaga, V. Doppalapudi, J. D. Buynak and J. R. Knox, *Biochemistry*, 2001, **40**, 6233-6239.
- <sup>121</sup> A. Patera, L. C. Blaszczyk, B. K. Shoichet, *J. Am. Chem. Soc.*, 2000, **122**, 10504-10512.
- <sup>122</sup> D. Golemi, L. Maveyraud, S. Vakulenko, J. P. Samama and S. Mobashery, *Proc. Natl. Acad. Sci. U.S.A.*, 2001, **98**, 14280-14285.
- <sup>123</sup> R. L. Charnas, J. R. Knowles, *Biochemistry*, 1981, **20**, 3214-3219.
- <sup>124</sup> C. H. Chen, O. Herzberg, *J. Mol. Biol.*, 1992, **224**, 1103-1113.
- <sup>125</sup> P. C. Moews, J. R. Knox, O. Dideberg, P. Charlier and J. -M. Frere, *Proteins*, 1990, **7**, 156-171.
- <sup>126</sup> C. Reading and P. Hepburn, *Biochem. J.*, 1979, **179**, 67-76.
- <sup>127</sup> R. P. A. Brown, R. T. Aplin and C. J. Schofield, *Biochemistry*, 1996, **35**, 38, 12421-12432.
- <sup>128</sup> L. W. Tremblay, J. E. Hugonnet and J. S. Blanchard, *Biochemistry*, 2008, **47**, 5312-5316.

- 
- <sup>129</sup> J. M. Thomson, A. M. Distler, F. Prati and R. A. Bonomo, *J. Biol., Chem.*, 2006, **281**, 36, 26734-26744; Y. Yang, K. Janota, K. Tabei, N. Huang, M. M. Siegel, Y. Lin, B. A. Rasmussen and D. M. Shlaes, *J. Biol. Chem.*, 2000, **275**, 35, 26674-26682; L. W. Tremblay, J. E. Hugonnet and J. S. Blanchard, *Biochemistry*, 2008, **47**, 5312-5316; S. M. Darwaz, C. R. Bethel, K. M. Hujer, K. N. Hurless, A. M. Distler, E. Caselli, F. Prati and R. A. Bonomo, *Biochemistry*, 2009, **48**, 4557-4566; D. Sulton, D. P. Rodriguez, X. Zhou, Y. Liu, A. M. Hujer, C. R. Bethel, M. S. Helfand, J. M. Thomson, V. E. Anderson, J. D. Buynak, L. M. Ng and R. A. Bonomo, *J. Biol. Chem.*, 2005, **280**, 42, 35528-35536; D. P. Rodriguez, X. Zhou, R. Simmons, C. R. Bethels, A. M. Hujer, M. S. Helfand, Z. Jin, B. Guo, V. E. Anderson, L. M. Ng and A. Bonomo, *J. Biol. Chem.*, 2004, **279**, 19, 19494-19501
- <sup>130</sup> P. Limphong, G. Nimako, P. W. Thomas, W. Fast, C. A. Makaroff and M. W. Crowder, *Biochemistry*, 2009, **48**, 8491-8493.
- <sup>131</sup> M. E. Stefanova, J. Tomberg, M. Olesky, J.V. Höltje, W. G. Gutheil and R. A. Nicholas, *Biochemistry*, 2003, **42**, 14614-14625.
- <sup>132</sup> R. K. Deka, M. Machius, M. V. Norgard and D. R. Tomchick, *J. Biol. Chem.*, 2002, **277**, 44, 41857-41864J; G. Nicola, S. Peddi, M. Stefanova, R. A. Nicholas, W. G. Gutheil, C. Davies, *Biochemistry*, 2005, **44**, 23, 8207-8217.
- <sup>133</sup> J. Y. Cha, A. Ishiwata and S. Mobashery, *J. Biol. Chem.*, 2004, **279**, 15, 14917-14921.
- <sup>134</sup> L. Lüthy, M. G. Grütter and P. R. E. Mittl, *J. Biol. Chem.*, 2002, **12**, 10187-10193.
- <sup>135</sup> P. R. E. Mittl, L. Lüthy, P. Hunziker and M. G. Grütter, *J. Biol. Chem.*, 2000, **275**, 23, 17693-17699.
- <sup>136</sup> K. M. Hoffmann, D. Williams, W. A. Shafer and R. G. Brennan, *J. Bacteriol.*, 2005, **187**, 14, 5008-5012.
- <sup>137</sup> M. Kojima, K. Masudaa, Y. Yada, Y. Hayase, T. Muratani, T. Matsumoto, *Int. J. Antimicrob. Agents*, 2008, **32**, 1, 50-54
- <sup>138</sup> S. A. Bernhard, *J. Biol. Chem.*, 1955, 961-969.
- <sup>139</sup> L. Lüthy, M. G. Grütter and P. R. E. Mittl, *J. Bacteriol.*, 2002, **277**, 10187-10193.
- <sup>140</sup> D. Li, M. Yang, J. Hu, Y. Zhang, H. Chang and F. Jin, *Water Res.*, 2008, **42**, 307-317.

- 
- <sup>141</sup> C. Bebrone, C. Moali, F. Mahy, S. Rival, J. D. Docquier, G. M. Rossolini, J. Fastrez, R. F. Pratt, J. M. Frere and M. Galleni, *Antimicrob. Agents Chemother.*, 2001, **45**, 6, 1868-1871.
- <sup>142</sup> J. E. Hugonnet, J. S. Blanchard, *Biochemistry*, 2007, **46**, 11998-12004.
- <sup>143</sup> D. Sulton, D. Pagan-Rodriguez, X. Zhou, Y. Liu, A. M. hujer, C. R. Bethel, M. S. Helfand, J. M. Thomson, V. E. Anderson, J. D. Buynak, L. M .Ng, R. A. Bonomo, *J. Biol. Chem.*, 2005, **280**, 42, 35538-35536
- <sup>144</sup> C. Saxena, R. E. Higgs, E. Zhen and J. E. Hale, *Expert Opinion Drug Disc.*, 2009, **4**, 7, 701-714.
- <sup>145</sup> T. T. Baird Jr., W. D. Wright and C. S. Craik, *Prot. Sci.*, 2006, **15**, 1229-1238.
- <sup>146</sup> T. T. Baird Jr., W. D. Wright and C. S. Craik, *Prot. Sci.*, 2006, **15**, 1229-1238.
- <sup>147</sup> E. Ortlund, M. W. Lacount, K. Lewinski and L. Lebioda, *Biochemistry*, 2000, **39**, 1199-1204.
- <sup>148</sup> K. Aghaiypour, A. Wlodawar and J. Lubowski, *Biochimica Biophys. Acta*, 2001, **1550**, 117-128.
- <sup>149</sup> A. Mazzariol, G. Cornaglia and H. Nikaido, *Antimicrob. Agents Chemother.*, 2000, **44**, 5, 1387-1390.
- <sup>150</sup> Y. Morita, K. Kodama, S. Shiota, T. Mine, A. Kataoka, T. Mizushima and T. S. Tsuchiya, *Antimicrob. Agents Chemother.*, 1998, **42**, 1778-1782.
- <sup>151</sup> H. Hirakawa, K. Nishino, J. Yamada, T. Hirata and A. Yamaguchi, *J. Antimicrob. Chemother.*, 2003, **52**, 576-582.
- <sup>152</sup> O. V. Martinez, H. G. Malinin and T. I. Ingram, *Cytometry*, 1982, **3**, 129-133.
- <sup>153</sup> H. B. Steen, E. Boye, K. Skarstad, B. Bloom, T. Godal and S. Mustafa, *Clinical Inf. Dis.*, 1982, **17**, Suppl. 2, 494-500.
- <sup>154</sup> R. S. Pore, *J. Antimicrob. Chemother.*, 1994, **34**, 613-627.
- <sup>155</sup> S. Wanandy, N. Brouwer, Q. Liu, A. Mahon, S. Cork, P. Karuso, S. Vemulpad and J. Jamie, *J. Microbiol. Methods*, 2005, **60**, 21-30.

- 
- <sup>156</sup> M. Berney, F. Hammes, F. Bosshard, H. U. Weilemann and T. Egli, *Applied Environ., Microbiol.*, 2007, **73**, 10, 3283-3290.
- <sup>157</sup> M. H. Malamy and B. L. Horecker, *Biochemistry*, 1964, **3**, 1889-1893.
- <sup>158</sup> G. F. L. Ames, C. Prody and S. Kustu, *J. Bacteriol.*, 1984, **160**, 1181-1183.
- <sup>159</sup> H. C. Neu and L. A. Heppel, *J. Biol. Chem.* 1965, **240**, 3685-3692.
- <sup>160</sup> M. K. Cha, W. C. Kim, C. J. Lim, K. Kim and I. H. Kim, *J. Biol. Chem.*, 2004, **279**, 8769-8778.
- <sup>161</sup> A. J. Link, K. Robinson and G. M. Church, *Electrophoresis*, 1997, **18**, 1259-1313.
- <sup>162</sup> K. Tao, *FEMS Microbiol. Lett.*, 2008, **289**, 41-45.
- <sup>163</sup> H. E. Ewis and C. D. Lu, *FEMS Microbiol. Lett.*, 2005, **253**, 295-301.
- <sup>164</sup> B. Ajouz, C. Berrier, A. Garrigues, M. Besnard and A. Ghazi, *J. Biol. Chem.*, 1998, **273**, 26670-26674.
- <sup>165</sup> W. M. Shafer, X.-D. Qu, A. J. Waring and R. I. Lehrer, *Proc. Natl. Acad. Sci. USA*, 1998, **95**, 1829-1833.
- <sup>166</sup> S. Rieg S, A. Huth, H. Kalbacher, W. V. Kern, *Int. J. Antimicrob. Agents*, 2009, **33**, 174-176
- <sup>167</sup> M. F. Burton and P. G. Steel, *Nat. Prod. Rep.*, 2009, 26, 12, 1572-1584
- <sup>168</sup> L. E. Alksne and P. M. Dunman, *Methods Mol. Biol.*, 2008, **431**, 271-283.
- <sup>169</sup> G. S. Wang, X. Li and Z. Wang, *Nucleic Acids Res.*, 2009, **37**, D933-D937.
- <sup>170</sup> M. Zasloff, *Nature*, 2002, **415**, 389-395.
- <sup>171</sup> R. L. Gallo, *J. Invest. Dermatol.*, 2008, **128**, 5.
- <sup>172</sup> A. M. Aerts, I. François, B. P. A. Cammue and K. Thevissen, *Cell. Mol. Life Sci.*, 2008, **65**, 2069.
- <sup>173</sup> J. Schaubert and R. L. Gallo, *J. Invest. Dermatol.*, 2007, **127**, 510-512; M. Zanetti, *Curr. Issues Mol. Biol.*, 2005, **7**, 179-196; M. Zanetti, *J. Leukocyte Biol.*, 2004, **75**, 39-48; P. Kougias,



- 
- H. Chai, P. H. Lin, Q. Z. Yao, A. B. Lumsden and C. Y. Chen, *J. Cell. Mol. Med.*, 2005, **9**, 3-10; R. Bals and J. M. Wilson, *Cell. Mol. Life Sci.*, 2003, **60**, 711-720; D. M. E. Bowdish, D. J. Davidson and R. E. W. Hancock, *Antimicrob. Pept. Human Dis.*, 2006, **306**, 27-66; De Smet and R. Contreras, *Biotechnol. Lett.*, 2005, **27**, 1337-1347; L. Tomasinsig and M. Zanetti, *Curr. Protein Pept. Sci.*, 2005, **6**, 23-34; O. E. Sorensen and N. Borregaard, *Comb. Chem. High Throughput Screening*, 2005, **8**, 273-280;
- <sup>174</sup> T. Uzzell, E. D. Stolzenberg, A. E. Shinnar and M. Zasloff, *Peptides*, 2003, **24**, 1655-1667; V. H. Maier, K. V. Dorn, B. K. Gudmundsdottir and G. H. Gudmundsson, *Mol. Immunol.*, 2008, **45**, 3723-3730; M. Scocchi, A. Pallavicini, R. Salgaro, K. Bociek and R. Gennaro, *Comp. Biochem. Physiol., Part B: Biochem. Mol. Biol.*, 2009, **152**, 376-38;
- <sup>175</sup> S. Y. Zhu, *Trends Microbiol.*, 2008, **16**, 353.
- <sup>176</sup> J. R. Lai, R. F. Epand, B. Weisblum, R. M. Epand and S. H. Gellman, *Biochemistry*, 2006, **45**, 15718-15730.
- <sup>177</sup> C. Roumestand, V. Louis, A. Aumelas, G. Grassy, B. Calas and A. Chavanieu, *FEBS Lett.*, 1998, **421**, 263-267.
- <sup>178</sup> K. Taylor, P. E. Barran and J. R. Dorin, *Biopolymers*, 2008, **90**, 1, 1-7; C. Herr, R. Shaykhiiev and R. Bals, *Expert Opin. Biol. Ther.*, 2007, **7**, 1449-146; P. S. Hiemstra, *Biochem. Soc. Trans.*, 2006, **34**, 276-278; T. Hirsch, F. Jacobsen, H. U. Steinau and L. Steinstraesser, *Protein Pept. Lett.*, 2008, **15**, 238-243; L. Steinstraesser, T. Koehler, F. Jacobsen, A. Daigeler, O. Goertz, S. Langer, M. Kesting, H. Steinau, E. Eriksson and T. Hirsch, *Mol. Med.*, 2008, **14**, 528-537; Y. Kai-Larsen and B. Agerberth, *Front. Biosci.*, 2008, **13**, 3760-3767
- <sup>179</sup> G. H. Gudmundsson, B. Agerberth, J. Odeberg, T. Bergman, B. Olsson and R. Salcedo, *Eur. J. Biochem.*, 1996, **238**, 325-332.
- <sup>180</sup> J. Stie, A. V. Jesaitis, C. I. Lord, J. M. Gripenrog, R. M. Taylor, J. B. Burritt and A. J. Jesaitis, *J. Leukocyte Biol.*, 2007, **82**, 161-172.
- <sup>181</sup> O. E. Sorensen and N. Borregaard, *Comb. Chem. High Throughput Screening*, 2005, **8**, 273-280.
- <sup>182</sup> M. Zaiou, V. Nizet and R. L. Gallo, *J. Invest. Dermatol.*, 2003, **120**, 810-816.

- 
- <sup>183</sup> J. Johansson, G. H. Gudmundsson, M. E. Rottenberg, K. D. Berndt and B. Agerberth, *J. Biol. Chem.*, 1998, **273**, 3718-3724.
- <sup>184</sup> O. E. Sorensen, L. Gram, A. H. Johnsen, E. Andersson, S. Bangsboll, G. S. Tjabringa, P. S. Hiemstra, J. Malm, A. Egesten and N. Borregaard, *J. Biol. Chem.*, 2003, **278**, 28540-28546.
- <sup>185</sup> K. Yamasaki, A. Di Nardo, A. Bardan, M. Murakami, T. Ohtake, A. Coda, R. A. Dorschner, C. Bonnart, P. Descargues, A. Hovnanian, V. B. Morhenn and R. L. Gallo, *Nat. Med.*, 2007, **13**, 975-980.
- <sup>186</sup> M. Murakami, B. Lopez-Garcia, M. Braff, R. A. Dorschner and R. L. Gallo, *J. Immunol.*, 2004, **172**, 3070-3077.
- <sup>187</sup> A. L. den Hertog, J. van Marle, H. A. van Veen, W. van't Hof, J. G. M. Bolscher, E. C. I. Veerman and A. V. N. Amerongen, *Biochem. J.*, 2005, **388**, 689-695; B. Lopez-Garcia, P. H. A. Lee, K. Yamasaki and R. L. Gallo, *J. Invest. Dermatol.*, 2005, **125**, 108-115; P. Bergman, L. Walter-Jallow, K. Broliden, B. Agerberth and J. Soderlund, *Curr. HIV Res.*, 2007, **5**, 410-415; G. S. Wang, K. M. Watson and R. W. Buckheit, *Antimicrob. Agents Chemother.*, 2008, **52**, 3438-3440
- <sup>188</sup> L. Steinstraesser, T. Koehler, F. Jacobsen, A. Daigeler, O. Goertz, S. Langer, M. Kesting, H. Steinau, E. Eriksson and T. Hirsch, *Mol. Med.*, 2008, **14**, 528-537; Y. P. Lai and R. L. Gallo, *Trends Immunol.*, 2009, **30**, 131-141; S. B. Coffelt and A. B. Scandurro, *Cancer Res.*, 2008, **68**, 6482-6485; N. Mookherjee, P. Hamill, J. Gardy, D. Blimkie, R. Falsafi, A. Chikatamarla, D. J. Arenillas, S. Doria, T. R. Kollmann and R. E. W. Hancock, *Molecular Biosystems*, 2009, **5**, 483-496
- <sup>189</sup> J. J. Oppenheim and D. Yang, *Curr. Opin. Immunol.*, 2005, **17**, 359-365.
- <sup>190</sup> A. Nijnik and R. E. W. Hancock, *Curr. Opin. Haem.*, 2009, **16**, 41-47.
- <sup>191</sup> S. L. Ball, G. P. Siou, J. A. Wilson, A. Howard, B. H. Hirst and J. Hall, *Journal of Laryngology and Otology*, 2007, **121**, 973-978.
- <sup>192</sup> H. Altman, D. Steinberg, Y. Porat, A. Mor, D. Fridman, M. Friedman and G. Bachrach, *J. Antimicrob. Chemother.*, 2006, **58**, 198-201.

- 
- <sup>193</sup> L. C. Huang, T. D. Petkova, R. Y. Reins, R. J. Proske and A. M. McDermott, *Investigative Ophthalmology & Visual Science*, 2006, **47**, 2369-2380.
- <sup>194</sup> M. Stahle, L. Mallbris, T. Wei, M. F. Nilsson, J. Heilborn, L. Carlen and F. Granath, *J. Invest. Dermatol.*, 2008, **128**, S8-S9.
- <sup>195</sup> M. Zasloff, *Proc. Natl. Acad. Sci. U.S.A.*, 2006, **103**, 8913-8914; R. Raqib, P. Sarker, P. Bergman, G. Ara, M. Lindh, D. A. Sack, K. M. N. Islam, G. H. Gudmundsson, J. Andersson and B. Agerberth, *Proc. Natl. Acad. Sci. U.S.A.*, 2006, **103**, 9178-9183; Y. Kida, T. Shimizu and K. Kuwano, *Mol. Immunol.*, 2006, **43**, 1972-1981; J. Schaubert, K. Iffland, S. Frisch, T. Kudlich, B. Schmausser, M. Eck, T. Menzel, A. Gostner, H. Luhrs and W. Scheppach, *Mol. Immunol.*, 2004, **41**, 847-854
- <sup>196</sup> S. Termen, M. Tollin, E. Rodriguez, S. H. Sveinsdottir, B. Johannesson, A. Cederlund, J. Sjovall, B. Agerberth and G. H. Gudmundsson, *Mol. Immunol.*, 2008, **45**, 3947-3955.
- <sup>197</sup> B. Agerberth, E. Buentke, P. Bergman, H. Eshaghi, S. Gabrielsson, G. H. Gudmundsson and A. Scheynius, *Allergy*, 2006, **61**, 422-430.
- <sup>198</sup> J. Cohen, *Nature*, 2002, **420**, 885-891.
- <sup>199</sup> R. Belas, J. Manos and R. Suvanasuthi, *Infect. Immun.*, 2004, **72**, 5159-5167; P. Bergman, L. Johansson, V. Asp, L. Plant, G. H. Gudmundsson, A. B. Jonsson and B. Agerberth, *Cell. Microbiol.*, 2005, **7**, 1009-1017; D. Islam, L. Bandholtz, J. Nilsson, H. Wigzell, B. Christensson, B. Agerberth and G. H. Gudmundsson, *Nat. Med.*, 2001, **7**, 180-185
- <sup>200</sup> K. Yamasaki, J. Schaubert, A. Coda, H. Lin, R. A. Dorschner, N. M. Schechter, C. Bonnart, P. Descargues, A. Hovnanian and R. L. Gallo, *FASEB J.*, 2006, **20**, 2068-2080.
- <sup>201</sup> Y. F. Li, X. Li and G. S. Wang, *Protein Expression Purif.*, 2007, **55**, 395-405; I. P. Hong, S. J. Lee, Y. S. Kim and S. G. Choi, *Biotechnol. Lett.*, 2007, **29**, 73; J. Y. Moon, K. A. Henzler-Wildman and A. Ramamoorthy, *Biochim. Biophys. Acta Biomembr.*, 2006, **1758**, 1351-1358; Y. F. Li, X. Li and G. S. Wang, *Protein Expression Purif.*, 2006, **47**, 498-505.
- <sup>202</sup> F. Porcelli, R. Verardi, L. Shi, K. A. Henzler-Wildman, A. Ramamoorthy and G. Veglia, *Biochemistry*, 2008, **47**, 5565-5572.
- <sup>203</sup> G. S. Wang, *J. Biol. Chem.*, 2008, **283**, 32637-32643.

- 
- <sup>204</sup> I. Zelezetsky, A. Pontillo, L. Puzzi, N. Antcheva, L. Segat, S. Pacor, S. Crovella and A. Tossi, *J. Biol. Chem.*, 2006, **281**, 19861-19871.
- <sup>205</sup> F. Morgera, L. Vaccari, N. Antcheva, D. Scaini, S. Pacor and A. Tossi, *Biochem. J.*, 2009, **417**, 727-735.
- <sup>206</sup> T. Sigurdardottir, P. Andersson, M. Davoudi, M. Malmsten, A. Schmidtchen and M. Bodelsson, *Antimicrob. Agents Chemother.*, 2006, **50**, 2983-2989.
- <sup>207</sup> M. H. Braff, M. A. Hawkins, A. Di Nardo, B. Lopez-Garcia, M. D. Howell, C. Wong, K. Lin, J. E. Streib, R. Dorschner, D. Y. M. Leung and R. L. Gallo, *J. Immunol.*, 2005, **174**, 4271-4278.
- <sup>208</sup> K. H. Lee, D. G. Lee, Y. Park, D. I. Kang, S. Y. Shin, K. S. Hahm and Y. Kim, *Biochem. J.*, 2006, **394**, 105.
- <sup>209</sup> T. Sigurdardottir, P. Andersson, M. Davoudi, M. Malmsten, A. Schmidtchen and M. Bodelsson, *Antimicrob. Agents Chemother.*, 2006, **50**, 2983-2989.
- <sup>210</sup> G. S. Wang, K. M. Watson and R. W. Buckheit, *Antimicrob. Agents Chemother.*, 2008, **52**, 3438-3440.
- <sup>211</sup> K. Okumura, A. Itoh, E. Isogai, K. Hirose, Y. Hosokawa, Y. Abiko, T. Shibata, M. Hirata, H. Isogai, *Cancer Lett.*, 2004, **212**, 185-194
- <sup>212</sup> E. M. Molhoek, A. L. den Hertog, A. de Vries, K. Nazmi, E. C. I. Veerman, F. C. Hartgers, M. Yazdanbakhsh, F. J. Bikker and D. van der Kleij, *Biol. Chem.*, 2009, **0**, 295-303
- <sup>213</sup> A. B. Meijer, R. B. Spruijt, C. Wolfs and M. A. Hemminga, *Biochemistry*, 2001, **40**, 5081-5086.
- <sup>214</sup> X. Li, Y. F. Li, H. Y. Han, D. W. Miller and G. S. Wang, *J. Am. Chem. Soc.*, 2006, **128**, 5776-5785.
- <sup>215</sup> M. H. Braff, M. Zaiou, J. Fierer, V. Nizet and R. L. Gallo, *Infect. Immun.*, 2005, **73**, 6771-6781.
- <sup>216</sup> E. Glukhov, L. L. Burrows and C. M. Deber, *Biopolymers*, 2008, **89**, 360-371.

- 
- <sup>217</sup> I. Nagaoka, K. Kuwaharß–Arai, H. Tamura, K. Hiramatsu and M. Hirata, *Inflammation Res.*, 2005, **54**, 66-73.
- <sup>218</sup> D. Tanaka, K. Y. Miyasaki and R. I. Lehrer, *Oral Microbiol. Immunol.*, 2000, **15**, 226-231.
- <sup>219</sup> B. Lopez-Garcia, W. Ubhayasekera, R. L. Gallo and J. F. Marcos, *Biochem. Biophys. Res. Commun.*, 2007, **356**, 107-113.
- <sup>220</sup> C. D. Ciornei, T. Sigurdardottir, A. Schmidtchen and M. Bodelsson, *Antimicrob. Agents Chemother.*, 2005, **49**, 2845-2850; M. J. Nell, G. S. Tjabringa, A. R. Wafelman, R. Verrijck, P. S. Hiemstra, J. W. Drijfhout and J. J. Grote, *Peptides*, 2006, **27**, 649-660; E. M. Molhoek, A. L. den Hertog, A. de Vries, K. Nazmi, E. C. I. Veerman, F. C. Hartgers, M. Yazdanbakhsh, F. J. Bikker and D. van der Kleij, *Biol. Chem.*, 2009, **0**, 295-303; I. Nagaoka, H. Tamura and M. Hirata, *J. Immunol.*, 2006, **176**, 3044-3052; Z. Oren, J. Hong and Y. Shai, *J. Biol. Chem.*, 1997, **272**, 14643-14649;
- <sup>221</sup> M. J. Nell, G. S. Tjabringa, A. R. Wafelman, R. Verrijck, P. S. Hiemstra, J. W. Drijfhout and J. J. Grote, *Peptides*, 2006
- <sup>222</sup> Z. Oren, J. Hong and Y. Shai, *J. Biol. Chem.*, 1997, **272**, 14643-14649.
- <sup>223</sup> E. Gazit, A. Boman, H. G. Boman and Y. Shai, *Biochemistry*, 1995, **34**, 11479-11488.
- <sup>224</sup> L. Tomasinsig, C. Pizzirani, B. Skerlavaj, P. Pellegatti, S. Gulinelli, A. Tossi, F. Di Virgilio and M. Zanetti, *J. Biol. Chem.*, 2008, **283**, 30471-30481.
- <sup>225</sup> E. Sevcsik, G. Pabst, A. Jilek and K. Lohner, *Biochim. Biophys. Acta Biomembr.*, 2007, **1768**, 2586-2595.
- <sup>226</sup> E. Sevcsik, G. Pabst, W. Richter, S. Danner, H. Amenitsch and K. Lohner, *Biophys. J.*, 2008, **94**, 4688-4699; F. Neville, M. Cahuzac, A. Nelson and D. Gidalevitz, *J. Phys.: Condens. Matter*, 2004, **16**, S2413-S2420; F. Neville, C. S. Hodges, C. Liu, O. Konovalov and D. Gidalevitz, *Biochim. Biophys. Acta Biomembr.*, 2006, **1758**, 232-240; F. Neville, M. Cahuzac, O. Konovalov, Y. Ishitsuka, K. Y. C. Lee, I. Kuzmenko, G. M. Kale and D. Gidalevitz, *Biophys. J.*, 2006, **90**, 1275-1287
- <sup>227</sup> G. S. Wang, *Biochim. Biophys. Acta Biomembr.*, 2007, **1768**, 3271-3281; R. Sood, Y. Domanov, M. Pietiainen, V. P. Kontinen and P. K. J. Kinnunen, *Biochim. Biophys. Acta*

---

*Biomembr.*, 2008, **1778**, 983-996; R. Sood and P. K. J. Kinnunen, *Chem. Phys. Lipids*, 2008, **154**, S29-S30.

<sup>228</sup> R. Sood and P. K. J. Kinnunen, *Biochim. Biophys. Acta Biomembr.*, 2008, **1778**, 1460-1466.

<sup>229</sup> A. J. Mason, A. Marquette and B. Bechinger, *Biophys. J.*, 2007, **93**, 4289-4299.

<sup>230</sup> Z. Oren, J. C. Lerman, G. H. Gudmundsson, B. Agerberth and Y. Shai, *Biochem. J.*, 1999, **341**, 501-513.

<sup>231</sup> Y. E. Lau, D. M. E. Bowdish, C. Cosseau, R. E. W. Hancock and D. J. Davidson, *Am. J. Respir. Cell Mol. Biol.*, 2006, **34**, 399-409.

<sup>232</sup> G. Ehrenstein and H. Lecar, *Q. Rev. Biophys.*, 1977, **10**, 1-34.

<sup>233</sup> J. M. Sanderson, *Org. Biomol. Chem.*, 2005, **3**, 201-212.

<sup>234</sup> K. A. Henzler Wildman, D.-K. Lee and A. Ramamoorthy, *Biochemistry*, 2003, **42**, 6545-6558.

<sup>235</sup> K. A. Henzler-Wildman, G. V. Martinez, M. F. Brown and A. Ramamoorthy, *Biochemistry*, 2004, **43**, 8459-8469.

<sup>236</sup> D. Avrahami, Z. Oren and Y. Shai, *Biochemistry*, 2001, **40**, 12591-12603.

<sup>237</sup> M. A. Holzl, J. Hofer, P. Steinberger, K. Pfistershammer and G. J. Zlabinger, *Immunol. Lett.*, 2008, **119**, 4-11.

<sup>238</sup> G. S. Tjabringa, J. Aarbiou, D. K. Ninaber, J. W. Drijfhout, O. E. Sorensen, N. Borregaard, K. F. Rabe and P. S. Hiemstra, *J. Immunol.*, 2003, **171**, 6690-6696.

<sup>239</sup> J. von Haussen, R. Koczulla, R. Shaykhiev, C. Herr, O. Pinkenburg, D. Reimer, R. Wiewrodt, S. Biesterfeld, A. Aigner, F. Czubayko and R. Bals, *Lung Cancer*, 2008, **59**, 12-23.

<sup>240</sup> S. B. Coffelt, R. S. Waterman, L. Florez, K. H. Bentrup, K. J. Zwezdaryk, S. L. Tomchuck, H. L. LaMarca, E. S. Danka, C. A. Morris and A. B. Scandurro, *Int. J. Cancer*, 2008, **122**, 1030-1039.

- 
- <sup>241</sup> S. Tokumaru, K. Sayama, Y. Shirakata, H. Komatsuzawa, K. Ouhara, Y. Hanakawa, Y. Yahata, X. J. Dai, M. Tohyama, H. Nagai, L. J. Yang, S. Higashiyama, A. Yoshimura, M. Sugai and K. Hashimoto, *J. Immunol.*, 2005, **175**, 4662-4668.
- <sup>242</sup> S. Pochet, S. Tandel, S. Querriere, M. Tre-Hardy, M. Garciß–Marcos, M. De Lorenzi, M. Vandenbranden, A. Marino, M. Devleeschouwer and J. P. Dehaye, *Mol. Pharmacol.*, 2006, **69**, 2037-2046.
- <sup>243</sup> S. M. Zughaier, W. M. Shafer and D. S. Stephens, *Cell. Microbiol.*, 2005, **7**, 1251-1262.
- <sup>244</sup> D. G. Perregaux, K. Bhavsar, L. Contillo, J. S. Shi and C. A. Gabel, *J. Immunol.*, 2002, **168**, 3024-3032.
- <sup>245</sup> A. Elssner, M. Duncan, M. Gavrilin and M. D. Wewers, *J. Immunol.*, 2004, **172**, 4987-4494.
- <sup>246</sup> A. Di Nardo, M. H. Braff, K. R. Taylor, C. R. Na, R. D. Granstein, J. E. McInturff, S. Krutzik, R. L. Modlin and R. L. Gallo, *J. Immunol.*, 2007, **178**, 1829-134.
- <sup>247</sup> D. Yang, Q. Chen, A. P. Schmidt, G. M. Anderson, J. M. Wang, J. Wooters, J. J. Oppenheim and O. Chertov, *J. Exp. Med.*, 2000, **192**, 1069-1074.
- <sup>248</sup> S. B. Coffelt, F. C. Marini, K. Watson, K. J. Zvezdaryk, J. L. Dembinski, H. L. LaMarca, S. L. Tomchuck, K. H. Z. Bentrup, E. S. Danka, S. L. Henkle and A. B. Scandurro, *Proc. Natl. Acad. Sci. U.S.A.*, 2009, **106**, 3806-3811.
- <sup>249</sup> A. Iaccio, F. Cattaneo, M. Mauro and R. Ammendola, *Arch. Biochem. Biophys.*, 2009, **481**, 94-100.
- <sup>250</sup> S. Y. Lee, M. S. Lee, H. Y. Lee, S. D. Kim, J. W. Shim, S. H. Jo, J. W. Lee, J. Y. Kim, Y. W. Choi, S. H. Baek, S. H. Ryu and Y. S. Bae, *FEBS Lett.*, 2008, **582**, 270.
- <sup>251</sup> Y. Rosenfeld, N. Papo and Y. Shai, *J. Biol. Chem.*, 2006, **281**, 1636.
- <sup>252</sup> P. J. Fisher, F. G. Prendergast, M. R. Ehrhardt, J. L. Urbauer, A. J. Wand, S. S. Sedarous, D. J. McCormik, P. J. Buckley, *Nature*, 1994, **368**, 6472, 651-653,
- <sup>253</sup> G. J. Kersh and P. M. Allen, *Nature*, 1996, **380**, 6574, 495-498.

- 
- <sup>254</sup> J. M. Webster, R. Zhang, S. S. Gambhir, Z. Cheng and F. A. Syud, *ChemBioChem*, 2009, **10**, 1293-1296.
- <sup>255</sup> M. Friedman, A. Orlova, E. Johansson, T. L. J. Eriksson, I. Hoiden-Guthenberg, V. Tolmachev, F. Y. Nilsson and S. Stahl, *J. Mol. Biol.*, 2008, **376**, 1388-1402.
- <sup>256</sup> F. Y. Nilsson and V. Tolmachev, *Curr. Opin. Drug Discovery Dev.*, 2007, **10**, 167-175.
- <sup>257</sup> P. A. Nygren, *FEBS J.*, 2008, **275**, 2668-2676.
- <sup>258</sup> S. Sandgren, A. Wittrup, F. Cheng, M. Jonsson, E. Eklund, S. Busch and M. Belting, *J. Biol. Chem.*, 2004, **279**, 17951-17956.
- <sup>259</sup> R. Lande, J. Gregorio, V. Facchinetti, B. Chatterjee, Y. H. Wang, B. Homey, W. Cao, B. Su, F. O. Nestle, T. Zal, I. Mellman, J. M. Schroder, Y. J. Liu and M. Gilliet, *Nature*, 2007, **449**, 564-566.
- <sup>260</sup> R. Bucki, F. J. Byfield and P. A. Janmey, *Eur. Respir. J.*, 2007, **29**, 624-632.
- <sup>261</sup> R. Bucki, A. G. Sostarecz, F. J. Byfield, P. B. Savage and P. A. Janmey, *J. Antimicrob. Chemother.*, 2007, **60**, 535-545
- <sup>262</sup> J. X. Tang, Q. Wen, A. Bennett, B. Kim, C. A. Sheils, R. Bucki and P. A. Janmey, *American Journal of Physiology-Lung Cellular and Molecular Physiology*, 2005, **289**, L599-L605.
- <sup>263</sup> L. J. Zhang and T. J. Falla, *Expert Opin. Pharmacother.*, 2006, **7**, 653-663.
- <sup>264</sup> R. E. W. Hancock and H. G. Sahl, *Nat. Biotechnol.*, 2006, **24**, 1551-1557.
- <sup>265</sup> J. B. McPhee and R. E. W. Hancock, *Journal of Peptide Science*, 2005, **11**, 677-687.
- <sup>266</sup> M. Zaiou, *J. Mol. Med.*, 2007, **85**, 317-329; A. A. Langham, H. Khandelia, B. Schuster, A. J. Waring, R. I. Lehrer and Y. N. Kaznessis, *Peptides*, 2008, **29**, 1085-1093; E. Matyus, C. Kandt and D. P. Tieleman, *Curr. Med. Chem.*, 2007, **14**, 2789-2798; C. D. Fjell, R. E. W. Hancock and A. Cherkasov, *Bioinformatics*, 2007, **23**, 1148-1155; C. Loose, K. Jensen, I. Rigoutsos and G. Stephanopoulos, *Nature*, 2006, **443**, 867-869; R. Hammami, J. Ben Hamida, G. Vergoten and I. Fliss, *Nucleic Acids Res.*, 2009, **37**, D963-D968;
- <sup>267</sup> G. A. Holdgate, *Biotechniques*, 2001, **31**, 164-184.



- 
- <sup>268</sup> B. Cravatt, A. T. Wright and J. W. Kozarich, *Annu. Rev. Biochem.*, 2008, **77**, 383-414.
- <sup>269</sup> C. Drahl, B. F. Cravatt and E. J. Sorensen, *Angew. Chem. Int. Ed.*, 2005, **44**, 5788-5809.
- <sup>270</sup> M. Hashimoto and Y. Hatanaka, *Eur. J. Org. Chem.*, 2008, 2513-2523
- <sup>271</sup> P. J. A. Weber, A. G. Beck-Sickinger, *J. Pept. Res.*, 1996, **49**, 5, 375-383
- <sup>272</sup> G. Dorman and G. D. Prestwich, *Biochemistry*, 1994, **33**, 19, 5661-5672
- <sup>273</sup> J.C. Kauer, S. Erickson-Viitanen S, H. R. Wolfe and W. F. DeGrado, *J. Biol. Chem.*, 1986, **261**, 10695-10700.
- <sup>274</sup> R. E. Galaray, L. C. Craig, J. D. Jamieon and M. P. Prinz, *J. Biol. Chem.*, 1974, **249**, 11, 3510-3518.
- <sup>275</sup> A. Saghatelian, N. Jessani, A. Joseph, M. Humphrey and B. F. Cravatt, *Proc. Nat. Academy Sci. U.S.A*, 101, **27**, 10000-10005
- <sup>276</sup> M.Völkert, K. Uwai, A.Tebbe, B. Popkirova, M. Wagner, J. Kuhlmann, and Herbert Waldmann, *J. Am. Chem. Soc.*, 2003, 125, 12749-12758
- <sup>277</sup> V. Pham and P. M. Sexton, *J. Pept. Sci*, 2004, **10**, 179-203
- <sup>278</sup> E. de Hoffmann and V. Stroobant in *Mass Spectrometry, Principles and Applications*, Wiley, Chichester, 2002,
- <sup>279</sup> M. L. Mayo, A. Rodriguez, M. del Mar Graciani and G. Fernandez, *J. Coll. Interface Sci.*, 2007, **316**, 2, 787-795.
- <sup>280</sup> C. -S. Lim, J. W. Kampf, V. Pecoraro, *Inorg. Chem.*, 2009, **48**, 5224-5233
- <sup>281</sup> M. S. Ozers, B. D. Marks, K. Gowda, K. R. Kupcho, K. M. Ervin, T. De Rosier, N. Qadir, H. C. Eliason, S. M. Riddle and M. S. Skekhani, *Biochemistry*, 2007, **46**, 683-695.
- <sup>282</sup> T. P. Hopp and K. R. Wood, *Proc. Natl. Acad. Sci., USA*, 1981, **78**, 3824-3828
- <sup>283</sup> R. B. Merrifield, *J. Am. Chem. Soc*, 1963, **85**, 2419-2422.
- <sup>284</sup> B. Blankemeyer-Menge, M. Nimtz, and R. Frank, *Tet. Lett.*, 1990, **31**, 12, 1701-1704.

- 
- <sup>285</sup> W. C. Chan and P. D. White, in *Basic Principles: Fmoc Solid Phase Peptide Synthesis: A Practical Approach*, ed. W. C. Chan and P. D. White, Oxford University Press, New York, 2000, pp 42-7.
- <sup>286</sup> N. Vavourakis, L. Leondiadis and N. Ferderigos, *Tet. Lett.*, 2002, **43**, 8343-8345.
- <sup>287</sup> J. Coste, D. LeNguyen and B. Castro, *Tet. Lett.*, 1990, **31**, 2, 205-208.
- <sup>288</sup> W. C. Chan and P. D. White, in *Basic Principles: Fmoc Solid Phase Peptide Synthesis: A Practical Approach*, ed. W. C. Chan and P. D. White, Oxford University Press, New York, 2000, pp 32-6.
- <sup>289</sup> S. A. Palsek, Z. J. Cox and J. M. Collins, *J. Pept. Sci.*, 2007, **13**, 143-148.
- <sup>290</sup> J. Coste, D. LeNguyen and B. Castro, *Tet. Lett.*, 1990, **31**, 2, 205-208.
- <sup>291</sup> E. Kaiser, R. L. Colescott, C. D. Bossinger and P. I. Cook, *Anal. Biochem.*, 1970, **35**, 595-599.
- <sup>292</sup> R. C. Milton, S. C. F. Milton and P. A. Adams, *J. Am. Chem. Soc.*, 1990, **112**, 6039- 6046.
- <sup>293</sup> F. Albericio, J. M. Bofill, A. El-Faham and S. A. Kates, *J. Org. Chem.*, 1998, **63**, 9678-9683.
- <sup>294</sup> S. A. Palasek, Z. J. Cox and J. M. Collins, *J. Pept. Sci.*, 2007, **13**, 143-148.
- <sup>295</sup> A. Galanis, F. Albericio and M. Grotli, *Org. Lett.*, 2009, 11, **20**, 4488-4491.
- <sup>296</sup> B. Basca, K. Horvita, S. Bosza, F. Andrae and O.C. Kappe, *J. Org. Chem.*, 2008, **73**, 7532-7542.
- <sup>297</sup> C.-S. Lim, J. W. Kampf and Vincent L. Pecoraro, *Inorg. Chem.*, 2009, **48**, 5224-5233
- <sup>298</sup> V. Ball and C Maechling, *Int. J. Mol. Sci.* 2009, **10**, 3283-3315;
- <sup>299</sup> E. Freire, *Chem. Biol. Drug Des.*, 2009, **74**, 468-472
- <sup>300</sup> M. Yamamoto, A. Ueda, M. Kudo, Y. Matsuo, J. Fukushima, T. Nakae, T. Kaneko and Y. Ishigatsubo, *Microbiology*, 2009, ASAP.

- 
- <sup>301</sup> K. E. van Holde, W. Curtis Johnson, P. Shing Ho in *Principles of Physical Biochemistry*, Prentice Hall, New Jersey, 1998, Chapter 6, pp 252-255.
- <sup>302</sup> G. Dorman and G. D. Prestiwich, *Biochemistry*, 1994, **33**, 19, 5661-5673
- <sup>303</sup> <http://prospector.ucsf.edu/prospector/mshome.htm>
- <sup>304</sup> P. Emsley P and K. Cowtan, *Acta Crystallographica Section D-Biological Crystallography*, 2004, **60**, 2126-2132
- <sup>305</sup> C. A Del Carpio, Y. Takahashi, S. Sasaki, *S. J. Mol. Graph.*, 1993, **11**, 23-29
- <sup>306</sup> N. Willand, B. Dirie, X. Carette, P. Bifani, A. Singhal, M. Desroses, F. Leroux, E., V. Mathys, R. Deprez-Poulain, *Nat. Med.*, 2009, **15**, 537-544
- <sup>307</sup> M. Klotzsche, C. Berens and Wolfgang Hillen, *J. Biol. Chem.*, 2005, **280**, 24591-24599.
- <sup>308</sup> A. G. Mazzariol, G. Cornaglia and H. Nikaido, *Antimicrob. Agents Chemother.*, 2000, **44**, 1387-1390
- <sup>309</sup> L. Zhang, PhD Thesis, 2009, Durham
- <sup>310</sup> Y. Morita, K. Kodama, S. Shiota, T. Mine, A. Kataoka, T. Mizushima, and T. Tsuchiya, *Antimicrobial. Agents Chemother.*, 1998, **42**, 7, 1778-1782
- <sup>311</sup> W. J. Stubbings, J. M. Bostock, E. Ingham and I. Chopra, *J. Antimicrob. Chemother.*, 2004, **54**, 1, 139-143.
- <sup>312</sup> E. Y. Chekmeneva, B. S. Vollmarb, K. T. Forseth, M. N. Manion, S. M. Jones, T. J. Wagner, R. L. Endicottc, B. P. Kyrissc, L. M. Homem, M. Pate, J. He, J. Raines, P. L. Gor'kov, W. W. Brey, D. J. Mitchell, A. J. Auman, M. J. Ellard-Ivey, J. Blazyk and M. Cotte, *Biochemica Biophysic Acta*, 2006, **1758**, 1359-1372; C. A. Elkins and L. B. Mullis, *Antimicrob. Agents Chemother.*, 2007, **51**, 3, 923-929; L. Otvos and M. Cudic, *Broth Microdilution Antibacterial assays of peptides*, in Peptide Characterisation and Application Protocols, Methods in Molecular Biology 386, ed. G. Fields, Human Press, Totowa, New Jersey, 2007

- 
- <sup>313</sup> L. Otvos and M. Cudic, *Broth Microdilution Antibacterial assays of peptides*, in *Peptide Characterisation and Application Protocols*, Methods in Molecular Biology 386, ed. G. Fields, Human Press, Totowa, New Jersey, 2007.
- <sup>314</sup> B. Ericksen, Z. Wu, W. Lu and R. Lehrer, *Antimicrob. Agents and Chemother.*, 2005, **49**, 1, 269-275
- <sup>315</sup> L. Otvos and M. Cudic, *Broth Microdilution Antibacterial assays of peptides*, in *Peptide Characterisation and Application Protocols*, Methods in Molecular Biology 386, ed. G. Fields, Human Press, Totowa, New Jersey, 2007
- <sup>316</sup> J. D. Brewster, *J. Microbiol. Methods*, 2003, **53**, 77-86.
- <sup>317</sup> M. Cudic, B. A. Condie, D. J. Weiner, E. S. Lysenko, Z.Q. Zhang, O. Insug, P. Bulet, L. Otvos, *Peptides*, 2002, **23**, 271-283
- <sup>318</sup> W. Boos, *Annu. Rev. Biochem.*, 1974, 43, 124-146; L. Rodrigues, D. Wagner, M. Viveiros, D. Sampaio, I. Couto, M. Vavra, W. V. Kern and L. Amaral, *J. Antimicrob. Chemother.*, 2008, **61**, 1076-1082
- <sup>319</sup> L. Rodrigues, D. Wagner, M. Viveiros, D. Sampaio, I. Couto, M. Vavra, W. V. Kern and L. Amaral, *J. Antimicrob. Chemother.*, 2008, 61, 1076-1082
- <sup>320</sup> Musiol, H.-J.; Siedler, F.; Quarzago, D.; Moroder, L. *Biopolymer* 1994, 34, 1553-1562.; Kaiser, T.; Nicholson, G.; Kohlbau, H. J. Voelter., *Tet. Lett.* 1996, 37, 1187-1190.
- <sup>321</sup> Moroder L, Besse D, Musiol HJ, RudolphBohner S, Siedler F, *Biopolymers*, 1996, 40, 2, 207-234
- <sup>322</sup> L. Kisfaludy, J. E. Roberts, R. H. Johnson, G. L. Mayers, J. Kovacs, *J. Org. Chem.*, 1970, **35**, 10, 3563-3565
- <sup>323</sup> L. Fattorinia, R. Gennarob, M. Zanettic, D. Tana, L. Brunoria, F. Giannonia, M. Pardinia, G. Orefici, *Peptides*, 2004, **25**, 7, 1075-1077
- <sup>324</sup> <http://www.expasy.ch/tools/protparam.html>

---

## 7 Appendix

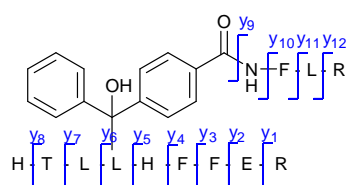
### 7.1 Data for mass spectrometric analysis of inhibitors 37 and 38 binding to MtrR

#### Characterisation of peak at 1269 by MS/MS using MALDI-LIFT

Observed m/z	Calculated m/z	Identity
86.065	86.096	L
87.028	87.0917	R
110.079	110.071	H
112.090	112.069	R
120.088	120.081	F
138.075	138.0662	H
175.079	175.119	y <sub>1</sub>
199.084	199.181	LL-28
223.086	223.155	LH-28
251.103	251.153	LH
257.092	257.140	TL+C <sub>3</sub> H <sub>3</sub> O <sub>2</sub> -28
259.105	259.101	FE-H <sub>2</sub> O
285.941	285.135	HF
364.091	364.234	LLH
369.073	369.223	TLL+C <sub>3</sub> H <sub>3</sub> O <sub>2</sub>

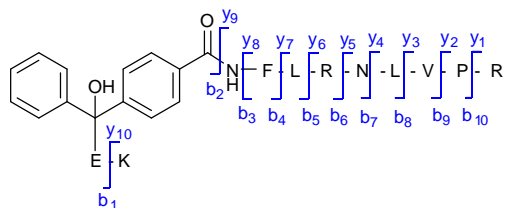
## 7.2 Data for MS /MS analysis of tryptic peptides after photo-insertion of peptide 243 into MtrR

### 7.2.1 Insertion into HTLLHFFER



m/z (observed)	m/z (calculated)	Identity
158.673	158.094	y <sub>1</sub> -NH <sub>3</sub>
175.678	175.112	y <sub>1</sub>
257.7345	257.1397	HF-28
285.7405	285.1346	HF
288.264	287.114	y <sub>2</sub> - NH <sub>3</sub>
581.287	581.272	y <sub>4</sub> - NH <sub>3</sub>
717.632	717.337	y <sub>5</sub> -H <sub>2</sub> O
972.098	970.049	LFLR+C <sub>14</sub> H <sub>10</sub> O <sub>2</sub> -28
1085.224	1081.525	TLHFRLR+ C <sub>14</sub> H <sub>10</sub> O <sub>2</sub>
1703.156	1702.8740	y <sub>11</sub>
1776.591	1777.9373	M-CH <sub>2</sub> N <sub>2</sub>
1824.667	1823.9380	MH-H <sub>2</sub> O

## 7.2.2 Insertion into EK



Observed m / z	Calculated m / z	Identity
158.9853	158.094	y <sub>1</sub> -NH <sub>3</sub>
175.0191	175.119	y <sub>1</sub>
186.9693	185.164	LV-28
243.0303	243.156	LR-28
257.9954	255.125	y <sub>2</sub> -NH <sub>3</sub>
358.0883	357.24	y <sub>3</sub> -NH <sub>3</sub>
373.0315	372.240	y <sub>3</sub>
450.1774	450.189	b <sub>2</sub> -NH <sub>3</sub>
470.1358	469.325	LRNL-28
487.15	487.106	F+C <sub>19</sub> H <sub>17</sub> NO <sub>5</sub>
563.2789	563.362	RNLVP-28
600.3719	600.019	FL+C <sub>19</sub> H <sub>17</sub> NO <sub>5</sub>
629.3973	627.361	FLRNL-NH <sub>3</sub>
1009.606	1011.621	y <sub>8</sub>
1109.157	1111.597	b <sub>7</sub>
1481.644	1481.287	M

---

### 7.3 Models generated for docking peptide 243 into MtrR

